

N 7 2 3 3 0 2 1

NASA CR-112157

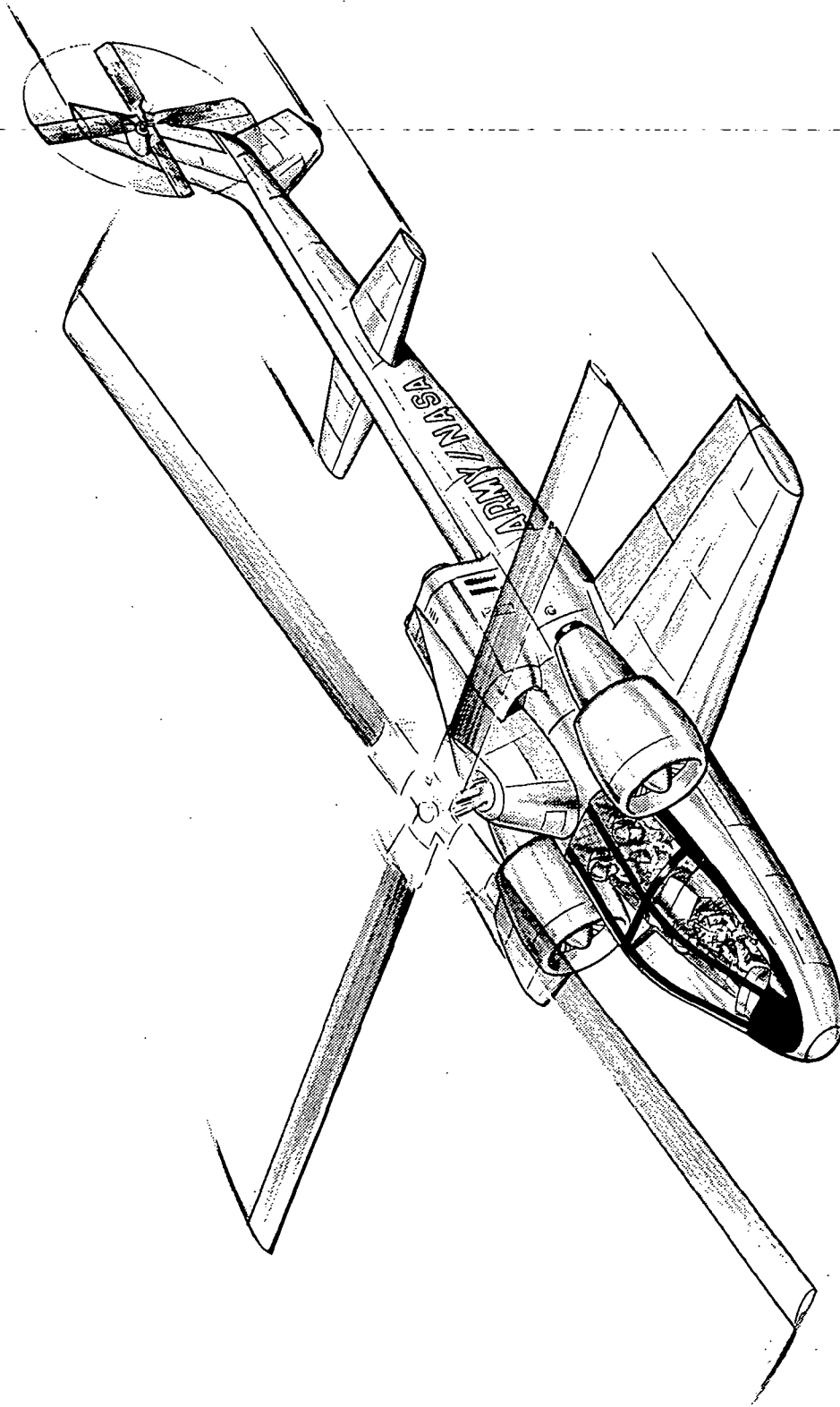
CASE FILE COPY

A CONCEPTUAL STUDY OF THE
ROTOR SYSTEMS RESEARCH AIRCRAFT

Prepared under Contract No. NAS1-11251 by
BELL HELICOPTER COMPANY
A Textron Company
Fort Worth, Texas

for

NATIONAL AERONAUTICS AND SPACE ADMINISTRATION



THE BELL HELICOPTER COMPANY
ROTOR SYSTEMS RESEARCH AIRCRAFT

TABLE OF CONTENTS

<u>Subject</u>	<u>Page</u>
INTRODUCTION AND SUMMARY	1
AIRCRAFT DESCRIPTION	2
WEIGHT AND BALANCE	4
PERFORMANCE	6
STABILITY AND CONTROL	14
DYNAMICS	18
NOISE	32
CONTROL SYSTEM	34
REFERENCES	38
SYMBOLS AND WEIGHT ESTIMATION PROCEDURES	Appendix A
FIGURES	Appendix B
TABLES	Appendix C

INTRODUCTION AND SUMMARY

This report describes the analytical comparison of the two candidate Rotor Systems Research Aircraft (RSRA) configurations selected by the Government at the completion of Part I of the RSRA Conceptual Pre-design Study. The purpose of the comparison was to determine the relative suitability of both vehicles for the RSRA missions described in the Government Statement of Work, and to assess their versatility in the testing of new rotor concepts.

The analytical comparison was performed primarily with regard to performance and stability and control. A weights, center-of-gravity, and inertia computation was performed for each iteration in the analysis process.

The dynamics investigation was not concerned so much with a comparison of the two vehicles, but explored the dynamic problems attending operation of any RSRA operating with large rotor RPM and diameter ranges over large forward speed ranges. Several means of isolating in- and out-of-plane rotor vibrations were analyzed, using the known dynamic characteristics of a Bell Helicopter Company (BHC) Model 309 helicopter to simulate the RSRA fuselage. An optimum isolation scheme was selected.

Existing BHC main and tail rotors were analyzed to determine their acceptability for use on either vehicle. A suitable four-bladed, gimbaled, hingeless rotor design was picked for the larger RSRA (646A) and a two-bladed semi-rigid rotor design was picked for the smaller RSRA (646B). Existing BHC tail rotor designs were found suitable for both vehicles.

A short study of RSRA noise problem potential was made, and means of mitigating noise problems are discussed.

Three candidates for an electronic control system were studied, all of which offered independent control of rotor and fixed-wing controls. The selected candidate provides a full-time mechanical backup for both rotor and fixed-wing controls.

The analytic comparison of the two vehicles shows that the 646A is the better selection for a RSRA. It possesses more research versatility and carries a third crew member. Main rotor mast tilt is shown to be of no advantage, so long as rotor power reasonably correlates with rotor size, and required wing incidence range is shown to be determined by wing lift requirements in the helicopter simulation mission rather than by rotor loading requirements in power-off autorotation.

As a result of the information gathered during this investigation, BHC made the following recommendations to the Government:

- Choose the BHC Model 646A as the RSRA
- Do not provide mast tilt

AIRCRAFT DESCRIPTION

A conceptual predesign has been accomplished for two compound helicopters which satisfy the RSRA mission requirements. The BHC Model 646A (Figure 1) is a new three-place machine in the 25,000-pound design gross weight class. The BHC Model 646B (Figure 2) is an extensive modification of the BHC Model 309 KingCobra and carries a crew of two. Table I lists the major characteristics of the two aircraft.

Both vehicles have wings sized to support the design gross weight at 150 KTAS, sea level, standard day. Full span lower flaps and partial span upper flaps are operable over a 30-degree range. The same surfaces (excluding the outer lower surfaces) operate over a range of 60 degrees for drag production. The upper outboard trailing edge surfaces serve as roll control devices. Wing beamwise and chordwise forces are measured by a flexural balance mounted in the fuselage-carry-through torque box. The wings are removable to leave a flush fuselage area (except for a small landing gear stub-out on the 646B).

Provisions are included for wing incidence control, main rotor mast tilt, computerized operation of any flight control, and variable mechanical advantages to main and tail rotor controls.

The main landing gear of both vehicles is fully retractable. The castoring tail wheel is partially panted by the ventral fin. Both the main and tail wheel struts are of the air-oil oleo type.

The 646A main rotor is a 55-foot diameter derivative of the BHC Model 240 UTTAS rotor. Blade twist has been decreased from minus eight degrees to zero degrees, and radius has been increased 0.5 foot. The 646B main rotor is a derivative of the BHC Model 645 rotor, with blade twist decreased from minus eight degrees to minus 2.5 degrees, and blade radius increased 1.0 foot. Antitorque for the 646A and 646B is provided by unmodified BHC Model 240 and 309 tail rotors, respectively.

Rotor engines are governable over an RPM range of 100 to 78 percent for the 646A (100 to 70 percent for the 646B), so that main rotor speed may be reduced in high-speed forward flight. Two-position exhaust nozzles are incorporated to decrease rotor engine wake drag in high-speed cruise. Auxiliary thrust engines are mounted on pylons which attach to the fuselage and incline upward to lessen engine/wing interference. The thrust engines are placed near the aircraft center of gravity, so that their removal will not greatly affect low-speed pitch trim in the pure helicopter mode.

Both vehicles have an escape system, consisting of a rotor severance and canopy removal system, in conjunction with a YANKEE crew extraction system. The YANKEE system has a zero altitude/zero airspeed ability. Rotor severance and/or canopy removal are available to the crew as independent options in ground emergencies.

An electronic control system which has a full-time mechanical backup is used to control the rotor and fixed-wing controls. The electronic system accepts computer or pilot inputs and controls a dual hydraulic system which powers the rotor and fixed-wing controls. Computer control of throttles is also possible. The overall system allows four modes of operation:

- Manual (dual hydraulically powered)
- Manual control of fixed-wing surfaces with holding ability for rotor parameters afforded by electronic control system (with or without computer).
- Computerized rotor control through the electronic control system and manual control of fixed-wing surfaces.
- Fully automatic control.

WEIGHT AND BALANCE

Weight and balance data of the Models 646A and 646B are presented in Tables II through IV. Table II shows the empty weight breakdown by major components and systems. A description of weight estimation methods used by BHC is given in Appendix A. Useful load and mission gross weights are listed in Table III for the primary and alternate missions (15- and 30-minute high speed cruise). Center-of-gravity and inertia data are tabulated in Table IV.

The horizontal and vertical reference datum planes for center-of-gravity location are defined with respect to the intersection of the rotor flapping axis and mast centerline (zero shaft tilt). For the Model 646A, the reference datum is located 213.0 inches forward (Fuselage Station 0.0) and 183.5 inches below (Water Line 0.0) the mast-flapping-axis intersection. The Model 646B reference datum is located 200 inches forward (Fuselage Station 0.0) and 160.2 inches below (Water Line 0.0) the mast-flapping-axis intersection.

The components and systems of each aircraft may be grouped by percentage of empty vehicle weight into existing, conventional, and new design categories:

<u>Vehicle</u>	<u>Existing</u>	<u>Conventional</u>	<u>New</u>
646A	30%	63%	7%
646B	49%	39%	12%

Existing Components

- 646A: thrust engines, shaft engines, main transmission, tail rotor, instruments, electronics, electrical system.
- 646B: main fuselage structure, cockpit, tail boom, thrust engines, main rotor transmission, shaft engines, tail rotor, tail rotor drive, cowling, nacelles, engine mounts, rotor controls, primary hydraulics, electrical system, most avionics.

Conventional Components

- 646A: body, wing, main rotor, landing gear, tail rotor drive gear-boxes, main rotor control system, fuel system, high lift devices, cowling, firewalls, air-conditioning, instrument packages.
- 646B: nose and instrument compartment structure, wing, main rotor, horizontal tail, landing gear, accessory gearbox, input drive shafts, fuel system, high-lift devices, firewalls, air-conditioning.

New Components

646A: variable wing incidence and balance mechanism, pylon vibration isolation system, rotor-wing-controls mixing box, crew escape systems, rotor shaft tilt mechanism.

646B: same as 646A.

A large portion of the 646A empty weight is composed of conventional design items. However, many of these items such as body and wing designs are conceptual in nature and entail high-weight estimation risk. Empirical prediction methods and techniques based on percentages were used, since comparable existing hardware was not available for weight verification. The Model 646B design utilizes major structural components and systems from the Bell Model 309 which have been strengthened or modified as necessary. Further, most required new 646B components are of conventional design. Because of the absence of major risk areas, the degree of confidence in the 646B configuration weight is higher than for the 646A.

AIRCRAFT PERFORMANCE

METHOD OF ANALYSIS

Rotor performance data published in NASA CR114 (Reference 1) were used for hover and high-speed calculations. At some high-speed conditions ($M_{1.0,90} > 0.9$ with nonzero twist) where data were not available, the BHC computer program BRAM was utilized. The BRAM program contains the essential elements and airfoil data as described in Reference 1 and shows good correlation with the referenced data.

Hovering download calculations were based on data presented in the Government Statement of Work. Figure 3 shows a plot of download factors, defined as:

$$\text{Download Factor} = \text{Planform Area} \times \text{Vertical Drag Coeff.} \times \frac{\text{Dynamic Pressure}}{\text{Disc Loading}}$$

The download factor is plotted as a function of rotor radius for each aircraft in both compound and variable (wings and thrust engines removed and optimum transmission installed) configurations. Figure 4 shows the download for both vehicles as a percentage of mission gross weights.

All fuel flow requirements are based on engine manufacturer data shown in Figures 5 through 12. Fuel flow degradation and engine inlet losses are included as noted on each curve. Fuel requirements for each mission are discussed in the corresponding performance sections that follow.

PARASITE DRAG ESTIMATIONS

The parasite drag of both vehicles was computed using three methods (Table V). The first method is that commonly employed in fixed wing aircraft drag estimation. The helicopter technique is employed as standard Bell Helicopter Company practice for helicopter drag estimation. It differs principally from the conventional aircraft method by allowing some separated flow regions. The third method utilizes a drag coefficient of 0.007 based on aircraft wetted area. This technique yields larger drag areas for the basic vehicle than the previous methods and thus no interference drag is included for this method. The wetted area drag values are used in all performance calculations.

Two-position exhaust nozzles are fitted to the rotor engines to reduce engine drag at low power, high-speed cruise. Therefore, no momentum drag is shown for the shaft engines. Main rotor and tail rotor hub drag are based on maximum rotor power available as given by the relationship

$$f_{\text{hub}} = 0.07 (\text{SHP}_{\text{rotor}})^{0.58}$$

PERFORMANCE WITH BASELINE ROTOR SYSTEMS

Both 646A and 646B configurations have been designed with the "baseline" rotor systems described previously in the aircraft description section. It is desired

that each aircraft be capable of performing a 300-knot high-speed cruise mission at sea level and at 9500-foot density altitude with the baseline rotors and with the aircraft operating in a compound helicopter (wings and thrust engines attached) configuration. In addition each vehicle should be capable of hover (OGE) for a 30-minute period at sea level standard and 95°F day conditions (also in compound configuration).

HIGH SPEED MISSION

High-speed cruise flight may be obtained for 15 or 30 minutes with either vehicle depending on payload requirements. The 15-minute sea level cruise duration is designated the primary mission, for which the 646A carries 3000 pounds of payload, and the 646B carries 2000 pounds. (Note that 1000 pounds of the payload of both vehicles are nonremovable instrumentation.) An alternate mission can be flown for 30-minute cruise duration with either aircraft, if 1000 pounds of payload are removed and full fuel capacity is carried.

For calculation purposes, the high-speed mission is divided into eight segments:

- warm up and takeoff
- flight at minimum airspeed
- climb
- acceleration
- high-speed cruise
- deceleration
- descent
- end-of-mission hover

The following assumptions were made to calculate fuel required in each segment of flight:

1. Warm Up and Takeoff. All engines operate at normal rated power for two minutes.
2. Flight at Minimum Airspeed. Shaft engines operate at normal rated power while thrust engines are brought to flight idle for a two-minute period.
3. Climb. The following force balance equations were solved by an iterative process to yield the minimum ascent time to 9500 feet.

$$\Sigma F_x = T - D - W \sin \gamma + (PF)_R = ma_x$$

$$\Sigma F_y = L_R + L_W - W \cos \gamma = 0$$

$$a_x = (V - V_0)/t$$

$$\sin \gamma = (R/C)/V = h/S_x$$

$$\cos \gamma = \sqrt{V^2 - (R/C)^2}/V$$

Some acceleration occurred during the climb with airspeed upon reaching 9500 feet, ranging from 105 to 150 knots. The climb was accomplished with all engines operating at military power.

The following assumptions were made concerning the flight conditions, airframe, and rotor parameters:

- (a) $V_0 = 50$ knots
 - (b) Rotor aerodynamic parameters were determined from a control plane angle of -8° and a $3/4$ -radius collective setting of 8°
 - (c) Rotor tip speed = 782 fps
 - (d) Wing lift coefficient = 0.4
4. Acceleration. The time required to accelerate to cruise speed was calculated from the relation:

$$t = m \int_{V_0}^{300} \frac{dV}{F(V)}$$

where $F(V)$ is the summation of forces in the direction of the acceleration and is a function of speed. The initial velocity, V_0 , was determined as that at the end of the minimum flight speed portion for sea level missions (approximately 50 knots) or that velocity at the termination of the climb. It was assumed that main rotor RPM, control plane angle of attack, and collective pitch remained constant during acceleration. A control angle of -4 degrees and a $3/4$ -radius collective pitch of 4 degrees place the rotor near its upper stall limit at 300 knots.

5. High-Speed Cruise. The high-speed cruise portion of the mission is accomplished with shaft engines near flight idle. Rotor controls are adjusted to give a zero-degree control plane angle of attack and a lift coefficient $C_L/\sigma = 0.4$. For these conditions the rotor loads are sufficient to prevent vibration problems and remain below the stall limits. Wing induced drag during high-speed cruise is determined using average gross weight values.
6. Deceleration. A deceleration time of one minute was assumed with all engines operating at flight idle. One minute was found to be conservative when deceleration time was calculated using the acceleration equation.
7. Descent. A conservative estimate for descent time was made by assuming equal time as required for climb. All engines operate at flight idle during descent.
8. End of Mission Hover. The fuel required to hover (OGE) for two minutes at the end of the mission was based on the horsepower required for the shaft engines while maintaining thrust engines at flight idle.

Fuel requirements for each segment of the high-speed 15- and 30-minute missions are listed in Table VI.

Table VII summarizes the high-speed mission performance for both vehicles. Note that the maximum speed of the 646B is 5 knots short of the 300-knot goal. The 300-knot cruise could be reached by decreasing drag area approximately 0.5 ft^2 . As Table V indicates, helicopter drag estimation methods would allow the 646B approximately 1.6 ft^2 drag area decrease at the 300-knot cruise condition.

Figures 13 and 14 illustrate the variation in high-speed cruise duration if fuel weight and payload weight are interchanged while maintaining a constant takeoff gross weight. The results show that the 646A is capable of a 30-minute cruise duration at both sea level and 9500 feet while carrying 1000 pounds of removable payload, in addition to the nonremovable instrumentation. The 646B is capable of 30-minute cruise duration only if all removable payload is off-loaded.

HOVER MISSION

Hover mission requirements for the vehicles with baseline rotors include fuel for a two-minute warm up and takeoff period, two minutes of flight at minimum airspeed, 30-minute OGE hover, a 10-nautical mile flight at optimum airspeed, and 2-minute end-of-mission hover -- plus 10-percent fuel reserve based on total fuel weight. A conservative estimate was made for the minimum speed flight and all hover requirements by assuming fuel flow values corresponding to transmission limited power inputs of 3600 and 2000 horsepower for the 646A and 646B respectively.

The hover performance of both vehicles is shown in Figure 15 for sea level standard and 95°F conditions. The results are presented in terms of hover duration versus payload for both machines in compound configuration. The hover ability shown is the maximum available without exceeding transmission torque limits of either vehicle.

The total payload ability of the 646B in hovering flight is about 1750 pounds (including 1000 pounds of nonremovable payload). The 646B therefore cannot accomplish the end-of-mission hover for the 15-minute high-speed mission, which requires the carrying of 1000 pounds of removable payload.

VEHICLE TEST VERSATILITY

The test versatility section shows the range of rotor sizes that may be used to replace the baseline rotor systems. While all performance described in the previous sections dealt only with the vehicles in compound configuration, this section discusses both compound and variable (pure helicopter with optimized transmission) performance.

In the compound configuration, wings and thrust engines are attached, and the transmission is unaltered; only changes to the rotor system are permitted. The transmission installed in the 646A is torque limited below 245 rotor RPM and is restricted to 3600 horsepower above this speed. Similarly, the 646B is torque limited below 299 RPM and is limited to 2000 horsepower at higher speeds. These rotor speeds correspond to 0.63 and 0.7 hover tip Mach numbers for 55- and 50-foot diameter rotors respectively.

In the variable configuration, the wings and thrust engines are removed and the transmission may be replaced. Engine power limits remain the same, but it is assumed that transmission torque limits are removed.

The largest diameter rotor that may be tested on either vehicle is determined by tail boom length. Thus, the baseline rotors are the largest diameter rotors at 55 and 50 feet respectively for the 646A and 646B. However, solidity may be increased to extreme values to give larger blade area than the baseline systems. A maximum solidity limit of 0.15 has been chosen for all rotor systems. This

limit is believed to exceed all conventional main rotor configurations. Likewise, a minimum solidity limit was determined using a blade aspect ratio of 28. For two-, four-, and six-bladed rotors the minimum allowable solidities are 0.023, 0.045, and 0.068. The four- and six-bladed limits are shown on the performance curves where applicable. The two-bladed minimum solidity was never reached.

HOVER TEST VERSATILITY

Fuel requirements for the hover versatility mission include fuel for a two-minute warm up and takeoff period, 30 minutes of hover plus a ten-percent reserve based on total fuel weight. Fuel flow rates were determined for maximum power settings during the 30-minute hover period. All hover performance is calculated using a negative 8-degree twist rotor operating at or between 0.5 and 0.7 tip Mach numbers.

Compound Configuration. Hover performance for the maximum diameter rotors is presented in Figure 16 for a range of solidities and tip Mach numbers. The largest rotor that may be tested on the 646A is 55 feet in diameter with 0.15 solidity. The heaviest OGE hover weight capability for this solidity is 26,700 pounds at 0.6 Mach number. (Note that by reducing solidity to 0.096 for the same Mach number, hover gross weight may be increased to 28,000 pounds.) Performance of the 50-foot diameter 646B rotor is shown in the lower set of curves. The maximum solidity that may be tested is restricted by minimum vehicle mission weight to .095 at 0.7 tip Mach number. By reducing solidity to .068, the gross weight may be increased to 15,900 pounds.

The smallest rotor capable of OGE hover for either machine in compound configuration is determined from Figure 17 at the vehicle minimum mission weight. The 646A will hover with approximately 3 feet less diameter, at a radius of 22.9 feet, while the 646B requires a 24.3-foot radius. However, the 646A requires approximately 67 percent greater solidity. Thus, in compound configuration, the 646A can test rotors in hover from 45.8 to 55 feet in diameter, while the 646B can test rotors from 48.6 to 50 feet in diameter.

Variable Configuration. Similar calculations for the largest and smallest rotors have been made for both vehicles as pure helicopters. The hover capability of both vehicles is considerably increased since download is reduced, and the transmission is limited only by power. Figure 18 shows that the 55-foot diameter 646A rotor allows a maximum gross weight at the 0.15 solidity limit for 0.5 tip Mach number. Similarly, a 0.15-solidity rotor may be tested on the 646B, but the optimum lifting ability occurs when solidity is reduced to 0.10.

The smallest rotors to be tested in OGE hover for the variable configuration are shown in Figure 19 at the minimum mission gross weights. The 646A will hover with a rotor of 14.4 feet radius, while the 646B requires a 16.3-foot radius. Both rotors require the maximum allowable solidity. In a pure helicopter mode, the hover test versatility for the 646A includes rotors ranging from 28.8 to 55 feet in diameter, while those for the 646B range from 32.6 to 50 feet in diameter. A summary of hover test versatility for both vehicles in compound and variable configurations is presented in Table VIII.

Maximum speed performance of the largest and smallest hovering rotors is presented in Figure 20 and summarized in Table IX for both vehicles in pure helicopter configuration. Rotor RPM is held constant until 0.9 advancing tip Mach number is attained and thereafter RPM varies to hold Mach number constant at 0.9. Note that due to solidity differences, the largest diameter 646B rotor performs better at the heavy gross weight. Note also that the small 646B rotor shows better performance in relation to its large rotor than does the small 646A rotor in relation to its large rotor. This characteristic occurs because the 646B is underpowered and requires a larger than optimum rotor for hover at minimum weight.

HELICOPTER SIMULATION VERSATILITY

The helicopter simulation versatility study determines the largest rotors that may be driven to the upper stall limit between 100 and 200 knots. In addition, the requirement for using shaft tilt to obtain the full envelope is examined. To perform the helicopter simulation mission the vehicles are in compound configuration and all transmission limits previously discussed are applied.

Rotor size is determined by using the procedure outlined in Figure 21. The first step was to define the baseline design rotors (largest diameter) for each vehicle. The performance at upper stall of each rotor was calculated (using BRAM) for four representative points within the flight envelope:

- 100 knots, $\Omega_R = 500$ fps
- 100 knots, $M_T = 0.9$
- 200 knots, $\Omega_R = 500$ fps
- 200 knots, $M_T = 0.9$

The corresponding lift, drag, and torque coefficients (C_L/σ , etc.) at upper stall were used to find the maximum blade area for each given flight condition. This was accomplished by balancing the forces acting on the vehicle while subjecting it to the following vehicle limitations:

<u>Limiting Factor</u>	<u>646A</u>	<u>646B</u>
Horsepower available	3600 @ 245 RPM	2000 @ 299 RPM
Maximum auxiliary thrust	10600 @ 100 Kt	6140 @ 100 Kt
	9300 @ 200 Kt	5920 @ 200 Kt
Wing $C_{L_{max}}$ with flaps	+2.54	+2.54
	-1.3	-1.3

During the execution of this procedure, its applicability was checked by computing the performance of several off-design rotors and comparing them with the baseline design rotors. Various combinations of solidity, number of blades, and diameter were investigated. Analysis of the results showed that if performance were expressed nondimensionally, neither solidity nor number of blades affected the calculations for maximum blade area.

On the other hand, diameter was found to have a significant effect. In general, a rotor smaller in diameter than the design rotor can either raise or lower the maximum blade area associated with the torque-horsepower limit. Whether or not the blade area limit is raised or lowered is difficult to determine since one cannot accurately predict the tradeoff in induced power versus profile power for the torque available. Also, there is a change in the auxiliary thrust required, and while the magnitude of the change cannot be predicted, the requirements will always be decreased. This occurs because smaller diameter rotors produce less drag to be overcome by the available auxiliary thrust.

Because of the effects of diameter, the versatility of each helicopter configuration, as shown in Figures 22 and 23, must be expressed in terms of solidity for a given rotor diameter. The constraints imposed by the helicopter designs, however, combine to make the limits shown generally valid for all practical diameters. In all cases, a smaller diameter rotor will have a higher torque limit because it must operate at a higher RPM for a given tip speed; thus, more horsepower will be available. Similarly, because of the smaller forces produced by a smaller diameter rotor, the auxiliary thrust limit will be higher.

Figures 22 and 23, therefore, show that the 646A is more versatile in its ability to test rotors than the 646B. The 646A can test a much larger rotor over a larger range of control plane angle of attack. Assuming a limit on solidity of 0.15, note that at 500 fps tip speed, the versatility is constrained only by autorotation (neglecting the difficulties of trimming at high negative α_c). At a tip Mach number of 0.9, however, the maximum rotor size that can be tested on either ship is a function of α_c : as rotor size increases, the applicable range of α_c decreases. In general, a given rotor size may be tested over a wider range of α_c on the 646A than on the 646B.

SHAFT TILT REQUIREMENTS

The preceding discussion has defined the maximum rotor sizes which can be tested to the upper stall limits, as determined by the available auxiliary lift and drag (wings + flaps) and propulsion (jets). It now remains to determine what wing incidence and shaft tilt ranges are necessary to assure that the vehicle can actually be trimmed at the desired conditions. The requirements, if any, for variable wing incidence and shaft tilt arises from the need to control flapping with respect to the mast, and to provide an ample range of control axis angles (in particular, the angles required to test at maximum power). To determine these ranges, trim investigations were conducted using a computer program developed by Bell Helicopter Company: the Rotorcraft Flight Simulation Analysis (C81).

The scope of the analytical trim investigations is illustrated by Figure 24 which shows the rotor lift at upper stall for the maximum size rotors for the Model 646B (rotors defined in Figures 22 and 23) and for the Model 646B design rotor ($\sigma = 0.070$). The symbols represent points at which detailed trim evaluations were conducted. Similar critical points were evaluated for the Model 646A. A key conclusion resulting from these trim studies was that variable shaft tilt is not necessary to control flapping if sufficient wing incidence variation is supplied. This results from the fact that the shaft can be positioned using pitch attitude. (The most critical point occurs during autorotation at 100 knots, where flapping reaches 6 degrees and -19 degrees wing incidence is required with zero shaft tilt.)

The second stated need for variable shaft tilt was to provide the negative control axis angles (α_c) needed, in some cases, to reach maximum power at the upper stall limit. Figure 25 shows the relationship between the control axis angle and the power loading coefficient for two rotor diameters (30 and 55 feet) at two airspeeds (100 and 200 knots). These are the endpoint rotor diameters and airspeeds under consideration for the helicopter simulation mission. With zero shaft tilt, the negative control axis limit is approximately -23.5 degrees (-10 degrees from pitch attitude, -13.5 degrees from cyclic control). With this limit, a C_Q/σ greater than 0.01 can be achieved for all cases except one (55 feet, 200 knots) where C_Q/σ is restricted to 0.0088. The following table shows that at maximum power (whether engine or transmission limited), typical power loading coefficients range between 0.0056 and 0.0080.

<u>Model</u>	<u>Max. Power, Sea Level, Std. Day)</u>	<u>C_Q/σ</u>
UH-1H		.0056
UH-1N		.0059
AH-1G		.0062
206A		.0062
OH-58A		.0065
King Cobra		.0080

The conclusion drawn from Figure 25 is that shaft tilt is not necessary to test both large and small rotors to power loadings commensurate with their size.

HIGH SPEED VERSATILITY

Figures 26 and 27 show the 300-knot high-speed cruise versatility that may be gained by replacing the baseline rotors with rotors having less drag. It is assumed that reduced fuel weight is compensated by increased payloads to maintain constant gross weights. The thrust limit of the 646B has been placed at a negative drag increment of 0.5 ft^2 to indicate that 300 knots cannot be achieved with the baseline rotor. Instead, a 5-knot penalty in maximum cruise has been accepted.

STABILITY AND CONTROL

GENERAL

BHC's Rotorcraft Flight Simulation Program (C81), described in BHC Report 599-068-904 was used to analyze the 646A and 646B RSRA. The C81 program was used to calculate trim conditions, including stick positions and stability characteristics.

Both candidates were evaluated with respect to (1) static and dynamic stability, (2) stabilizer incidence requirements, (3) control response, power, and margins, (4) trim change with auxiliary thrust variations, (5) autorotation characteristics, and (6) requirements of applicable specifications.

USABLE CENTER-OF-GRAVITY RANGE

The principal stability and control task during this phase was an investigation of the usable center-of-gravity range. This investigation showed that both configurations will have ample usable cg ranges, with the forward limit defined by the aft cyclic control margin in rearward flight, and the aft limit by the forward cyclic control margin, and the phugoid mode instability in compound and helicopter modes. Since in the RSRA concept the stabilator incidence is controlled independently of the rotor cyclic, and will be programmed to meet the requirements of a given configuration, the optimum incidence for each cg location may be obtained. This allows the RSRA vehicle to have a wider range of usable cg than helicopters with fixed or geared stabilizers. The stabilator incidence requirements, as a function of cg location and airspeed are discussed below.

A reasonable estimate of the allowable cg range may be made by calculating the cg range which results in ± 5 degrees of flapping with respect to the mast. This allows for reasonable maneuvering margins at lower speeds, and flapping caused by gusts at high speeds. This criterion indicates a range of 15.9 inches for the 646A and 16.5 inches for the 646B. For reference, the AH-1G has a cg range of 9 inches, and the UH-1D/H has a range of 10 inches.

DYNAMIC STABILITY CHARACTERISTICS - SCAS OFF

Lateral-directional and longitudinal stability characteristics were investigated for compound and helicopter configurations. Only the longitudinal stability is discussed here since it is the critical case.

Compound Mode

For both the 646A and 646B, the SCAS-off dynamic stability characteristics at neutral cg easily meet the requirements of MIL-H-8501A. Figures 28 and 29 show the longitudinal stability variation with airspeed for the 646A and 646B respectively. In both cases the short period mode is highly damped, and the phugoid mode is stable throughout a range of airspeeds from 40 KTAS to 300 KTAS. Increasing stabilizer incidence generally tended to decrease the frequency of both the short period and phugoid modes, while increasing the short period damping, with negligible effect upon phugoid damping, as shown in Figure 29.

Helicopter Mode

In the pure helicopter configuration the phugoid mode is less stable than in compound mode. Figures 30 and 31 are root locus plots at neutral cg for the 646A and 646B respectively. The effect of cg location and stabilizer incidence on the stability characteristics are also indicated. As shown in Figure 31, a 20-inch change in cg has negligible effect on the highly damped short period characteristics. The phugoid mode is slightly unstable at low speeds for both cg locations. The phugoid mode becomes aperiodic divergent with increasing speed at the aft cg location but continues to meet the military specification VFR damping requirements.

Stability boundaries for the phugoid mode as a function of cg location and stabilator incidence are discussed below.

STABILATOR INCIDENCE REQUIREMENTS

Stabilator incidence requirements were determined over a range of cg locations. To establish these requirements the following limits were used:

- longitudinal cyclic control margin of not less than ten percent
- main rotor longitudinal flapping not more than five degrees
- longitudinal cyclic position gradient positive with increasing airspeed (collective pitch constant or variable)
- if a dynamic instability exists, the time to double must be in excess of ten seconds

Trim conditions were calculated for various cg locations with the stabilator incidence held constant over a range of airspeed up to maximum speed. Fore and aft cyclic position and blade flapping (a_{1s}) was then plotted versus airspeed to determine where the limits defined above were exceeded. Figure 32 is an example of the 646A fore and aft cyclic position versus airspeed for several stabilator incidence at an aft cg. Stabilator incidence and airspeed have the usual effect on trim stick position. At a fixed airspeed, nose down incidence requires forward cyclic pitch to trim. As the stabilator incidence becomes more positive, aft cyclic stick motion is required. Note that at this cg a stabilator incidence of -4 degrees results in the 10-percent forward control margin boundary being encountered at 150 knots. A stabilator incidence of 0 degrees results in an unacceptable stick gradient. A -2-degree incidence meets requirements for a positive stick position gradient, but exceeds the 90-percent forward stick limit prior to reaching 300 knots. Therefore, it is necessary to schedule stabilator motion independently of the cyclic stick position, by means of the automatic flight control system, to achieve a positive stick position gradient without exceeding the stick position limits. To determine if an incidence schedule which satisfies these two requirements is acceptable, one must also determine that blade flapping and dynamic stability requirements are also met. To facilitate this task, all limiting values (except stick gradient) were mapped at four airspeeds for the compound configuration: 40, 100, 200, and 300 knots. At each of these speeds

the stabilator incidence was swept for a cg range, and blade flapping, cyclic pitch, and stability characteristics were calculated. The equivalent plot for the 646B is shown as Figure 33. The collective schedule is shown and is similar to that used for the 646A, except that a large collective change has been made at the addition of auxiliary thrust, which provides a means of avoiding the forward stick limit.

Compound Mode

Figures 34 through 41 show the limits of elevator incidence as a function of cg.

The region below the "Stabilator Stalled" line of Figure 34 represents a stalled condition for this surface. It is seen from this figure that, at this low speed, variations in stabilator incidence have almost no effect on main rotor flapping or fuselage attitude, regardless of whether the surface is stalled. In Figure 35, it is seen that an aft cg limit exists at F.S. 234, denoted by the intersection of the dynamic stability and five degrees flapping boundary. The "Stabilizer $\alpha = 0^\circ$ " line denotes the stabilizer position for neutral stabilizer speed stability. At 200 KTAS (Figure 36) an aft cg limit of F.S. 233 is again determined by dynamic stability and longitudinal cyclic control margin. Maximum allowable longitudinal flapping limits nose up stabilator incidence for cg travel as far aft as F.S. 224, where dynamic stability becomes a limit. At 300 KTAS, Figure 37, longitudinal flapping and control margin define a rather narrow band of stabilizer incidence. BHC experience with high-speed compound helicopters indicates that the maintenance of nominal rotor thrust at high speeds is required to minimize rotor loads. Two main rotor thrust values are plotted which show that the development of adequate thrust at 300 KTAS does not present a stability and control problem.

Figures 38 through 41 show corresponding information for the 646B. The stabilator incidence requirements of the 646B are very similar to those of the 646A, and as with the 646A, main rotor flapping control margin sets the incidence requirements.

Figure 42 summarizes the 646A stabilator incidence requirement for the compound mode, at three different cg locations. Note that the positive stick gradient requirement must also be imposed. A positive stick gradient is obtained by scheduling the stabilator incidence as indicated. The 646B stabilator incidence (Figure 43) requirement is very similar to that of the 646A. The requirement for an independently controllable stabilator for high-speed compound mode of flight is clear from the stabilator trim requirements shown.

Helicopter Mode

In helicopter mode, with wings and auxiliary propulsion removed, dynamic instability establishes the stabilator incidence requirements and the aft cg limits. Figures 44 through 47 show the 646A incidence limits as a function of cg location. The 646B limits (Figures 48 through 51) are similar.

The stabilator incidence requirements in helicopter mode are similar to those of conventional helicopters. In light of the larger tail volume characteristic of both the 646A and 646B, an ample aft cg range can be obtained even with a simple stabilator-longitudinal cyclic gearing. A positive stick gradient with airspeed change is readily obtained. Figures 52 and 53 show stick position versus airspeed for several stabilizer incidence angles.

CONTROL RESPONSE WITH SCAS

The BHC Stability and Control Augmentation System (SCAS), like most such devices, uses high gains to oppose disturbances. Unlike most Stability Augmentation Systems (SAS), the BHC SCAS uses an electronic sensor to determine whether the sensed angular velocity is caused by external forces or pilot inputs. If caused by pilot inputs, a special network allows the SCAS actuator to cause more swashplate motion than would normally occur, and then washes out that motion within a specified time (usually about 3.5 seconds).

Figures 54 and 55 show the vehicle responses, about all three axes, to step rotor control inputs of one-inch stick displacement in hover with SCAS engaged. The response curves are similar up to the maximum speed obtainable without auxiliary thrust.

Figures 56 and 57 show that damping and control power about all axes meet MIL-H-8501A VFR requirements, in both the helicopter and compound modes, with the SCAS engaged. The data for this plot were obtained from Figures 54 and 55, using the relationships that damping is the inverse of the response time constant, and control power is determined by the initial slope of the rate response time history.

Figures 58 and 59 present time history responses, about all three axes, to step fixed-wing control inputs of one-inch stick displacement at 300 KTAS with SCAS engaged. To illustrate the effect of the pilot input loop the yaw response is shown with the pilot loop open. With the pilot input loop closed the yaw rate response is similar to that shown for pitch and roll.

WING INCIDENCE FOR AUTOROTATION

Program C81 was used to investigate the power-off autorotational characteristics of the 646A and 646B in the compound mode. A rotor mast inclination of four degrees forward was used for both vehicles, with flapping being held to less than ten degrees. Evaluations of autorotational characteristics were made for a heavy and light weight for each vehicle.

Figure 60 presents the results of this investigation. The minimum rate of descent, for both vehicles, is about 35 feet per second, and is obtained at approximately 80 knots. It is seen that wing incidence range requirements are relatively small for autorotation. Unlike most winged helicopters, negative wing incidence is not required to load the rotor. The small blade twist angles result in poor performance at low forward speeds, and minimum sink rates are obtained at large wing lifts.

Wing incidence range is therefore determined by helicopter simulation mission wing-lift requirements.

EFFECT OF AUXILIARY THRUST ON TRIM

The effects of loss of auxiliary thrust on pitch trim are slight at any speed, because of the small difference in vertical location of the aircraft center of gravity and the engine thrust line.

Figures 61 and 62 depict the cyclic control change necessary to retrim following loss of auxiliary thrust at 200 and 300 KTAS, for both the upper and lower limit of cg travel. The required cyclic stick travel is well within the three-inch maximum allowed by MIL-H-8501A even at the worst case.

DYNAMIC ANALYSIS

PROBLEM STATEMENT

The broad mission requirements of the RSRA in terms of rotor size, rotational speed, and number of blades results in the predominant rotor excitation frequency being coincident with fuselage natural frequencies for certain vehicle loading configurations and operating conditions. Variations in rotor thrust with wing loading will result in significant changes in the magnitude of the rotor excitations. To provide adequate crew comfort and to protect components, structure, and instrumentation over the entire flight, rotor speed, and frequency range, it is necessary to isolate both inplane and vertical rotor excitations from the fuselage. Further, due to the wide variation of rotor types and excitation characteristics, it is necessary to provide inplane isolation of both shears and moments.

The fuselage vibration level is a function of many variables. The parameters considered as primary are:

1. Fuselage response characteristics
2. Frequency of rotor excitation (predominant harmonic)
3. Magnitude of rotor excitation (predominant harmonic)
4. Rotor and airframe lift and drag
5. Power required
6. Isolation system effectivity

Flight mode, crew comfort, or reconfiguration time requirements were not specified by the procuring agency. Guidelines established by the Contractor include the isolation system requirements to achieve the widest operating range for a crew vibration level not to exceed ± 0.2 g at the predominant frequency with the least number of isolator configurations. Tradeoffs in terms of rotor configuration, rotor speed, airspeed, isolation system complexity and reconfiguration times were evaluated. The major trade-off items are to be discussed.

FUSELAGE RESPONSE CHARACTERISTICS

To estimate vibration levels and evaluate the isolation system requirements, a baseline fuselage was assumed. The Bell Model 309 fuselage, clean wing (no stores) configuration with a gross weight of 10,000 pounds, was analytically modeled using NASTRAN methods as shown in Figure 63. The pylon was rigidly locked to the fuselage in the vertical, pitch, and roll directions.

The acceleration response at the pilot, gunner, and rotor hub per 1000 pounds hub shear force applied separately in the vertical, lateral, and fore-and-aft directions are shown in Figures 64, 65, and 66 respectively. The response to a pitching moment of 10,000 inch-pounds is shown in Figure 67. These response values are valid for the baseline fuselage only; however, they are considered representative of the RSRA fuselage.

Since operation in resonance would be difficult with any significant degree of transmissibility, a brief study was made, varying the attachment stiffness of the tail boom to shift fuselage natural frequencies. The frequencies obtained are shown in Figure 68 as a function of attachment stiffness. The primary range of interest is from 6 to 30 cps. Although a significant effect is shown, this approach is not desirable since it requires considerable structural complexity.

ROTOR EXCITATION FREQUENCY

The range of rotor excitation frequencies was calculated, based on the RSRA design envelopes. The rotor size and rotational speed design envelope is shown in Figure 69. The rotor speed/airspeed operational envelope is shown in Figure 70. Rotor diameters of 35, 40, 45, and 50 feet were considered. Boundaries of the operational envelope were based on a minimum tip speed (ΩR) of 500 fps, a maximum tip speed of 0.9 M, and a maximum rotor speed of 300 rpm. The predominant harmonic was calculated for rotors of $b = 2, 3, 4, 5,$ and 6 , as shown in Figure 71. Extrapolation to other rotor diameters can easily be made.

MAGNITUDE OF ROTOR EXCITATION FUNCTIONS

Magnitude vs Airspeed

The magnitudes of rotor excitation forces and moments used in this evaluation were based on published data of the Sikorsky NH-3A compound helicopter and measured BHC data. The Sikorsky data, Reference 2, shows a wide band of rotor hub force magnitudes. It is assumed for purposes of this study that:

1. The rotor excitation sources are proportional to rotor thrust at a particular airspeed.
2. The maximum values shown in Figure 72 taken from Reference 2 represents the maximum thrust condition of 19,000 pounds.
3. The minimum values shown represent a minimum thrust of 4900 pounds.
4. The roll-off in vertical force and increase in lateral force are a function of rotor plane tilt.

A comparison of the rotor forces from BHC data and the maximum values reported by Sikorsky normalized on gross weight and referenced to five blades is shown in Figure 73 as a function of airspeed. Also shown in these figures are the normalized values, shown by the heavy solid lines, used in this study. As can be seen, the vertical forces are in good agreement while the assumed curves for vertical and lateral forces exaggerate the forces of the two-bladed semirigid rotor and underestimate the values for the five-bladed articulated rotor.

Magnitude vs Number of Blades

The magnitudes of the rotor hub forces are assumed to decrease inversely with the square of the number of blades. This assumption is established by a comparison of the BHC and Sikorsky measured data at 150 knots as shown in Figure 72.

ROTOR LIFT AND DRAG

The ranges of rotor lift and drag as a function of airspeed is shown in Figures 74 and 75, respectively. These ranges are based on rotor lift at minimum and maximum control plane angle of attack, and for maximum and minimum tip speed. Rotor lift is at the upper stall limit in all cases. The minimum lift is zero. The minimum propulsive force is zero, and the lift and propulsive force is in the axis of the relative wind. For example, at 100 knots with $\alpha_c = 0$ and $\Omega R = 832$ fps, the rotor lift is 23,000 pounds and the rotor drag is 1760 pounds, while with $\alpha_c = 16^\circ$ and $\Omega R = 500$ fps, the rotor lift is 7800 pounds, and the rotor propulsive force is 1920 pounds.

ISOLATION SYSTEM REQUIREMENTS

The requirements of isolation in the vertical, fore-and-aft, and lateral directions have been established by calculating the nonisolated fuselage response using the force magnitudes and frequencies defined previously. The procedure used in these calculations is shown by the flow diagram in Figure 76. The steps are:

1. Check inputs against design and operational envelopes given in Figures 69 and 70.
2. From Figure 73 and the airspeed, determine the hub force per unit thrust (FH_j/T).
3. Assume a wing lift and subtract it from the gross weight to get the rotor thrust ($GW - L = T$).
4. Multiply the rotor thrust by the hub force per unit thrust to get the hub force ($FH_j = [FH_j/T][T]$). This hub force is referenced to a five-bladed system.
5. An adjustment of hub force as a function of the number of blades can be determined using Figure 72 and the number of blades or the equation:

$$\frac{FH_i}{FH_j} = \left[\frac{5}{b_i} \right]^2$$

6. Multiply the ratio of hub forces from step 5 by the hub force (FH_j) to get the actual hub force (FH_i) for the particular number of blades being considered, i.e.:

$$\left[\frac{FH_i}{FH_j} \right] FH_j = FH_i$$

7. The predominant rotor frequency is given by dividing the rotor speed (RPM) by sixty and multiplying by the number of blades:

$$\frac{RPM}{60} [b] = \text{freq}$$

8. Figures 64, 65, and 66 and the frequency will yield the 'g' level per 1000-pound hub force.

$$\frac{g}{1000\# FH_i}$$

9. Multiply the hub force by the 'g' level and divide by 1000 to get the nonisolated 'g' level, i.e.:

$$\left[\frac{g}{1000\# H_i} \right] \left[\frac{FH_i}{1000\#} \right] = g$$

10. Multiply this level by the isolation effectivity (η) for the actual 'g' level experienced.

Estimates of vibration levels are shown for rotors with 2, 3, 4, 5, and 6 blades in Figures 77a through 77e for vertical response. Levels for lateral response are shown in Figures 78a through 78e, and for fore-and-aft response in Figures 79a through 79e. The contour lines represent the calculated vibration levels in g's per 1000-pound rotor lift for no vertical isolation. As an example, the pilot stations vertical response at 220 RPM and 115 knots (see Figure 77a) is 0.04 g per 1000-pound rotor lift.

Assuming a value of $\alpha_c = 16^\circ$ and a tip speed of 832 fps, Figure 74 shows a rotor lift of 13,500 pounds for a two-bladed, 50-foot diameter rotor. Hence, the 2/rev vibration level is:

$$0.04 \text{ g/1000 pounds} \times 13,500 \text{ pounds} = 0.54 \text{ g}$$

No attempt was made to superimpose the response due to forces in the various directions, although a superposition dependent upon phase relationships occurs. For simplicity, vibration isolation is treated for each axis independently.

METHODS OF ISOLATION

A number of methods of isolation were considered (see Figure 80). These are as follows:

Inplane (Fore-and-Aft and Lateral)

Passive

1. Bipod focal pylon
2. Tetrapod focal pylon

Vertical

Passive

1. Nodal beam

Servo-Controlled

1. Nodal beam
2. Servo-null sprung pylon

Each of these are discussed in the following paragraphs.

INPLANE ISOLATION SYSTEMS

The inplane isolation systems considered are two types of focal pylons:

- (1) a bipod system similar to that employed on the OH-58A helicopter, and
- (2) a linkage focal pylon system similar to that on BHC's Model 609.

A study was made of these two systems. First, a static deflection criterion was established, then calculations were made of the spring rates and focal depths required to obtain optimum force and moment isolation at specific frequencies from 5 to 30 cps, in each the pitch and roll directions.

In general, either design approach could be combined with either the nodal beam or servo-null systems considered for vertical isolation. Some of the tradeoffs are discussed later. The determination of the system transmissibilities is described in the subsequent paragraphs.

Static Deflections

Although it may be possible to operate satisfactorily in some configurations below the selected static criterion line, rapid and high 'g' transient maneuvers result in significant transient relative angular motions between the pylon and fuselage. The selected criterion shown on Figures 81 and 82 is equivalent to that of the AH-1J pylon in pitch.

Force Isolation

Optimum focal depth and spring rate loci for 1000 pounds hub force are shown for the predominant harmonics at 5, 10, 15, 20, and 30 cps in Figure 81.

For static pylon deflections of 0.09-inch hub deflection per 1000 pounds hub force, the optimum focal point for hub force isolation varies from WL 132.5 to WL 96.6 in the upper focal region, and from WL -60.0 to WL 46.2 in the lower focal region, as the excitation frequency varies from 5 to 30 cps, respectively. Typical system response curves are shown in Figures 83, 84, and 85.

Moment Isolation

Optimum moment isolation is a function of focal depth, pylon spring rate, effective rotor inertia, and flapping spring stiffness. Optimum focal depth and spring rate loci for 10000 in.-lb moment are shown for the predominant harmonics at 5, 10, 15, 20, and 30 cps in Figure 68.

For static pylon rotation of 0.5 degrees hub rotation per 10000 in.-lb moment, the optimum focal point for hub moment isolation varies from WL 149.5 to WL 144.2 in the upper focal region, and from WL 26.8 to WL 51.0 in the lower focal region, as the excitation frequency varies from 5 to 30 cps, respectively. A typical fuselage angular response curve is shown in Figure 86.

Transmissibility

Frequency response plots were calculated for combinations of focal depth and spring rate equal to the static criterion wherein optimum shear and moment isolation is achieved at frequencies of 5, 10, 15, 20, and 30 cps. Transmissibilities in the pitch and roll planes due to hub shears are shown in Tables X and XI, respectively. Similarly, transmissibility of hub moments in the pitch and roll planes are shown in Tables XII and XIII, respectively.

Bipod Focal Pylon

With no pylon restoring spring, the fuselage is isolated when attached at the pylon center of percussion (see Figure 81). However, for finite values of restoring spring stiffness, the optimum point moves toward the rotor hub. As the excitation frequency is increased, the optimum point moves away from the rotor hub. The sensitivity to focal point, spring rate, and rotor speed changes is much greater for the upper focal region than for the lower focal region.

The optimum isolation of a shear requires a different focal point from that required for optimum isolation of a moment. A reasonable compromise for shear and moment isolation can be achieved for lower focal points.

It is desirable to locate the fore-and-aft focal axis at the transmission input, WL 80.25, to minimize shaft misalignments. Also, for shaft tilt considerations, it is necessary to pivot about this axis, or alternately to provide another pivot axis and means to accommodate the shaft misalignment.

The bipod design provides a focal point in the lower focal region for roll isolation and a focal axis in the upper focal region for pitch isolation. In addition, rotor antitorque restraint is provided. The system, when tailored for an individual rotor system, weighs less than one percent of gross weight including mount and attachment hardware, and is thus the lightest configuration for isolation of inplane forces.

With the bipod fore-and-aft focal axis located at the lateral shaft input axis, frequency response plots were calculated for varying spring rates. From each of these response plots, the transmissibility at frequencies of 5, 10, 15, 20, 25, and 30 cps was obtained. Table XIV shows the transmissibility of hub forces and hub moments in pitch.

The bipod attachments can be made at locations other than the lateral shaft input axis with some improvement in force isolation. However, accommodating pylon tilt with the focal axis offset from the lateral shaft axis necessitates excessive coupling misalignment.

The bipod configuration would isolate best in roll with a focal point at WL 45 and a torsional spring rate of 15×10^6 in.-lb/rad. The focal axis in pitch would be at the shaft axis, WL 80.25, with the minimum spring rate which meets the static criterion (7.2×10^6 in.-lb/rad for 2/rev isolation).

Tetrapod Focal Pylon

The tetrapod focal pylon can be focused over a broad range of lower focal depths and spring rates while achieving relatively good isolation of both forces and moments over a large frequency range. In the lower focal region, the minimum

response curves for shear and moment are in relatively close proximity, while the response gradient for off-optimum focal points or spring rates is low. For example, for a focal depth of -5.4 inches (WL 46.2) with a spring rate of 14.9×10^6 in.-lb/rad, the isolation achieved is shown in the following tabulation.

FORCE AND MOMENT ISOLATION
FOR TETRAPOD DESIGN CONFIGURATION.

	FREQUENCY - CPS					
	5	10	15	20	25	30
Isolation to:						
Force in Pitch	63%	94%	98%	99%	99%	100%
Moment in Pitch	73%	100%	96%	95%	94%	94%
Force in Roll	38%	90%	97%	98%	99%	100%
Moment in Roll	54%	100%	95%	93%	92%	92%

Trade-Offs for Inplane Isolation Systems

The trade-offs between the bipod and tetrapod isolation systems, where the upper bipod attachment was predetermined, are essentially between the requirements for a lightweight system and one which provides improved moment isolation. The major trade-off items are listed in Table XV. The principal advantage of the tetrapod system is that excellent (better than 90 percent) isolation is achieved in the pitch and roll planes for hub forces and moments. On the other hand, the tetrapod system requires additional hardware for both torque restraint and tilting. The torque restraint system alone increases the weight approximately 50 percent. In addition, the design must accommodate the relative motions between the pylon and fuselage, including tilting, and the mean and oscillatory deflections. In all cases, pylon-control coupling must be evaluated to ensure rotor-ylon stability, and in the case of articulated rotors, the pylon mounting frequency must be placed above one-per-rev and/or sufficient damping be provided to preclude mechanical instability.

VERTICAL ISOLATION SYSTEMS

Nodal Beam

General

Nodal beam isolation was recently developed and demonstrated by BHC. Results of fractional scale model tests and full-scale flight tests using this principle are described in References 2 and 3.

To permit a broad scope of investigation in terms of frequency range, tip mass and spring rate variations, the beam's mass and stiffness distribution were held constant, and a symmetric geometry was assumed. The two-dimensional analytical model is shown in Figure 87 while the three-dimensional model is shown in Figure 88.

A beam overall length of 68 inches with a beam bending stiffness of 500×10^6 lb-in² and a mass distribution of 0.2 lb-in was selected. The beam was hinged at mid-span and restrained with a torsional spring about the hinge. Beam tip masses were varied from 25 pounds to 200 pounds and the torsional spring rate was varied from 10,000 to 1,000,000 in-lb/rad. A bipod focal pylon, hinged at the upper attachment point was used in the analysis, but the results also apply to the tetrapod focal pylon. A static deflection criterion of 0.75 in/g--same as for the Model 206 dynamic module--at the mid-span of the beam, was used.

Two approaches were evaluated to show the extremes of complexity and the related isolation ranges:

- (1) a nodal beam with an elastomeric hinge at mid-span with fixed nodal points, fixed spring rates, and fixed masses (passive);
- (2) a nodal beam with a variable elastomeric hinge at mid-span and constant tip weights.

Passive System

The center-hinged nodal beam was analyzed statically and dynamically. Static deflections and the moment distribution of the installed beam were calculated. Figure 89 typifies this calculation. The torsional spring rate and the tip mass were also varied. The response of the rotor, transmission, and beam assembly was then obtained at various frequencies and the nodal points determined.

An example of the variation in nodal point location with spring rate, maintaining a 50-pound tip mass, is shown in Figures 90 through 94. The mode shapes are based on a rotor speed of 300 rpm. From these and similar results with tip masses of 0, 25, 100, and 150 pounds, the curves shown in Figure 95 were obtained.

Results from the Model 206 dynamic module studies show that the natural frequency of the pylon and beam assembly should be placed at a frequency of approximately 0.8 times the frequency to be isolated. Thus the required spring rate for a given tip mass can be determined.

Fixed Nodal Points, Fixed Spring Rate, Fixed Tip Mass

The simplest in-flight mechanical system is achieved from a system with fixed nodal points, fixed spring rate, and fixed masses. With this system, isolation is obtained for relatively narrow rotor speed corridors, as shown in Figure 96 for a system with $K_{\theta} = 172,000$ in-lb/rad, $M_{tip} = 100$ pounds, and nodal points at 17 inches from centerline.

Thus to meet the RSRA requirements, a number of fixed design configurations must be provided. Coverage of the complete operating regime, i.e., airspeed, rpm, and number of blades, would require approximately four configurations as indicated in Table XVI. This necessitates structural provisions in the beam and the fuselage for varying the nodal attachment points. The total weight of the vertical isolation system consists of the tip mass indicated in Table XVI plus the beam and attachment weights.

Variable Spring Rate

To achieve a broader operating range requires more complexity. This could be in the form of (1) a servo-drive used to move the tip masses along a track in a predetermined amount as a function of rotor speed, (2) a servo-drive used to move nodal attachments along a track, or (3) by varying the torsional spring rate as a function of rotor speed.

Due to the high-g level of the tip masses, and the high steady loads at the nodal points, combined with the difficulty of maintaining a preload across the track, the first two were not considered further. The requirements for varying the torsional spring rate as a function of tip mass and initial nodal point location are shown in Figures 97 through 101. From these figures, two sets of fixed nodal point locations were selected to avoid compromise of the design at the extremities of the frequency range.

With the nodal points 10 inches from the beam centerline, two-per-rev isolation can be achieved with 200 pounds tip masses over a rotor speed range from 190 rpm to 300 rpm as shown in Figures 102 and 103. With the nodal points 14 inches from the beam centerline, six-per-rev isolation can be achieved with 50 pound tip masses over a rotor speed range from 190 to 300 rpm as shown in Figures 104 and 105.

The spring rate variation from 300,000 to 900,000 in-lb/rad is accomplished as shown in Figure 106 with two liquid springs having linear spring rates of 7200 lb/in acting at a distance of 3.36 inches from the hinge axis at 190 rpm and 5.6 inches from the hinge axis at 300 rpm. Note that theoretical values of less than 0.05g/1000 pounds vertical shear is achieved in each case.

Servo-Null Spring Pylon

A second vertical isolation system was evaluated in an effort to obtain one configuration which provides isolation over the entire frequency range, all rotor speeds and diameters shown in Figures 70 and 71, and maneuvers up to 2.5g at the high rpm. This system, shown in Figure 107, uses an inertial cancellation effect. The system functions as follows:

1. The linkages from the focal pylon attach to four arms connected to torque tubes which are in turn attached to the fuselage through elastomeric mounts which provide additional isolation of the high frequencies.
2. The torque tubes are connected through an interlocking tube which constrains the torque tubes to rotate in opposing directions. This allows only vertical motions of the pylon and, therefore, decouples the vertical and inplane isolation systems. This is necessary to maintain a defined focal point.
3. Vertical restraint is provided by springs about the torque tube axis. This is accomplished by placing two linear springs, one at each side of the pylon, between arms connected to each of the torque tubes. The final design spring rate includes the contribution of the arms, torque tubes, and elastomeric mounts.

4. The isolation capability is extended over the required frequency range by providing a means of varying the vertical spring rate as a function of rotor speed. This is accomplished by screw jacks which are integral to the spring support arms and are driven by interlocking drive motors. Thus, as the arm length is changed, the torsional spring rate is varied.
5. Two servo-actuated hydraulic actuators are used in series with the two linear springs to minimize the static and transient deflections. Pylon vertical position transducers are used to control the servo-valves and thus maintain a fixed static reference position. The motion resulting from transients is a function of the spring rates and the flow rate available to the actuators. The actuator is not required to follow the oscillatory motions as these are sensed by the springs.
6. Pylon tilting is provided by a screw-jack in the interlocking tube used to decouple the vertical and inplane motions. Extending the tube produces forward pylon tilt of 15 degrees about a fixed point.
7. Inertia amplification is produced by inertia arms attached to the torque tubes. A mechanical advantage of approximately five is used. The inertia masses are thus accelerated five times that of the pylon and thus amplify the inertia of the pylon. This provides greater isolation with lower oscillatory motions with some degradation in isolation at the higher frequencies as the inertia masses are increased. The inertia mass is varied dependent upon the rotor to be isolated.

In effect, the system acts as a soft-mounted pylon wherein the rotor forces are largely reacted by the pylon inertia forces. The remaining forces enter the fuselage through the torque tube support points, thus perfect isolation is not achieved. However, good isolation is obtained throughout the rotor speed range by means of the tuning feature, while the large relative motions which usually preclude isolation in this manner are eliminated by the servo-null feature. Positive stops, with rubber contacting surfaces, can be set in close proximity to the pylon support arms to limit the total travel to approximately one-half inch.

A summary of servo-null isolation design requirements are shown in Table XVII. For a 15,000-pound fuselage, the system requirements are:

- (1) two linear elastomeric springs with a spring rate of 1,150 lb/in, capable of 13,000 pounds steady force and five inches of displacement,
- (2) a 3,000 psi hydraulic pump with a 5 hp capacity.

Trade-Off Study Summary

The trade-offs for the vibration isolation system are essentially dependent upon the user's requirements in terms of: the flight mode restrictions (limitations on airspeed and rotor speed for a given configuration), the reconfiguration time limitations (acceptable time permitted for reconfiguration between flights), and an acceptable vibration level.

This study shows that simple passive systems can provide a high degree of isolation over a limited rotor speed range. An example of the simple passive system is the nodal beam. It is estimated that at least four configurations would be required to cover the proposed frequency range.

A much more complex system is necessary if one configuration is required to accommodate all of the rotor systems and provide isolation over the entire rotor speed range of each rotor. Two examples of a more complex system have been described: the nodal beam with variable pivot spring and the servo-null sprung pylon. Trade-offs between these systems are given in Table XV. The prime consideration between these two systems is essentially one of configuration compatibility--i.e., how well can it be integrated into the total vehicle design. It is concluded that the servo-null sprung pylon is fully compatible and is the isolation system recommended to fulfill the RSRA requirements.

ROTOR DYNAMICS

The calculation of rotor dynamics is based on the assumption that all blades of a particular rotor are identical. For specified radial distributions of stiffness and weight, the dynamics of a single blade are determined as functions of the boundary conditions at the rotor centerline. The boundary conditions are specified by the type of hub geometry, the number of blades, and the frequency ratio of the applied airloads to the rotor speed. For semirigid (stiff inplane) rotors, the inplane and out-of-plane boundary conditions must be treated as paired sets. When the coupling effects due to collective pitch and twist are included, each set of boundary conditions defines a distinct type of mode which is excited only by prescribed harmonics of the external airloads.

Collective Mode

The boundary conditions for the collective mode are cantilevered in the vertical (out-of-plane) direction, and pinned in the plane of rotation. For the collective mode, vertical and lead-lag motions of all blades are in phase, as indicated in the following sketch.

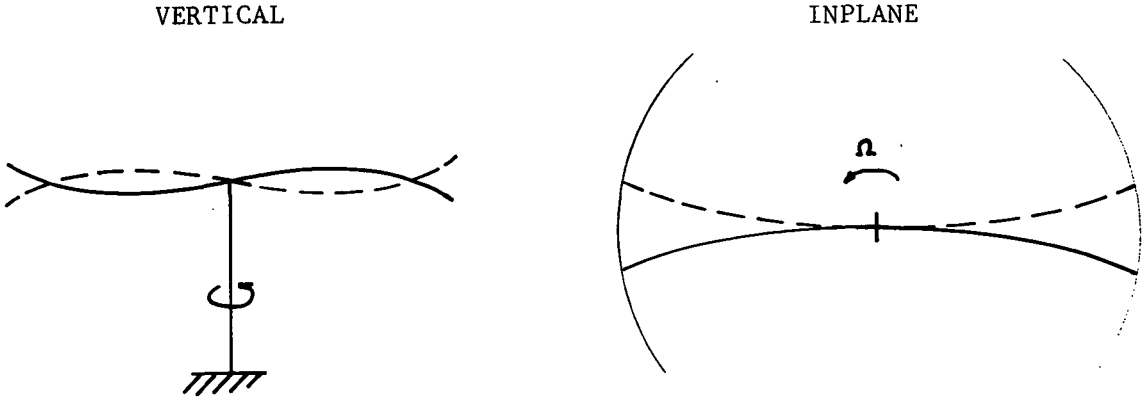


Collective-mode boundary conditions may be modified by input data. An equivalent axial spring rate of the mast may be included to allow vertical displacement at the rotor centerline, and an equivalent torsional inertia may be included to restrain wind-up at the mast.

The collective modes are excited only by harmonic components of airloads, i.e., frequencies equal to the rotor speed multiplied by the number of blades and integer multiples thereof.

Cyclic Mode

The boundary conditions for the cyclic mode are pinned in the vertical direction and cantilevered in the plane of rotation. For the cyclic mode, vertical and lead-lag motions of the blades are out of phase, as indicated below.

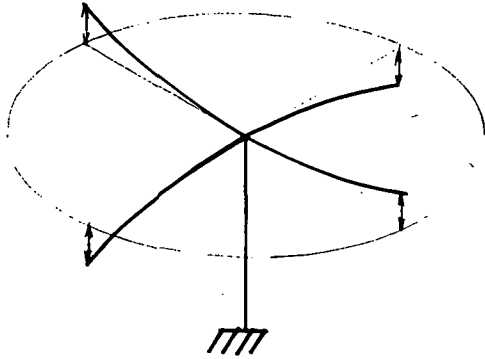


Cyclic-mode boundary conditions may be modified by input data to allow inplane displacement at the rotor centerline (mast bending) and to include the effects of a flapping spring between rotor and mast. The cyclic modes are excited only by harmonic components of airloads at odd-integer multiples of the rotor speed times the number of blades.

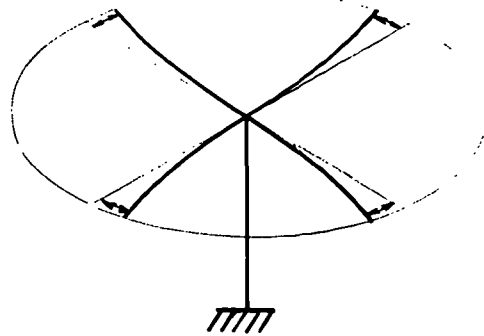
Rigid Mode

The boundary conditions for the rigid mode are cantilevered both inplane and out of plane. This mode, known as the scissors mode, is used only for multibladed gimbaled rotors where the vertical shears and inplane moments from one pair of opposed blades are reacted by another pair of opposed blades as shown in the following sketch. For a four-bladed rotor, the rigid modes are excited only by harmonic components of airloads at frequencies equal to the rotor speed multiplied by 2, 6, 10, etc.

VERTICAL



INPLANE



IMPACT OF FLIGHT PARAMETERS ON ROTOR DYNAMICS

At the design forward speed of 300 KTAS, it is desirable to limit the advancing blade tip Mach number to 0.90 for noise considerations. This establishes a minimum rotational tip speed for the rotor of 495 feet per second. Based on the Phase I performance studies, Mach 0.70 was selected as the rotational tip speed for hover and low-speed flight. Thus, the variation of rotational tip speed is from Mach 0.447 to Mach 0.70. The corresponding rotor speeds are 176 to 277 rpm for the 646A rotor (55-foot diameter), and 191 to 299 rpm for the 646B rotor (50-foot diameter). In terms of the upper value, the range of rotor speed is 36 percent for the conditions of Mach 0.90 advancing-blade tip speed at 300 knots and Mach 0.70 tip speed in hover.

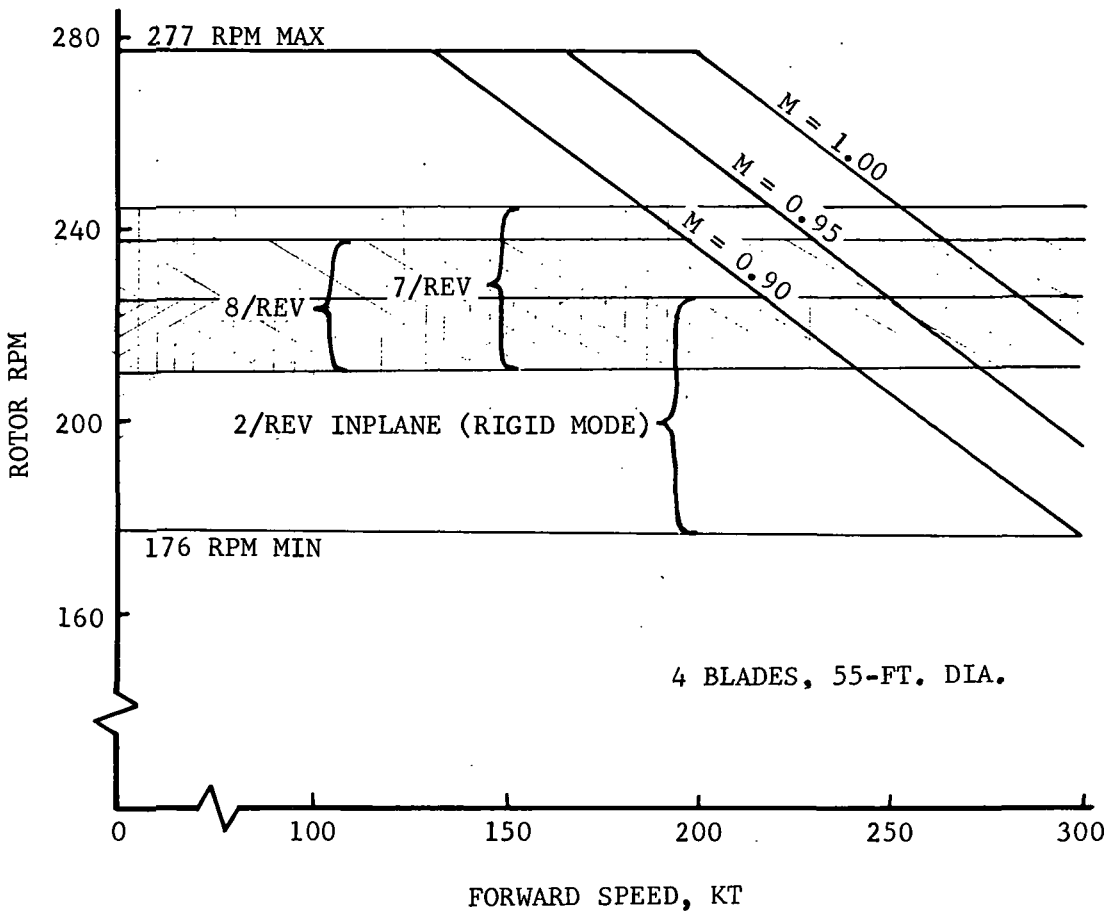
The requirement for a wide range of rotor speeds has an adverse effect on the dynamic design of a rotor. Good design practice involves dynamic tuning to separate all coupled rotor natural frequencies from the excitation frequencies by at least 0.3/rev for all combinations of collective pitch and rpm in the flight envelope. As the range of rotor speed is increased, the avoidance of resonant conditions becomes more difficult.

Typical helicopters are operated at constant rotor speed, with design provisions for 5 to 10 percent rpm variation during autorotational landings, severe maneuvers, etc. In such designs, several approaches may be used to achieve good separation between rotor natural frequencies and the basic aerodynamic excitation frequencies, but only for a narrow range of operating rotor speeds.

To allow a narrow range of rotor speeds in the RSRA, several constraints must be relaxed. The range of maximum rotor speeds may be reduced by selecting Mach 0.60 (instead of Mach 0.70) as the rotational tip speed for hover and low-speed flight. This would change the rotor-speed range from 36 percent to 25 percent. This results in a small improvement in performance for the 646A but in a hovering performance penalty for the 646B. Allowing Mach 1.0 tip speed at 300 knots, (combined with a hover tip speed of Mach 0.60) would result in a nine percent range of rotor speed. Figures 108 and 109 show the considered operational envelopes of the 646A and 646B rotors. The desirability of using the smallest range of rotor speeds is illustrated by the following rotor-dynamic evaluations.

646A ROTOR

Plots of computed coupled natural frequencies versus rotor speed and collective pitch are presented in Figures 110, 111, and 112 for the Model 646A 55-foot diameter, 25-inch chord, four-bladed gimbaled rotor. The following sketch shows bands of rpm where high loads are expected, due to the crossing of excitation frequencies by rotor natural frequencies. The width of the bands are determined from the empirical frequency separation rule, i.e., 0.3/rev separation between natural and excitation frequencies.



As rotor speed is reduced from the maximum of 277 rpm, resonances will be encountered at seven-per-rev (cyclic mode) and eight-per-rev (collective mode). Since vertical modes will be excited in both cases, aerodynamic damping will limit the maximum amplitude of these high-frequency loads to reasonable values. The highest levels of seven-per-rev and eight-per-rev rotor loads will occur in the range of 215-240 rpm.

Reducing rotor speed to approximately 220 rpm will shift the inplane rigid-mode natural frequency to about 1.7-per-rev, or within 0.3-per-rev of resonance with two-per-rev airloads. Further reductions in rotor speed will cause a rapid increase in chordwise bending moments. Inplane motions are very lightly damped by aerodynamic forces, hence the inplane two-per-rev bending moments may approach or exceed the yield strength of the rotor structure if the rotor speed is reduced below 215 rpm.

Based on the constraint of operating the rotor at or above 215 rpm, a forward speed of 300 knots can be attained for the condition of Mach 1.0 at the advancing blade tip.

646B ROTOR

Plots of computed coupled natural frequencies versus rotor speed and collective pitch are shown in Figures 113 and 114 for the Model 646B 50-foot diameter, 33-inch chord, two-bladed teetering rotor.

At the maximum design rotor speed of 299 rpm, and particularly for low values of collective pitch, beamwise bending moments in the mid-span region of the blade will be amplified by the close proximity of the first elastic vertical cyclic mode to three-per-rev. Fatigue damage probably will be accumulated for all forward speeds (above sidewind velocity) for which maximum design rotor speed is maintained. Reducing the rotor speed to 250 rpm should be sufficient to avoid fatigue damage from three-per-rev bending moments.

At approximately 217 rpm, resonances will occur at both seven-per-rev (cyclic mode) and eight-per-rev (collective mode). Since vertical modes will be excited in each case, aerodynamic damping will limit to reasonable values the maximum amplitude of these high-frequency loads. An eight-per-rev inplane resonance (collective mode) at 250 rotor rpm is also indicated and must be considered in a detailed design with respect to drive system torsional modes.

For rotor speeds less than 210 rpm, a buildup in rotor loads is expected as the second collective mode approaches four-per-rev resonance. As a result, rotor speeds below 210 rpm should be avoided. In addition, excitation of this mode transfers a vertical force to the fuselage, hence the frequency placement and level of force transferred are subject to tuning by the vibration isolation system. Based on the constraints of operating the rotor at or above 210 rpm, a forward speed of 300 knots can be attained for the condition of Mach .95 at the advancing blade tip.

For both rotors, dynamic problems will be encountered if the maximum rotor speed is based on a rotational tip speed of Mach 0.70, and the minimum rotor speed is based on the advancing-blade tip speed of Mach 0.9 at a forward speed of 300 knots, as was considered during the initial phases of the study. Based on the rotor dynamic analyses, it is recommended that the rotor speed range be reduced by lowering the maximum design rotor speed and considering operation at higher advancing-blade tip Mach numbers.

NOISE CONSIDERATIONS

The amount of noise radiated into areas adjacent to and below flight test corridors depends on the rotor system's acoustical signature and on how the vehicle is flown.

Figure 115 shows that rotor noise varies principally with disk loading and advancing-tip Mach number, the latter a function of tip speed and forward airspeed. Rotors with disk loadings ranging from 5 to 20 lb/ft² will generate perceived noise levels from about 85 to 110 PNdb at a sideline distance of 500 feet during landing and takeoff operations. Low altitude, high speed flyovers at high Mach numbers can produce intense noise as high as 130 PNdb.

Noise-abatement flight testing of the RSRA is mandatory. The most offensive sounds of the vehicle can be eliminated by performing high-speed flights at the highest practical altitude. Low altitude high-speed flyovers should be performed only over unpopulated areas. During approach and landing, the "slapping" of a main rotor can be avoided by pilot techniques. The airspeed at which he converts to an approach glide slope, the glide slope, and the initiation of the flare can be safely coordinated to avoid slap regimes caused by the blade interacting with the wake.

Noisy flight regimes can be identified beforehand for each rotor configuration. Hence, tests can be scheduled and pilot techniques quickly developed to prevent excessive noise exposure in the test corridor.

AUTOMATIC FLIGHT CONTROL SYSTEM

STUDY GUIDELINES

Prior to beginning a study of possible control systems, a statement of assumptions and requirements was formulated as a guide in control system selection.

- Conventional collective and cyclic controls are required for compound helicopter operation.
- A control integration scheme is required that allows continuous integration of fixed wing surfaces and conventional helicopter controls.
- Tradeoffs must consider failure of primary electronic components and include a backup system for safety.
- A rotor controls "phase-out" system is required for high-speed operation.
- The position of the pilot's controls must agree with the fixed wing controls at all times.
- The pilot can override the electronic control system at any time.
- Rotor control must be possible independently of fixed wing controls.
- No failure shall require an immediate landing.
- Mission continuance after a malfunction is not required.
- The aircraft must meet all handling qualities and control system failure requirements of MIL-H-8501A.

TRADEOFF STUDY (PRIMARY FLIGHT CONTROLS)

Comparisons were made for longitudinal cyclic and fixed wing pitch and roll control systems. Lateral cyclic and collective controls were considered to be comparable with longitudinal cyclic, and yaw controls were considered analogous to the fixed wing portion of the pitch controls.

CONCEPT I

The first concept considered was that shown in the original BHC RTV proposal. The concept uses an electronic control system with a mechanical backup. Figure 116 depicts this system.

The Fly-By-Wire (FBW) actuator (full authority) responds to pilot and computer commands, which together with the limited authority SCAS actuator inputs, positions the fixed wing controls. The sloppy link and clutching mechanism allows the mechanical backup system to be disconnected for a limited range to allow the FBW actuator enough motion to perform normal movements. A FBW system failure would cause the clutching mechanism to slowly center, lock the sloppy link, and bypass the FBW actuator to allow mechanical backup system operation.

The control phasing mechanism is used to select the mechanical control system—swashplate motion ratio for varying flight conditions to minimize the SCAS authority required. The control phasing mechanism has dual phasing actuators for safety. These are slow-moving actuators which shut off automatically if a disagreement of signals is sensed. In event of failure, the pilot may reactivate one of the actuators to achieve a change in control motion ratios. Dual rotor SCAS actuators are also used. A failure of one will be counteracted by the other and the monitor will shut off and slowly center and lock both actuators.

Computer controlled FBW is accomplished by deactivating the sloppy link to allow the stick to follow the computer controlled motions.

Independent rotor control may be accomplished by the rotor SCAS actuators independently of the fixed wing control motions and method of operation (manual, FBW, Computer Controlled FBW, or mechanical backup).

CONCEPT II

Figure 117 shows a design concept using triply redundant FBW rotor controls and conventional fixed-wing controls. Fixed-wing FBW control is accomplished by the parallel FBW (SCAS) actuators which accepts computer commands and positions the fixed-wing controls. The fixed-wing dual SCAS system is conventional. A disengaging of the SCAS will cause the SCAS actuators to slowly center and lock. During manual fixed-wing control, the FBW actuator becomes a force-feel actuator to provide desired control forces to the pilot's stick. The FBW/FF (Fly-By-Wire/Force Feel) actuator is monitored continuously for failures, which, if they occur, will bypass the actuator and allow the mechanical control system to operate in a conventional manner.

Independent rotor control is provided by the triply redundant FBW rotor control system. Each of the three independent FBW systems is identical, with independent input signals. An equalization (tracking) system is required to prevent each of the three FBW systems from opposing inputs of the others. The amount of equalization needed is determined by the signal tolerance buildup for the systems. Any disagreement between the actuator forces above the equalization level indicates a fail condition which will be signalled to the pilot. The failure of one of the three will not cause a runaway since the other two are still in agreement and will overpower the failed system. This system can also be flown without the computer.

CONCEPT III

Figure 118 shows Concept III which uses the same fixed-wing controls as Concept II, but with a mechanical backup system for the rotor controls. Independent rotor control is provided by actuators 2 and 3. These SCAS actuators add to or subtract from the mechanical control system motion to provide the rotor inputs required. Actuators 2 and 3 receive signals from identical sources, and must always have the same motions (within the signal tolerance). An out-of-tolerance disagreement between these actuators will indicate a failed condition and the actuators are then centered and locked to allow a rigid mechanical backup control to the rotor.

The gain change mechanism is used to adjust the control system-to-swashplate coupling. This is a slow-moving device and may be controlled by the computer or pilot. A monitor is required to shut off and hold position of this device should a failure occur. Several important functions are provided by this device. In addition to changing the control system-to-swashplate coupling, it limits the authority of actuators 2 and 3, and provides a rotor control lockout. This device can be programmed to provide sensitivity change with airspeed, altitude, or other flight conditions.

COMPARISON

Table XVIII shows a brief summary of comparisons for the three concepts discussed.

SELECTED CONCEPT

Concept III was chosen as the best, and is recommended as the one which best meets the requirements and philosophy already presented. There are several important reasons for this choice:

1. A rigid mechanical link is always present to both the rotor (if not phased out) and fixed-wing controls to allow the pilot immediate and proportional mechanical inputs in case of FBW system malfunction.
2. The FBW actuator is available to provide the pilot with a force-feel system during manual operation of fixed-wing controls. This is provided for very small additional cost and requires no additional development time or expense.
3. The gain change mechanism provides a means of limiting inputs to the rotor from computer, pilot, or rotor control (SCAS) actuators to safe levels.
4. The proposed control system concept provides more operational flexibility with the least development effort and good safety features.

THROTTLE CONTROL

The throttle control system for the auxiliary thrust engines required a minimum of concept studies. The requirements of this system are:

1. Slow-moving, full-authority actuators.
2. Fail safe for all single failures.
3. Pilot can override automatic functions.

The system proposed for these controls is shown in Figure 119. The two operating modes permitted are: manual, and automatic control by computer. During manual operation, the hydraulic actuator is bypassed to eliminate interference. During automatic control, the throttle handles are moved by the actuator as programmed by the computer. If the pilot overrides the automatic function, the actuator will automatically bypass to allow manual operation.

A hydraulic actuator is used which permits easy force limiting, velocity limiting, and bypassing. Dual and independent sensors are used to detect any failed condition which causes a difference in the two signals. Independent electronic controls will then automatically bypass the actuator and alert the pilot of the fail condition.

FLAP CONTROLS

The lower flaps are powered by either of two independent hydraulic motors operating from separate hydraulic systems. The upper flaps are powered by a single hydraulic motor. The requirements are:

- No single failure can prevent operation of the lower flaps.
- The upper and lower flaps will lock in position should the driving hydraulic motor fail or electronic control be lost. The pilot may elect to close upper and/or lower flaps after any failure.
- Upper and lower flaps may be operated as speed brakes simultaneously by an independent control.

The tradeoff for the lower flap control system was between two active systems, or one active and one passive system. The latter system was selected and is shown in Figure 120, with the upper flap control system. This selection deletes the requirement for a force equalization system between the two drive systems. System 2 operates as a monitor, automatically assuming control should System 1 fail. If an electronic or electrical system failure of either 1 or 2 occurs, both will be deactivated and lower flaps will be locked in that position. Systems 1 or 2 (whichever is good) may then be operated manually by pilot to position the lower flaps.

Operation of the speed brakes, as shown in Figure 120, is performed by directing the same input to both upper and lower flap controls, which causes equal displacement of both in opposite directions. This signal will be in the form of a ramp voltage of the desired rate.

REFERENCES

1. Tanner, Watson H. "Charts for Estimating Rotary Wing Performance in Hover and at High Forward Speeds", NASA CR114, November 1964.
2. Fenaughty, R. and Beno, E., "NH-3A Vibratory Airloads and Vibratory Rotor Loads, Volume I", Sikorsky Aircraft Division of United Aircraft Corporation, Report SER 611493, January 1970.
3. White, J. A., "Fractional-Scale Model Investigation and Full-Scale Flight Tests of Fuselage Nodalization Concepts", Bell Helicopter Co. Report 220-909-001, April 1972.
4. Shipman, D.P., White, J. A., and Cronkhite, J. D., "Fuselage Nodalization", paper 612 presented at the 28th Annual National Forum of the American Helicopter Society, May 1972.

APPENDIX A
SYMBOLS
AND
WEIGHT ESTIMATION PROCEDURES

LIST OF SYMBOLS

a	aircraft acceleration along flight path, ft/sec ²
b	number of blades
D	total vehicle drag, lb
f	frequency, Hz
FH/T	rotor hub force per unit thrust
h	altitude gain, ft
$K\theta$	nodal beam torsional spring rate, in-lb/rad
L_R	rotor lift, lb
L_W	wing lift, lb
m	aircraft mass, slugs
M_T	rotor tip Mach number; nodal beam tip weight, lb
$(PF)_R$	rotor propulsive force, lb
R	rotor radius, ft
R/C	aircraft rate of climb, ft/sec
S_X	distance traveled along flight path, ft
t	time, sec
T	thrust (rotor or auxiliary engines), lb
V	aircraft velocity, ft/sec or knots
V_0	aircraft velocity before acceleration phase of mission, ft/sec
X, Y	directions parallel and perpendicular to aircraft flight path
α	angle of attack
α_c	rotor control plane angle-of-attack, deg
γ	aircraft climb angle with respect to horizon, deg
Ω	rotor rotational speed, rad/sec

WEIGHT ESTIMATION METHODS

Component weights were derived from existing components and systems, where possible. New components were either estimated from conceptual predesign layouts or determined analytically. Weights derived analytically were verified by use of statistical methods and/or comparison of unit weights of functionally similar designs.

- Rotor Group: The four-bladed gimbaled rotor of the Model 646A is a close derivative of the BHC Model 240 (twist was decreased to 0.0 degrees and radius increased 0.5 foot). The two-bladed hingeless rotor of the 646B is the BHC Model 645 rotor with twist decreased to 2.5 degrees and 1.0 foot added to the radius. Close estimation was possible for this group.
- Wing Group: Wing weight was estimated using the following equation:

$$\text{Wing Weight} = 52 \left[\frac{\text{Wing Area}}{100} \right]^{.68} (\text{Load Factor})^{.32} \left[\frac{\text{Gross Weight}}{1000} \right]^{.64}$$

This equation does not include an allowance for high-lift devices, fuel cells, or exterior finish. These were estimated separately as was the wing-tilt mechanism.

- Tail Group: Tail rotor hub, shaft, and blade weights for the 646A and 646B were taken from the BHC Model 240 and 309 tail rotors, to which they are identical. Ventral fin weights were estimated from a comparison with the BHC Model 309. Dorsal fin weights were estimated from the equation:

$$\text{Weight} = 1.04 (\text{Area}) \left[\frac{\text{Gross Weight}}{1000} \right]^{.41}$$

Horizontal surface weight was estimated from the equation:

$$\text{Weight} = 1.22 (\text{Area}) \left[\frac{\text{Gross Weight}}{1000} \right]^{.18}$$

- Body Group: Model 646A body group weights were based on ratios of actual body weight to design gross weights for Bell AH-1G and AH-1J helicopters. For the 646A a value of 10.8 percent was used. Although the 646A has greater fuselage width than the AH-1, the differences are not large when resulting gains in lateral and torsional stiffness are considered.

Model 646B body group weights were estimated from known BHC Model 309 values, with allowances made for a one-foot tail boom extension and structural buildup necessary to allow 4.0 g's and 18,500-pound gross weight.

- Landing Gear: The main landing gear was estimated as 3.5 percent of DGW, as is common for vehicles which land at relatively high speeds and sink rates. The tail gear was estimated from layout drawings.
- Flight Controls: The flight control systems in the 646A and 646B are the same design, differing only in physical size. They are both similar to the control system in the BHC Model 309, which served as a baseline for weight estimations based on gross weight ratios. The controls which are not common with the 309 (rudder, wing, rotor phase-out, and pylon-tilt controls) were estimated from layout drawings.
- Engine Section: Mount weights for the T53 and T55 engines were taken from previous BHC installations of these engines. Firewall and cowl weights (646B) were referenced to the twin-engined installation in the BHC Model 309. For the 646A, cowl weights were calculated based on the equation:

$$\text{Weight} = .86 (\text{Surface Area}) A_v$$

where A_v is a velocity factor of 0.5 for 360 KTAS.

Engine section weights (including pylons) for the JT12A-8 engines were based on the NAR Actual Weight Report (NA-63-1347) for the T-39 aircraft. Engine section weights for the F102-LD-100 engines are based on a ratio of the size of that engine to the JT12A-8.

- Propulsion Group: All engine weights are actual weights. The air induction system for the T55 and T53 rotor engines, including bellmouth assembly and screens (but no particle separator) was estimated from previous BHC installations of these engines. The air induction system for the JT12A-8 engine was taken directly from the T-39A installation. The air induction system for the F102-LD-100 is based on a ratio of the size of that engine to the JT12A-8.
- Drive Trains: Main rotor transmission weights were available from the manufacturers. The tail rotor drive train of the 646B is existing, and that of the 646A was estimated as a part of the BHC UTTAS effort. Weights of other gear boxes, shafts, and couplings were estimated from layout drawings.
- Electrical System: Weights were based on the Model 309 KingCobra, with an added AC generator.
- Avionics: Actual weights were used.

- Air-Conditioning: Weight was based on the T55-powered Model 309, with an allowance for larger cockpit volumes (646A). This weight includes the air-conditioning unit, jet-pump rain removal system, and canopy defroster.
- Special Provisions: The crew escape system weight was based on system weights provided by Stanley Aviation, Inc. The vibration isolation system, wing-high lift devices, wing-tilt device, and flexural balance weights were estimated from layout drawings.

APPENDIX B

FIGURES

LIST OF FIGURES

<u>Figure</u>	<u>Title</u>	<u>Page</u>
1	Three-View and Inboard Profile, 646A	1
2	Three-View and Inboard Profile, 646B	2
3	Download Factor Versus Radius	3
4	Percent Download Versus Rotor Radius	4
5	T53-L-13 Engine Performance, Sea Level, Standard Day	5
6	T53-L-13 Engine Performance, 9500 Feet, Standard Day	6
7	JT12A-8 Engine Performance, Sea Level, Standard Day	7
8	JT12A-8 Engine Performance, 9500 Feet, Standard Day	8
9	T55-L-7C Engine Performance, Sea Level, Standard Day	9
10	T55-L-7C Engine Performance, 9500 Feet, Standard Day	10
11	F102-LD-100 Engine Performance, Sea Level, Standard Day	11
12	F102-LD-100 Engine Performance, 9500 Feet, Standard Day	12
13	High-Speed Mission Performance, Sea Level, Standard Day	13
14	High-Speed Mission Performance, 9500 Feet, Standard Day	14
15	Hover Mission Performance	15
16	Hover Versatility, Largest Rotor, Compound Configuration	16
17	Hover Versatility, Smallest Rotor, Compound Configuration	17
18	Hover Versatility, Largest Rotor, Variable Configuration	18
19	Hover Versatility, Smallest Rotor, Variable Configuration	19
20	Level Flight Power Required, Variable Configuration	20
21	Procedure Used to Determine Maximum Rotor Size	21
22	Rotor Test Versatility, 100 Knots	22
23	Rotor Test Versatility, 200 Knots	23
24	Model 646B, Maximum Size Rotors, Rotor Lift at Upper Stall Limit	24
25	C_Q/σ at Upper Stall Limit, Smallest and Largest Rotors	24
26	High-Speed Mission Versatility, Sea Level, Standard Day	25
27	High-Speed Mission Versatility, 9500 Feet, Standard Day	26
28	Model 646A Longitudinal Mode Root Locus, Compound Configuration	27
29	Model 646B Longitudinal Mode Root Locus, Compound Configuration	28

LIST OF FIGURES (Continued)

<u>Figure</u>	<u>Title</u>	<u>Page</u>
30	Model 646A Longitudinal Mode Root Locus, Helicopter Configuration	29
31	Model 646B Longitudinal Mode Root Locus, Helicopter Configuration	30
32	Model 646A Fore and Aft Cyclic Stick Position Variation with Stabilizer Incidence	31
33	Model 646B Fore and Aft Cyclic Stick Position Variation with Stabilizer Incidence	32
34	Model 646A Stabilizer Incidence Limits, Compound Configuration, 40 KTAS	33
35	Model 646A Stabilizer Incidence Limits, Compound Configuration, 100 KTAS	34
36	Model 646A Stabilizer Incidence Limits, Compound Configuration, 200 KTAS	35
37	Model 646A Stabilizer Incidence Limits, Compound Configuration, 300 KTAS	36
38	Model 646B Stabilizer Incidence Limits, Compound Configuration, 40 KTAS	37
39	Model 646B Stabilizer Incidence Limits, Compound Configuration, 100 KTAS	38
40	Model 646B Stabilizer Incidence, Compound Configuration, 200 KTAS	39
41	Model 646B Stabilizer Incidence Limits, Compound Configuration, 300 KTAS	40
42	Model 646A Compound Configuration Stabilizer Incidence Limits Versus Airspeed	41
43	Model 646B Compound Configuration Stabilizer Incidence Limits Versus Airspeed	42
44	Model 646A Stabilizer Incidence Limits, Helicopter Configuration, Hover	43
45	Model 646A Stabilizer Incidence Limits, Helicopter Configuration, 40 KTAS	44
46	Model 646A Stabilizer Incidence Limits, Helicopter Configuration, 100 KTAS	45
47	Model 646A Stabilizer Incidence Limits, Helicopter Configuration, 150 KTAS	46
48	Model 646B Stabilizer Incidence Limits, Helicopter Configuration, Hover	47

LIST OF FIGURES (Continued)

<u>Figure</u>	<u>Title</u>	<u>Page</u>
49	Model 646B Stabilizer Incidence Limits, Helicopter Configuration, 40 KTAS	48
50	Model 646B Stabilizer Incidence Limits, Helicopter Configuration, 100 KTAS	49
51	Model 646B Stabilizer Incidence Limit, Helicopter Configuration, 130 KTAS	50
52	Model 646A Fore and Aft Cyclic Position Variation with Stabilizer Incidence, Helicopter Configuration	51
53	Model 646B Fore and Aft Cyclic Position Variation with Stabilizer Incidence, Helicopter Configuration	52
54	Model 646A Response to Step Control Inputs, Compound Configuration, Hover, SCAS Operative	53
55	Model 646B Response to Step Control Inputs, Compound Configuration, Hover, SCAS Operative	54
56	Control Power and Damping in Hover for the Model 646A, Compound Configuration (SCAS Off and On)	55
57	Control Power and Damping in Hover for the Model 646B, Compound Configuration (SCAS Off and On)	56
58	Model 646A Response to Step Control Inputs, Compound Configuration, 300 KTAS, SCAS Operative	57
59	Model 646B Response to Step Control Inputs, Compound Configuration, 300 KTAS, SCAS Operative	58
60	Wing Incidence for Autorotation at Minimum Rate of Descent	59
61	Model 646A Trim Change with Auxiliary Jet Thrust, Compound Configuration	60
62	Model 646B Trim Change with Auxiliary Jet Thrust, Compound Configuration	61
63	RSRA 646B Fuselage Analytical Model	62
64	Vertical Response to Vertical Force Excitation of 646B Without Vertical Isolation	63
65	Vertical Response to Lateral Force Excitation of 646B Without Roll Isolation	64
66	Vertical Response to Fore and Aft Force Excitation of 646B Without Pitch Isolation	65
67	Vertical Response to Pitching Moment Excitation of 646B Without Pitch Isolation	66
68	Fuselage Vertail Natural Frequencies as a Function of Tail Boom Junction Moment Restraint Stiffness	67
69	Rotor Size and Rotational Speed Design Envelope	68

LIST OF FIGURES (Continued)

<u>Figure</u>	<u>Title</u>	<u>Page</u>
70	Rotor Operational Envelope	69
71	Frequency of Predominant Harmonic as a Function of Rotor Diameter and Number of Blades	70
72	Oscillatory Vertical Rotor Force Versus Number of Blades	71
73	Rotor Hub Oscillatory Forces Normalized on Five-Bladed Rotor Versus Airspeed	72
74	Rotor Lift Versus Airspeed	73
75	Rotor Drag Versus Airspeed	74
76	Isolation System Study Flow Diagram	75
77(a)	Pilot's Station Vertical Response (g/1000-Pound Rotor Lift) to Vertical Excitation for Two-Bladed Rotor	76
77(b)	Pilot's Station Vertical Response (g/1000-Pound Rotor Lift) to Vertical Excitation for Three-Bladed Rotor	76
77(c)	Pilot's Station Vertical Response (g/1000-Pound Rotor Lift) to Vertical Excitation for Four-Bladed Rotor	77
77(d)	Pilot's Station Vertical Response (g/1000-Pound Rotor Lift) to Vertical Excitation for Five-Bladed Rotor	77
77(e)	Pilot's Station Vertical Response (g/1000-Pound Rotor Lift) to Vertical Excitation for Six-Bladed Rotor	78
78(a)	Pilot's Station Lateral Response (g/1000-Pound Rotor Lift) to Lateral Excitation for Two-Bladed Rotor	79
78(b)	Pilot's Station Lateral Response (g/1000-Pound Rotor Lift) to Lateral Excitation for Three-Bladed Rotor	79
78(c)	Pilot's Station Lateral Response (g/1000-Pound Rotor Lift) to Lateral Excitation for Four-Bladed Rotor	80
78(d)	Pilot's Station Lateral Response (g/1000-Pound Rotor Lift) to Lateral Excitation for Five-Bladed Rotor	80
78(e)	Pilot's Station Lateral Response (g/1000-Pound Rotor Lift) to Lateral Excitation for Six-Bladed Rotor	81
79(a)	Pilot's Station Vertical Response (g/1000-Pound Rotor Lift) to Fore and Aft Excitation for Two-Bladed Rotor	82
79(b)	Pilot's Station Vertical Response (g/1000-Pound Rotor Lift) to Fore and Aft Excitation for Three-Bladed Rotor	82
79(c)	Pilot's Station Vertical Response (g/1000-Pound Rotor Lift) to Fore and Aft Excitation for Four-Bladed Rotor	83

LIST OF FIGURES (Continued)

<u>Figure</u>	<u>Title</u>	<u>Page</u>
79(d)	Pilot's Station Vertical Response (g/1000-Pound Rotor Lift) to Fore and Aft Excitation for Five-Bladed Rotor	83
79(e)	Pilot's Station Vertical Response (g/1000-Pound Rotor Lift) to Fore and Aft Excitation for Six-Bladed Rotor	84
80	Methods of Isolation	85
81	Loci of Minimum Fuselage Response to Hub Force Excitation	86
82	Loci of Minimum Fuselage Response to Hub Moment Excitation	87
83	Typical Fuselage Angular Response for Focal Pylon Isolation of Two-Per-Rev, Upper Focal Region, Force Excitation	88
84	Typical Fuselage Angular Response for Focal Pylon Isolation of Two-Per-Rev, Lower Focal Region, Force Excitation	89
85	Typical Fuselage Angular Response for Focal Pylon Isolation of Six-Per-Rev, Upper Focal Region, Force Excitation	90
86	Typical Fuselage Angular Response for Focal Pylon Isolation of Six-Per-Rev, Upper Focal Region, Moment Excitation	91
87	Two-Dimensional Analytical Model of Nodal Beam and Pylon Assembly	92
88	Three-Dimensional Analytical Model of Nodal Beam and Pylon Assembly	93
89	Displacement and Bending Moment Distribution for $n_z = 1.0$ g with 15,000 Pounds Lift	94
90	Natural Mode and Forced Response of Pylon and Nodal Beam Assembly with $M_{TIP} = 50$ Pounds, $K_\theta = 10,000$ In.-Lb/Rad	95
91	Natural Mode and Forced Response of Pylon and Nodal Beam Assembly with $M_{TIP} = 50$ Pounds, $K_\theta = 50,000$ In.-Lb/Rad	96
92	Natural Mode and Forced Response of Pylon and Nodal Beam Assembly with $M_{TIP} = 50$ Pounds, $K_\theta = 100,000$ In.-Lb/Rad	97
93	Natural Mode and Forced Response of Pylon and Nodal Beam Assembly with $M_{TIP} = 50$ Pounds, $K_\theta = 150,000$ In.-Lb/Rad	98
94	Natural Mode and Forced Response of Pylon and Nodal Beam Assembly with $M_{TIP} = 50$ Pounds, $K_\theta = 200,000$ In.-Lb/Rad	99
95	RSRA Nodal Beam Natural Frequency with Variations of M_{TIP} and K_θ	100

LIST OF FIGURES (Continued)

<u>Figure</u>	<u>Title</u>	<u>Page</u>
96	Model 309 Frequency Response to a 1000-Pound Vertical Hub Shear	101
97	Nodal Point Location as a Function of Frequency and K_θ for RSRA Nodal Beam with $M_{TIP} = 25$ Pounds	102
98	Nodal Point Location as a Function of Frequency and K_θ for RSRA Nodal Beam with $M_{TIP} = 50$ Pounds	103
99	Nodal Point Location as a Function of Frequency and K_θ for RSRA Nodal Beam with $M_{TIP} = 100$ Pounds	104
100	Nodal Point Location as a Function of Frequency and K_θ for RSRA Nodal Beam with $M_{TIP} = 150$ Pounds	105
101	Nodal Point Location as a Function of Frequency and K_θ for RSRA Nodal Beam with $M_{TIP} = 200$ Pounds	106
102	Low RPM Two-Per-Rev Vertical Isolation with Nodal Beam	107
103	High RPM Two-Per-Rev Vertical Isolation with Nodal Beam	108
104	Low RPM Six-Per-Rev Vertical Isolation with Nodal Beam	109
105	High RPM Six-Per-Rev Vertical Isolation with Nodal Beam	110
106	RSRA Nodal Beam Vertical Isolation System	111
107	Servo-Null Vertical Isolation System	112
108	Operational Envelope Considered and Regimes of Blade Load Amplification - 646A	113
109	Operational Envelope Considered and Regimes of Blade Load Amplification - 646B	114
110	646A Rotor Coupled Natural Frequencies Collective Mode	115
111	646A Rotor Coupled Natural Frequencies Cyclic Mode	116
112	646A Rotor Coupled Natural Frequencies Rigid Mode	117
113	646B Rotor Coupled Natural Frequencies Collective Mode	118
114	646B Rotor Coupled Natural Frequencies Cyclic Mode	119
115	Rotor Noise Generation	120
116	Control System Concept No. I	121
117	Control System Concept No. II	122
118	Control System Concept No. III	123
119	Throttle Control	124
120	Flap Controls	125

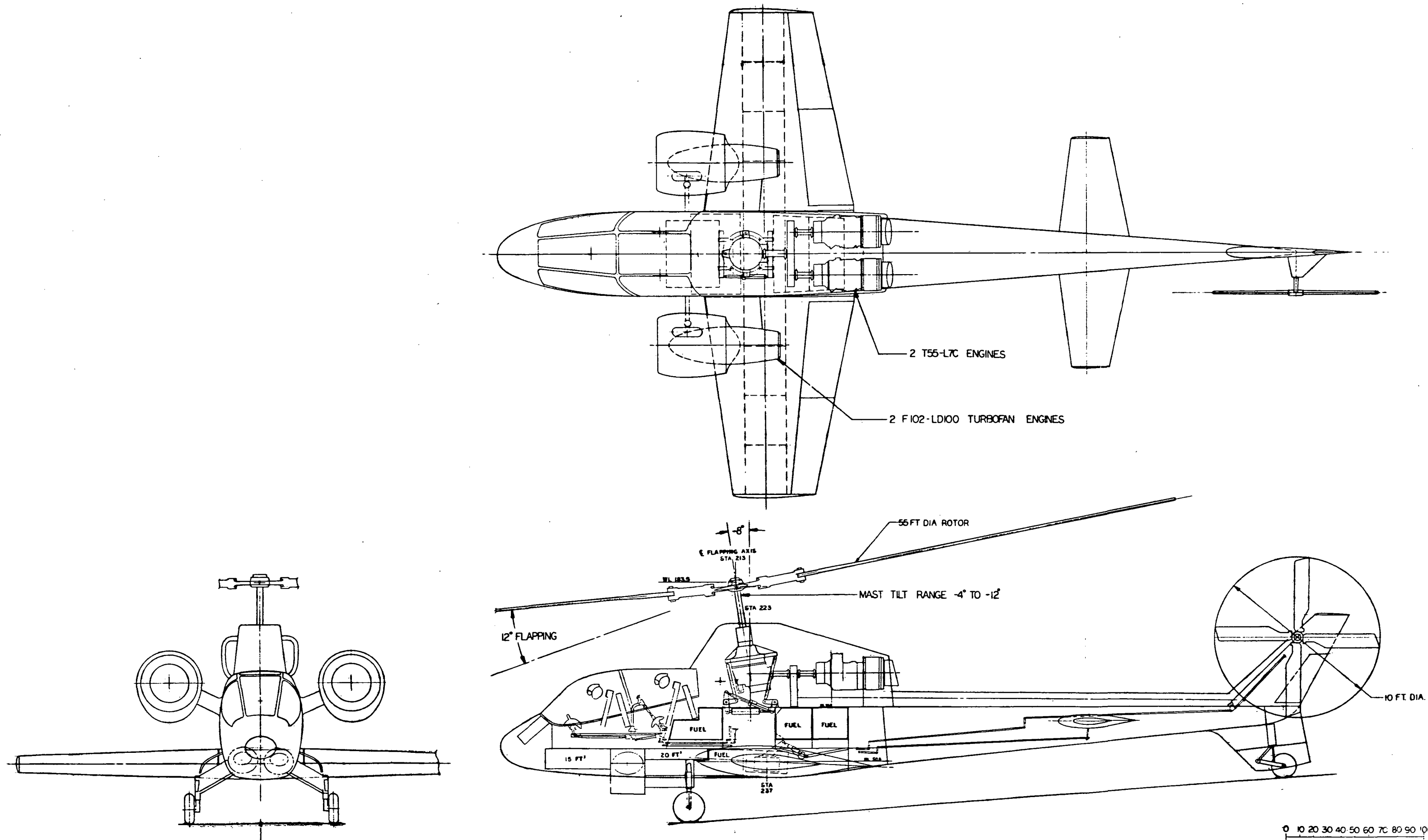


Figure 1. Three-View and Inboard Profile, 646A.

DESIGN PROPOSAL	
INBOARD PROFILE R S R A	
DESIGNED BY R. REBER	DATE 12-72
DRAWING NO. 646-900-001	

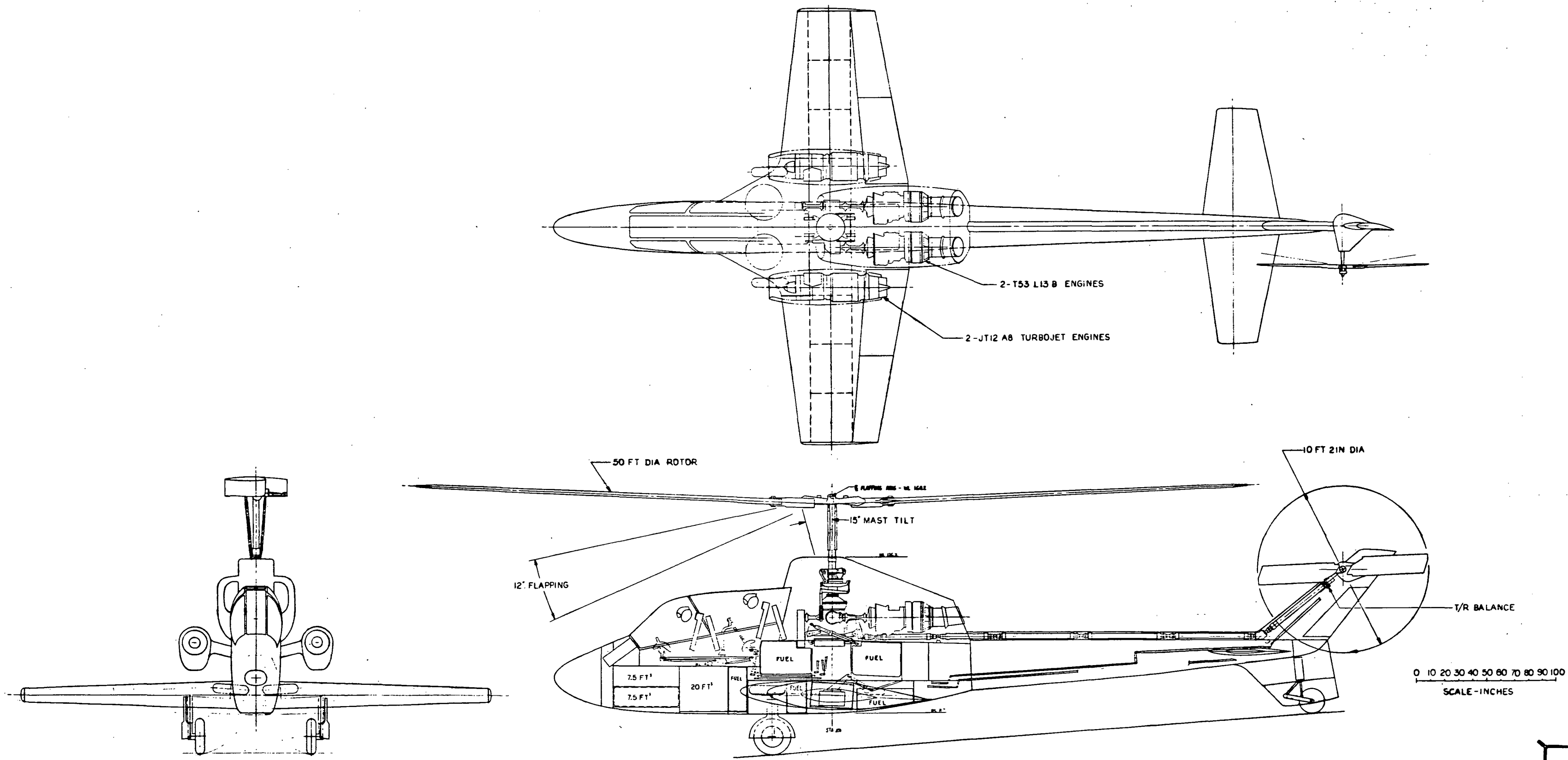


Figure 2. Three-View and Inboard Profile, 646B.

bh		DESIGN PROPOSAL	
TITLE RTV-INBOARD PROFILE			
DESIGNED BY R. Reiter	DATE 3/22/64	SCALE 3/4" = 1'-0"	NO. 1/0
APPROVED BY		646-960-001	
		646-099-001	

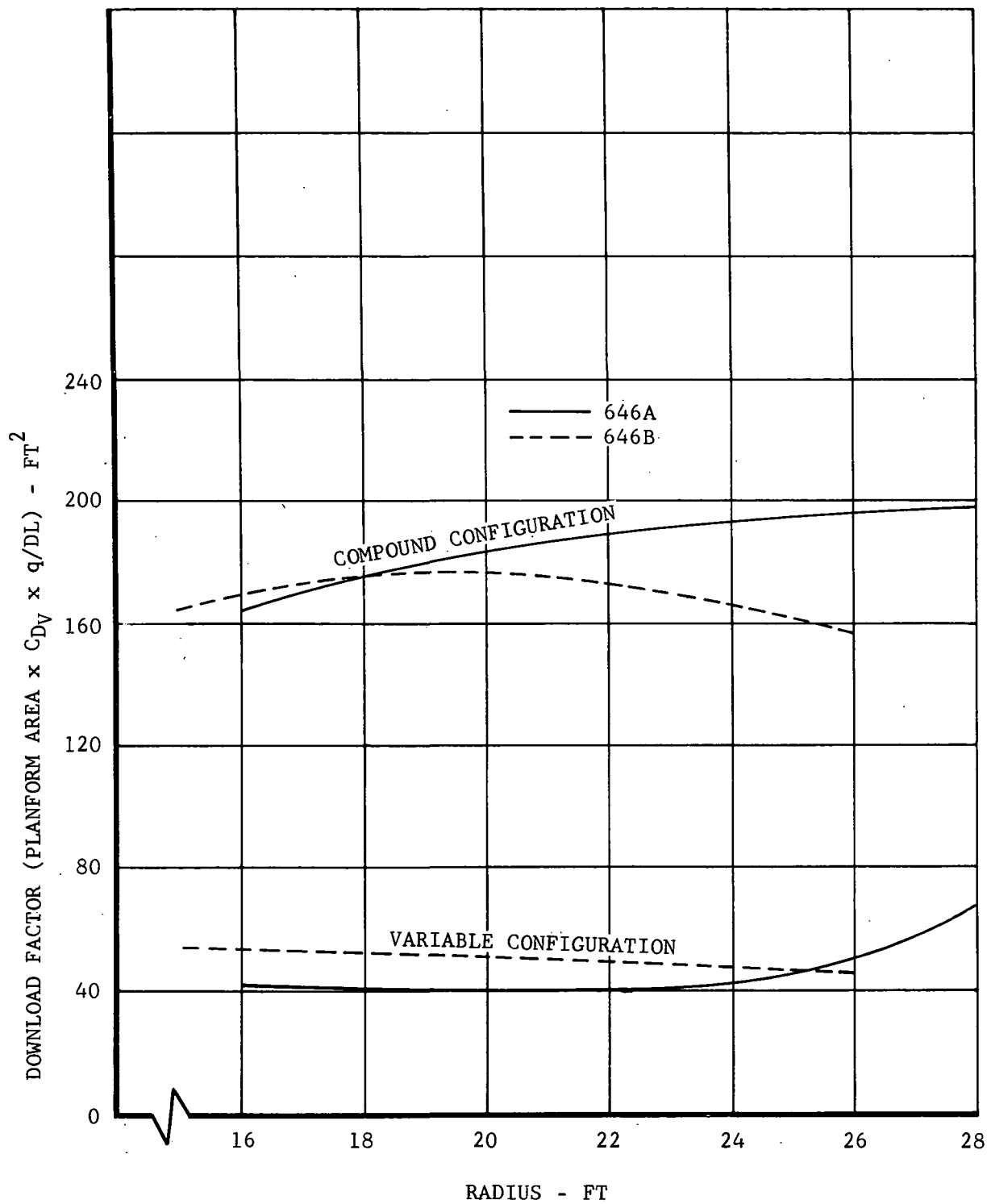


Figure 3. Download Factor Versus Radius.

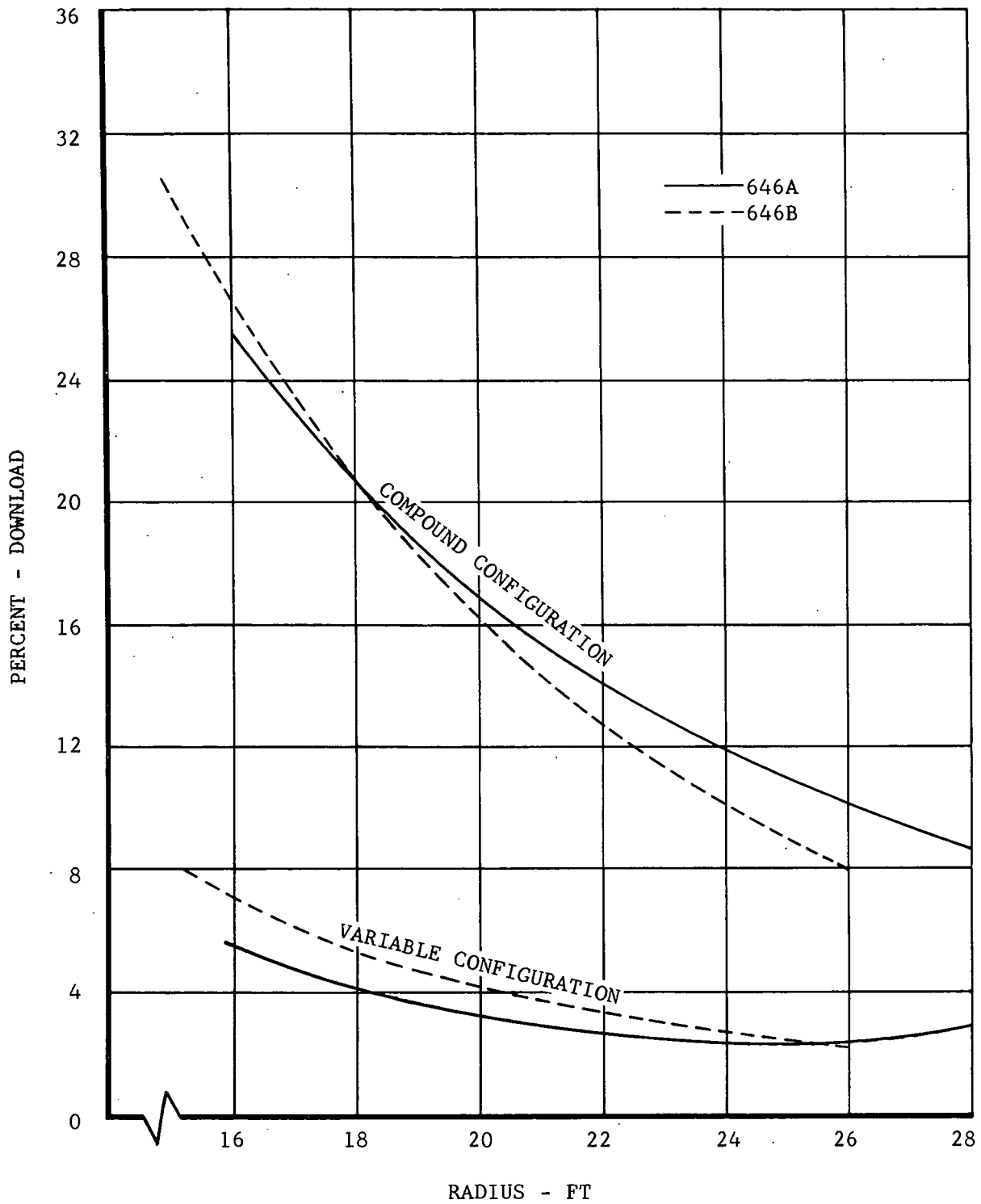


Figure 4. Percent Download Versus Rotor Radius.

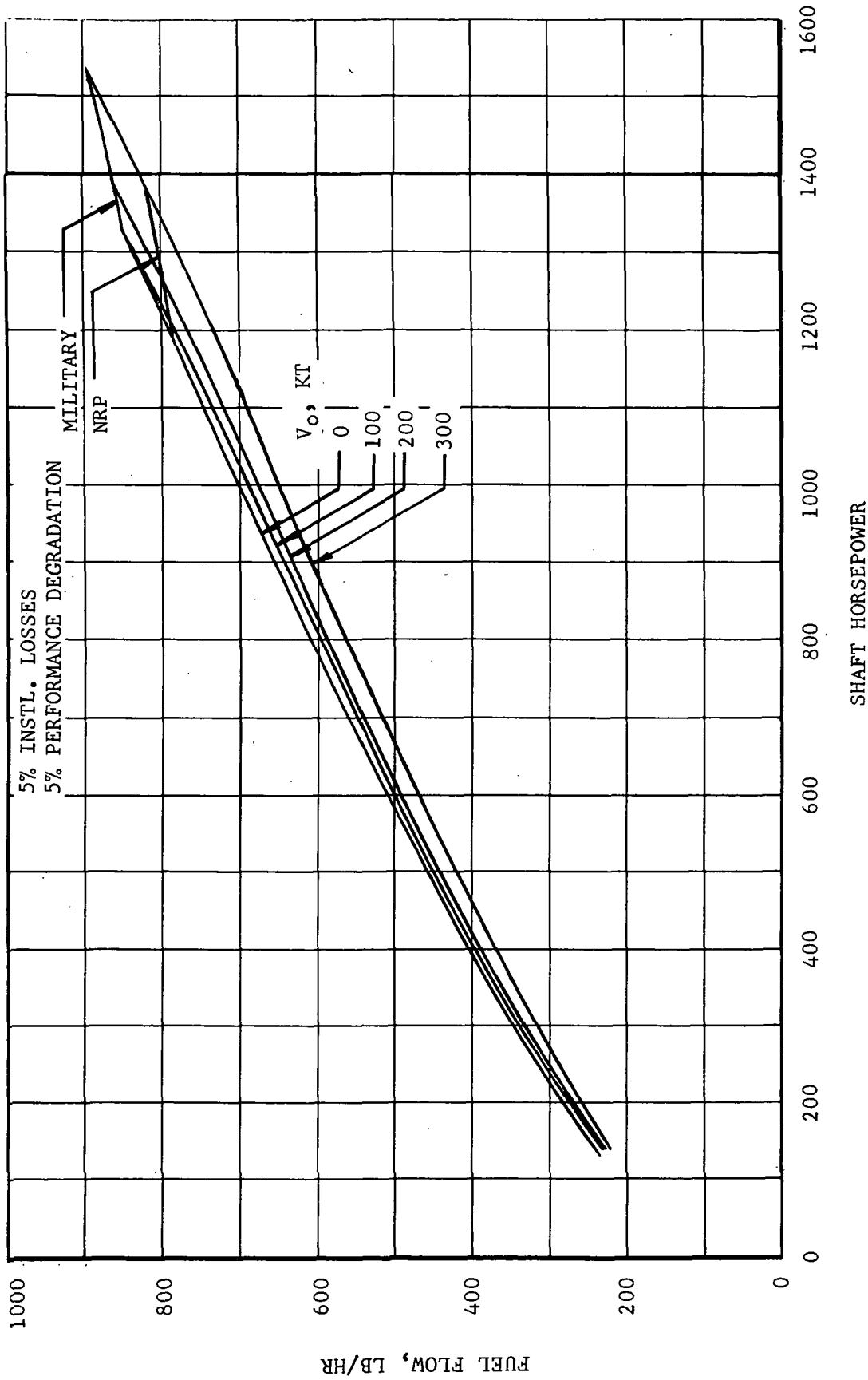


Figure 5. T53-L-13 Engine Performance, Sea Level, Standard Day.

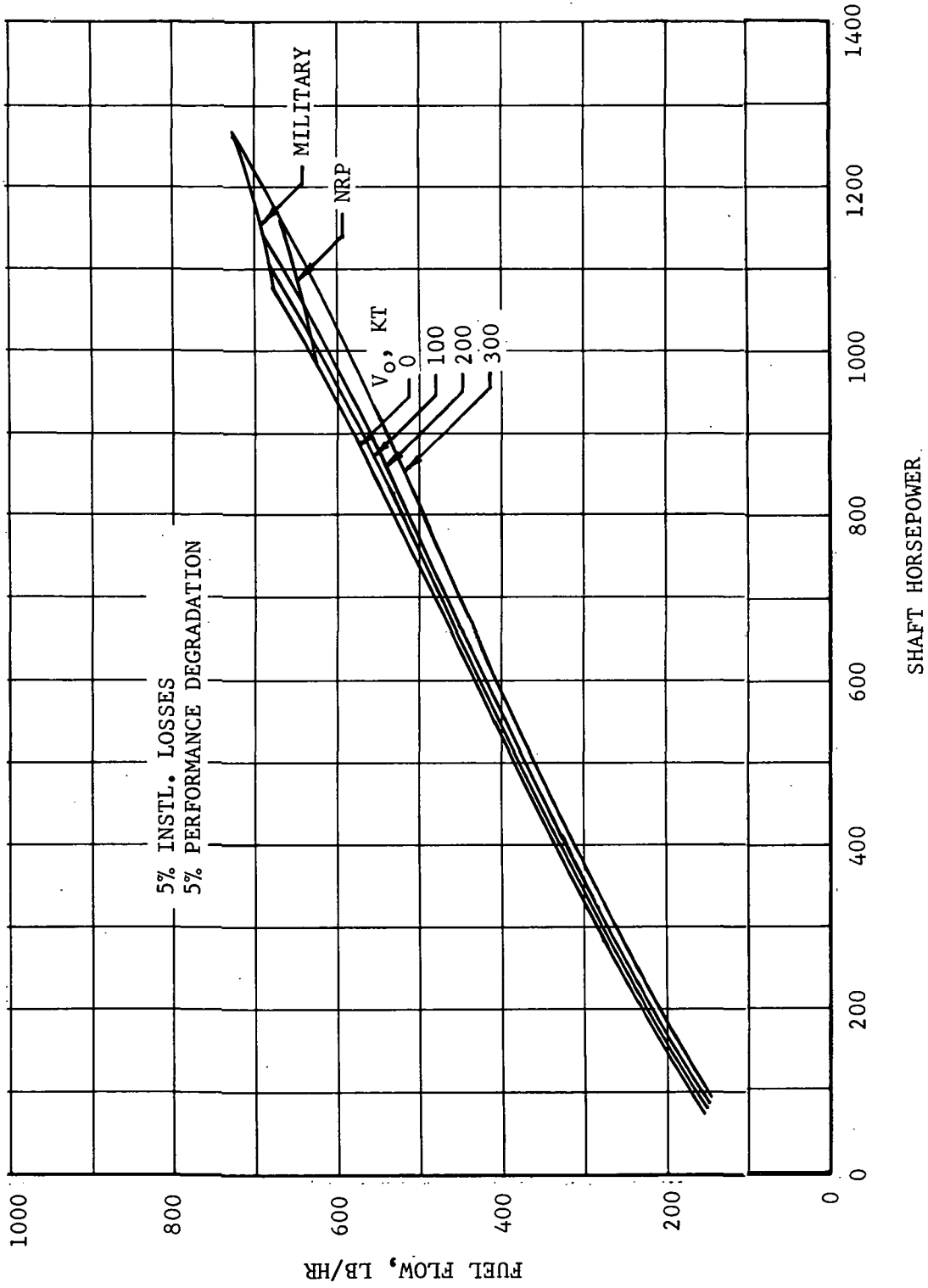


Figure 6. T53-L-13 Engine Performance, 9500 Feet, Standard Day.

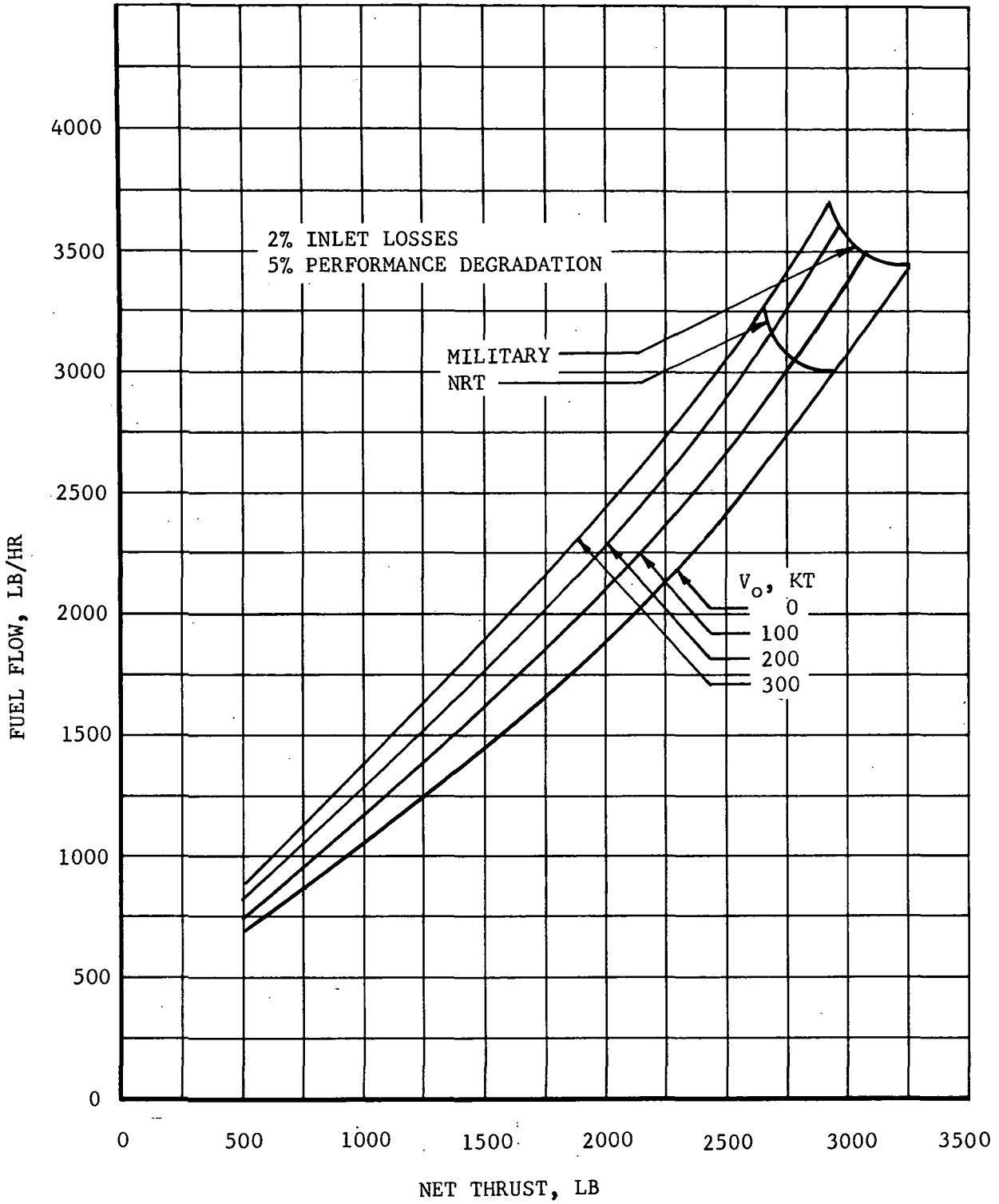


Figure 7. JT12A-8 Engine Performance, Sea Level, Standard Day.

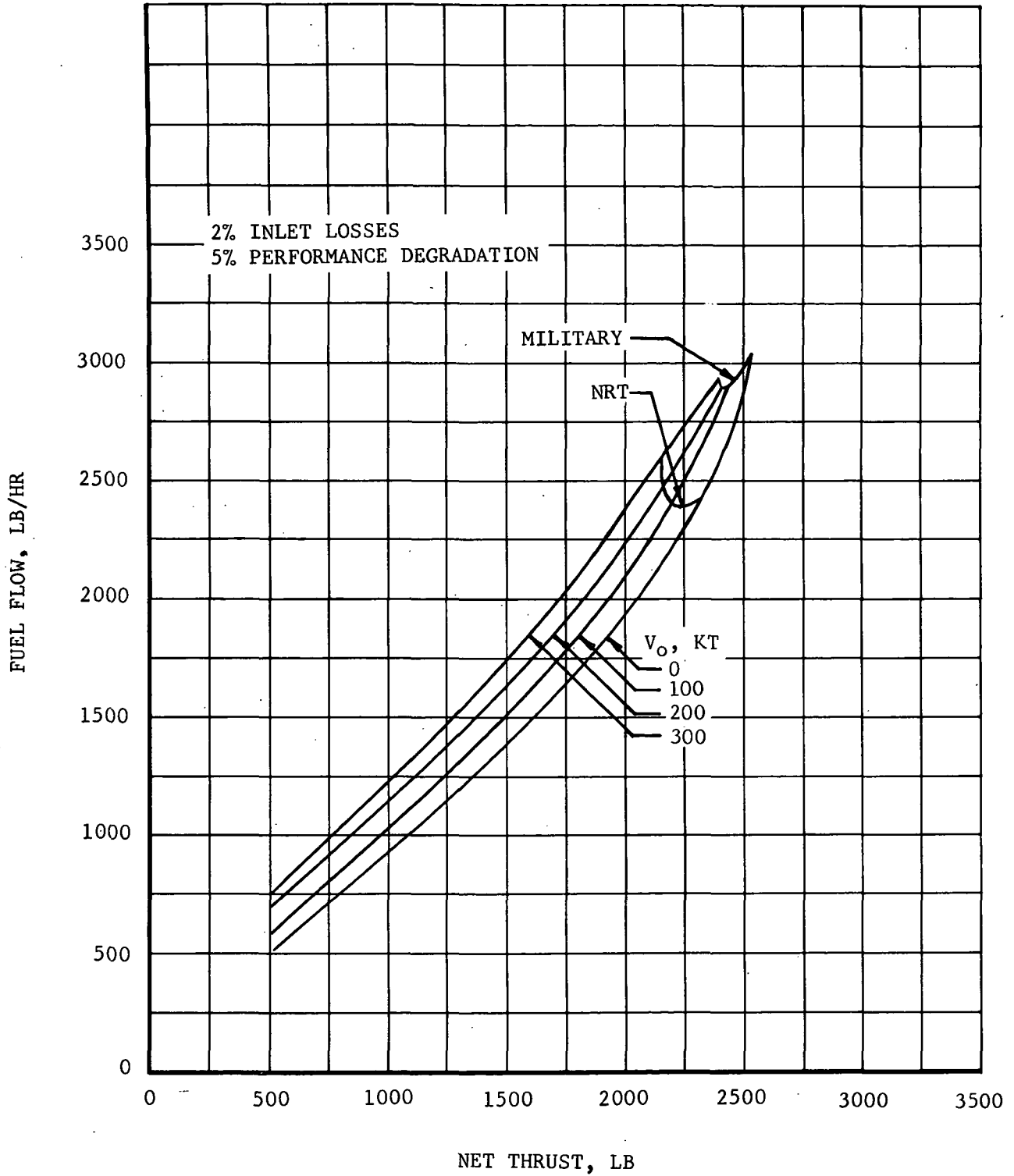


Figure 8. JT12A-8 Engine Performance, 9500 Feet, Standard Day.

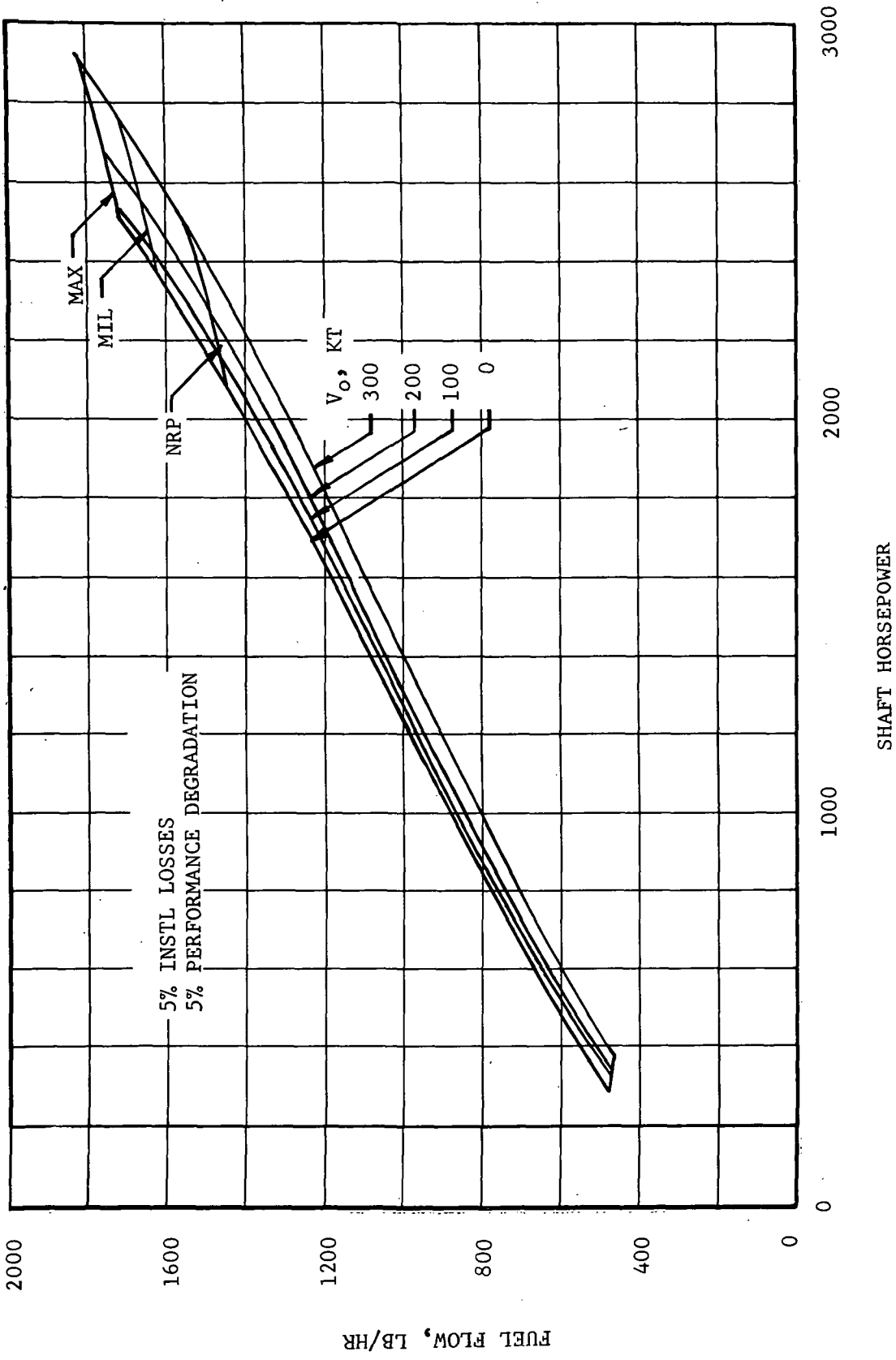


Figure 9. T55-L-7C Engine Performance, Sea Level, Standard Day.

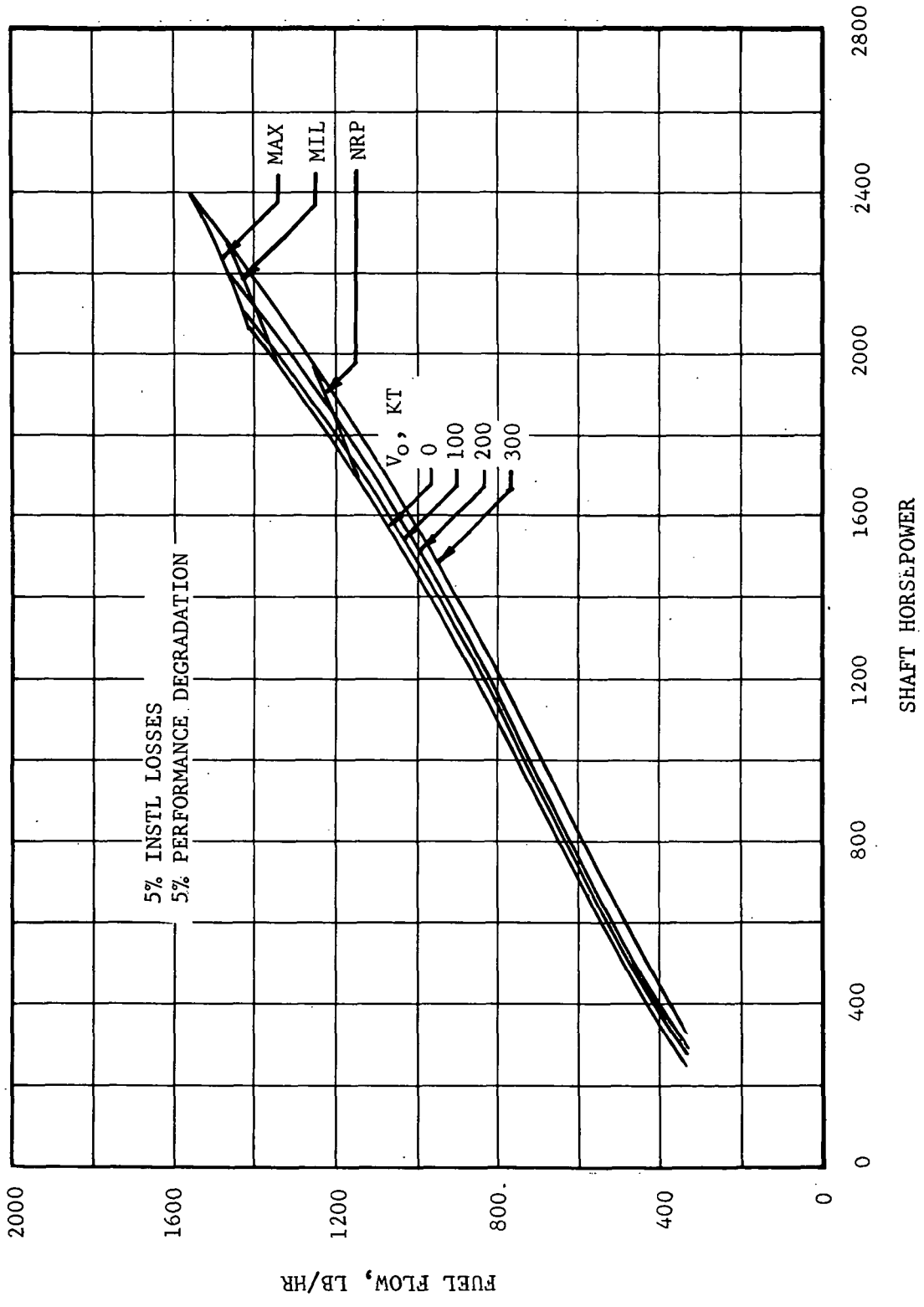


Figure 10. T55-L-7C Engine Performance, 9500 Feet, Standard Day.

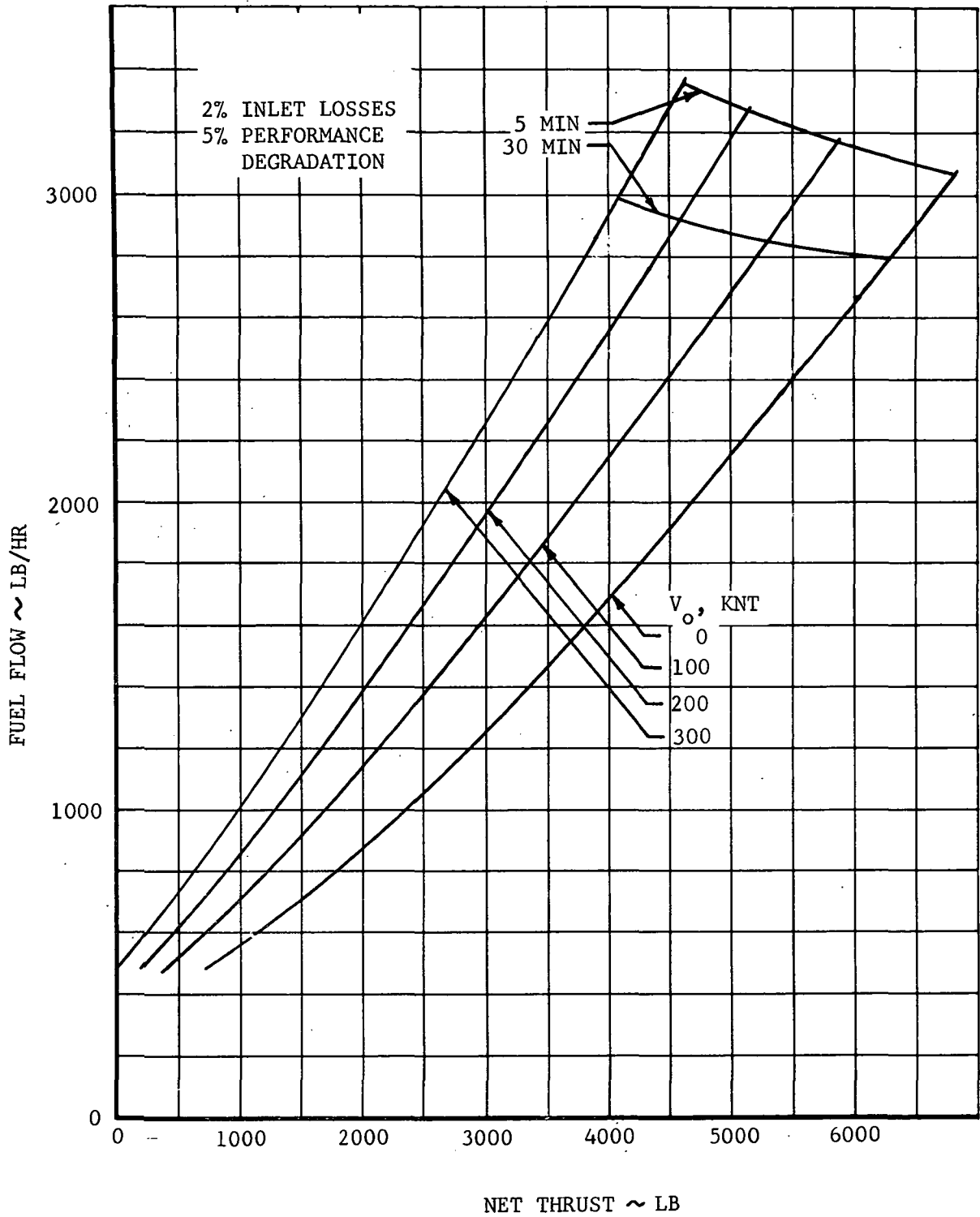


Figure 11. F102-LD-100 Engine Performance, Sea Level, Standard Day.

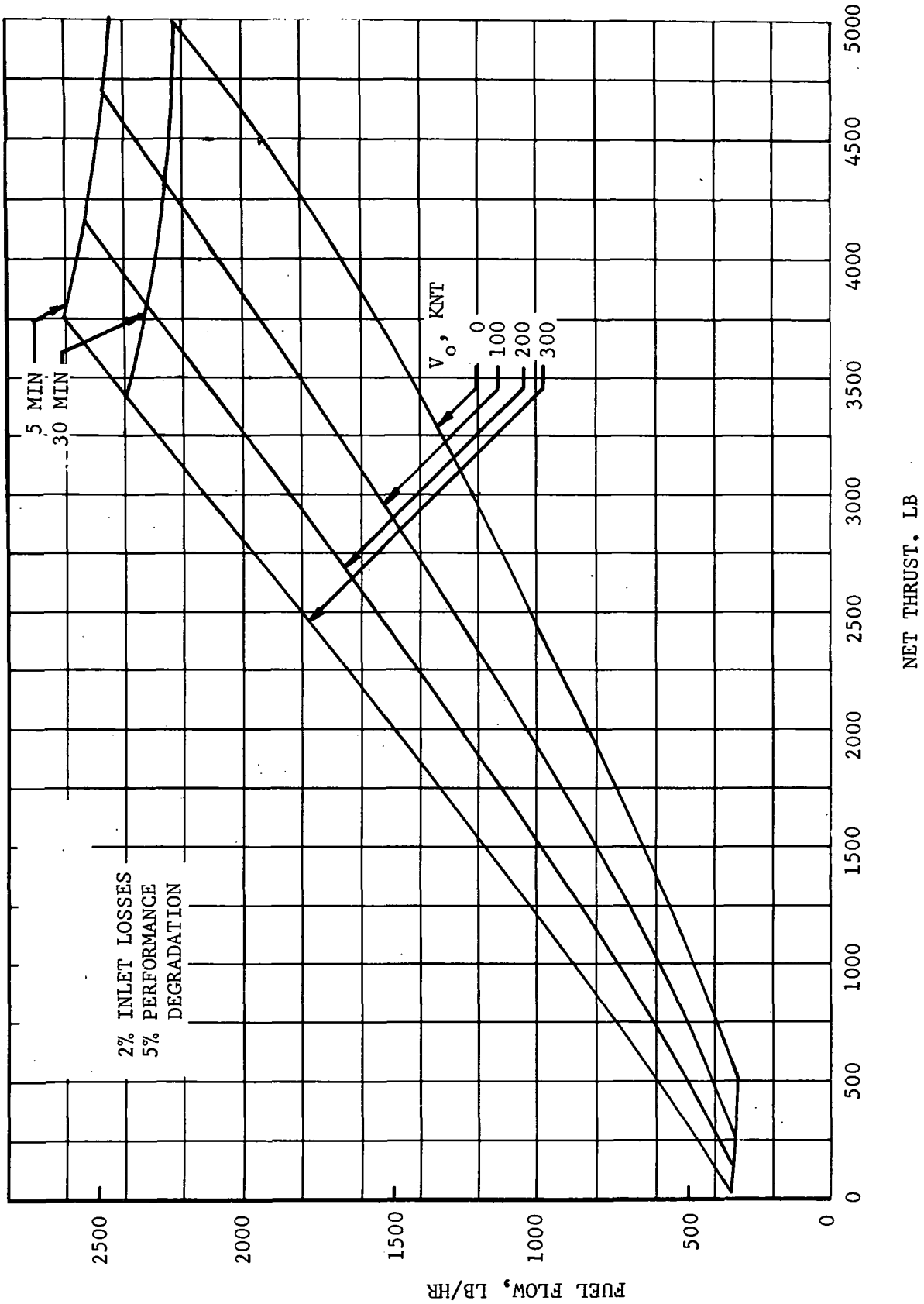


Figure 12. F102-LD-100 Engine Performance, 9500 Feet, Standard Day.

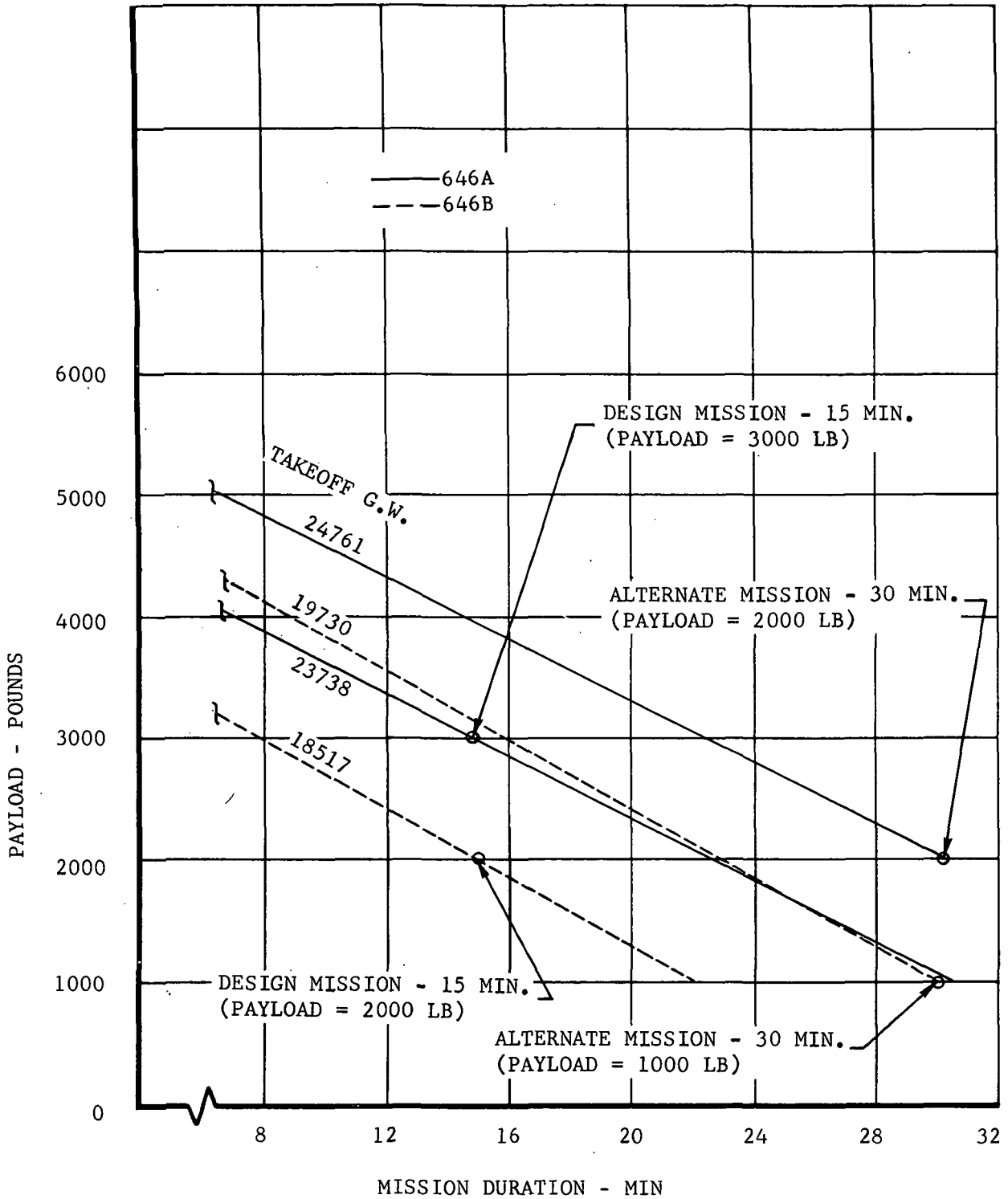


Figure 13. High-Speed Mission Performance, Sea Level, Standard Day.

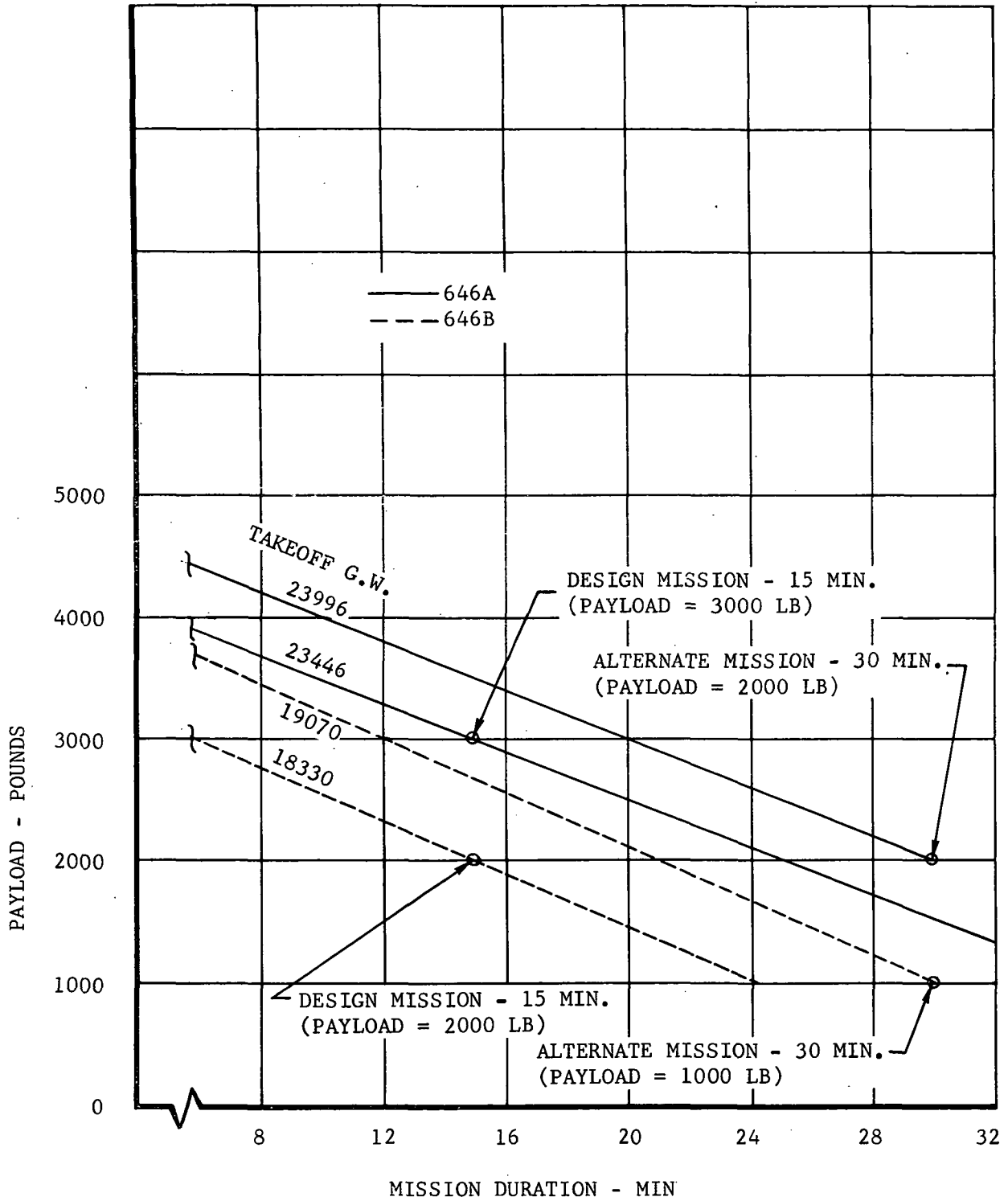


Figure 14. High-Speed Mission Performance, 9500 Feet, Standard Day.

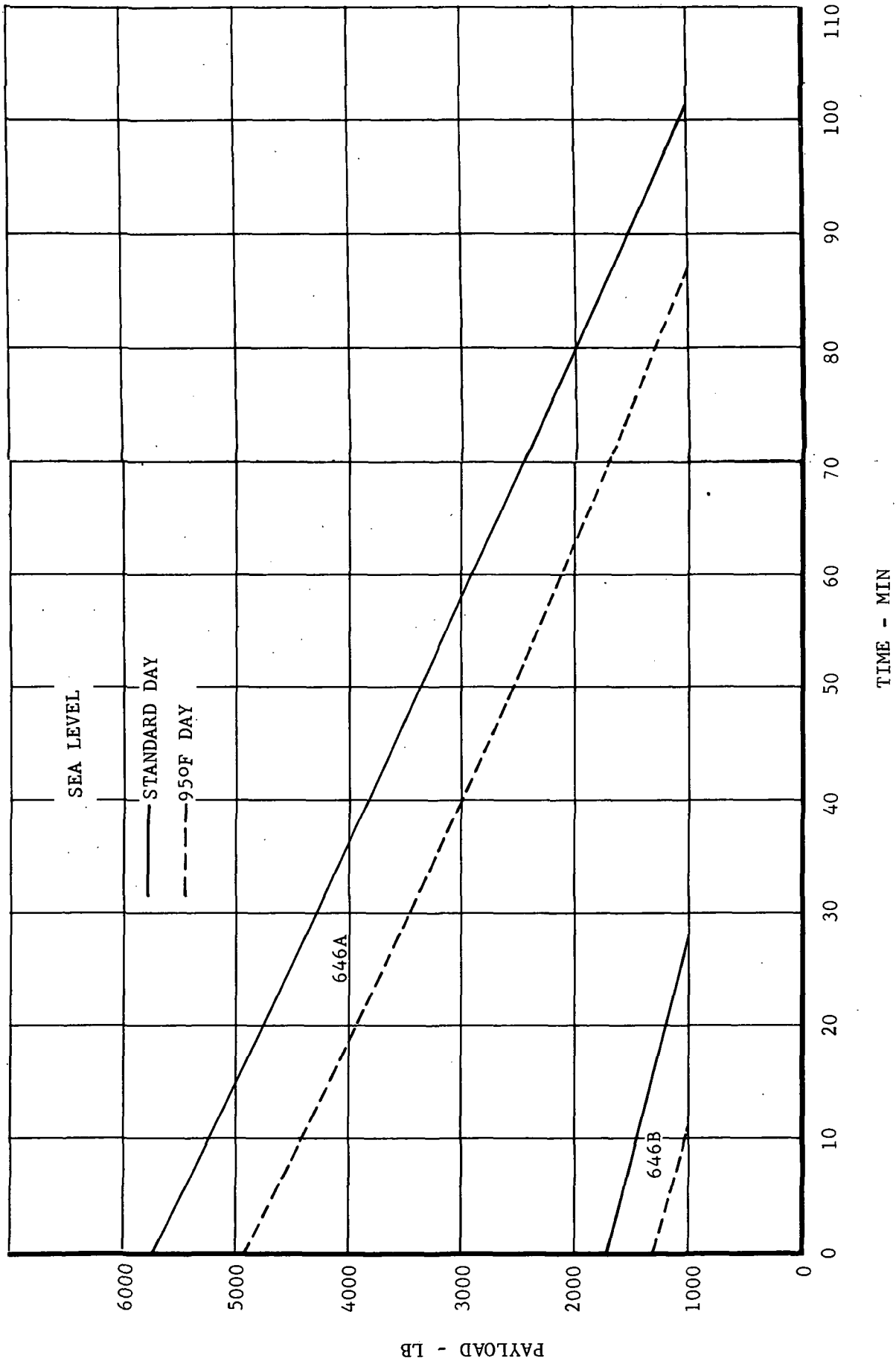


Figure 15. Hover Mission Performance.

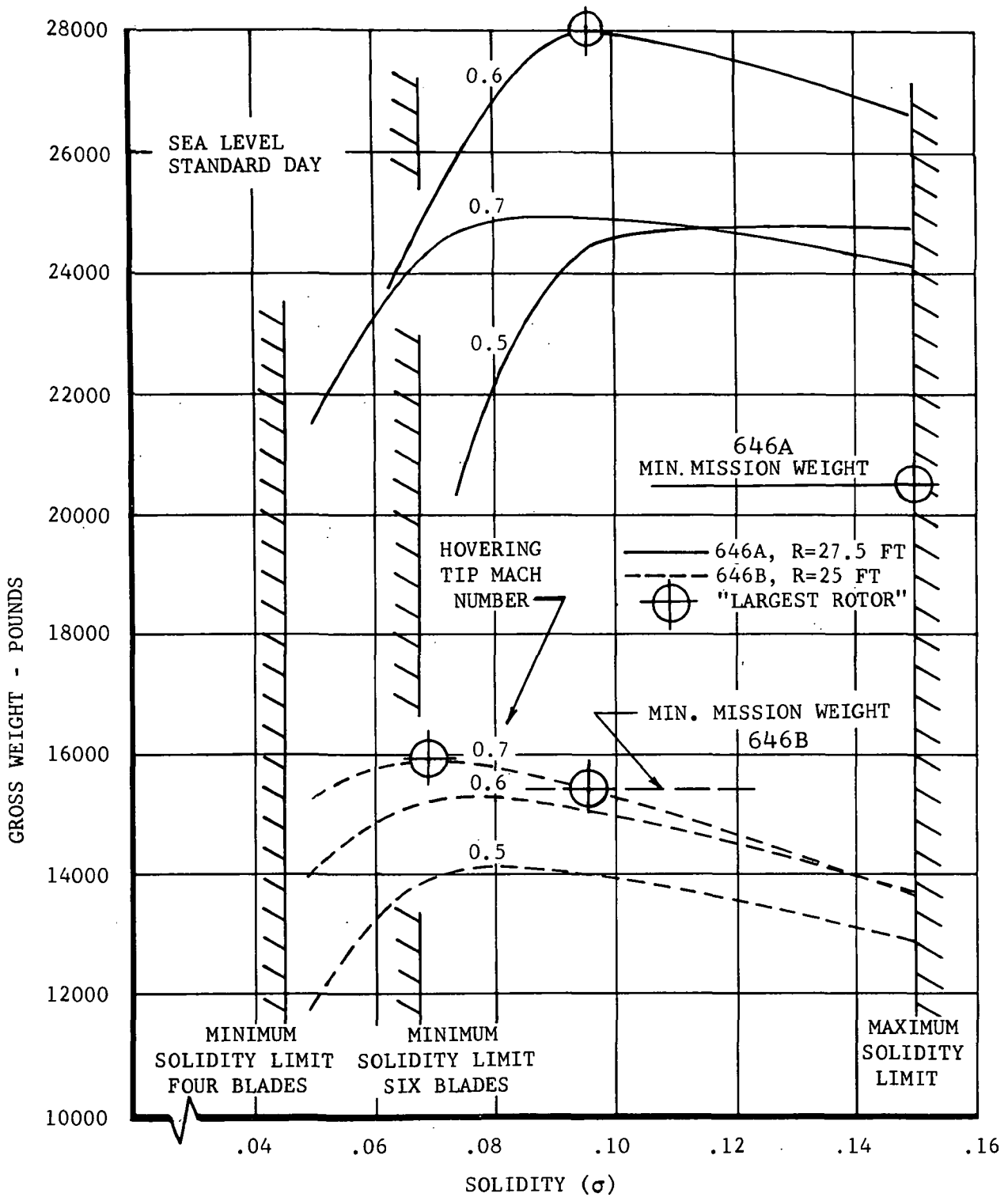


Figure 16. Hover Versatility, Largest Rotor, Compound Configuration.

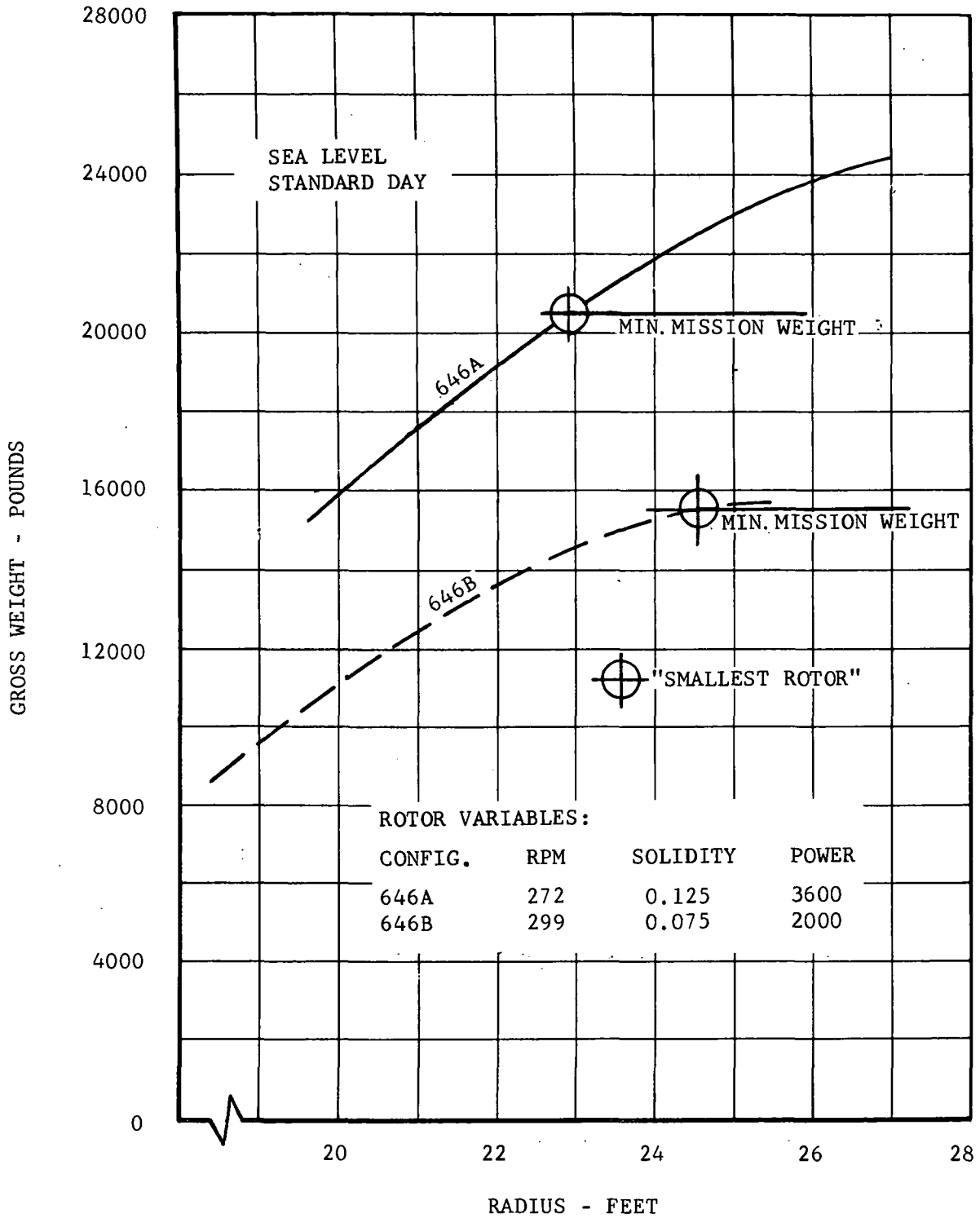


Figure 17. Hover Versatility, Smallest Rotor, Compound Configuration.

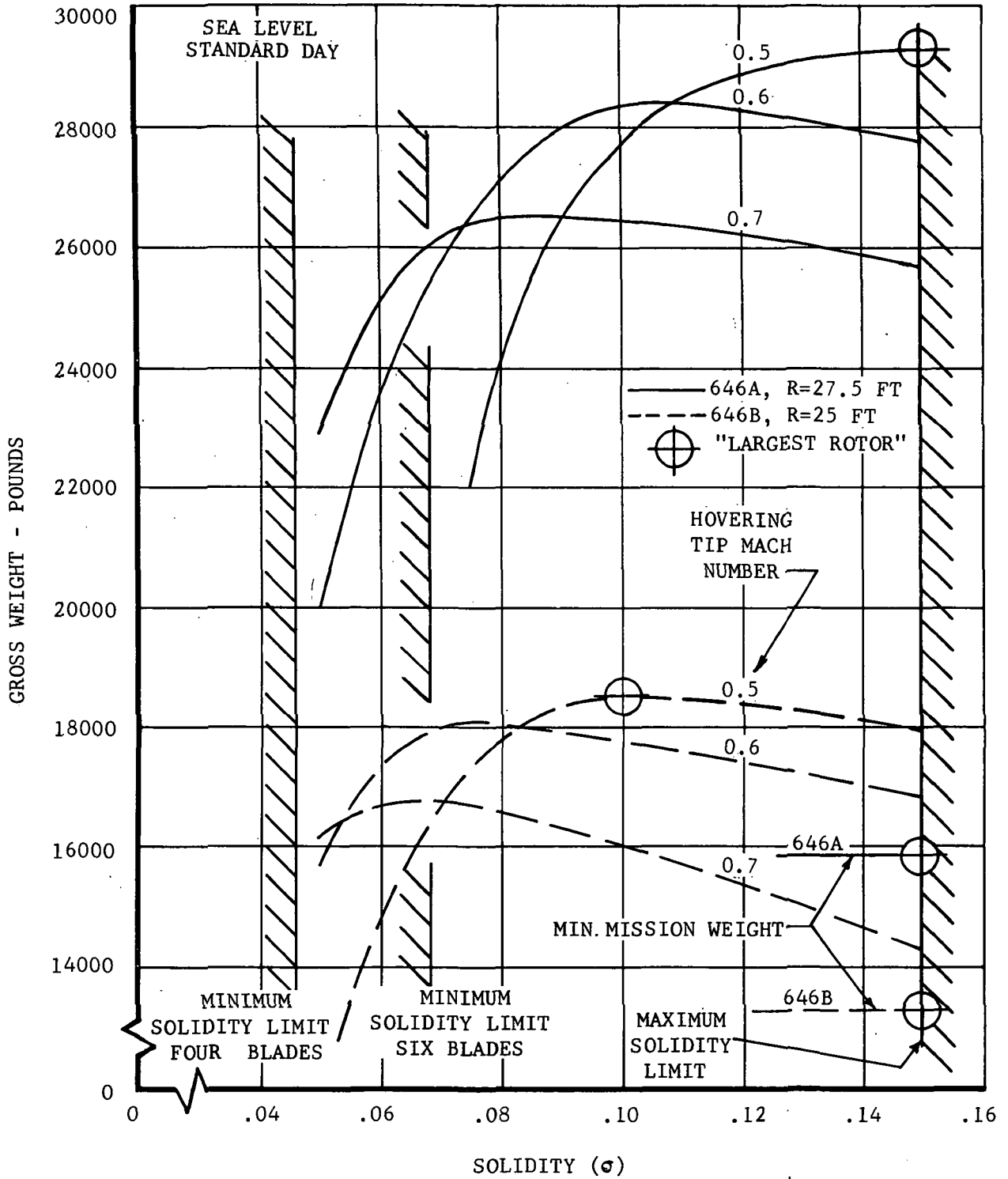


Figure 18. Hover Versatility, Largest Rotor, Variable Configuration.

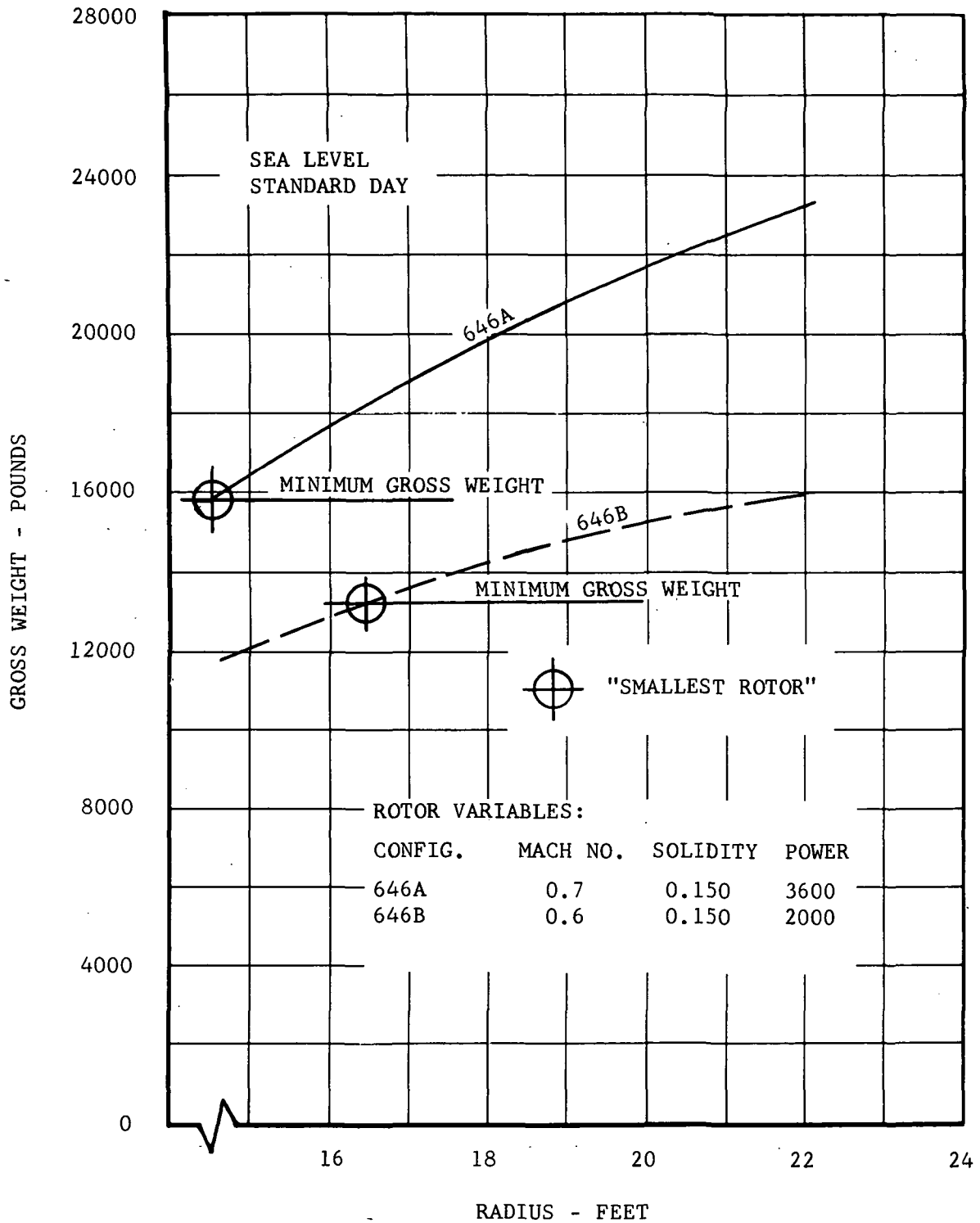


Figure 19. Hover Versatility, Smallest Rotor, Variable Configuration.

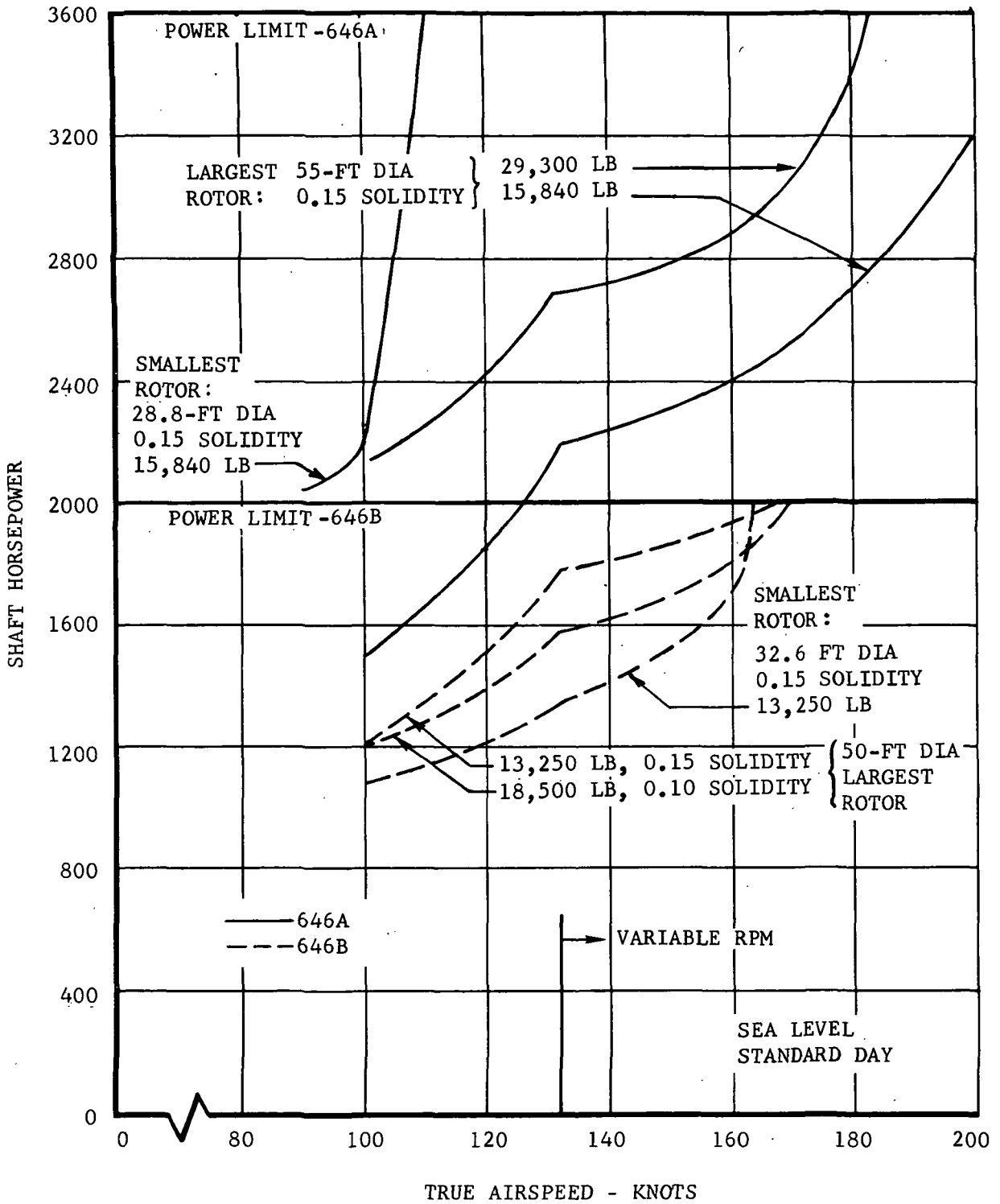
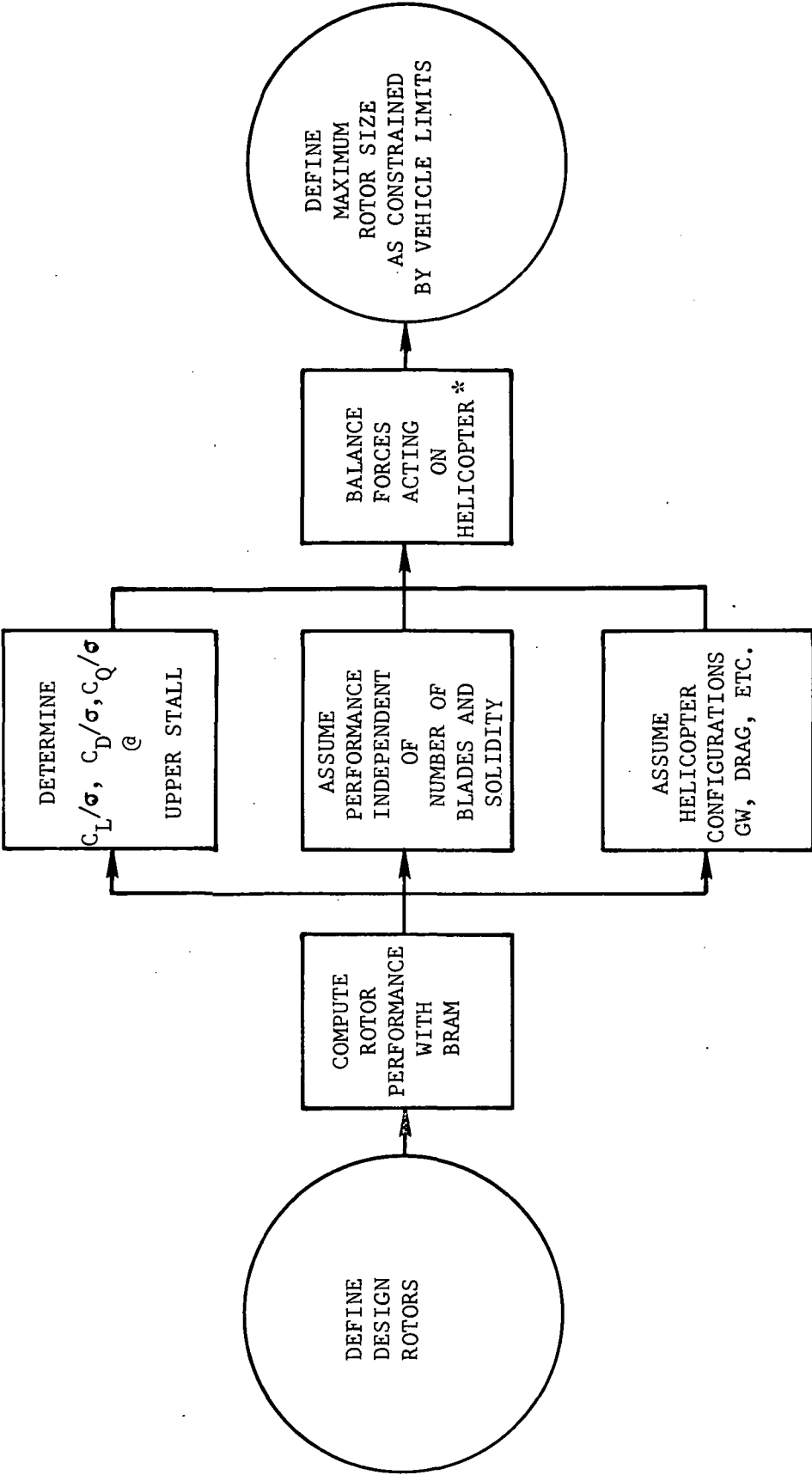


Figure 20. Level Flight Power Required, Variable Configuration.



* Jet Thrust = Parasite Drag + Rotor Drag + Induced Drag + Flap Drag
 Gross Weight = Rotor Lift + Wing Lift

Figure 21. Procedure Used to Determine Maximum Rotor Size.

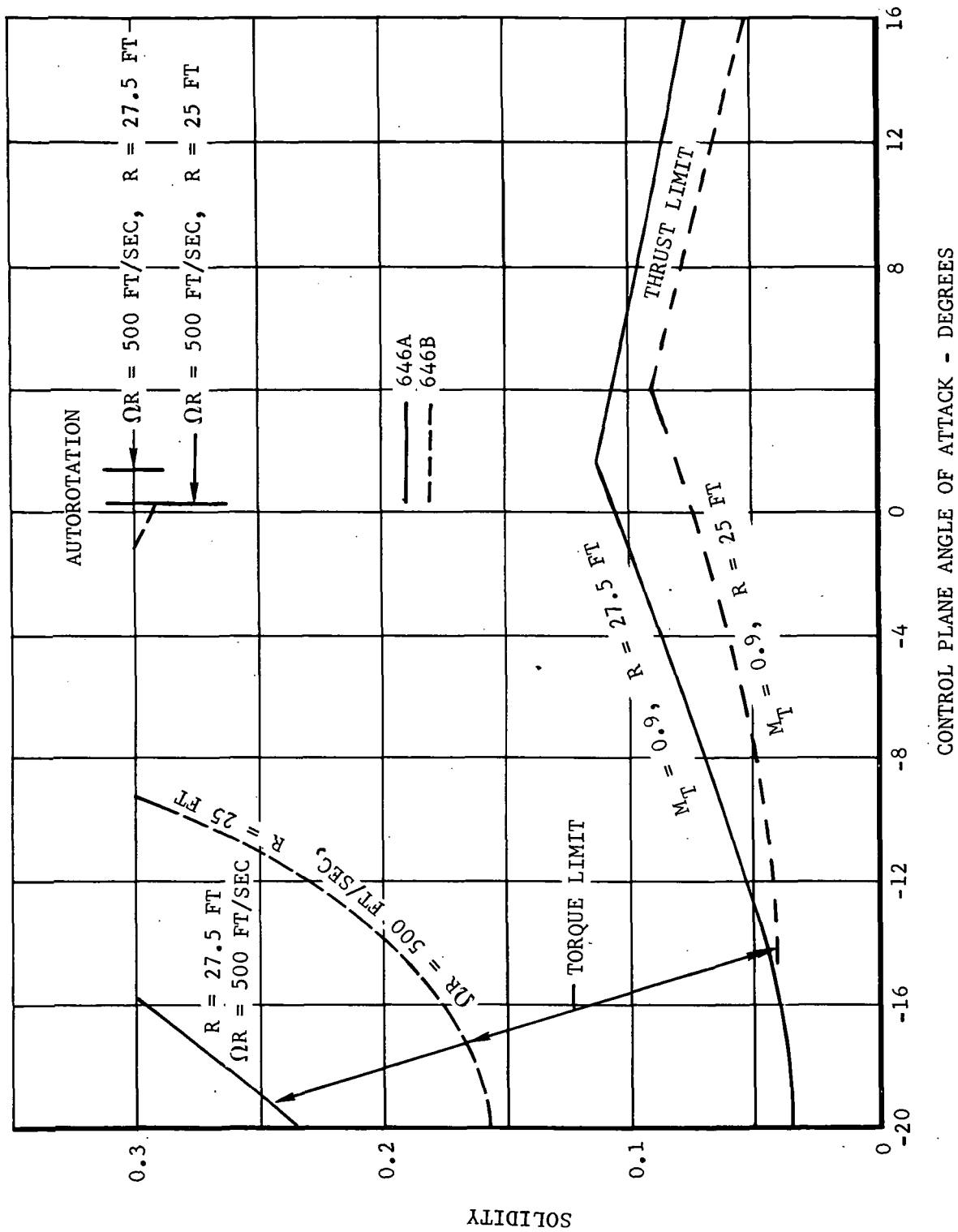
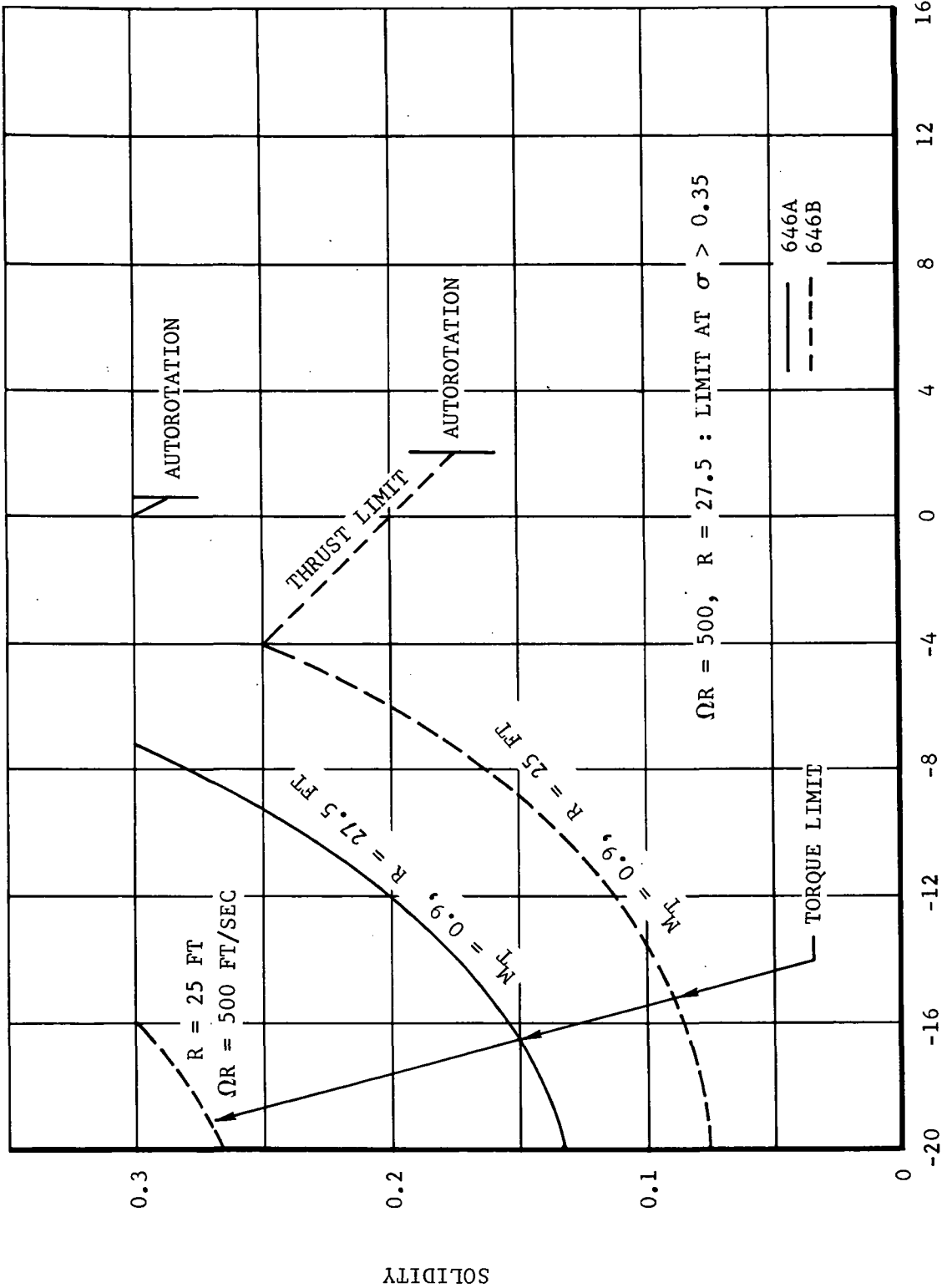


Figure 22. Rotor Test Versatility, 100 Knots.



CONTROL PLANE ANGLE OF ATTACK - DEGREES

Figure 23. Rotor Test Versatility, 200 Knots.

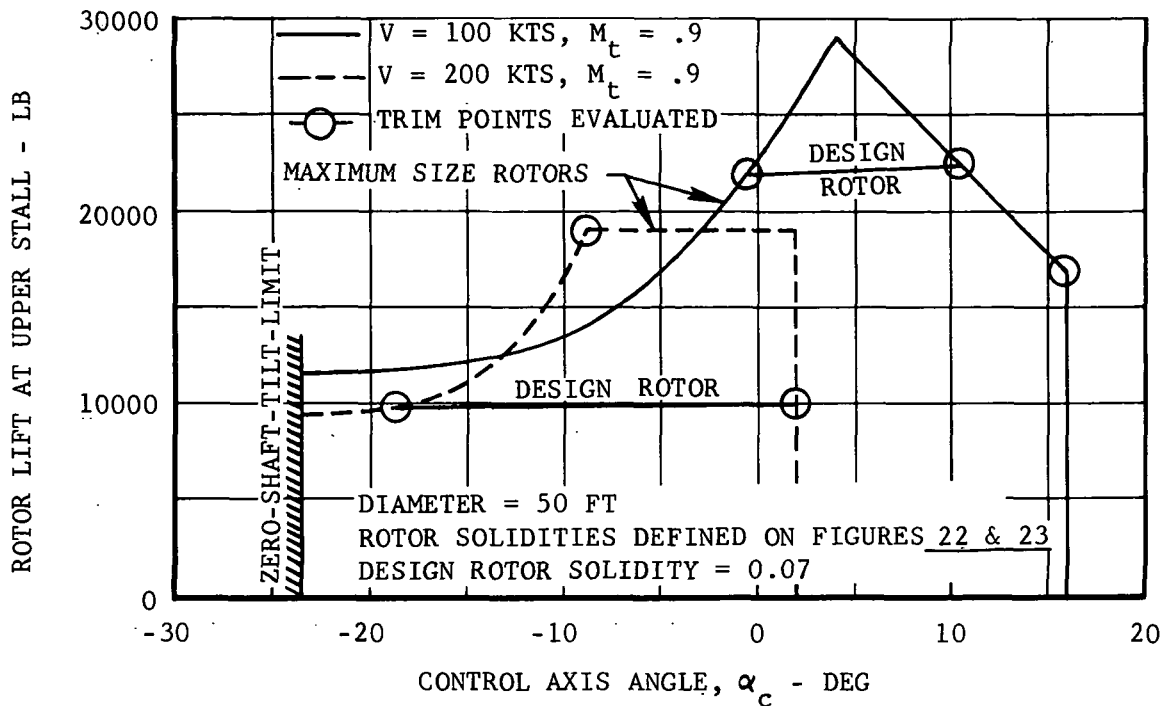


Figure 24. Model 646B, Maximum Size Rotors, Rotor Lift at Upper Stall Limit.

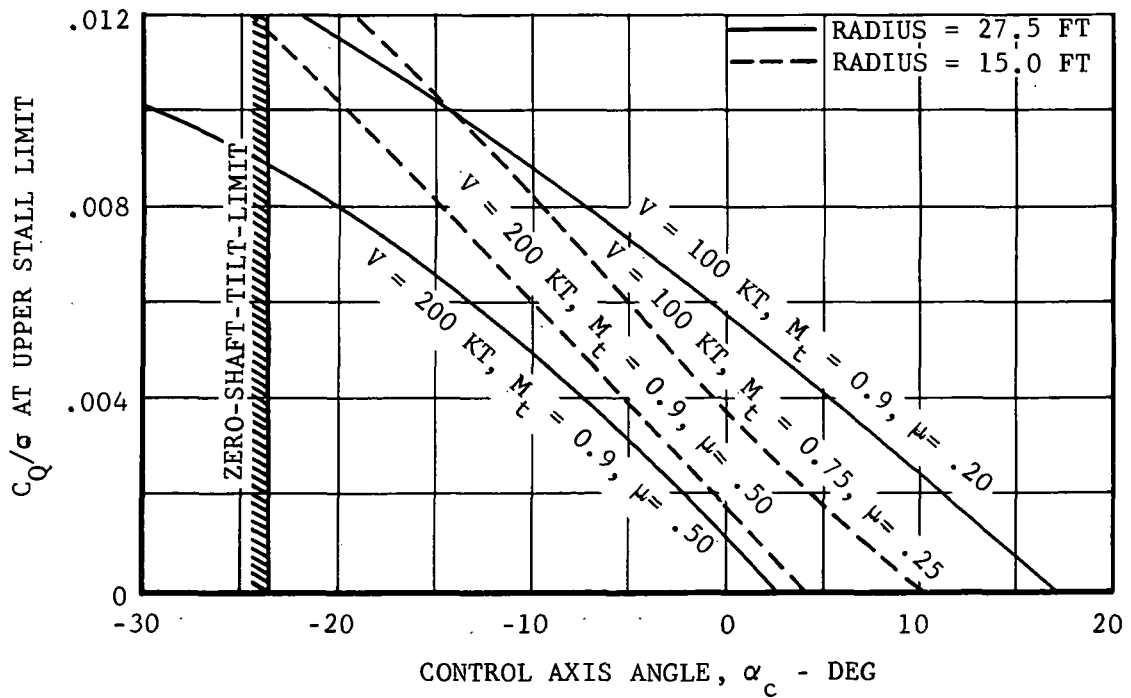


Figure 25. C_Q/σ at Upper Stall Limit, Smallest and Largest Rotors.

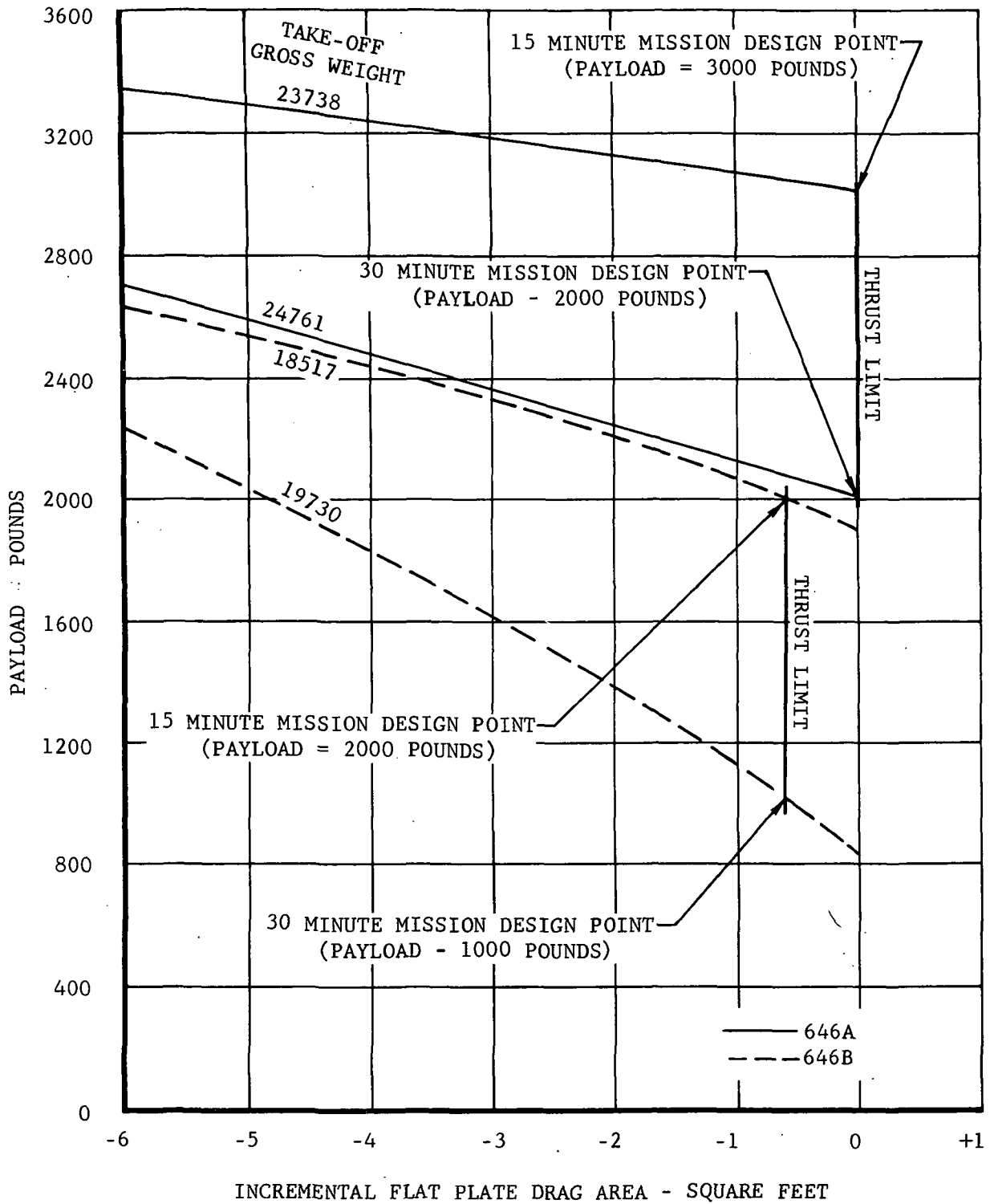


Figure 26. High-Speed Mission Versatility, Sea Level, Standard Day.

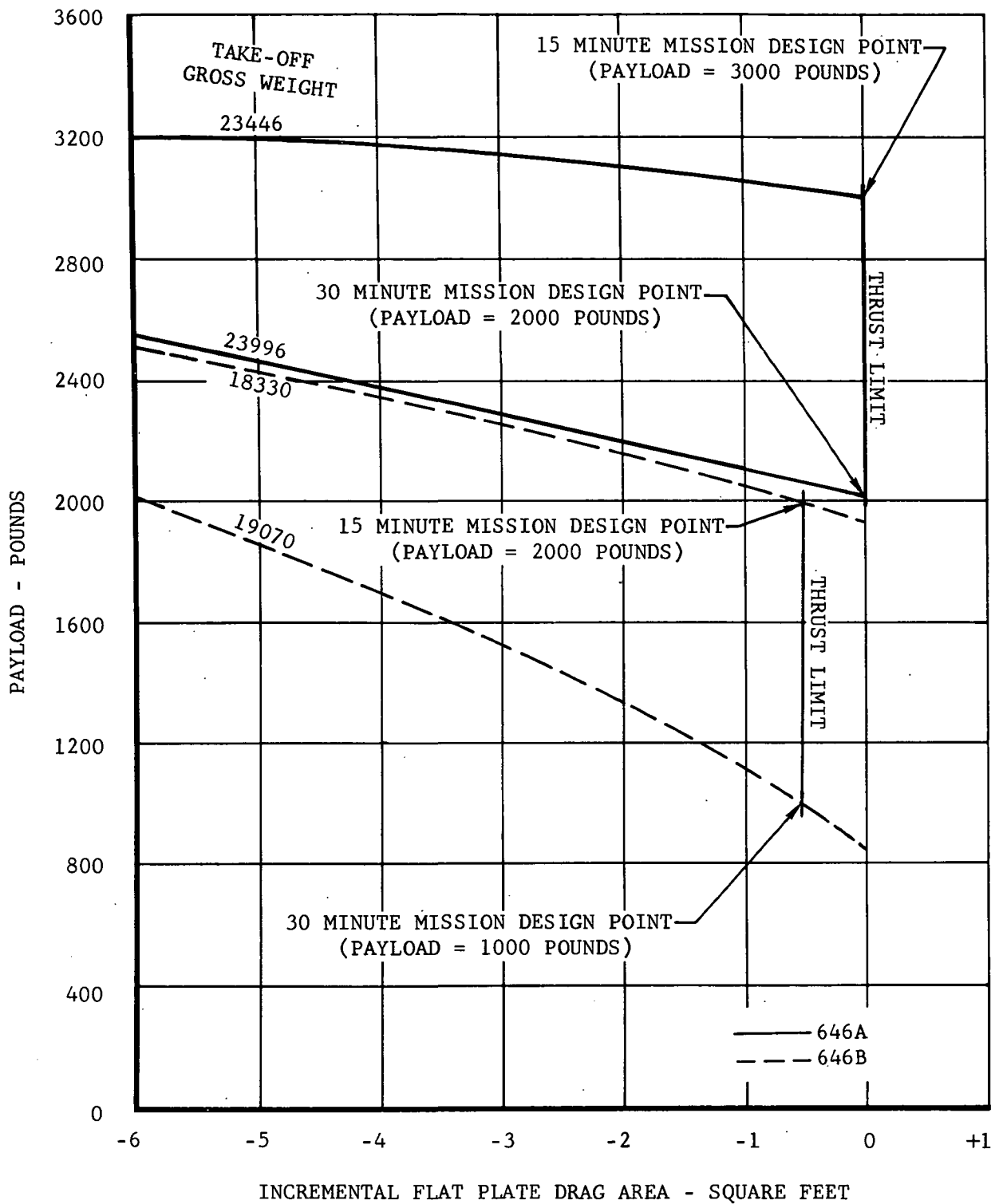


Figure 27. High-Speed Mission Versatility, 9500 Feet, Standard Day.

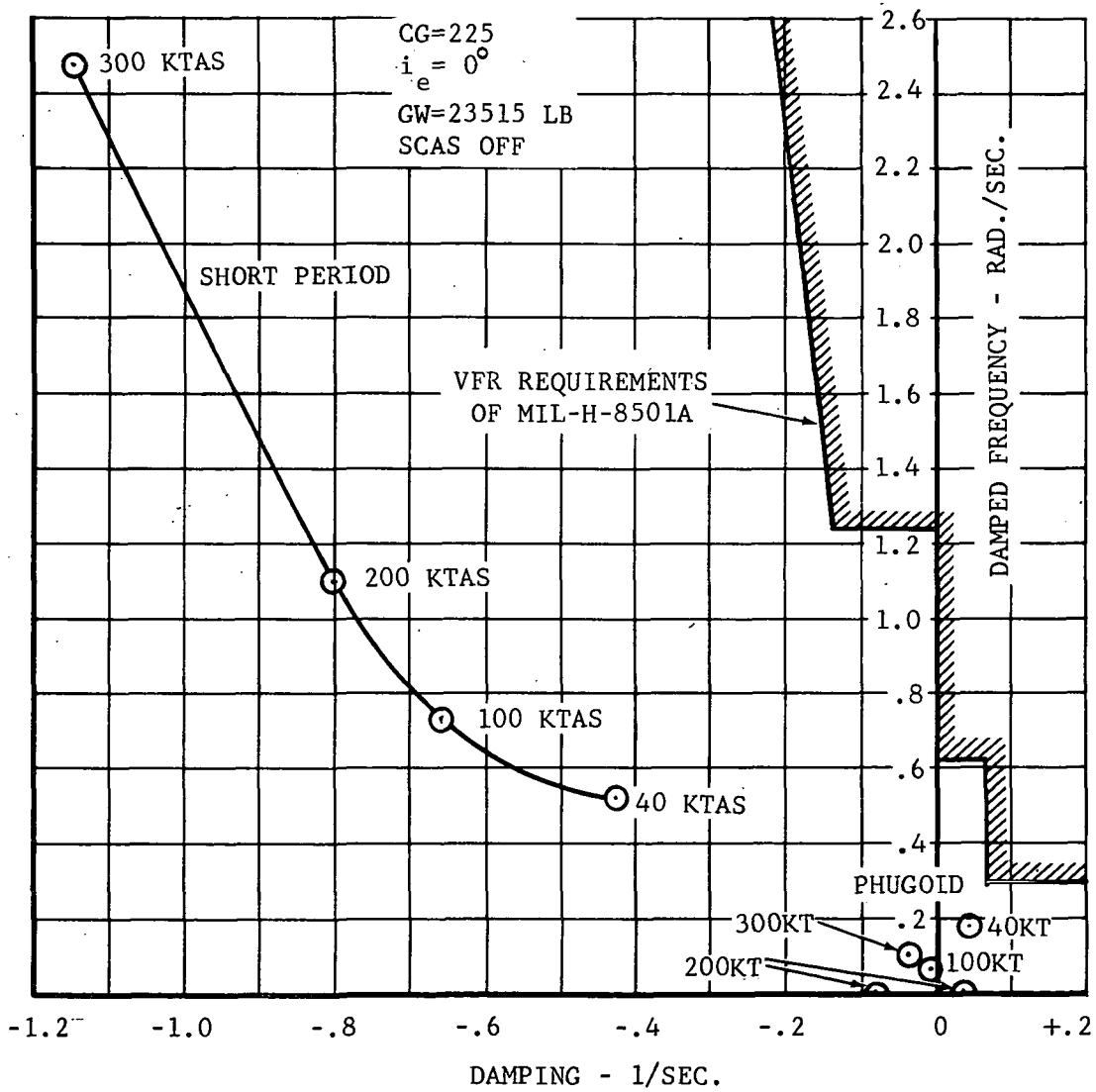


Figure 28. Model 646A Longitudinal Mode Root Locus, Compound Configuration.

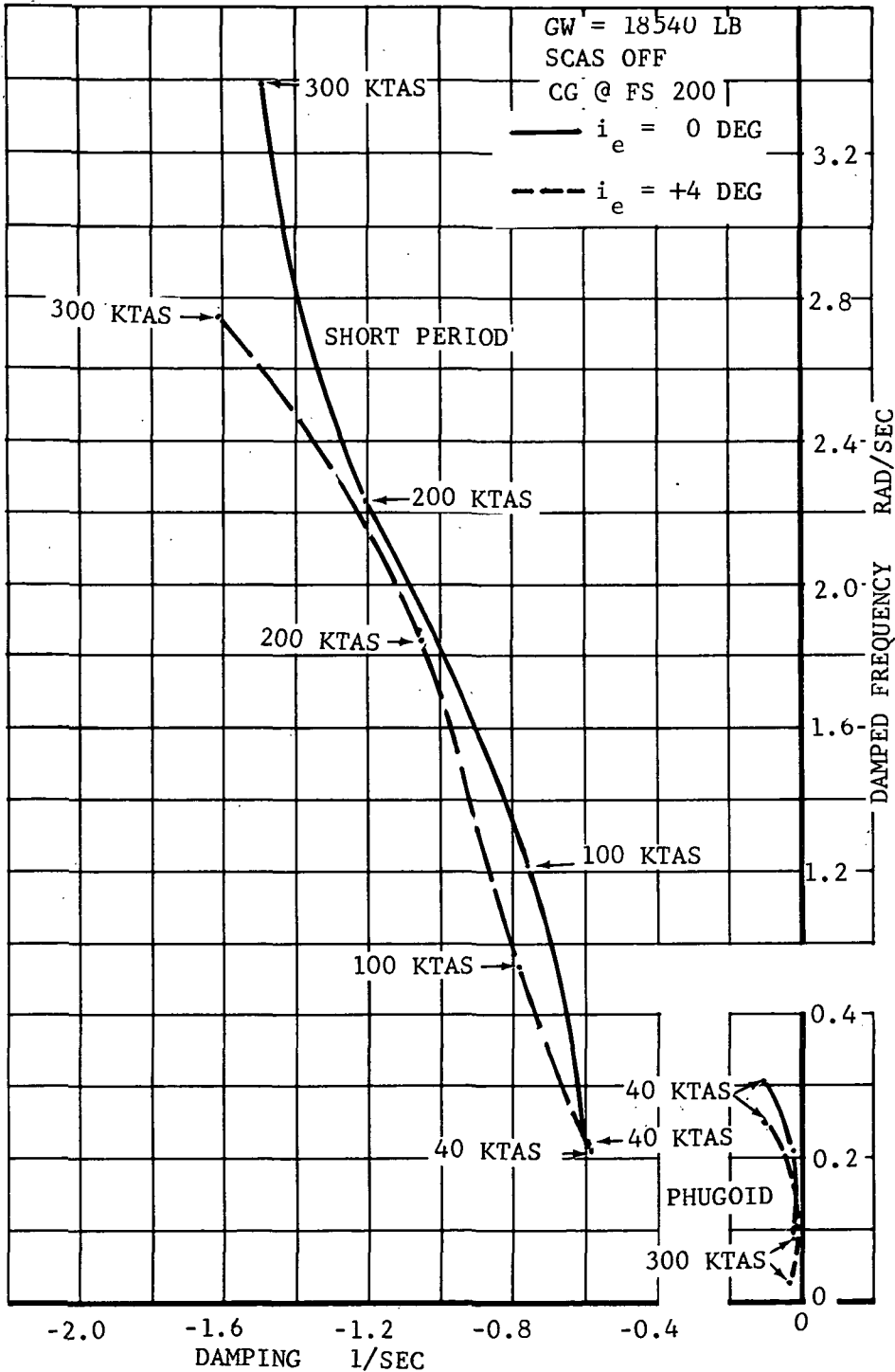


Figure 29. Model 646B Longitudinal Mode Root Locus, Compound Configuration.

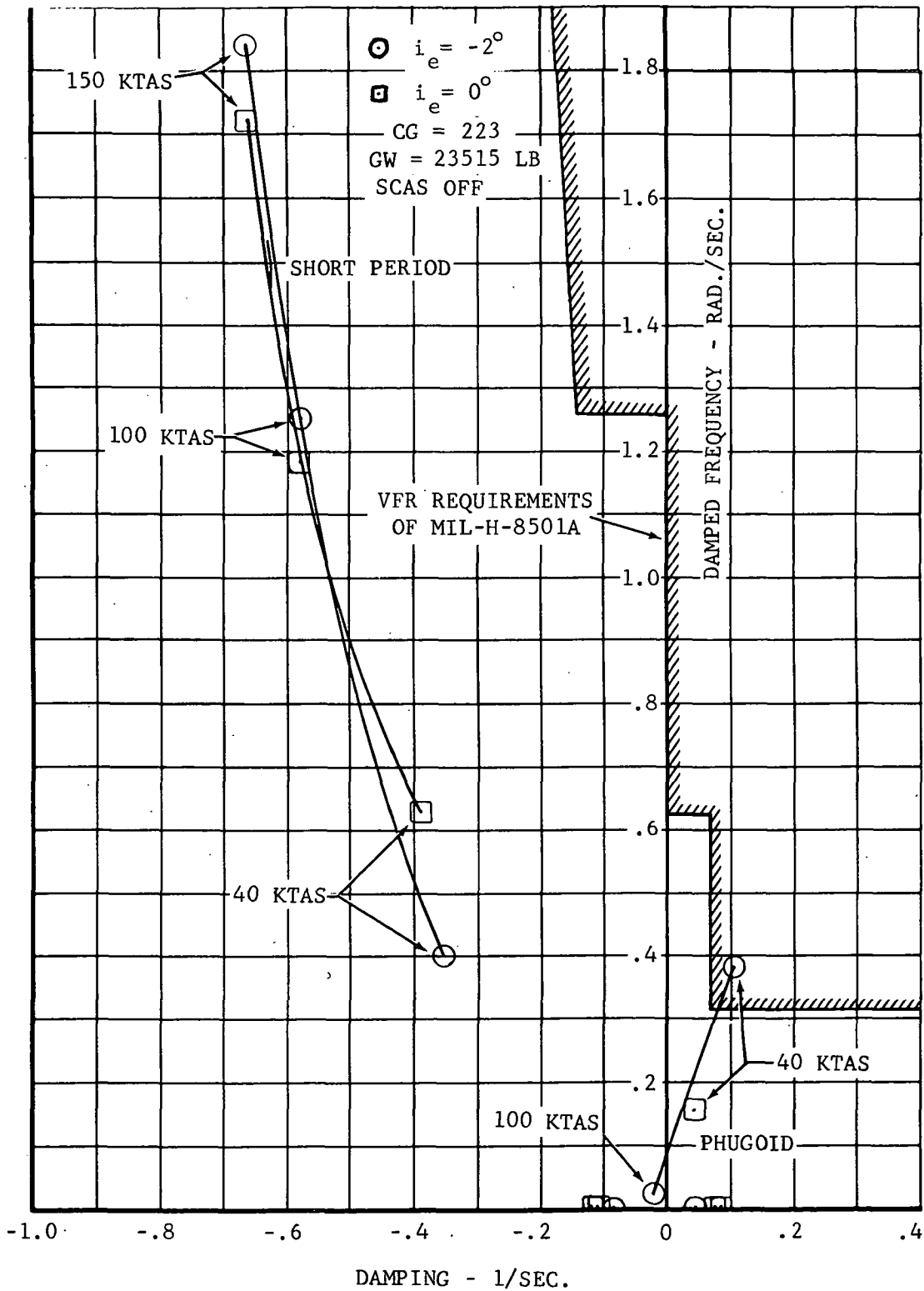


Figure 30. Model 646A Longitudinal Mode Root Locus, Helicopter Configuration.

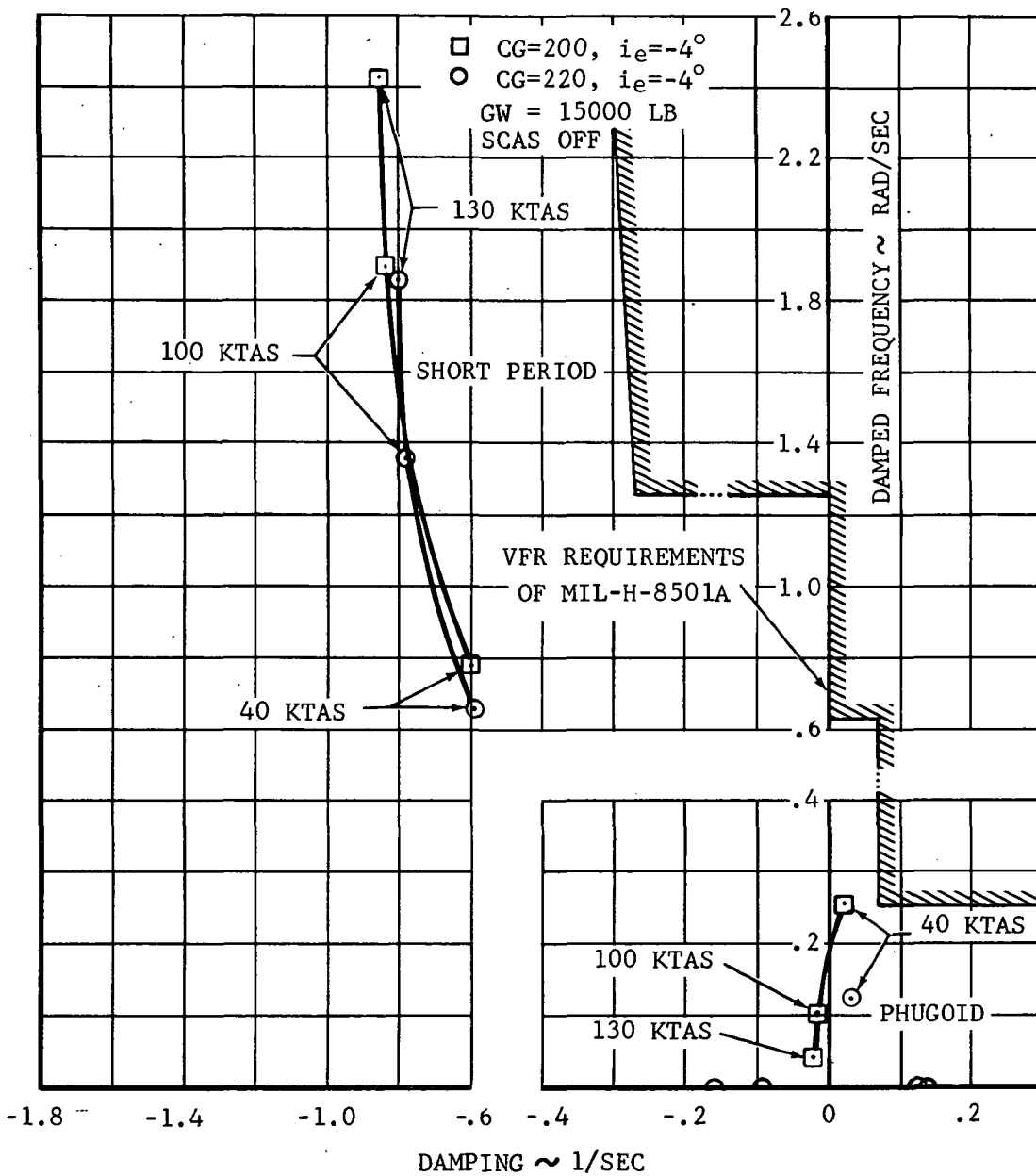


Figure 31. Model 646B Longitudinal Mode Root Locus, Helicopter Configuration.

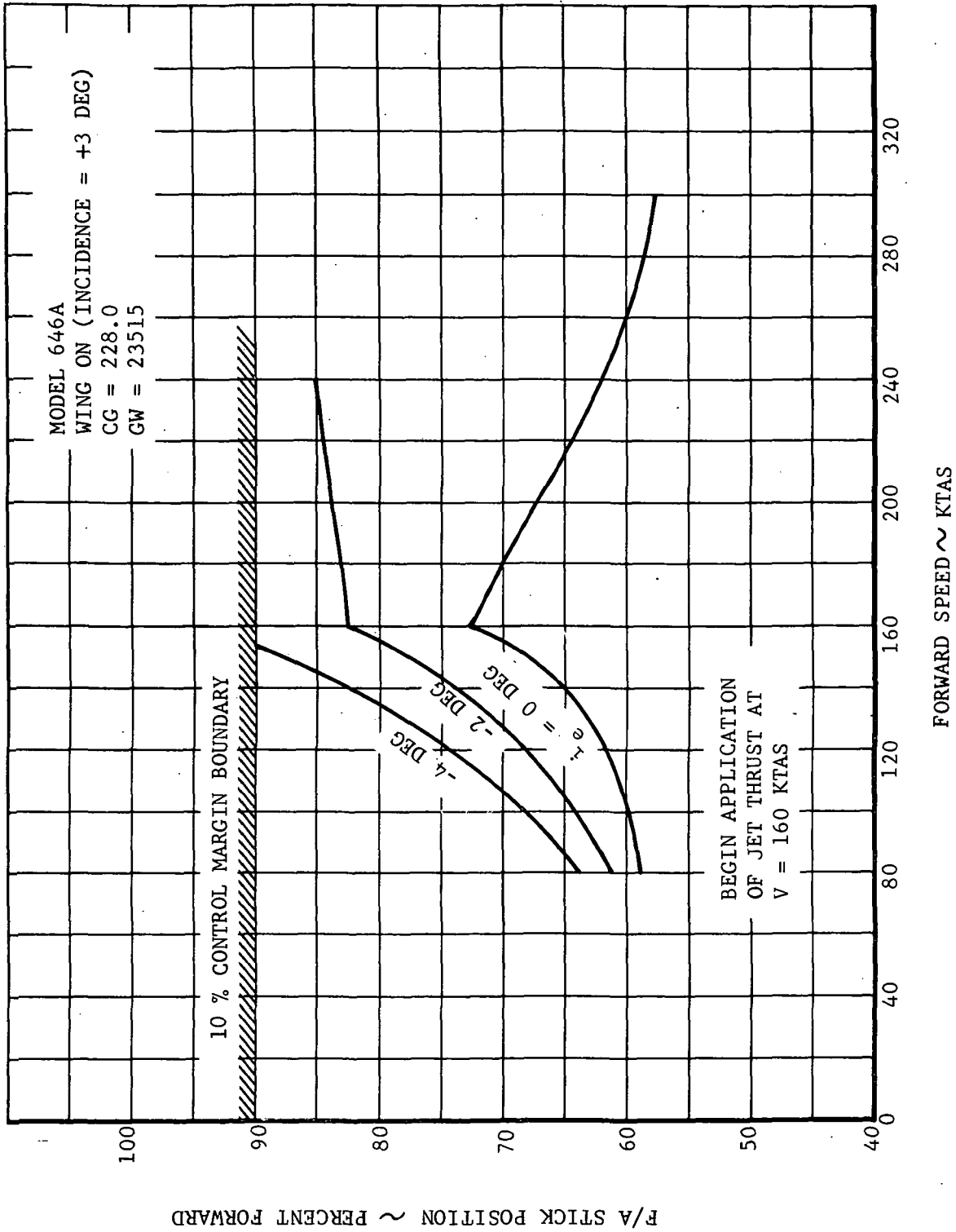


Figure 32. Model 646A Fore and Aft Cyclic Stick Position Variation with Stabilizer Incidence.

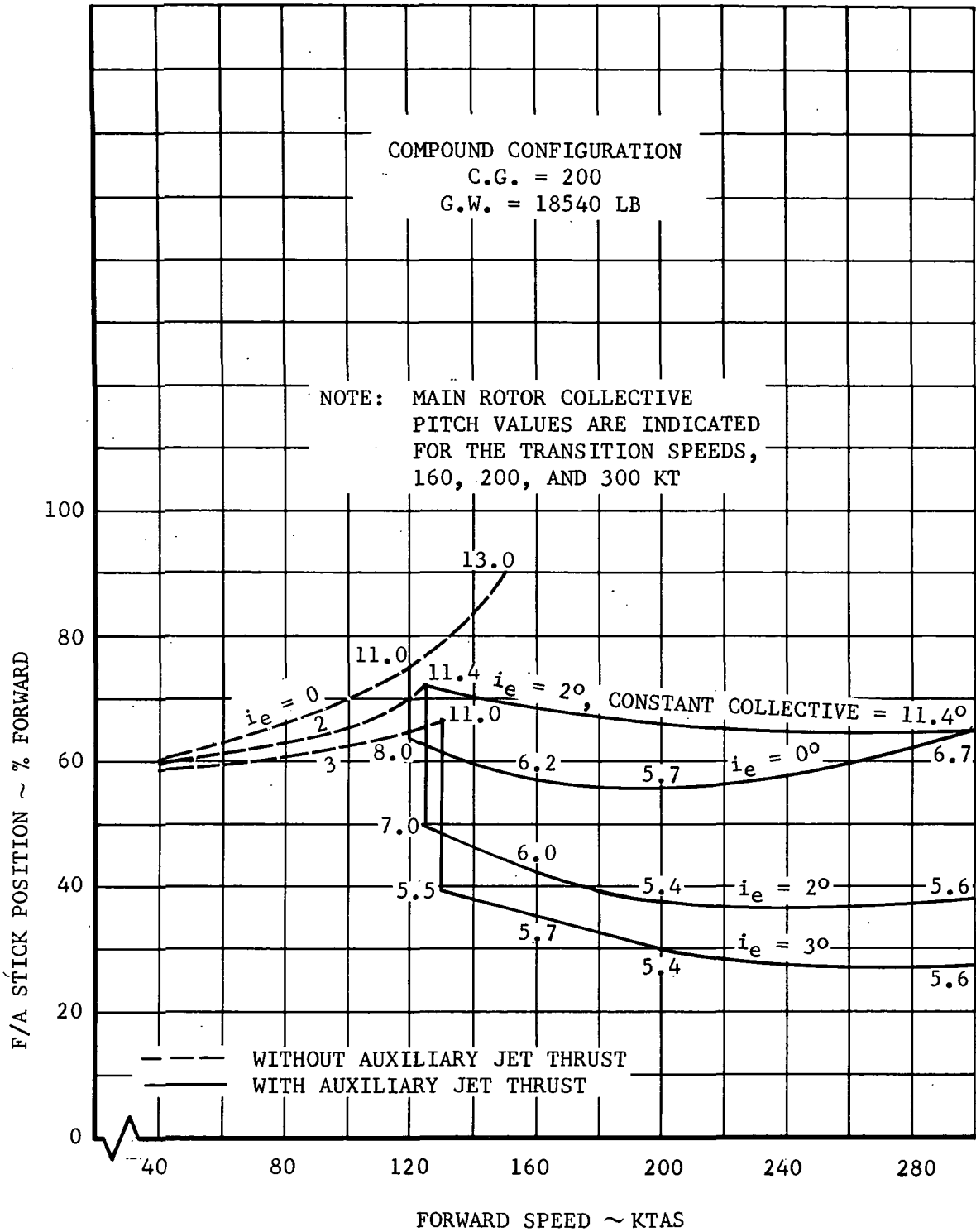


Figure 33. Model 646B Fore and Aft Cyclic Stick Position Variation with Stabilizer Incidence.

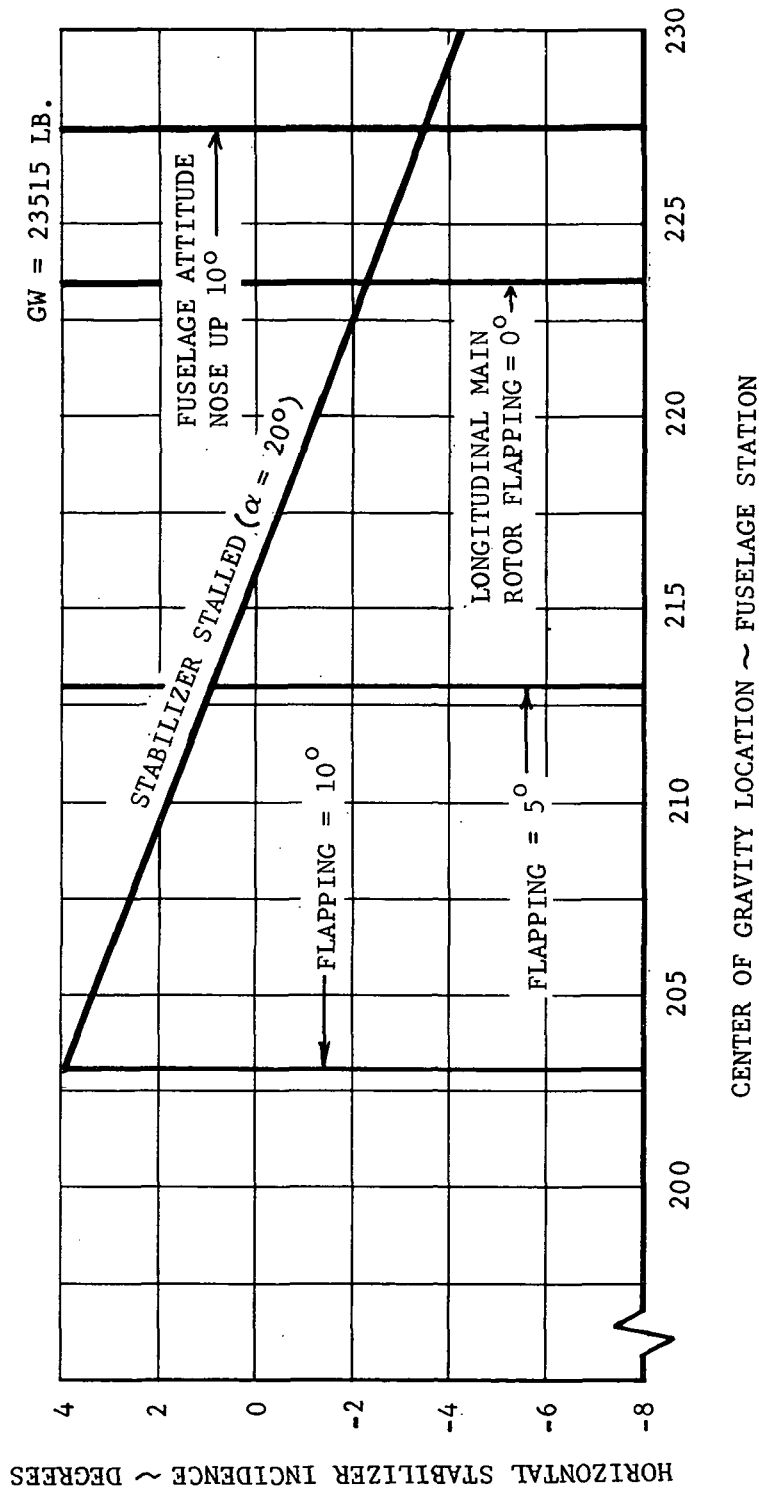


Figure 34. Model 646A Stabilizer Incidence Limits, Compound Configuration, 40 KTAS.

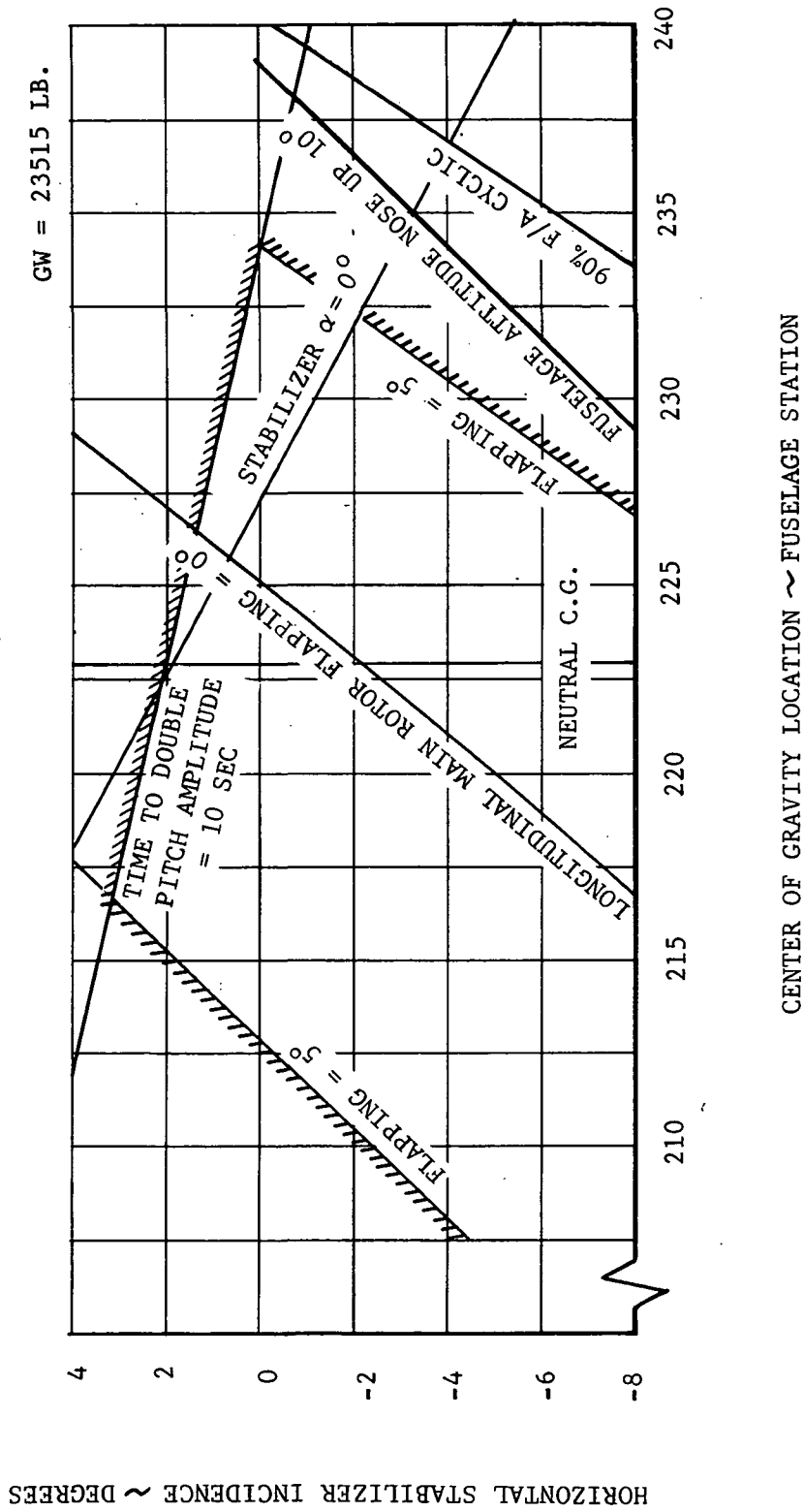


Figure 35. Model 646A Stabilizer Incidence Limits, Compound Configuration, 100 KTAS.

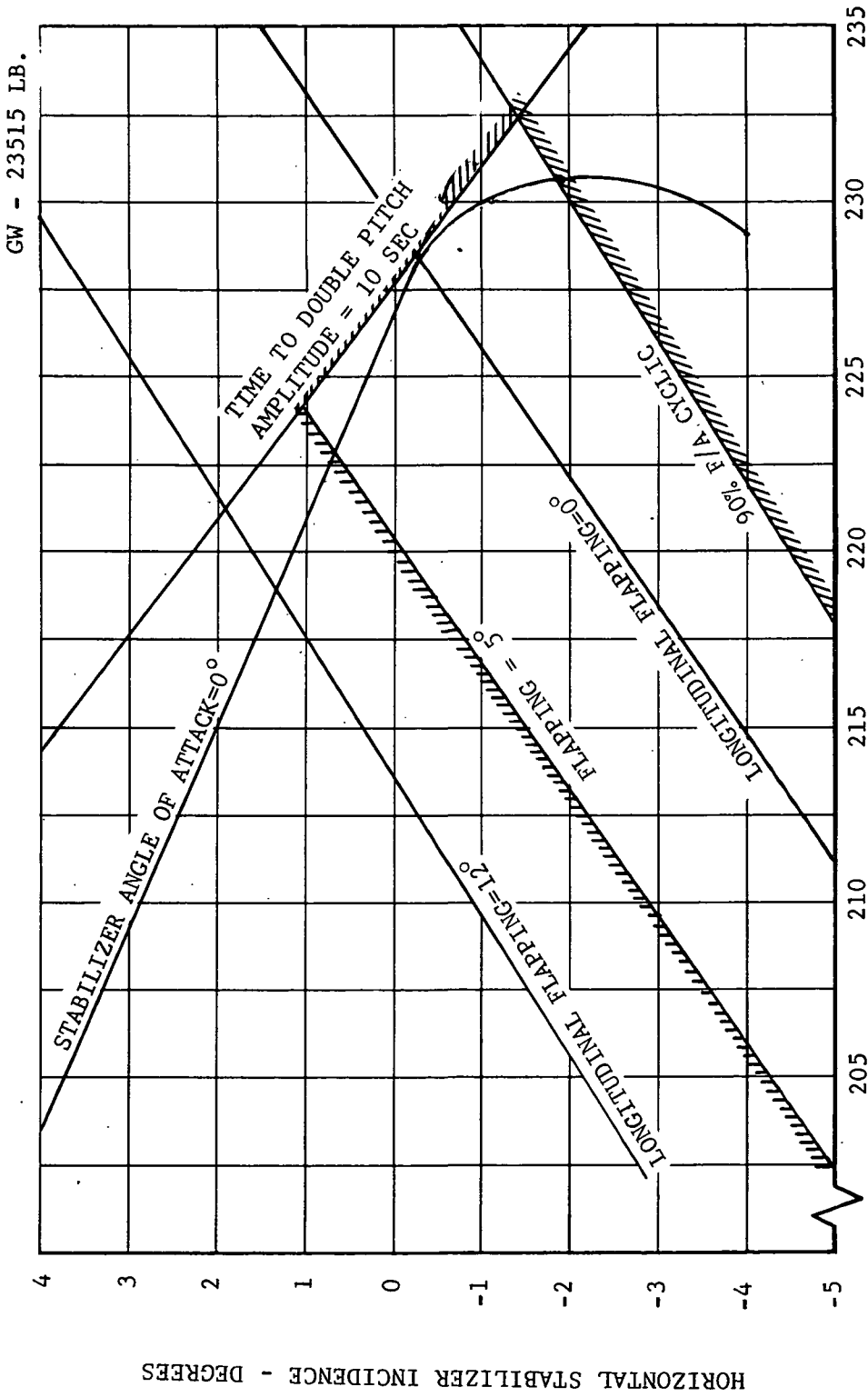


Figure 36. Model 646A Stabilizer Incidence Limits, Compound Configuration, 200 KTAS.

GW = 23515 LB

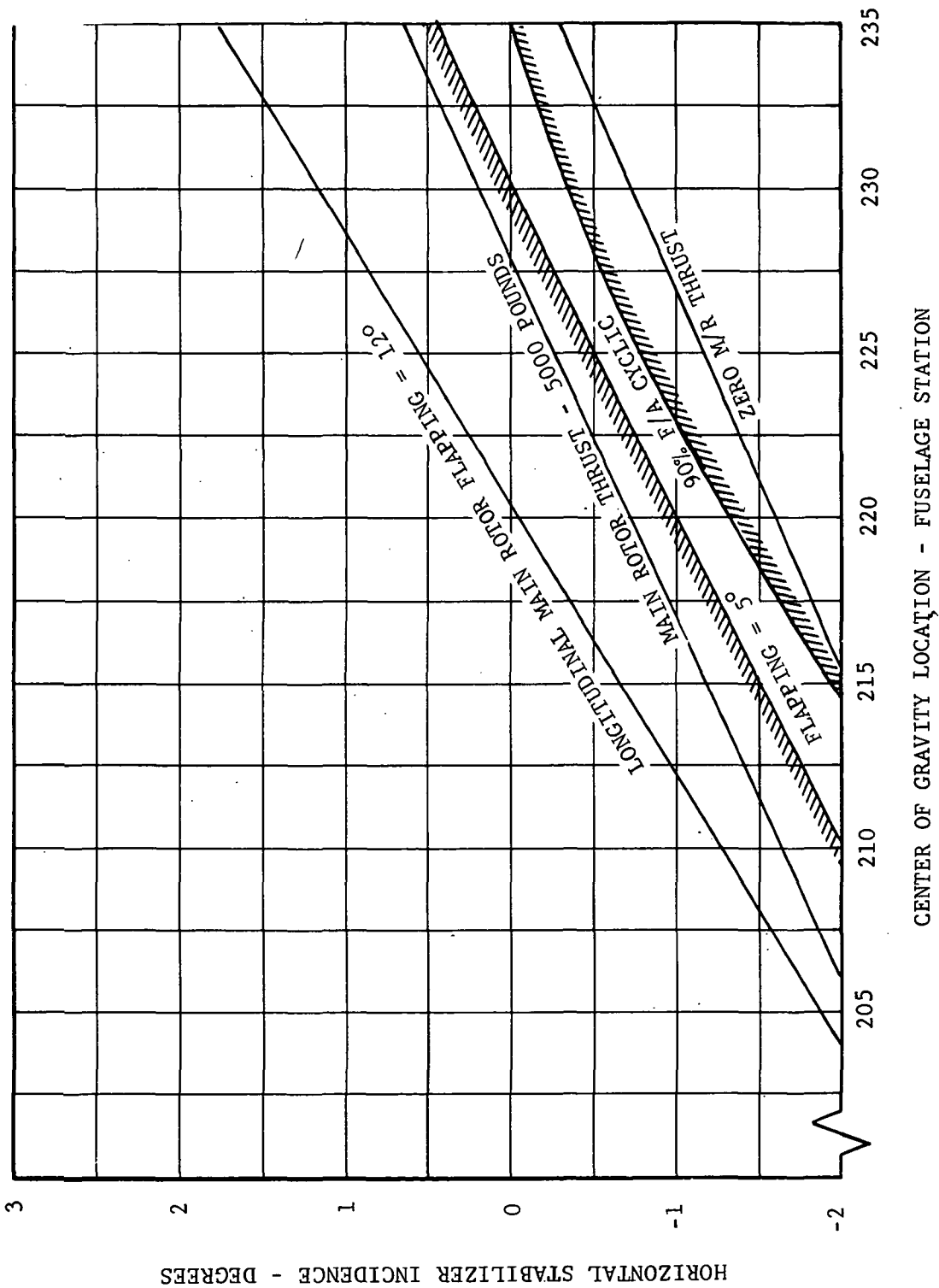


Figure 37. Model 646A Stabilizer Incidence Limits, Compound Configuration, 300 KTAS.

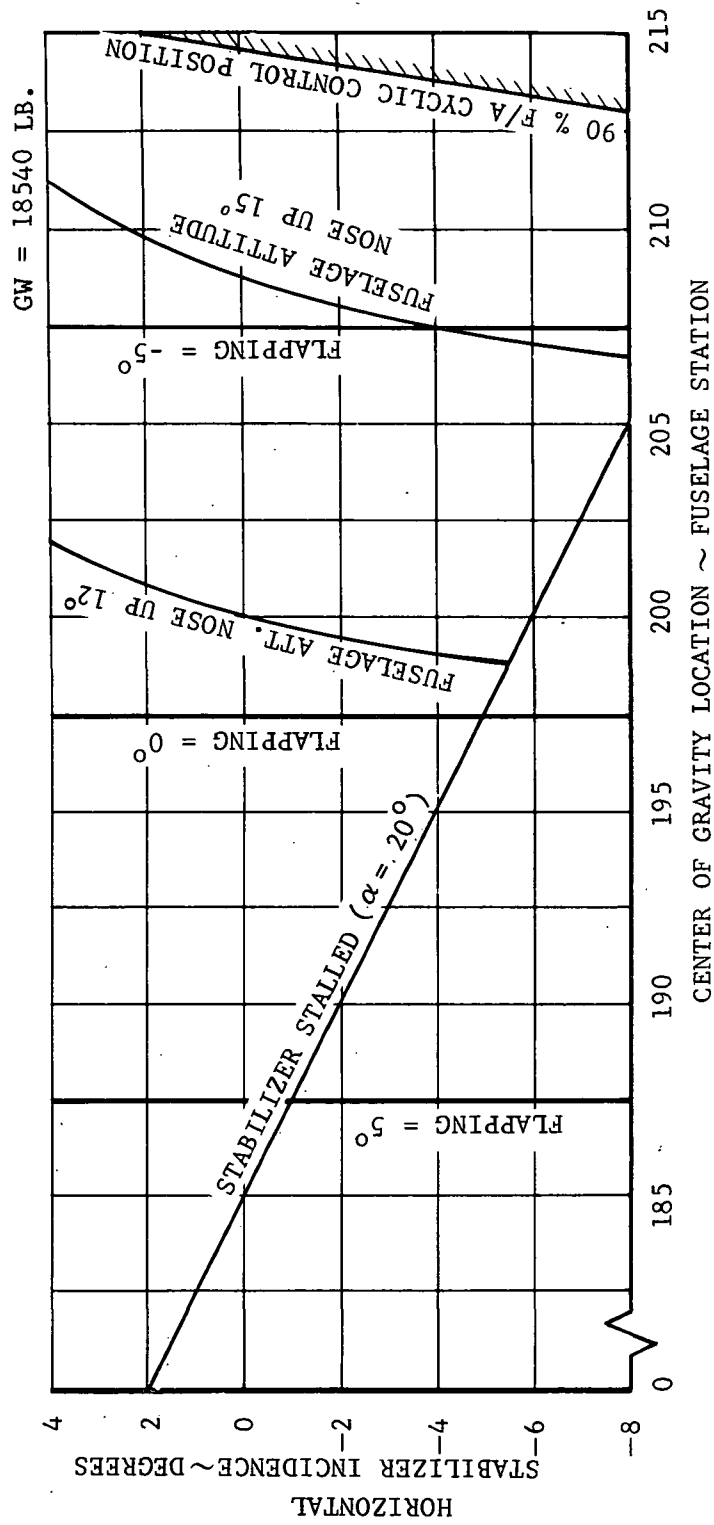


Figure 38. Model 646B Stabilizer Incidence Limits, Compound Configuration, 40 KTAS.

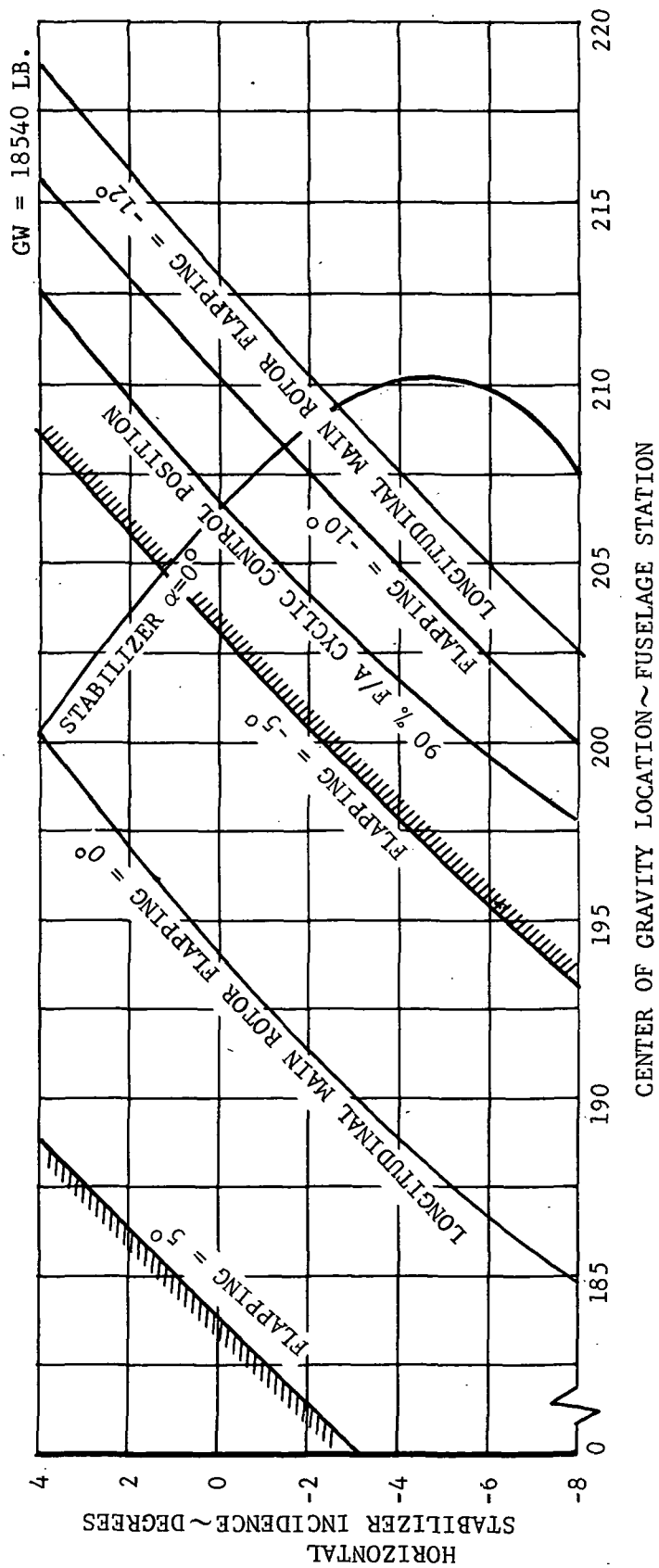
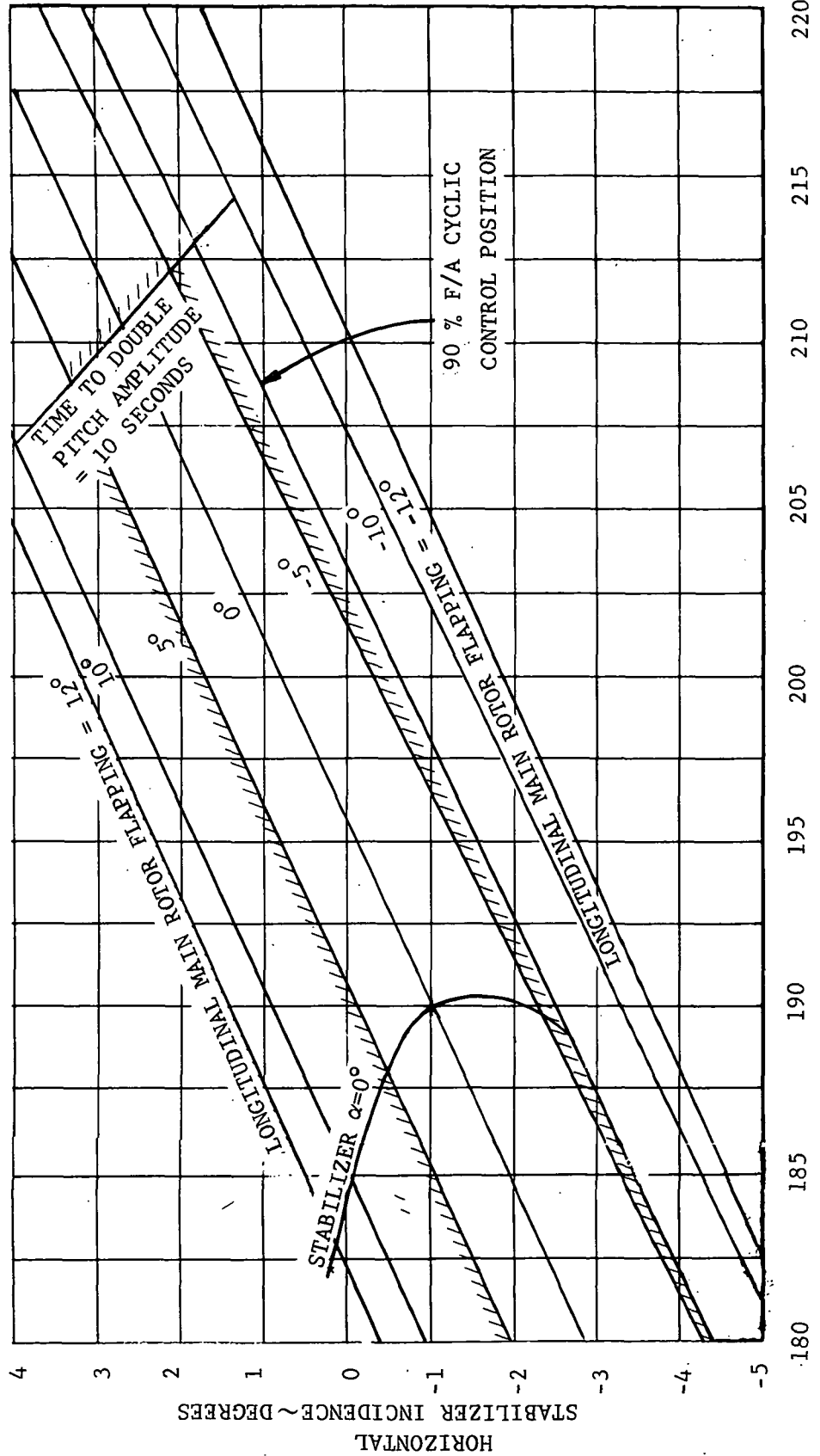


Figure 39. Model 646B Stabilizer Incidence Limits, Compound Configuration, 100 KTAS.

GW = 18540 LB.



CENTER OF GRAVITY LOCATION ~ FUSELAGE STATION

Figure 40. Model 646B Stabilizer Incidence, Compound Configuration, 200 KTAS.

CW = 18540 LB

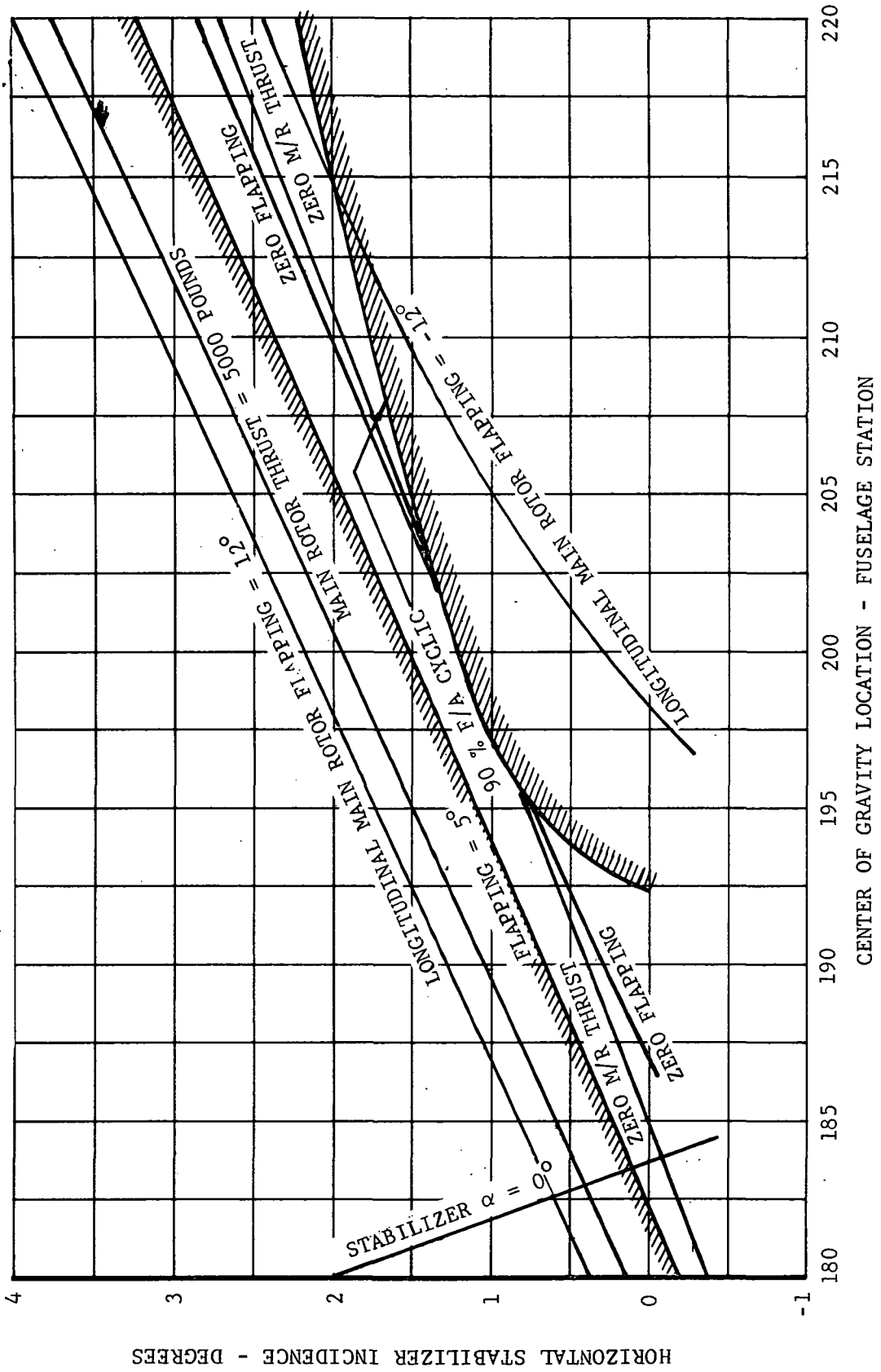
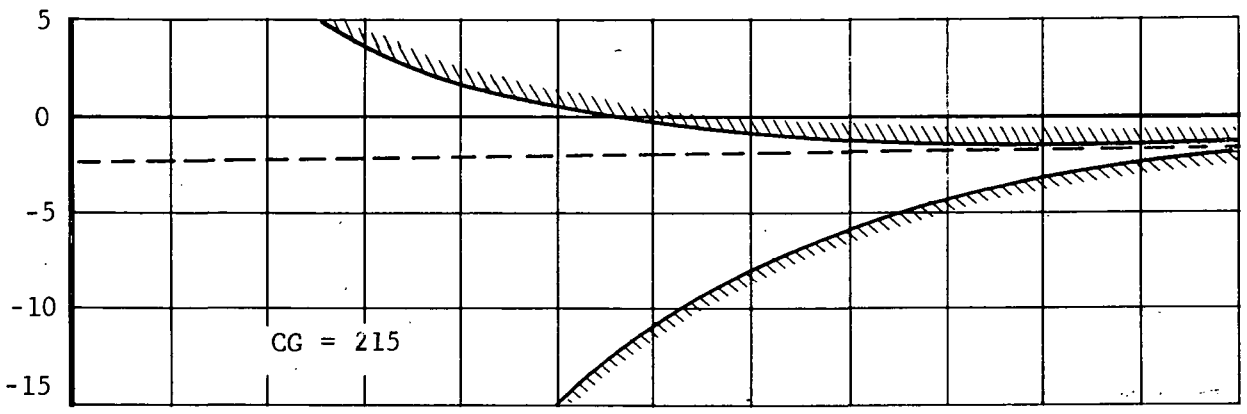


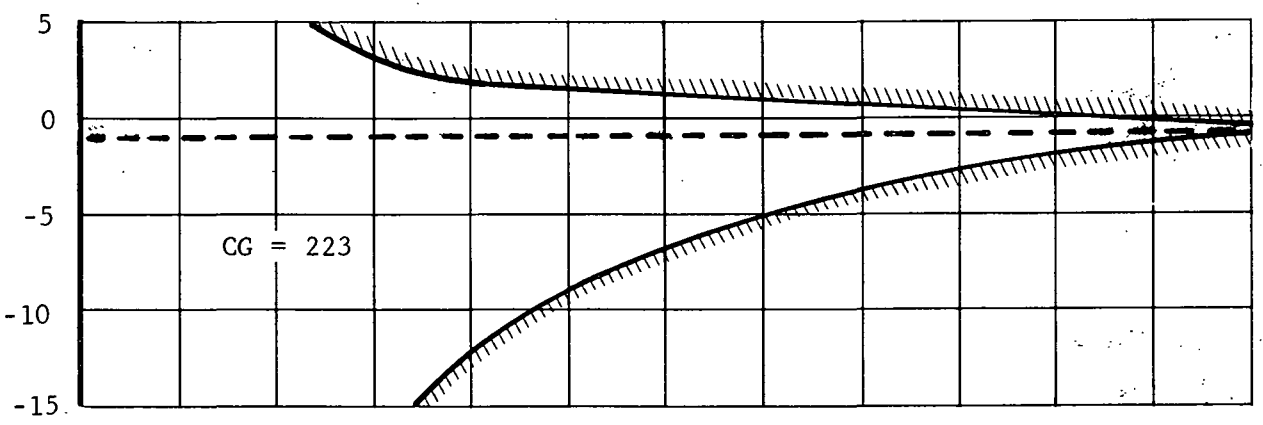
Figure 41. Model 646B Stabilizer Incidence Limits, Compound Configuration, 300 KTAS.

STABILIZER INCIDENCE - DEG.

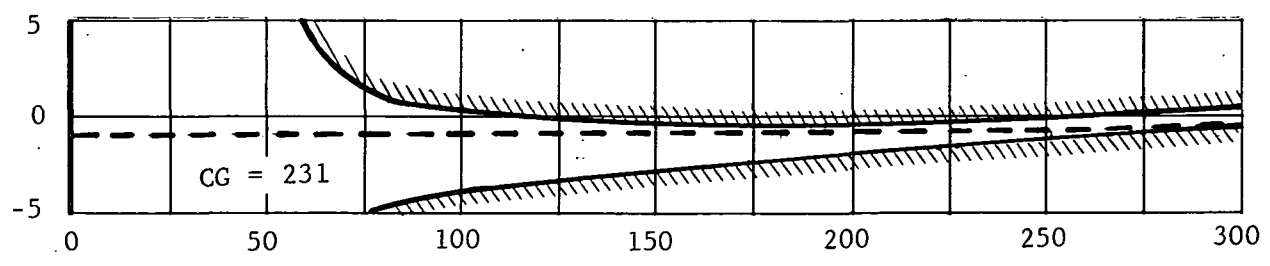


----- INCIDENCE FOR POSITIVE F/A POSITION GRADIENT

STABILIZER INCIDENCE - DEG.



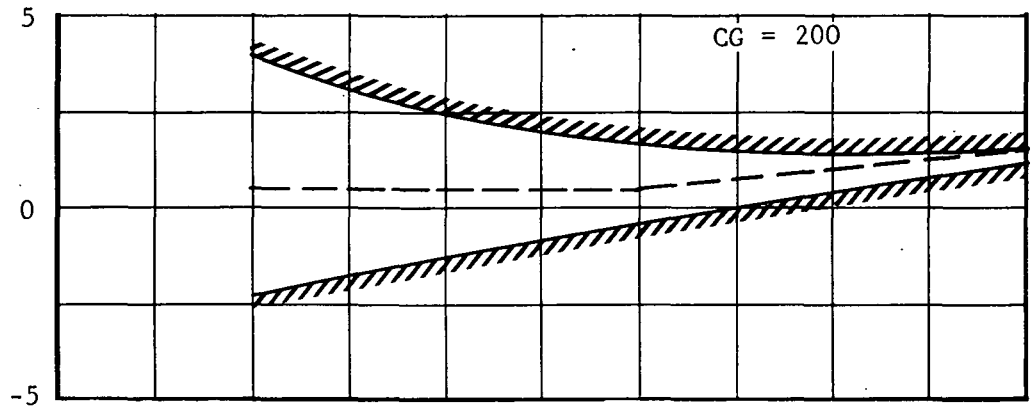
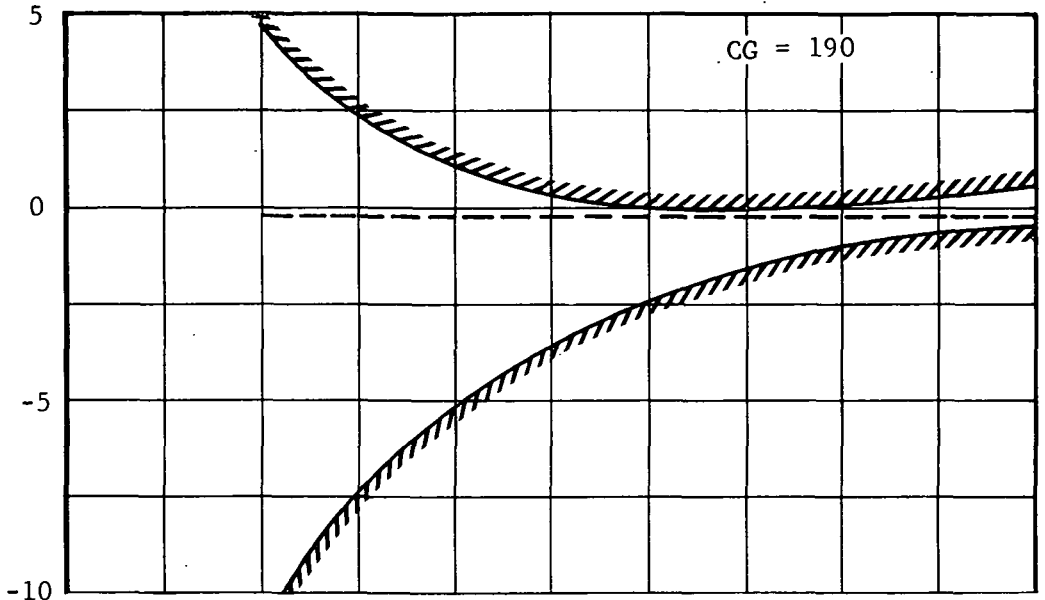
STABILIZER INCIDENCE - DEG.



FORWARD SPEED - KTAS .

Figure 42. Model 646A Compound Configuration Stabilizer Incidence Limits Versus Airspeed.

STABILIZER INCIDENCE ~ DEG



--- INCIDENCE FOR POSITIVE F/A STICK GRADIENT

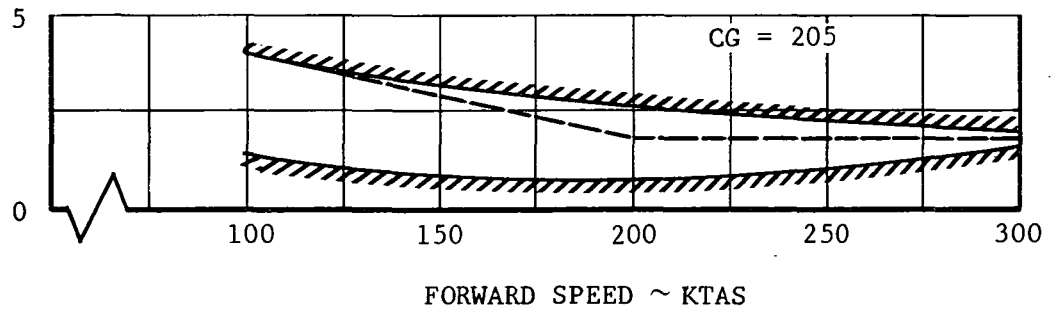


Figure 43. Model 646B, Compound Configuration, Stabilizer Incidence Limits Versus Airspeed.

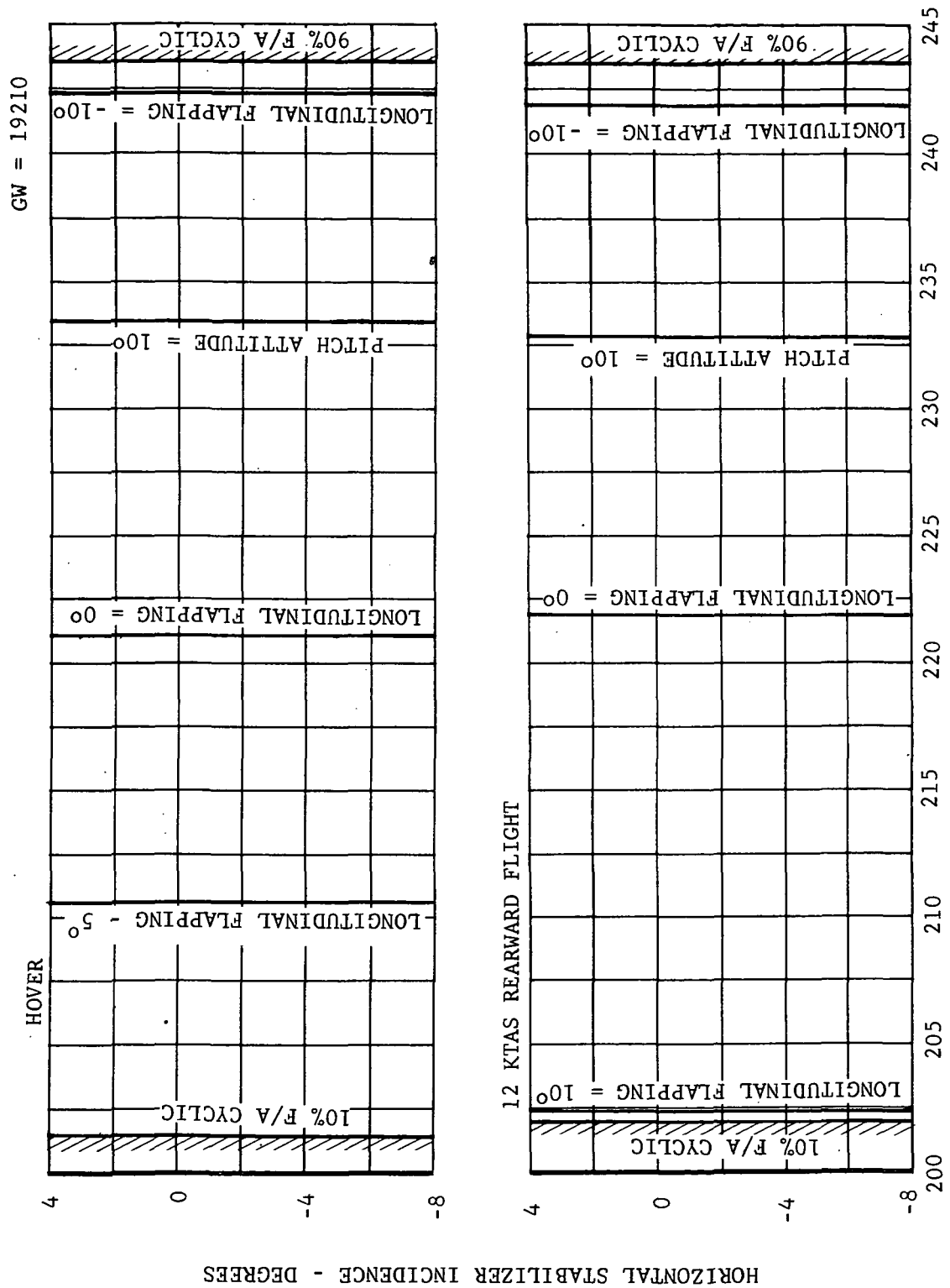


Figure 44. Model 646A Stabilizer Incidence Limits, Helicopter Configuration, Hover.

HORIZONTAL STABILIZER INCIDENCE - DEGREES

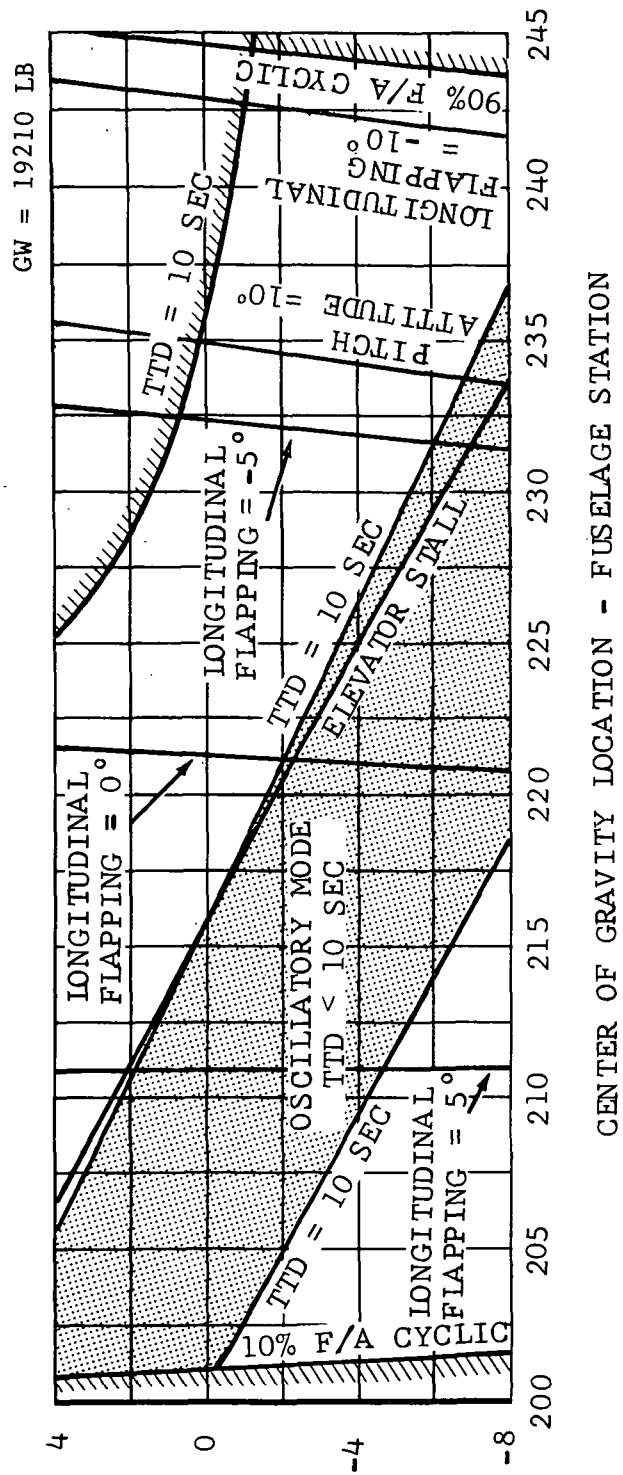


Figure 45. Model 646A Stabilizer Incidence Limits, Helicopter Configuration, 40 KTAS

HORIZONTAL STABILIZER INCIDENCE - DEGREES

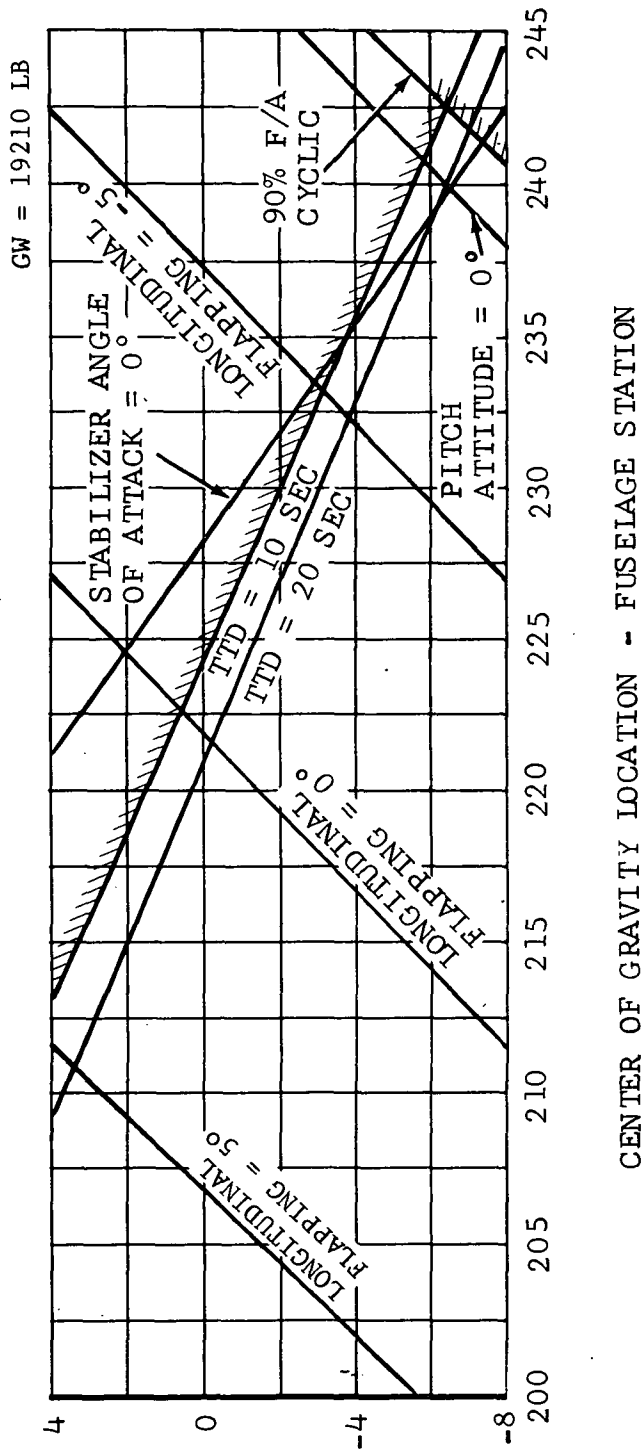


Figure 46. Model 646A Stabilizer Incidence Limits, Helicopter Configuration, 100 KTAS.

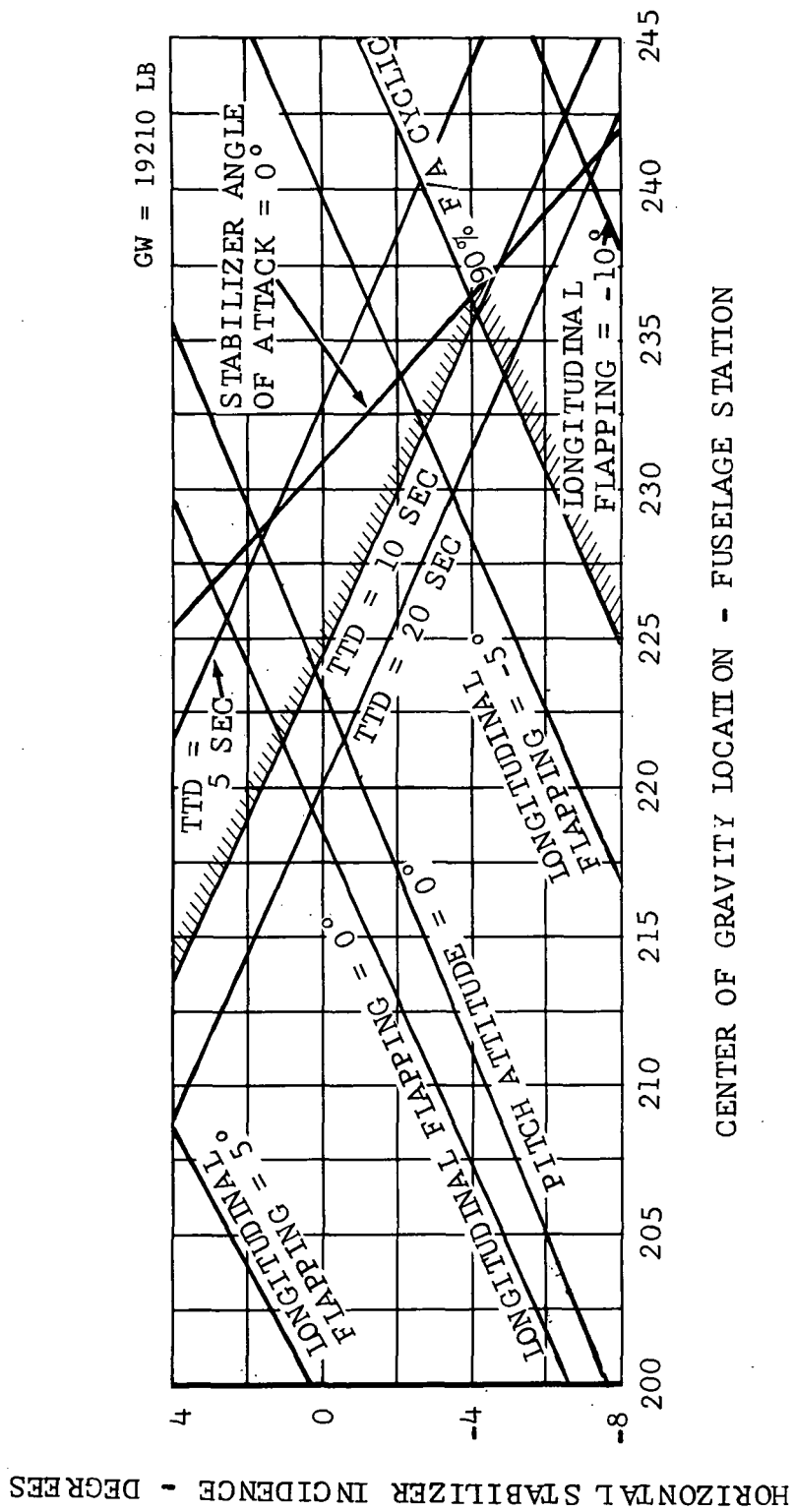
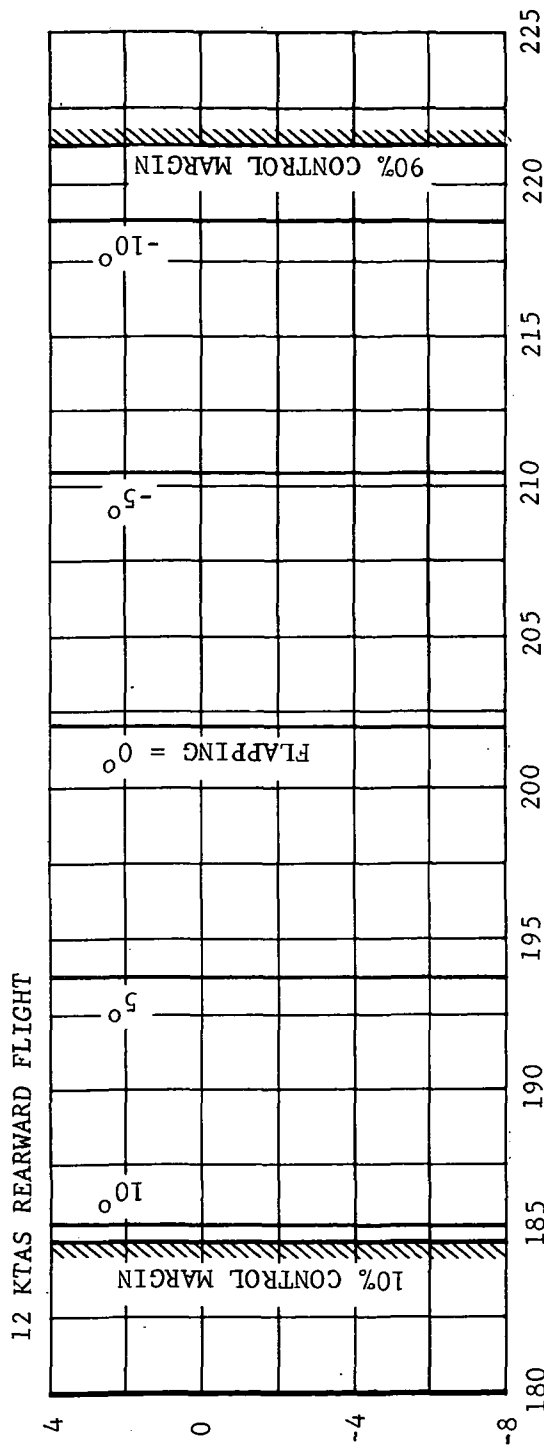
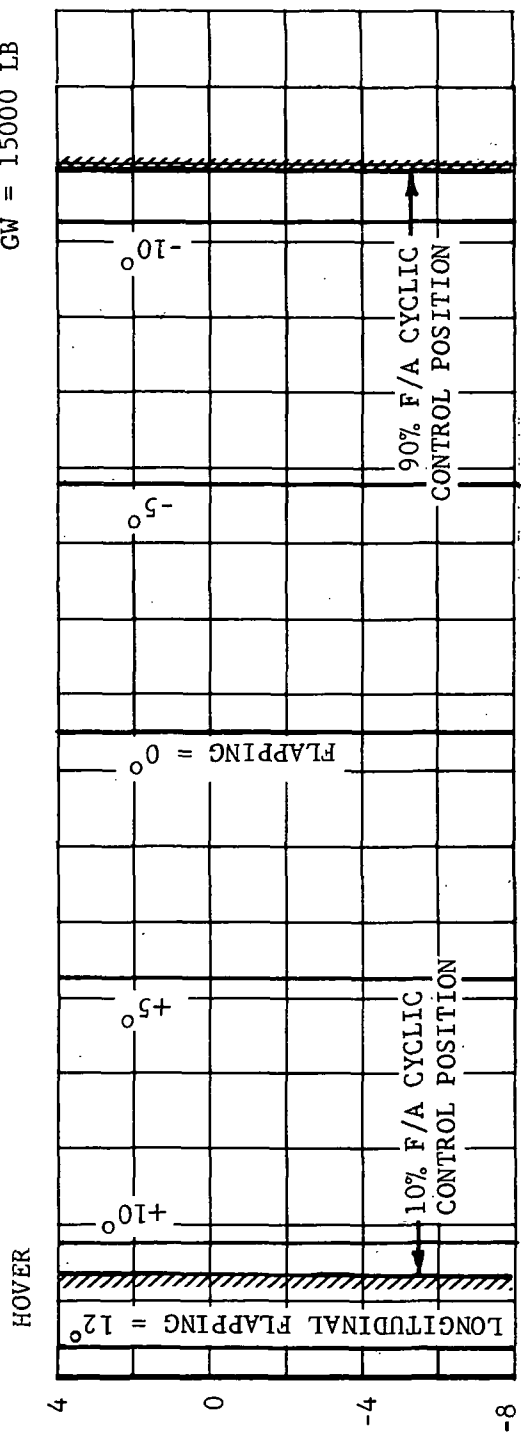


Figure 47. Model 646A Stabilizer Incidence Limits, Helicopter Configuration, 150 KTAS.

GW = 15000 LB



C.G. LOCATION - FUSELAGE STATION

Figure 48. Model 646B Stabilizer Incidence Limits, Helicopter Configuration, Hover.

HORIZONTAL STABILIZER INCIDENCE - DEG

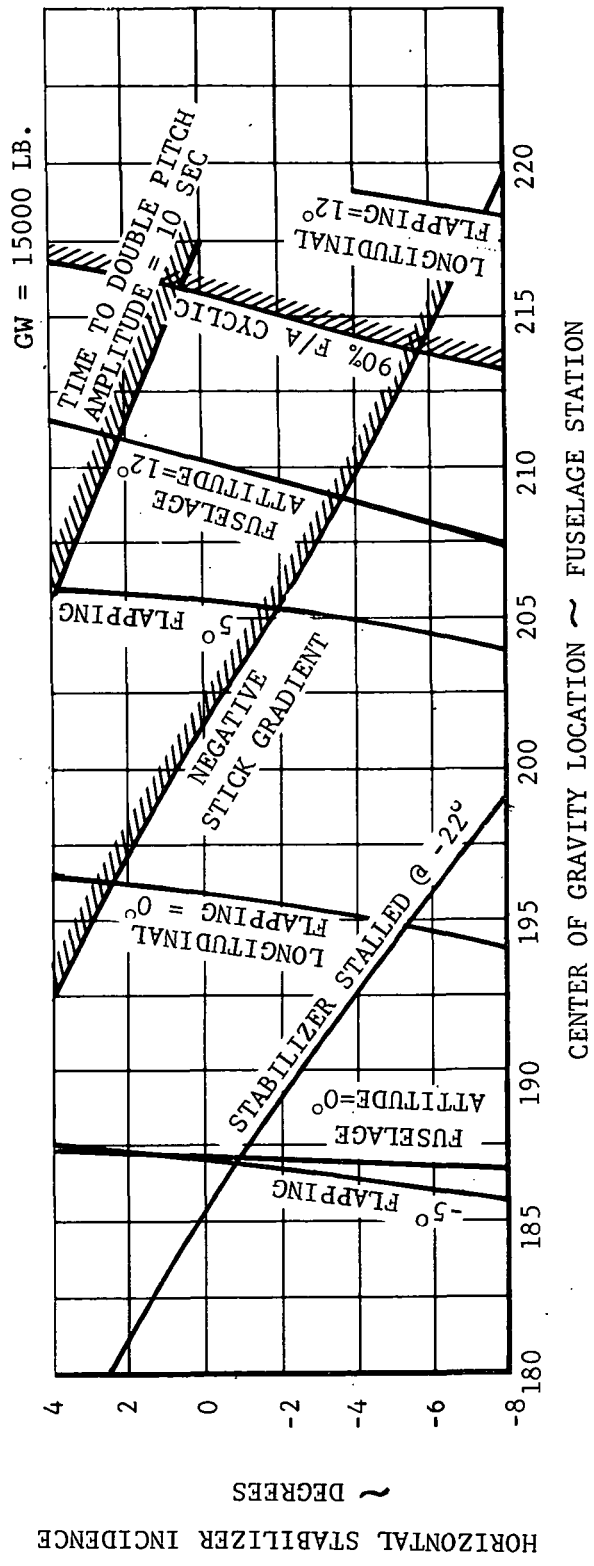


Figure 49. Model 646B Stabilizer Incidence Limits, Helicopter Configuration, 40 KTAS.

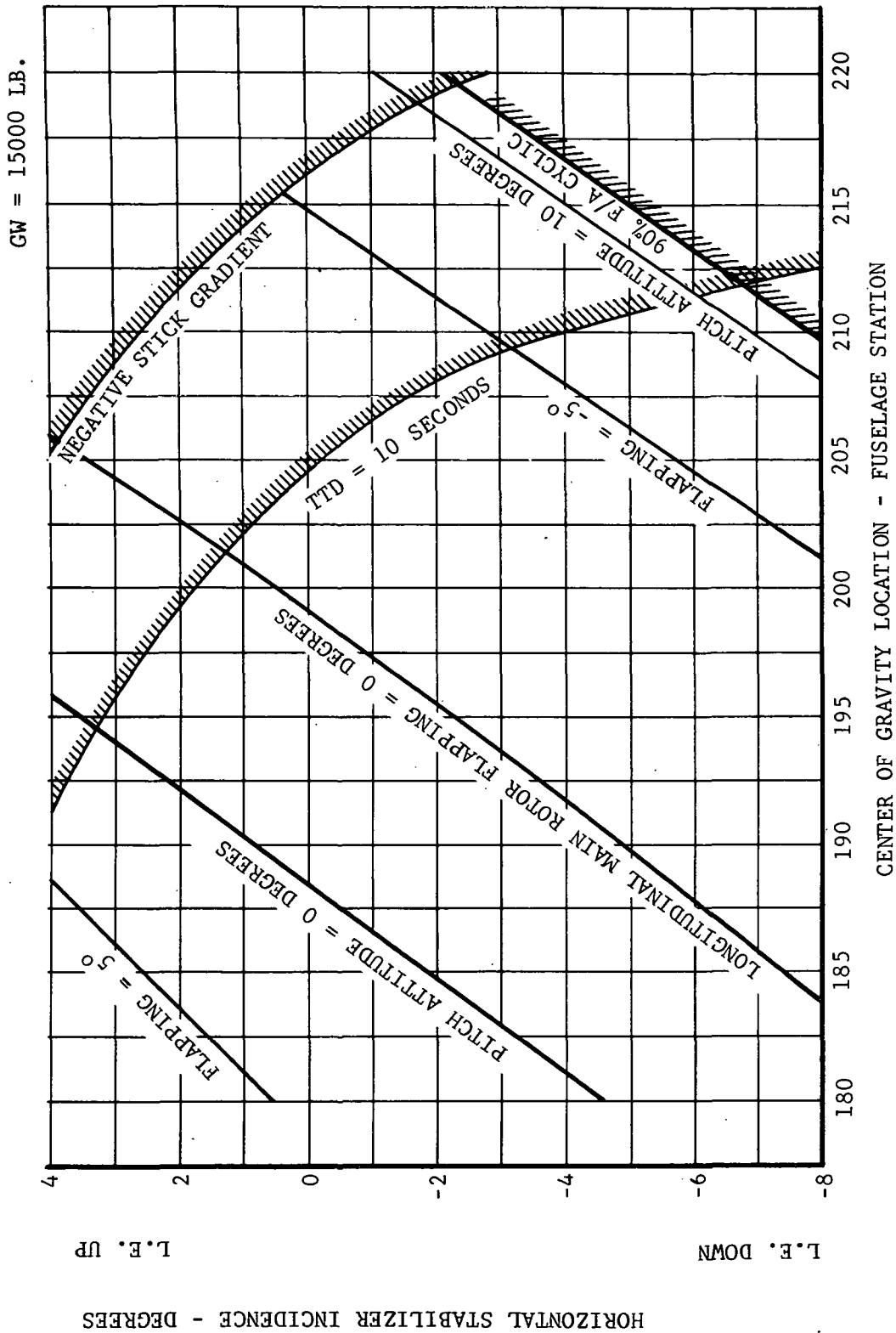


Figure 50. Model 646B Stabilizer Incidence Limits, Helicopter Configuration, 100 KTAS.

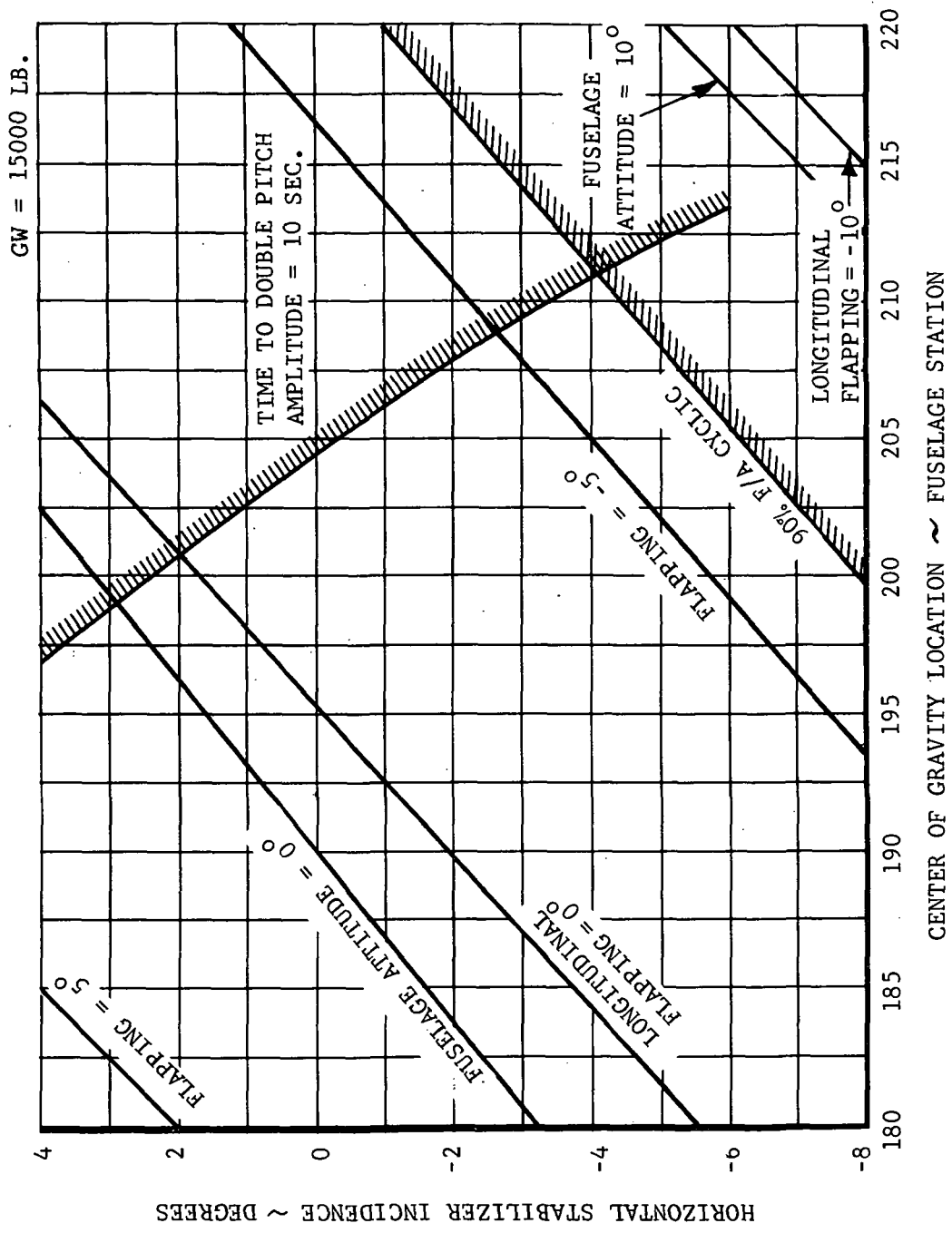


Figure 51. Model 646B Stabilizer Incidence Limit, Helicopter Configuration, 130 KTAS.

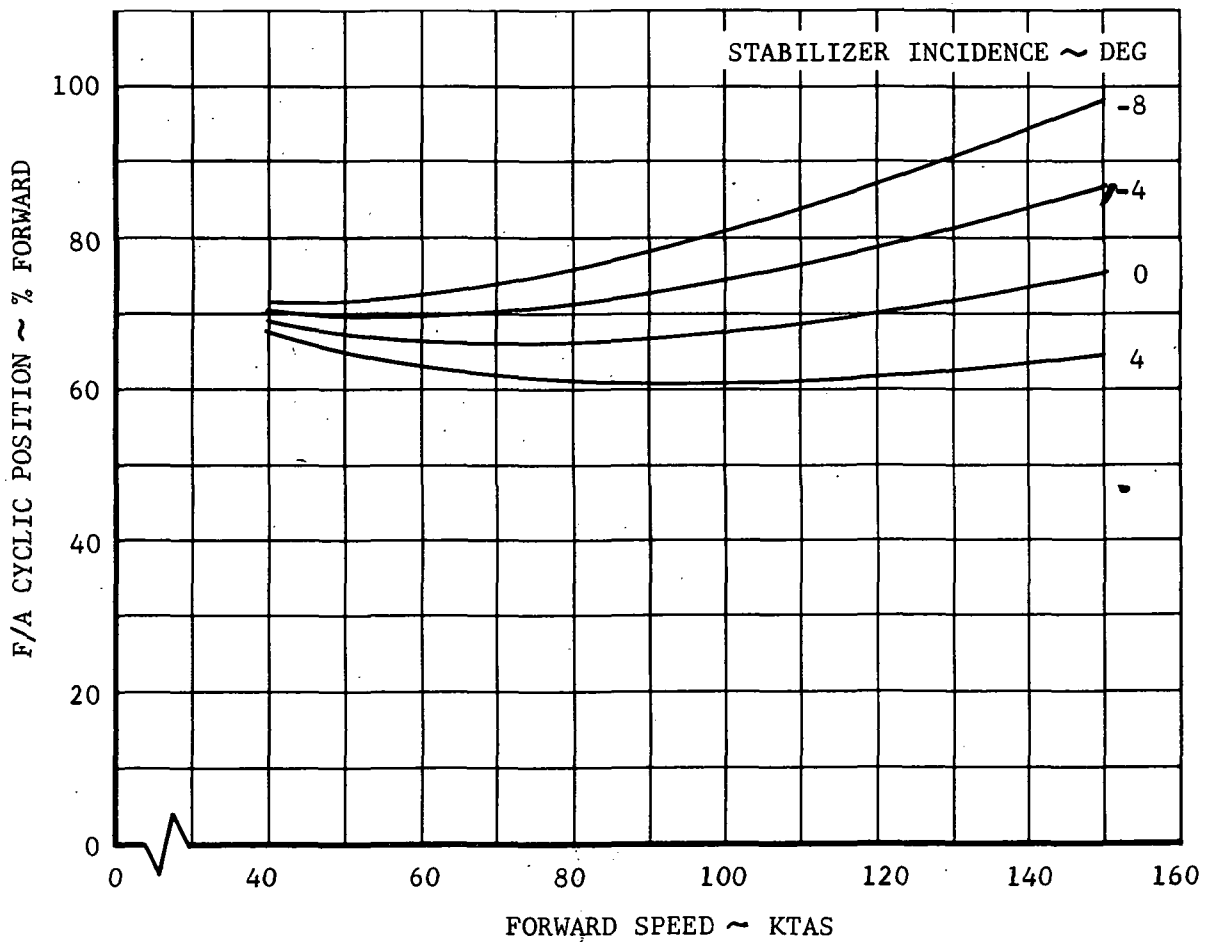


Figure 52. Model 646A Fore and Aft Cyclic Position Variation with Stabilizer Incidence, Helicopter Configuration.

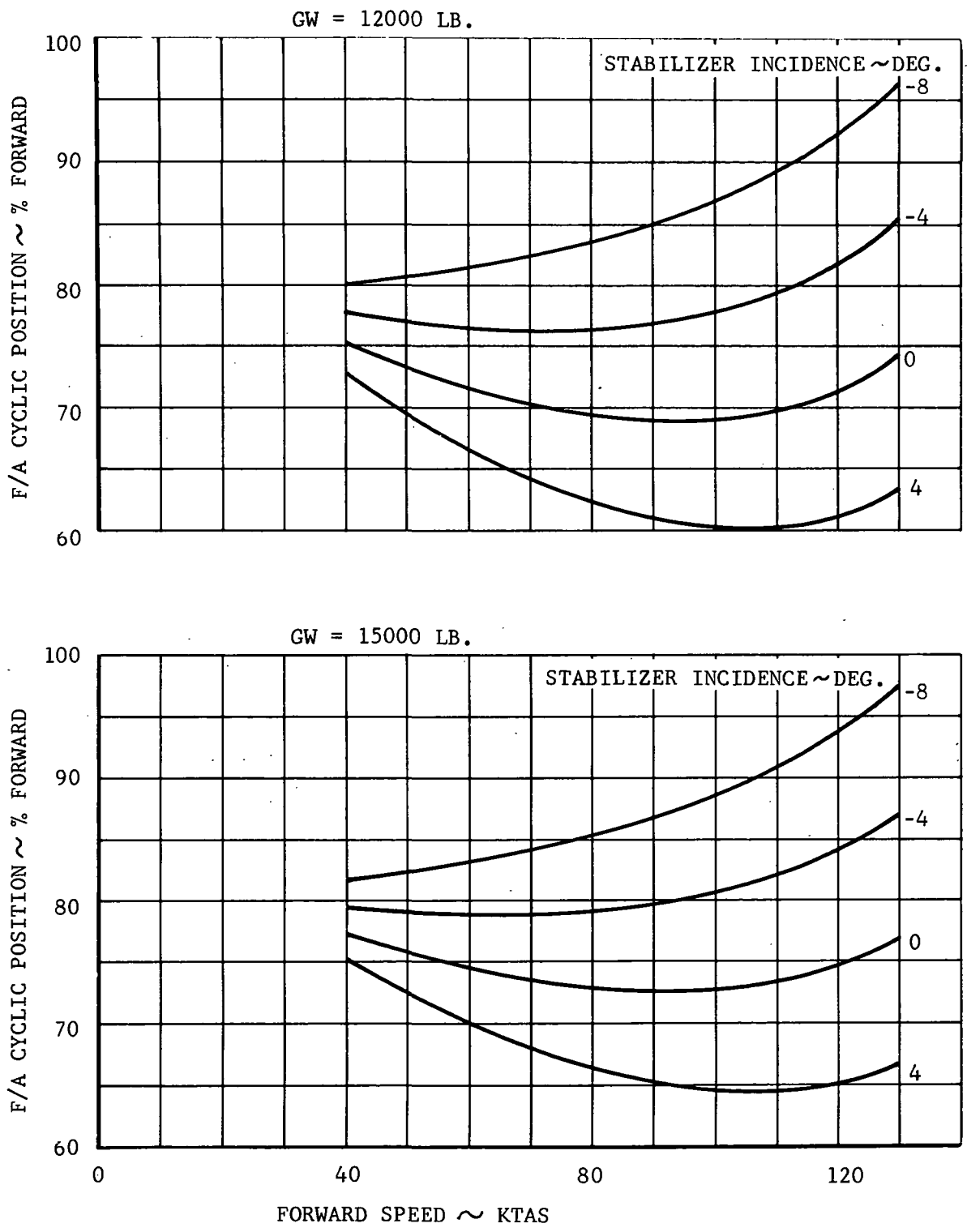


Figure 53. Model 646B Fore and Aft Cyclic Position Variation with Stabilizer Incidence, Helicopter Configuration.

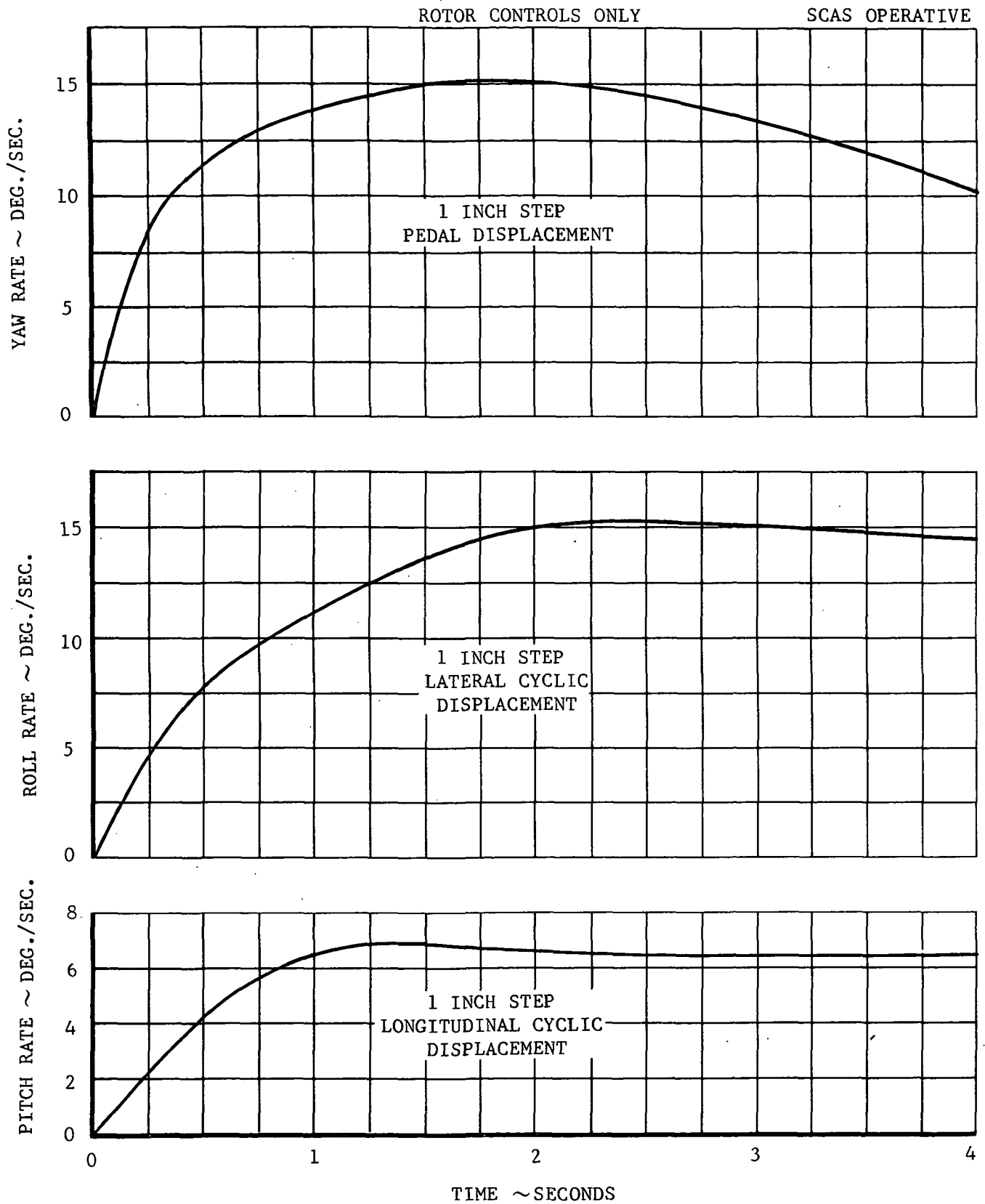


Figure 54. Model 646A Response to Step Control Inputs, Compound Configuration, Hover, SCAS Operative.

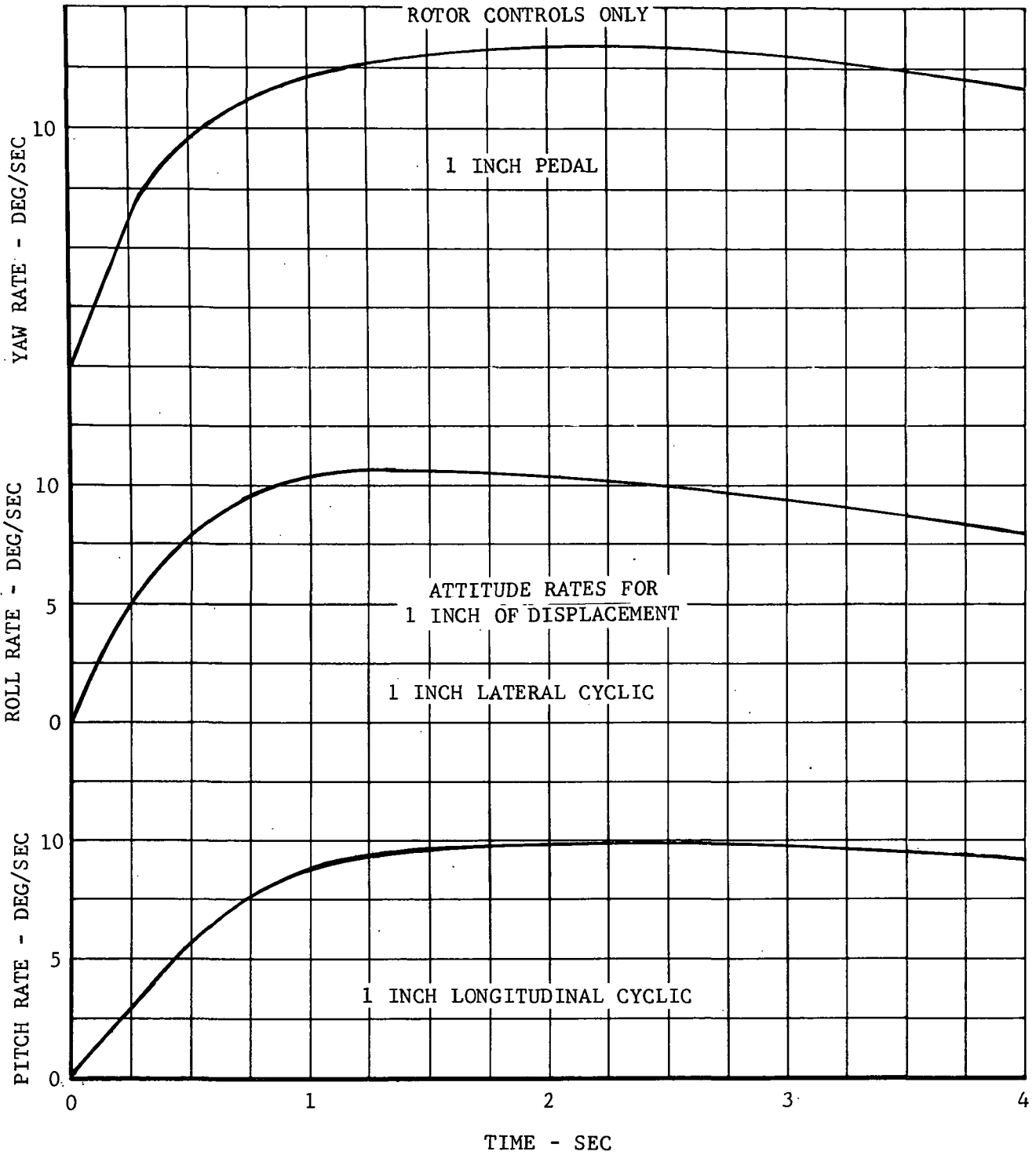
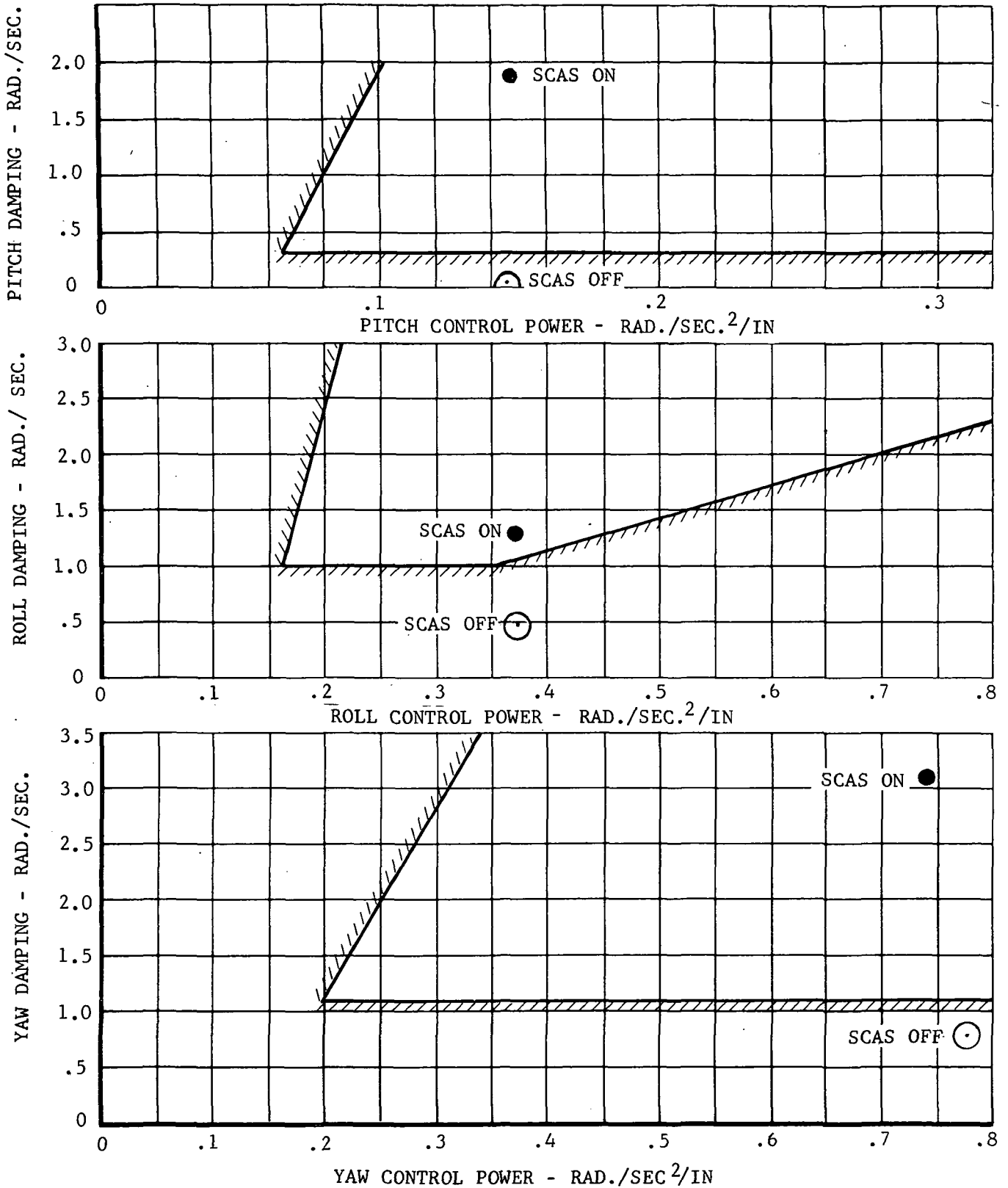


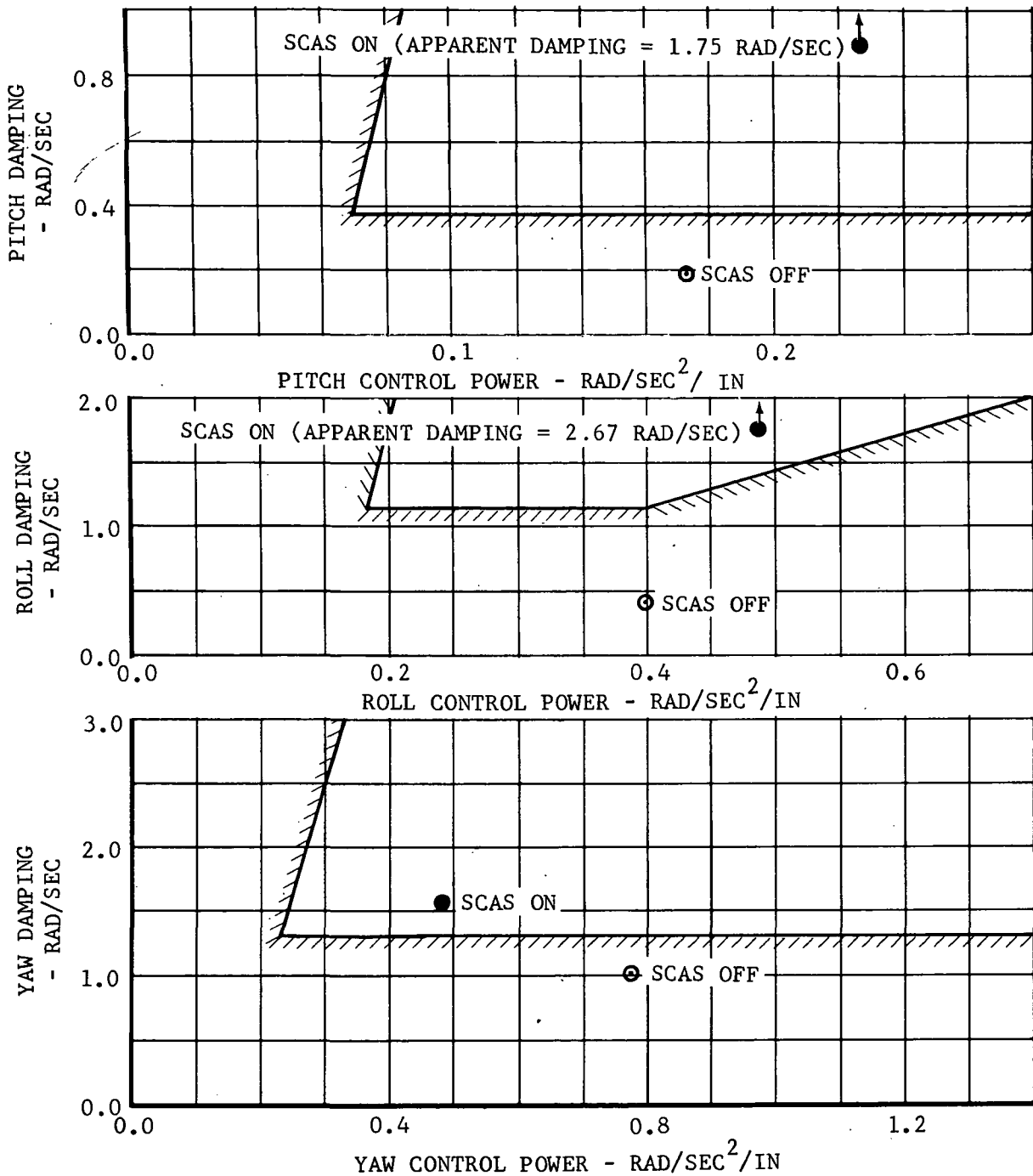
Figure 55. Model 646B Response to Step Control Inputs, Compound Configuration, Hover, SCAS Operative.

GW/CG = 19210/223



BOUNDARIES SHOWN ARE THE VFR REQUIREMENTS OF MIL-H-8501A

Figure 56. Control Power and Damping in Hover for the Model 646A, Compound Configuration (SCAS Off and On).



BOUNDARIES SHOWN ARE THE VFR REQUIREMENTS OF MIL-H-8501A

Figure 57. Control Power and Damping in Hover for the Model 646B, Compound Configuration (SCAS Off and On).

FIXED WING CONTROLS ONLY

SCAS OPERATIVE

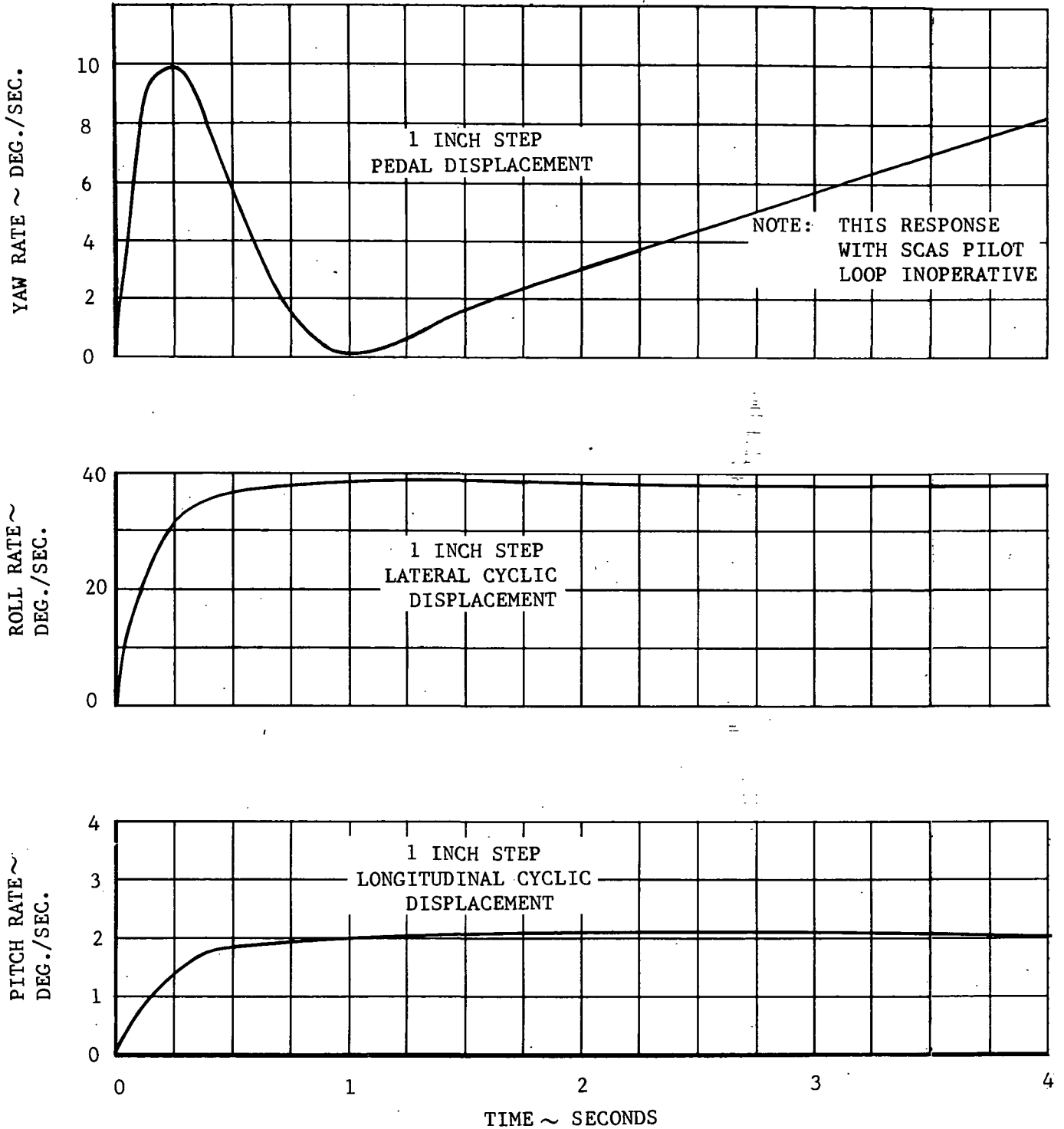


Figure 58. Model 646A Response to Step Control Inputs, Compound Configuration, 300 KTAS, SCAS Operative.

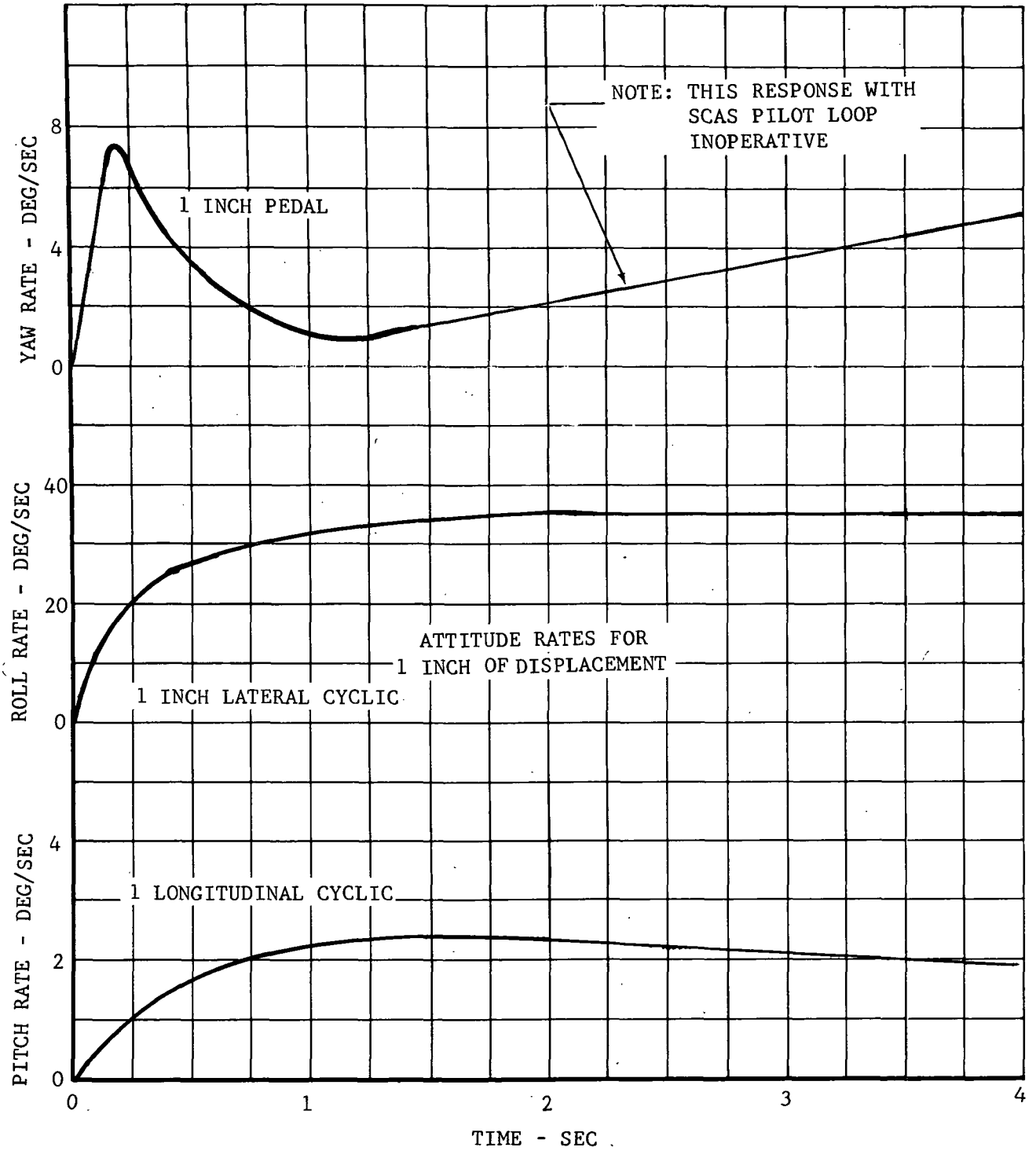
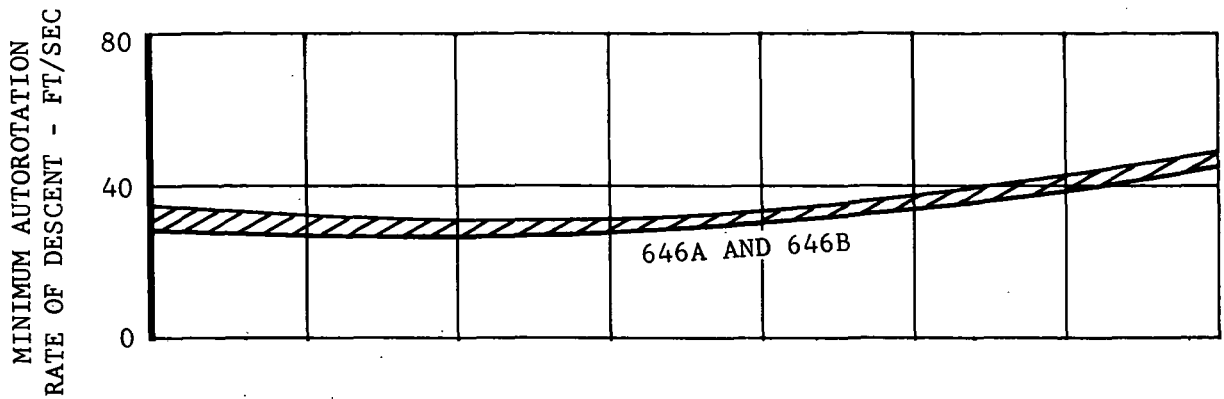


Figure 59. Model 646B Response to Step Control Inputs, Compound Configuration, 300 KTAS, SCAS Operative.



ALL DATA FOR ZERO-POWER (SHAFT AND JET) TRIMS AT ZERO PITCH ATTITUDE

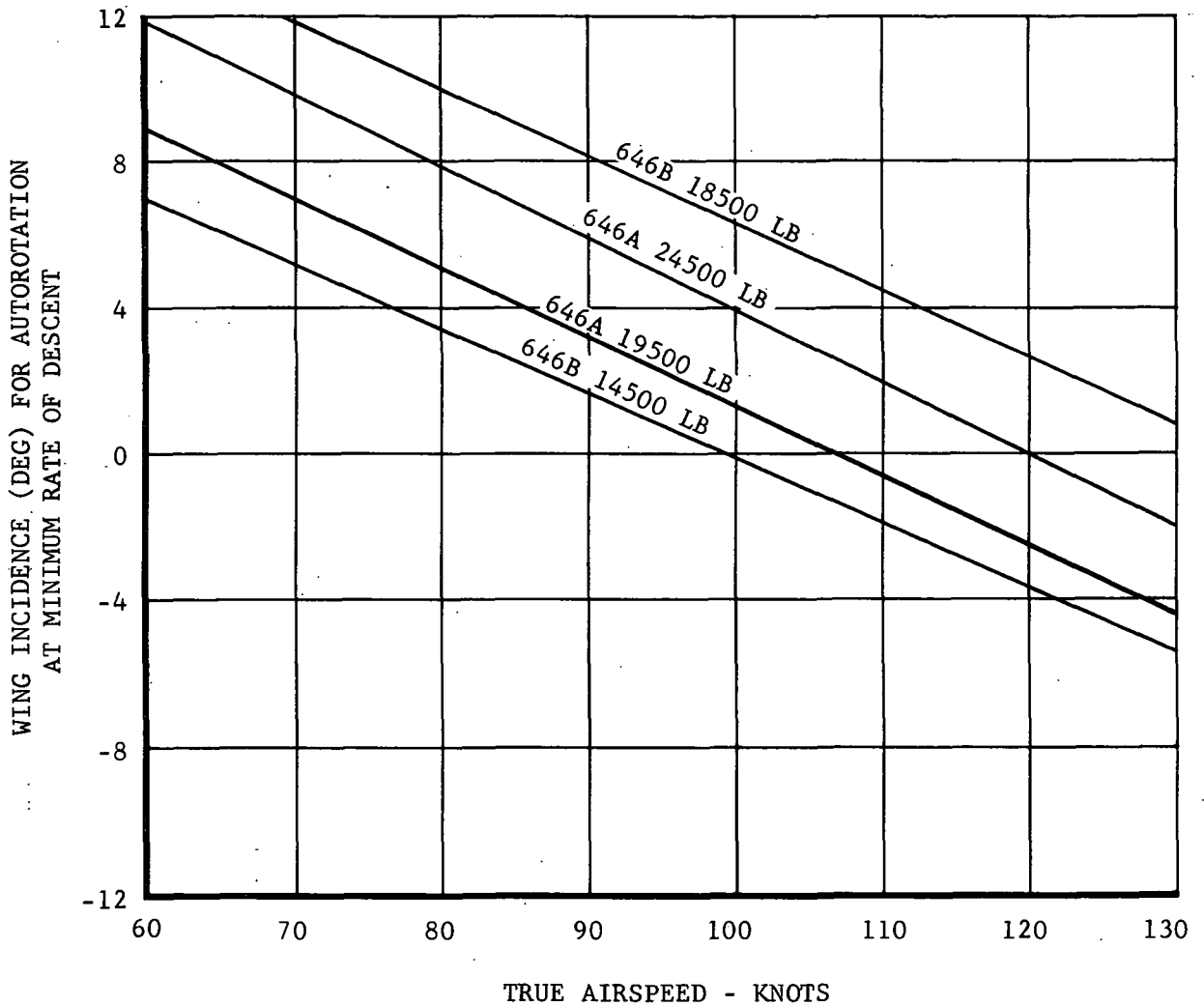


Figure 60. Wing Incidence for Autorotation at Minimum Rate of Descent.

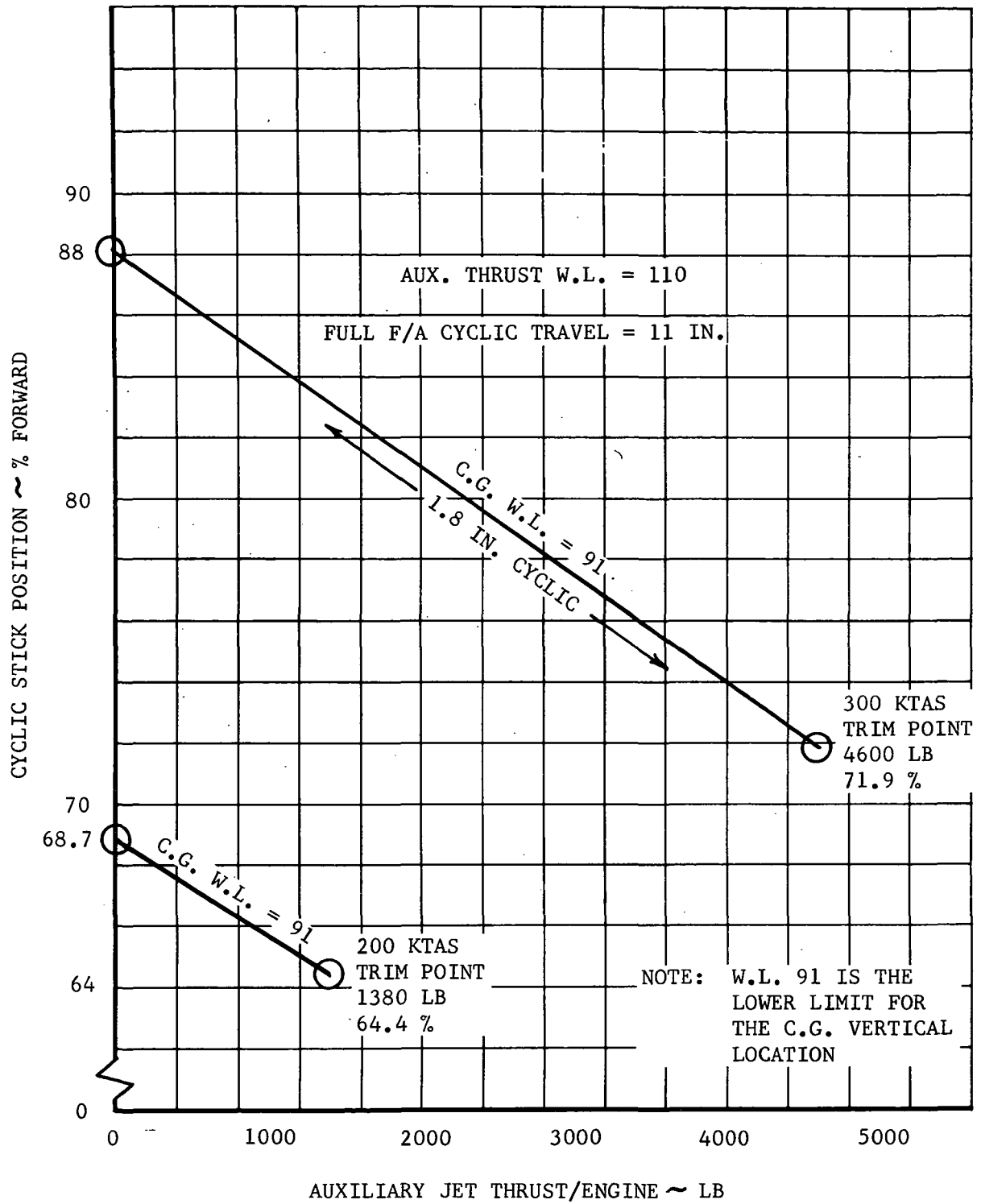


Figure 61. Model 646A Trim Change with Auxiliary Jet Thrust, Compound Configuration.

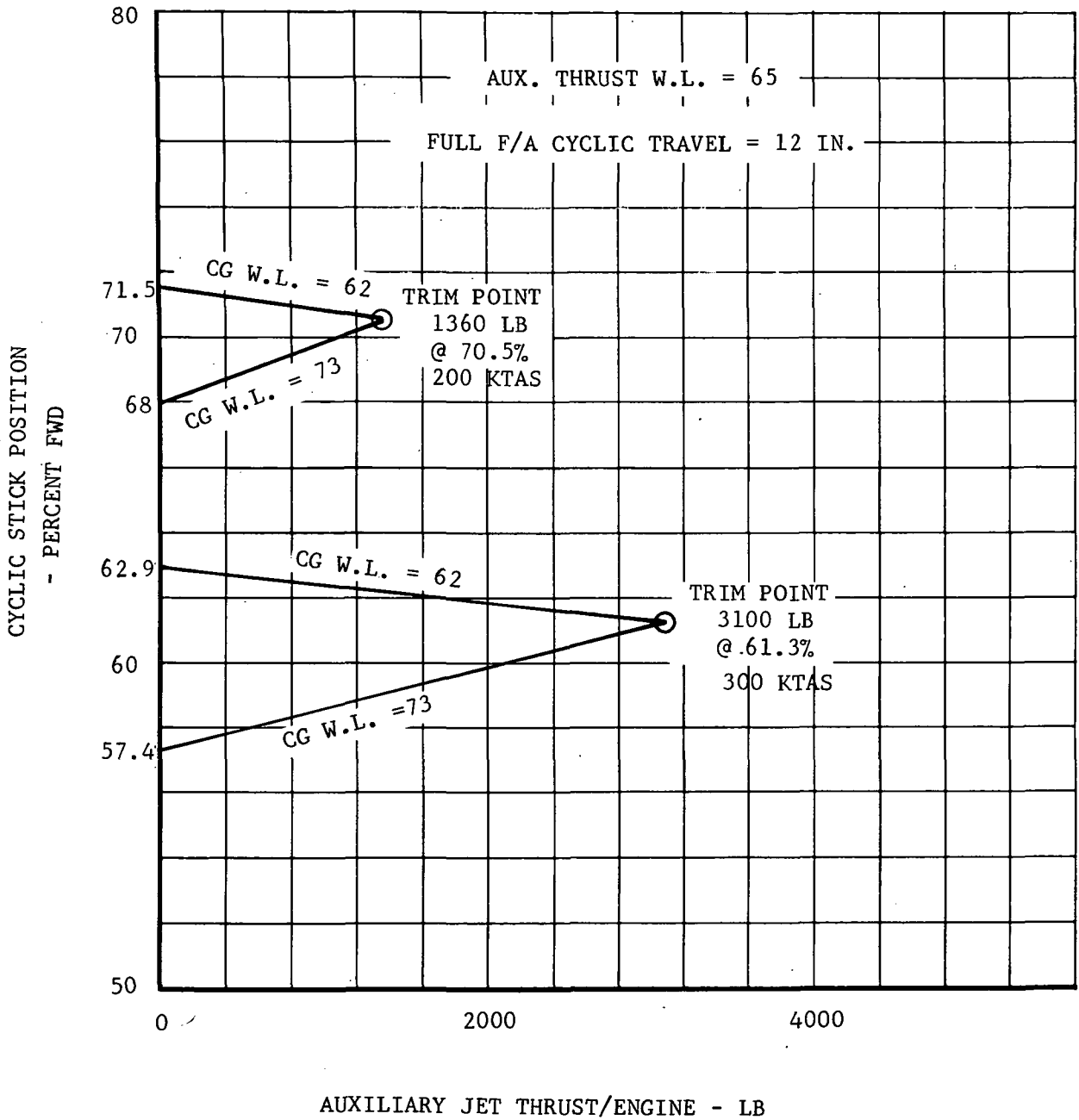


Figure 62. Model 646B Trim Change with Auxiliary Jet Thrust, Compound Configuration.

NOTE: NUMBERS INDICATE NASTRAN CONTROL POINTS

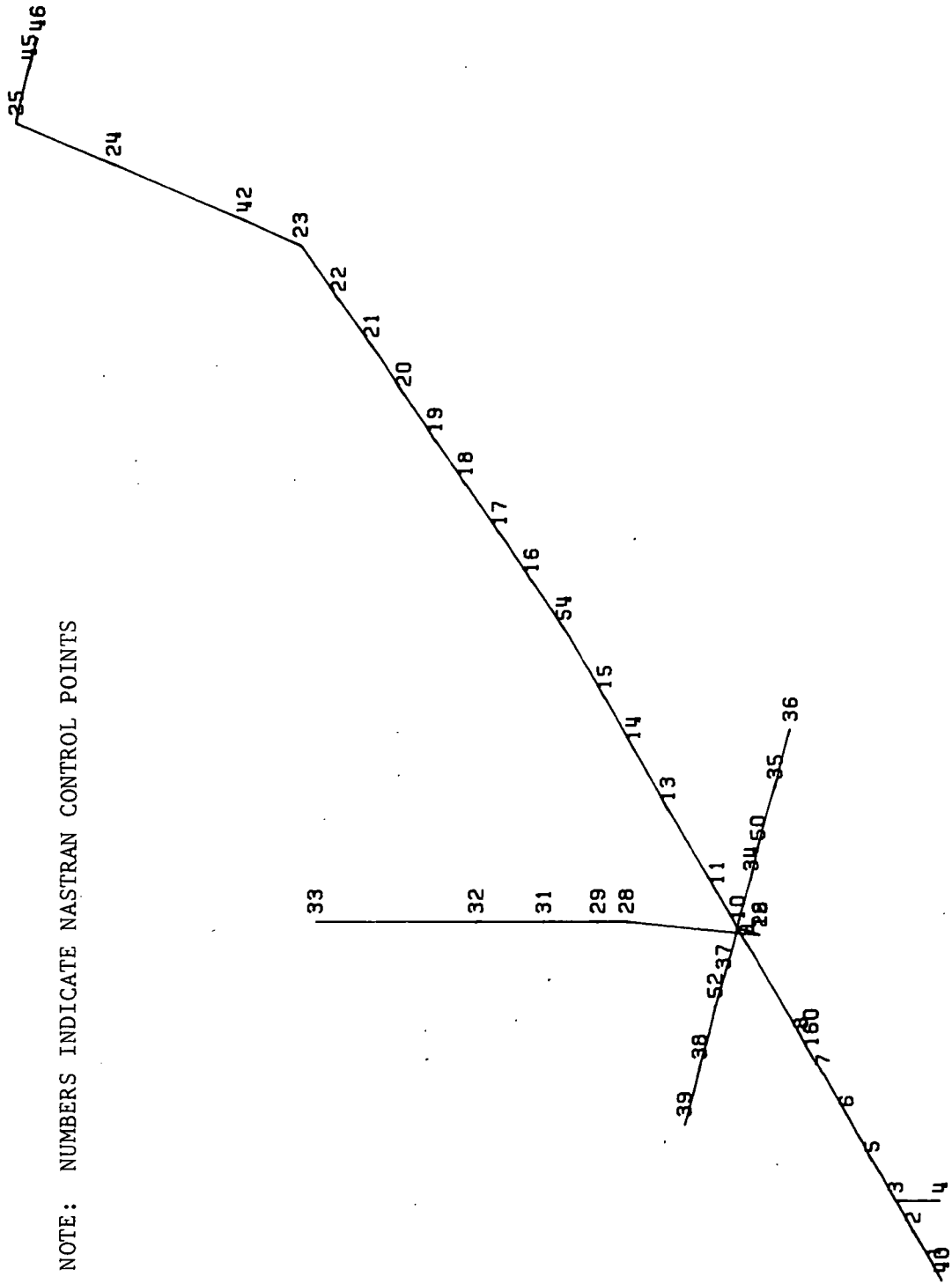


Figure 63. RSRA 646B Fuselage Analytical Model.

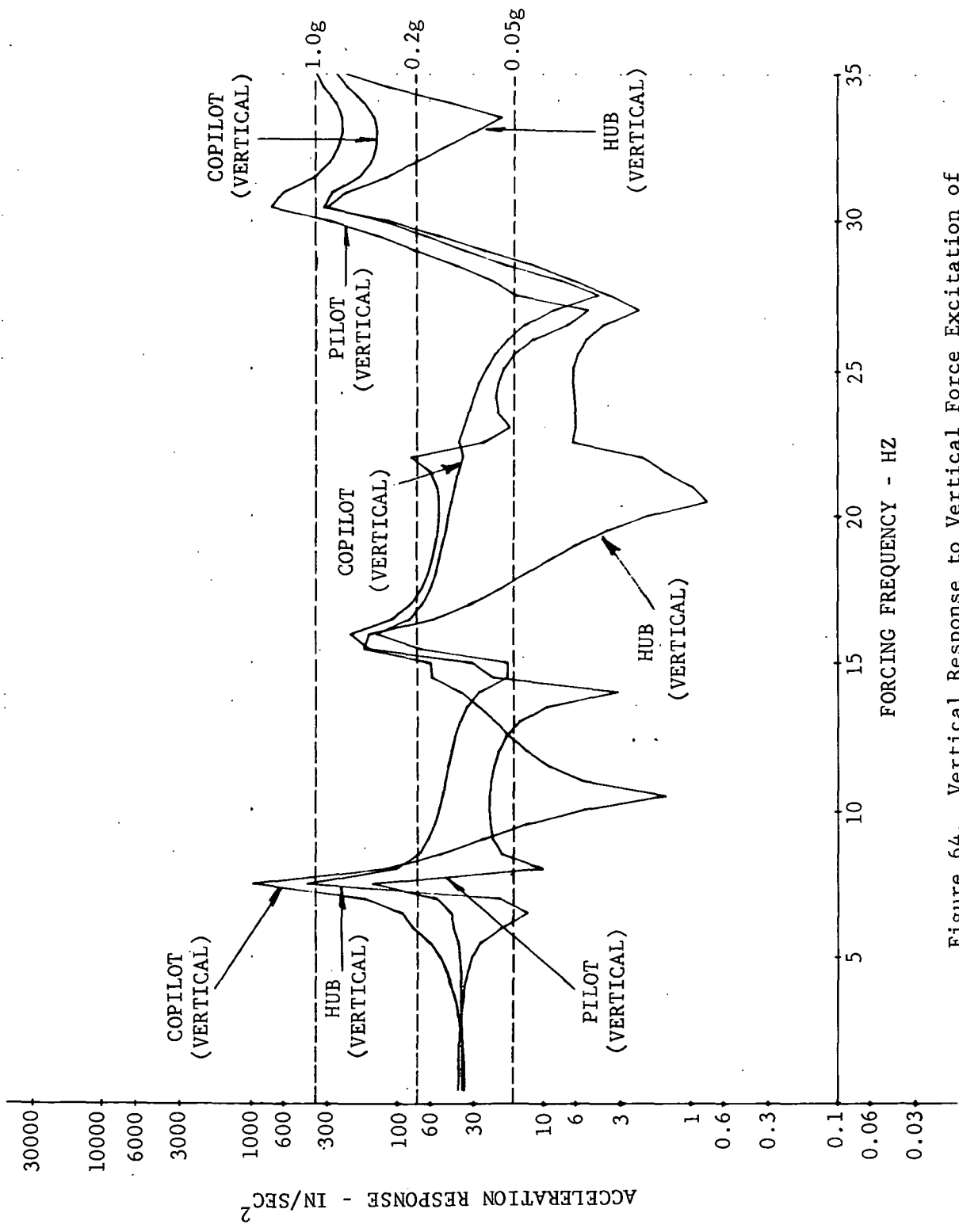


Figure 64. Vertical Response to Vertical Force Excitation of 646B Without Vertical Isolation.

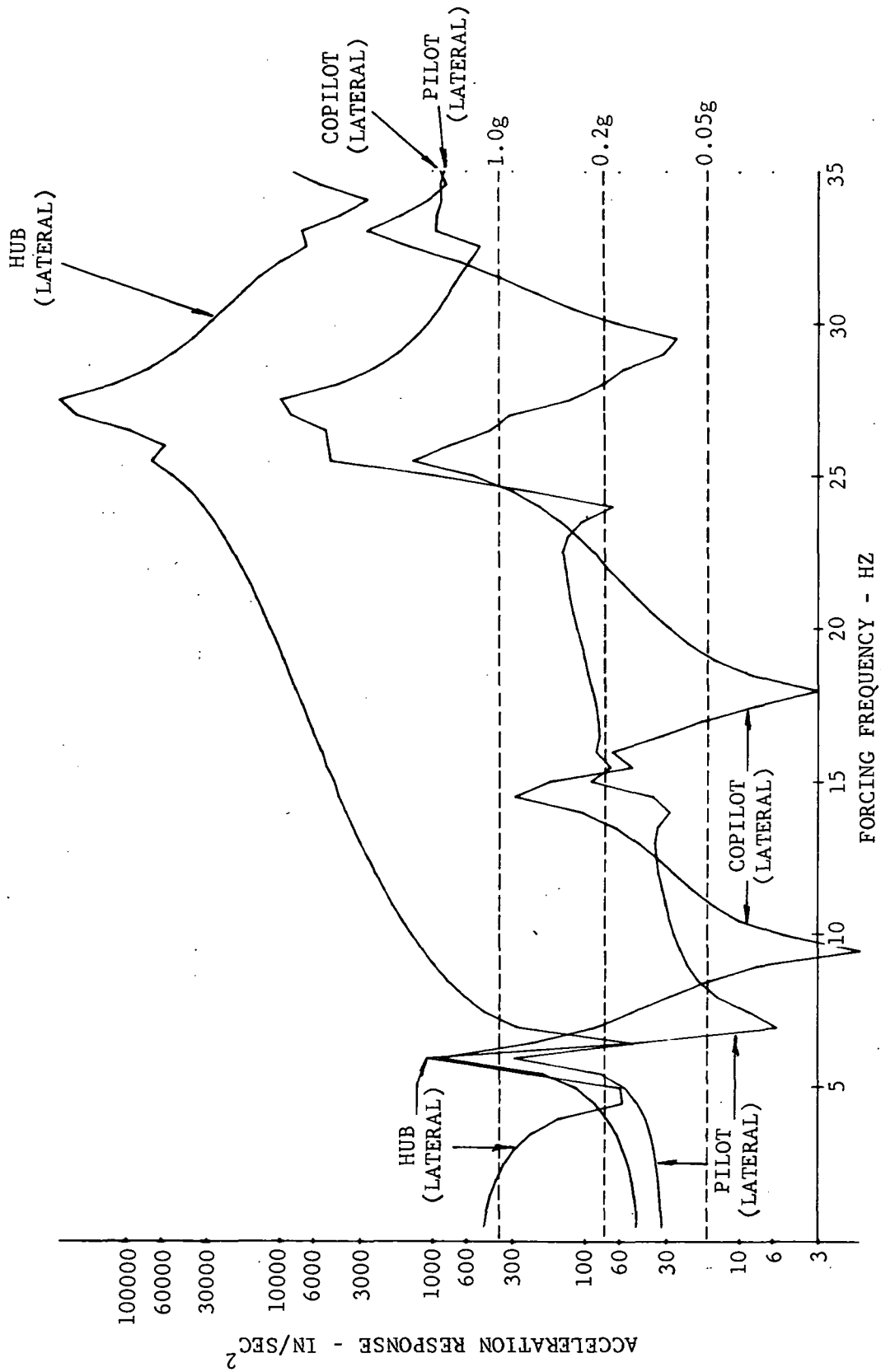


Figure 65. Vertical Response to Lateral Force Excitation of 646B Without Roll Isolation.

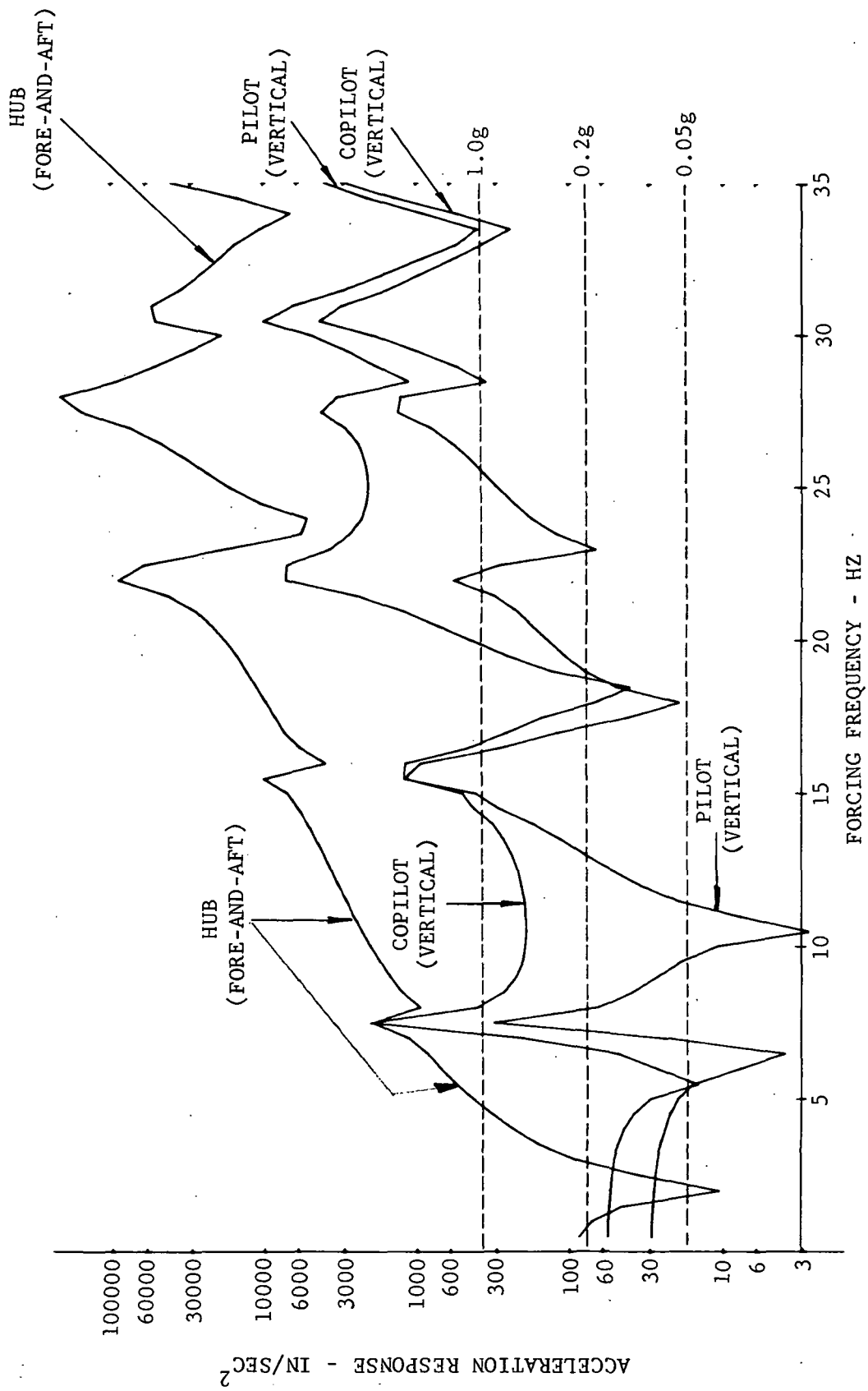


Figure 66. Vertical Response to Fore and Aft Force Excitation of 646B Without Pitch Isolation.

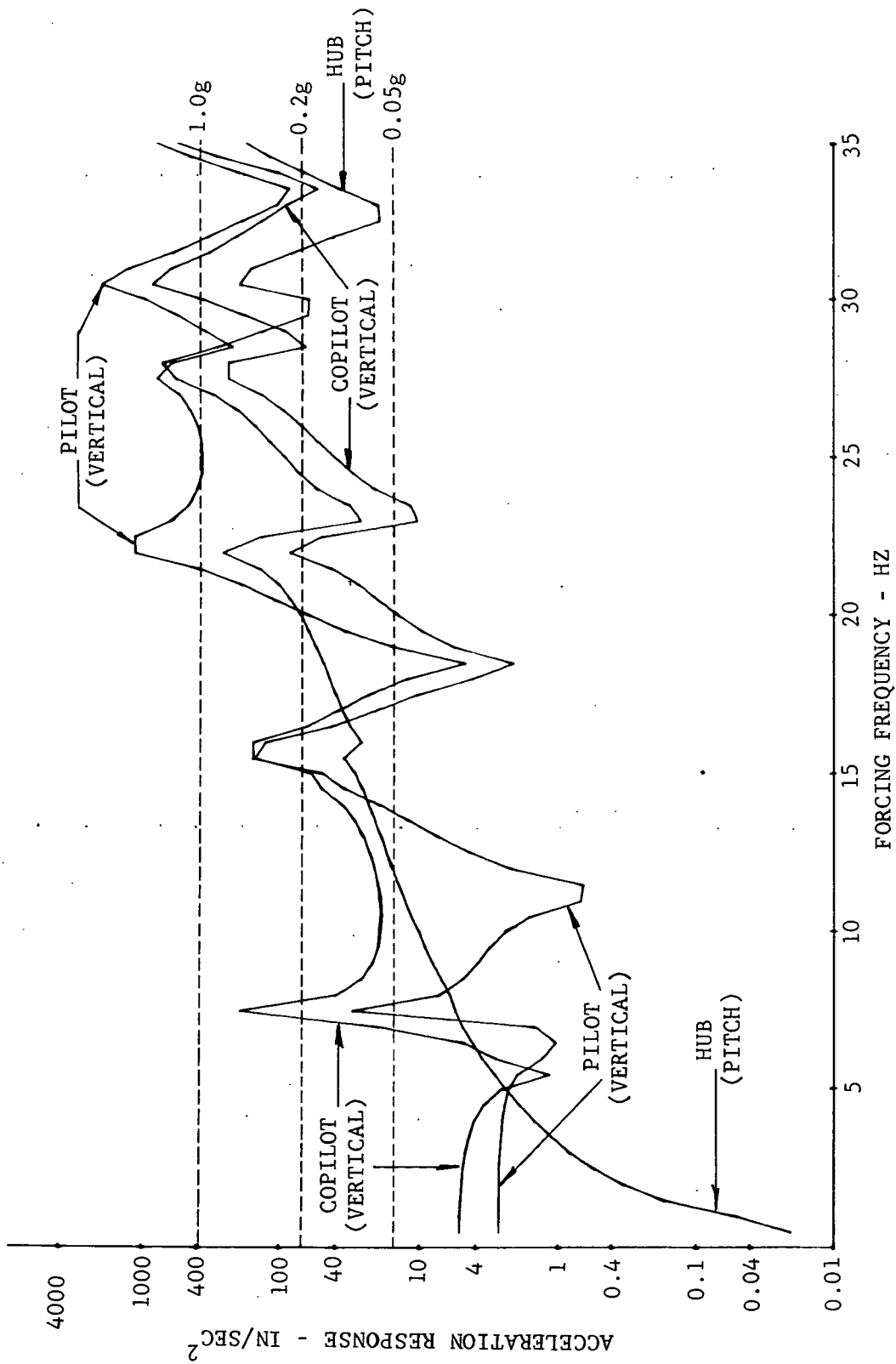


Figure 67. Vertical Response to Pitching Moment Excitation of 646B Without Pitch Isolation.

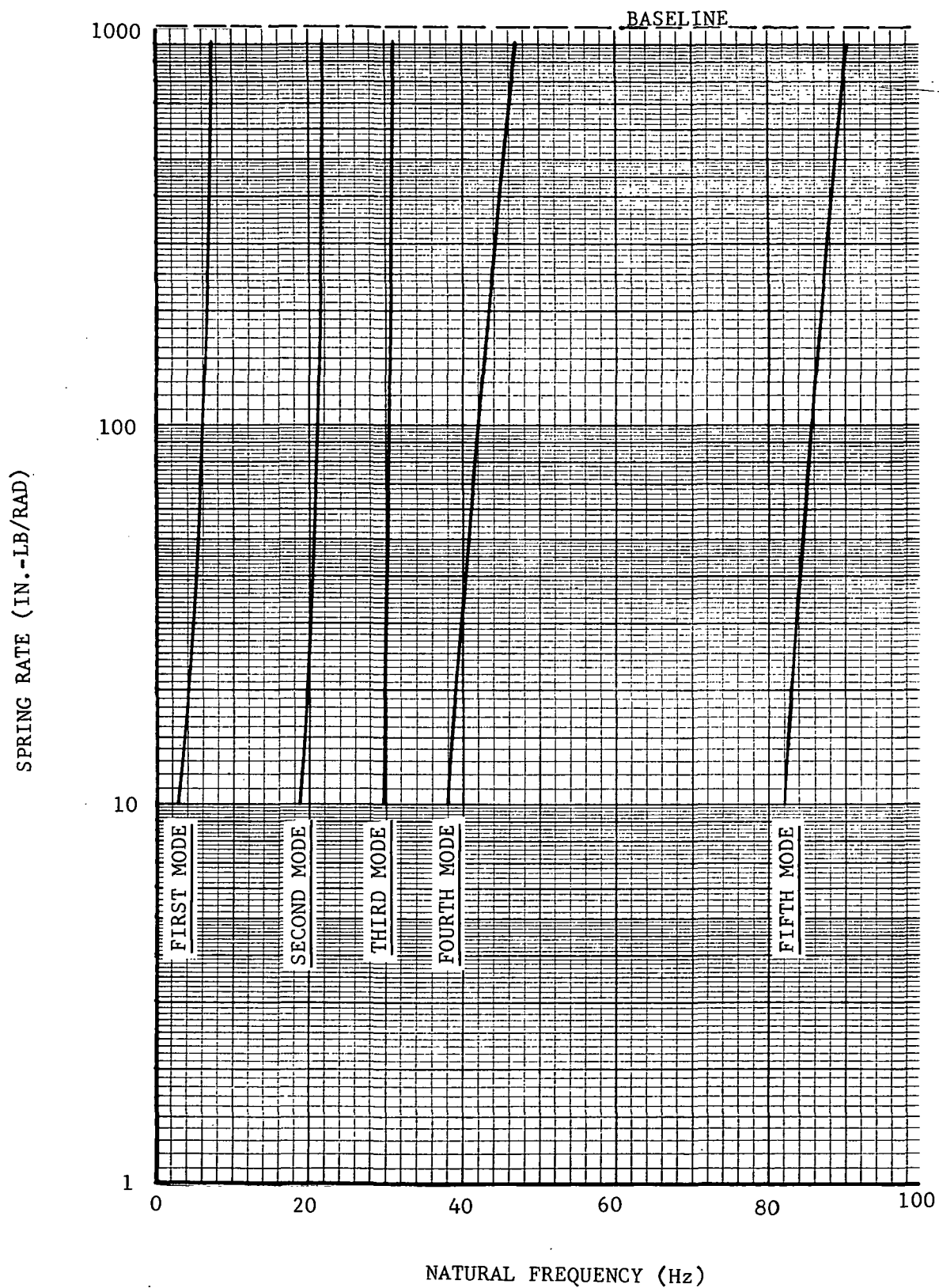


Figure 68. Fuselage Vertical Natural Frequencies as a Function of Tail Boom Junction Moment Restraint Stiffness.

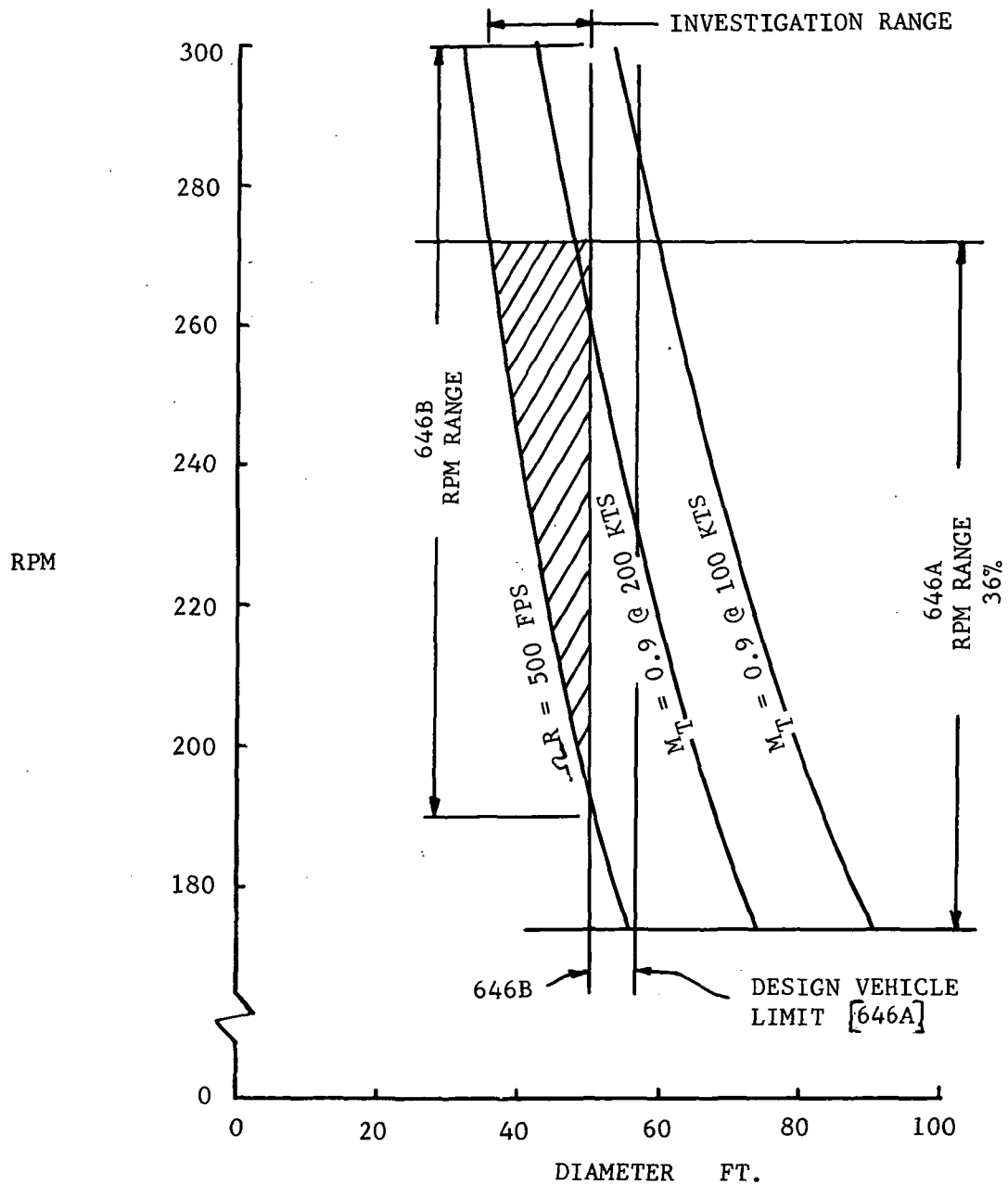


Figure 69. Rotor Size and Rotational Speed Design Envelope.

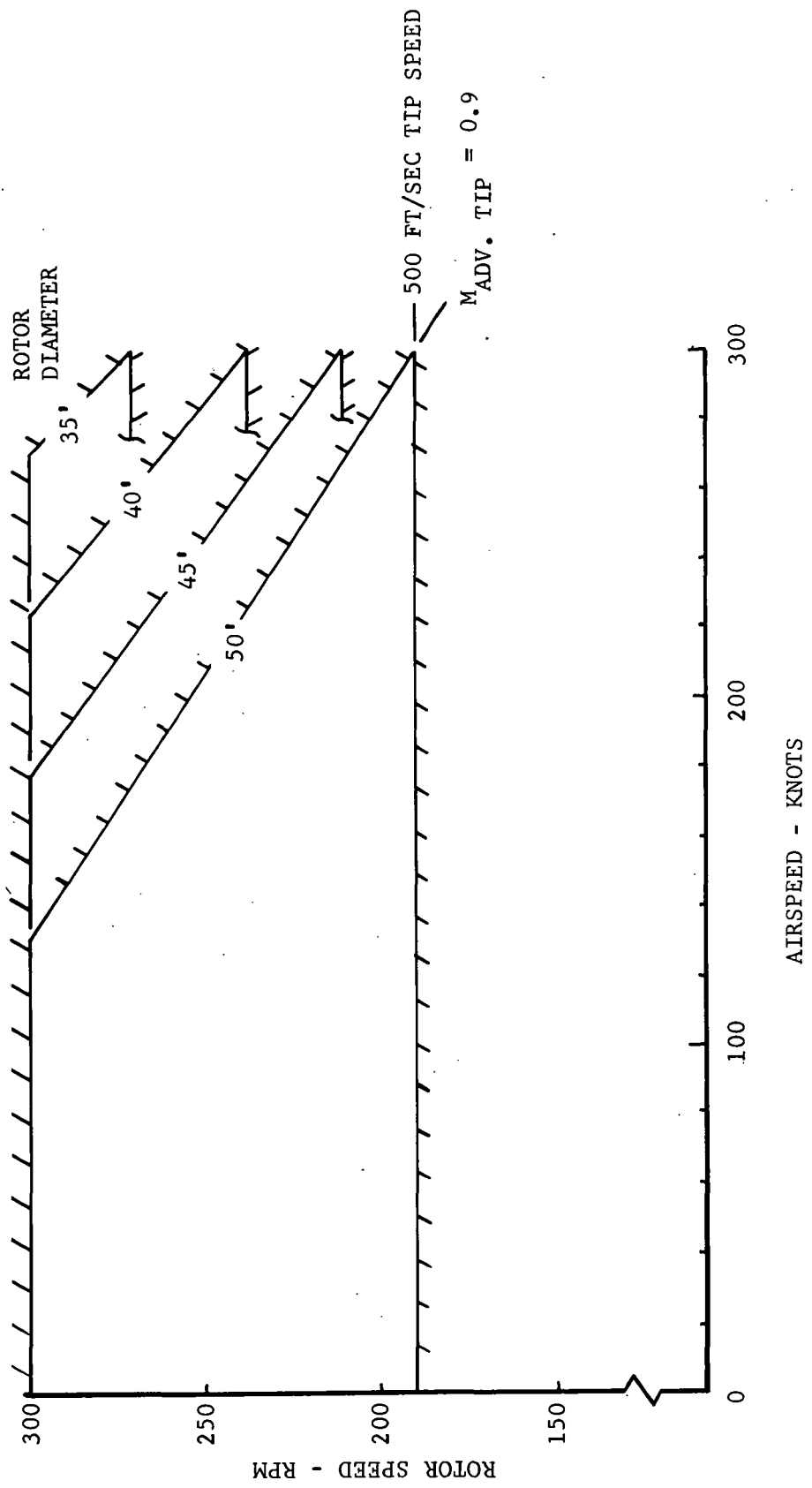


Figure 70. Rotor Operational Envelope.

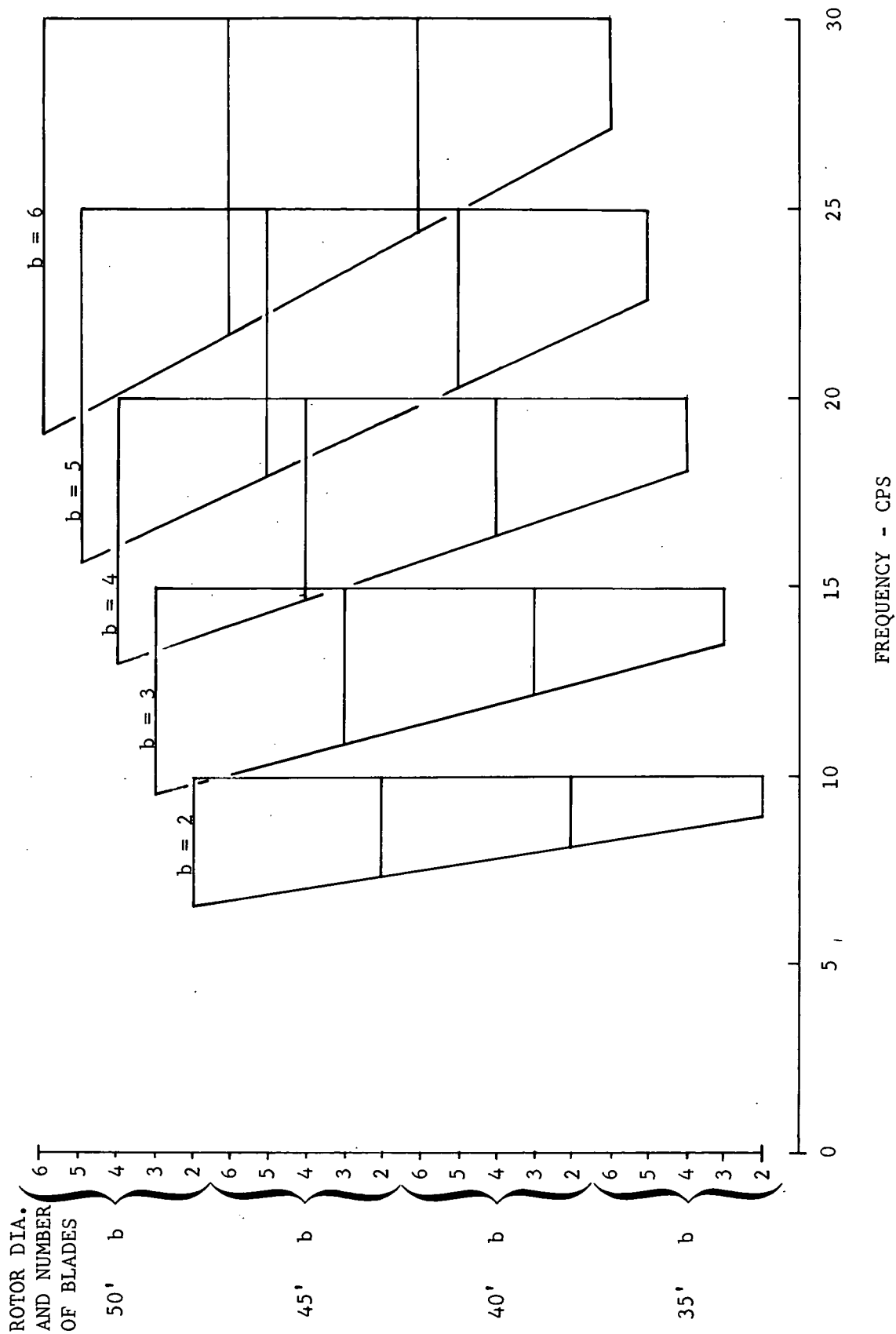


Figure 71. Frequency of Predominant Harmonic as a Function of Rotor Diameter and Number of Blades.

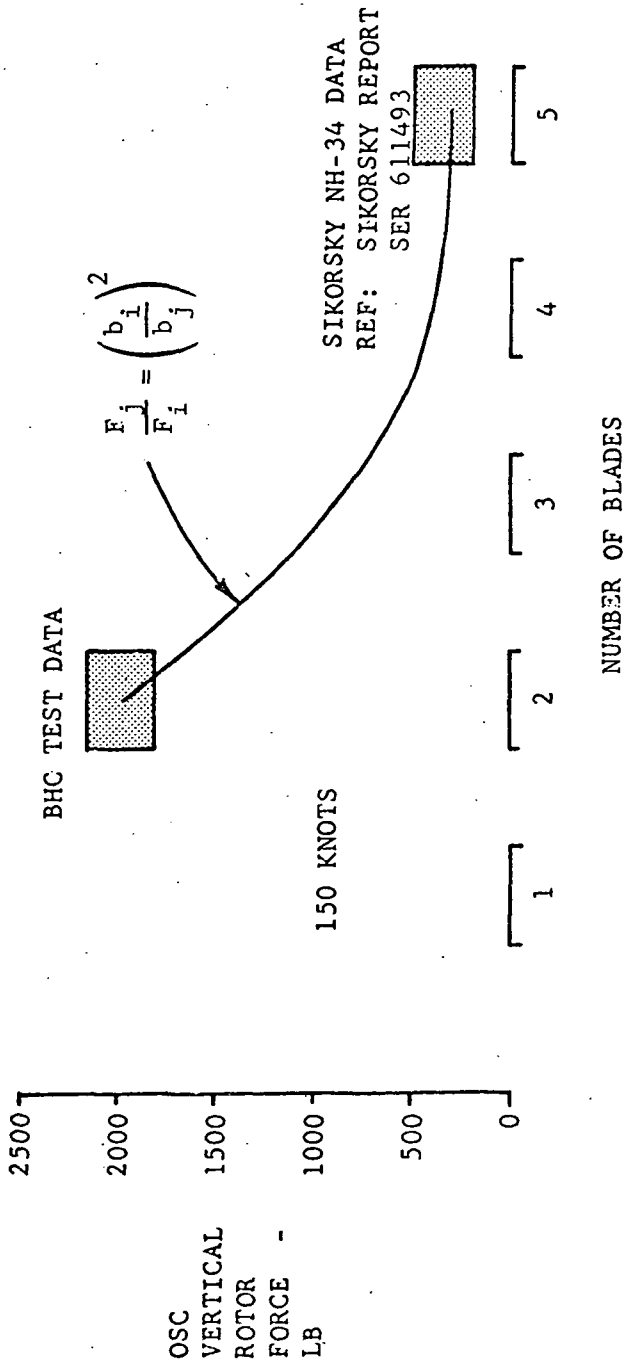


Figure 72. Oscillatory Vertical Rotor Force Versus Number of Blades.

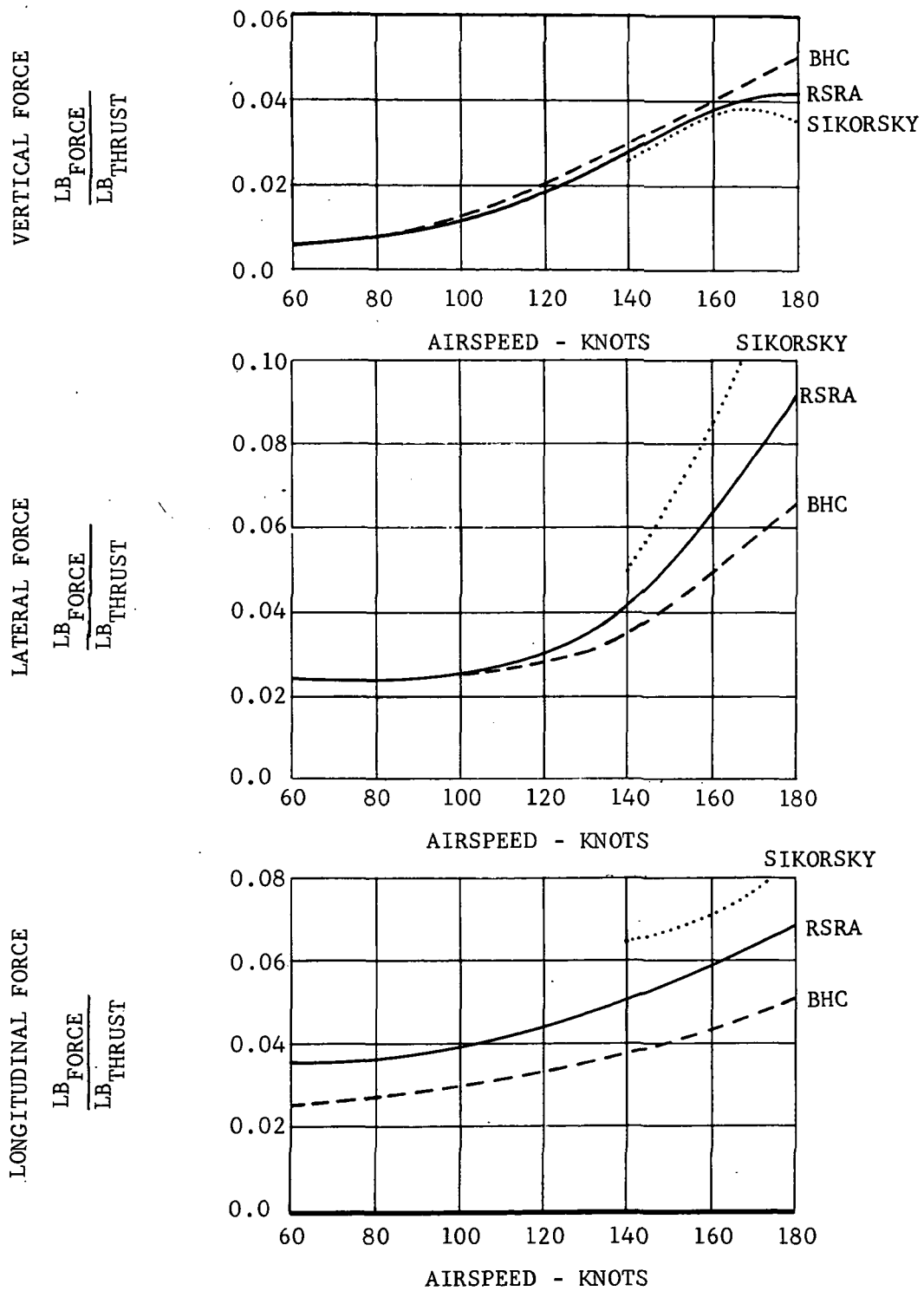


Figure 73. Rotor Hub Oscillatory Forces Normalized on Five-Bladed Rotor Versus Airspeed.

RSRA - BRAM

TWIST = -4° $\sigma = 0.075$ 2 BLADES
50 FT DIA SLS

--- $\Omega R = 832$ FPS @ 100 KTAS:
661 @ 200; 490 @ 300

— $\Omega R = 500$ FPS @ ALL SPEEDS

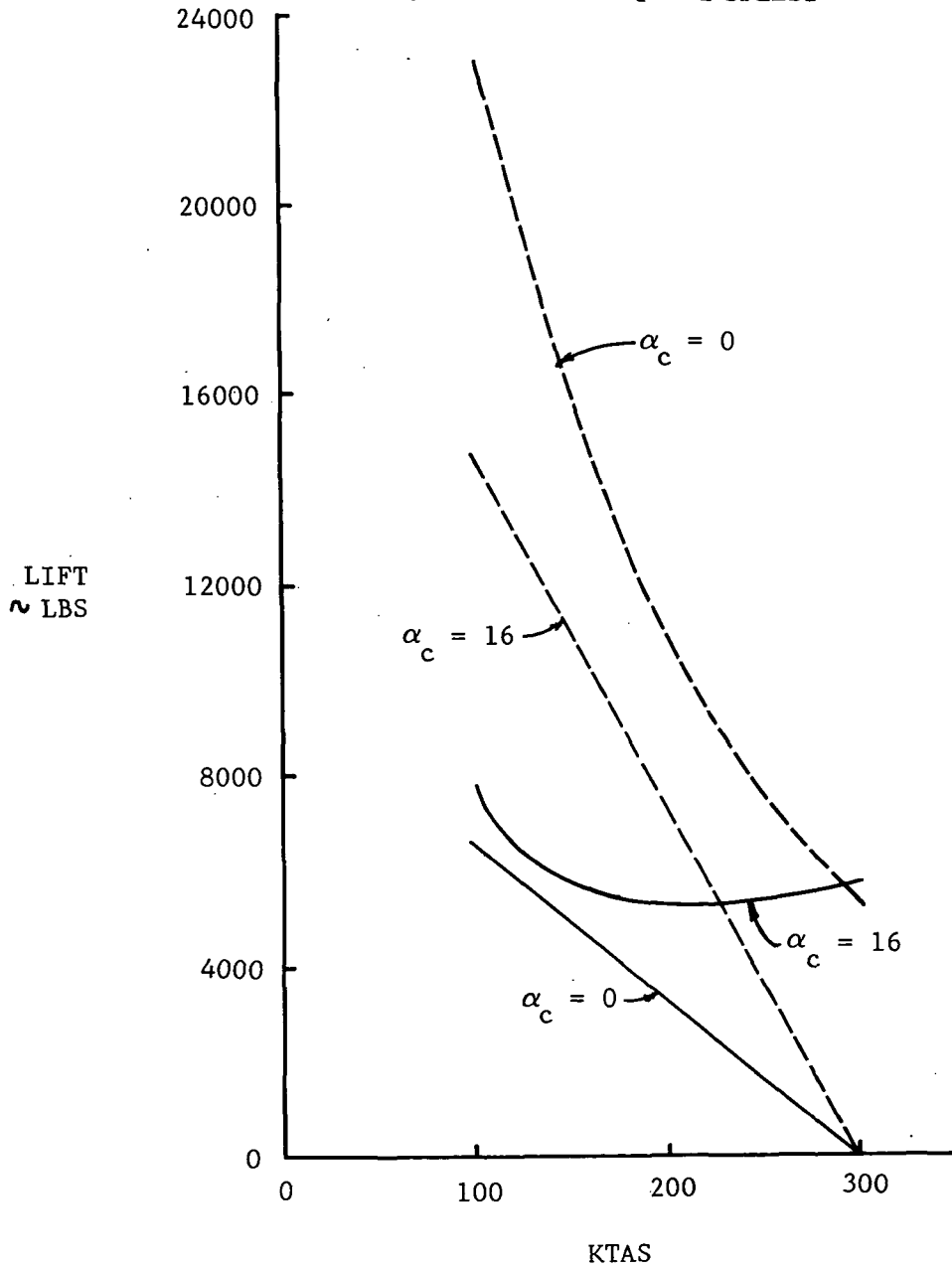


Figure 74. Rotor Lift Versus Airspeed.

RSRA - BRAM

TWIST = -4° $\sigma = 0.075$ 2 BLADES
50 FT DIA SLS

--- $\Omega R = 832$ FPS @ 100 KTAS:
661 @ 200: 490 @ 300

— $\Omega R = 500$ FPS @ ALL SPEEDS

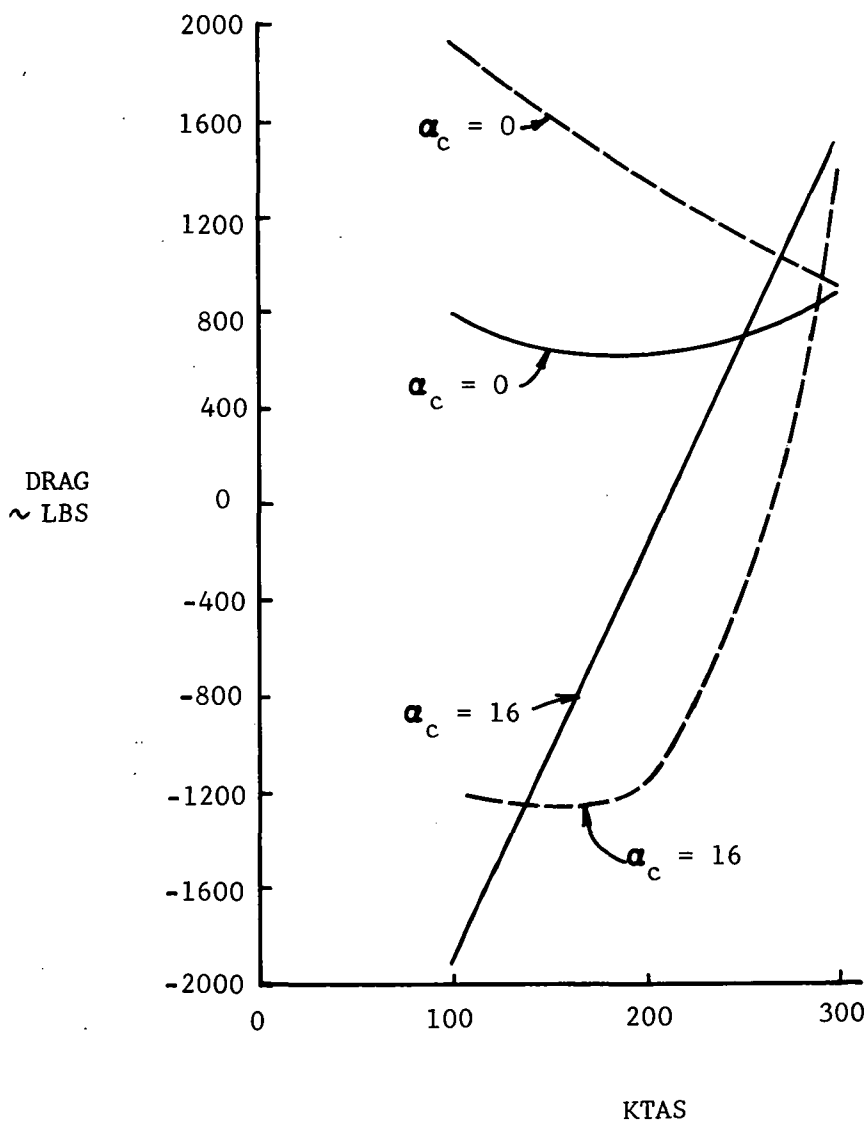


Figure 75. Rotor Drag Versus Airspeed.

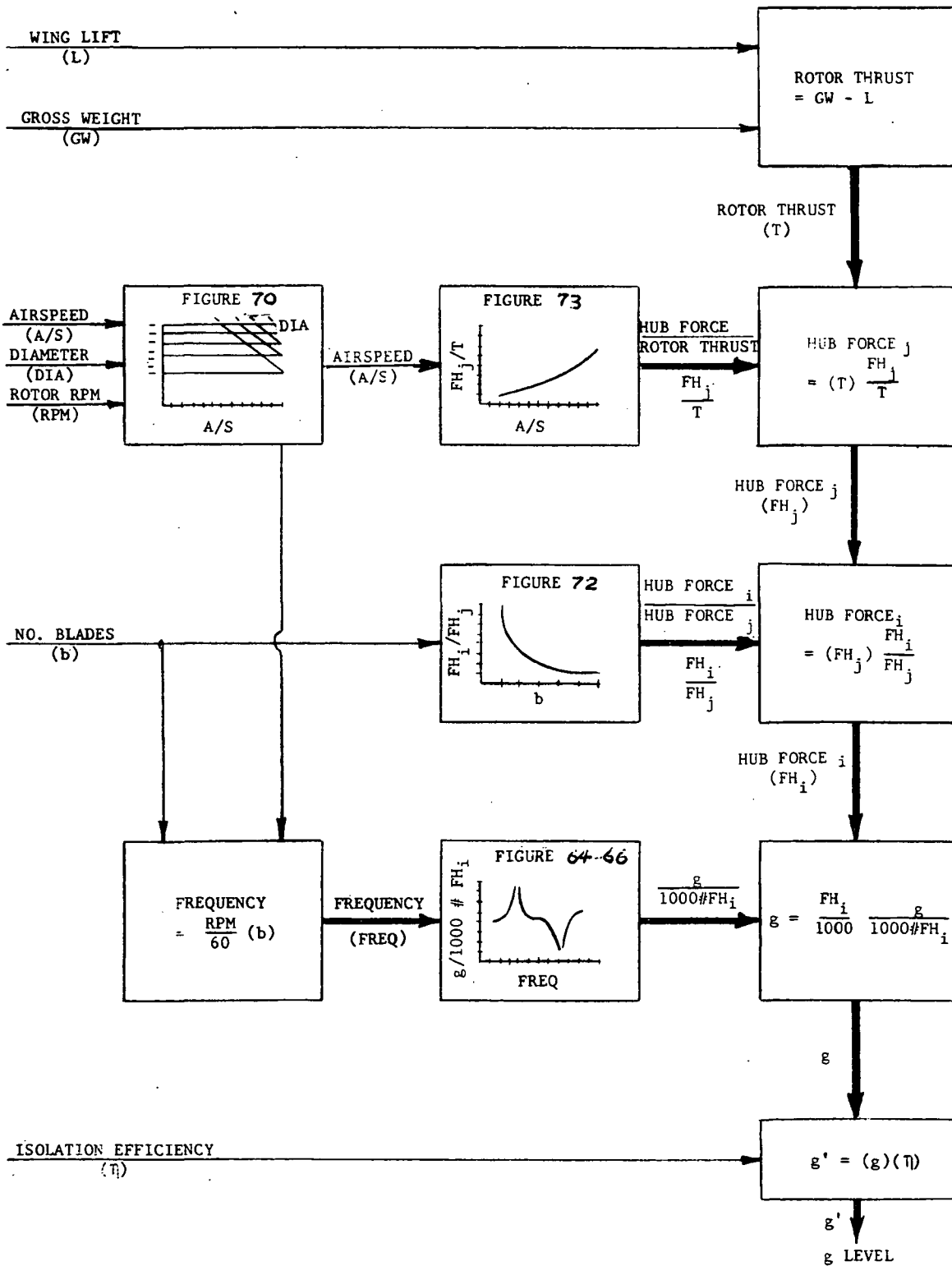


Figure 76. Isolation System Study Flow Diagram.

6

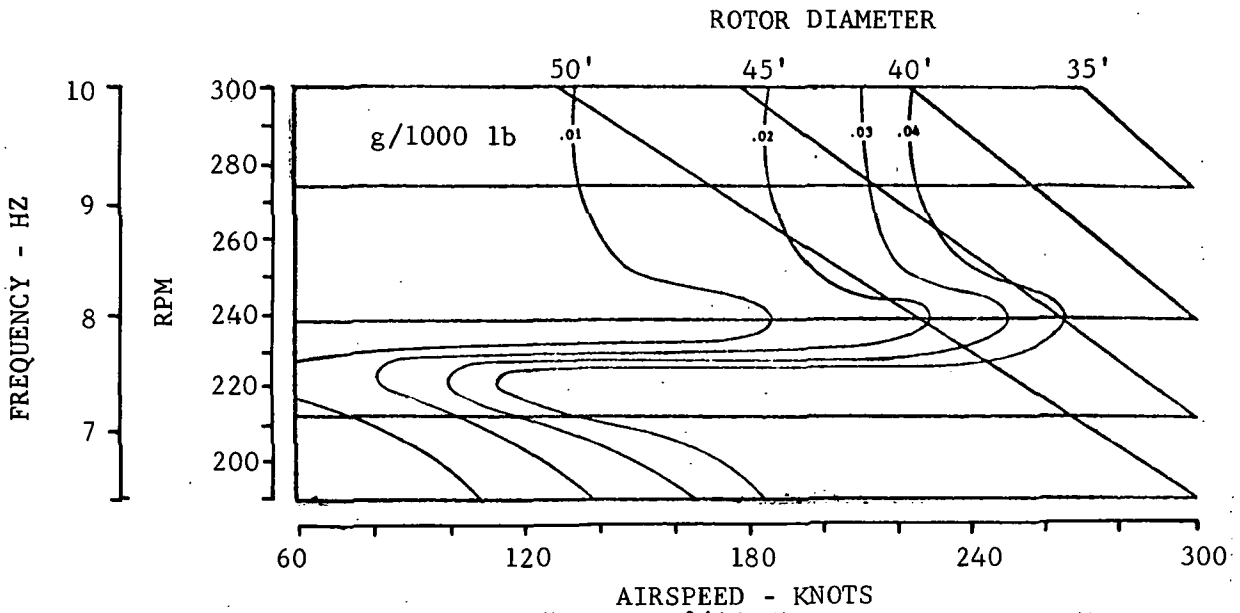


Figure 77(a). Pilot's Station Vertical Response (g/1000-Pound Rotor Lift) to Vertical Excitation for Two-Bladed Rotor.

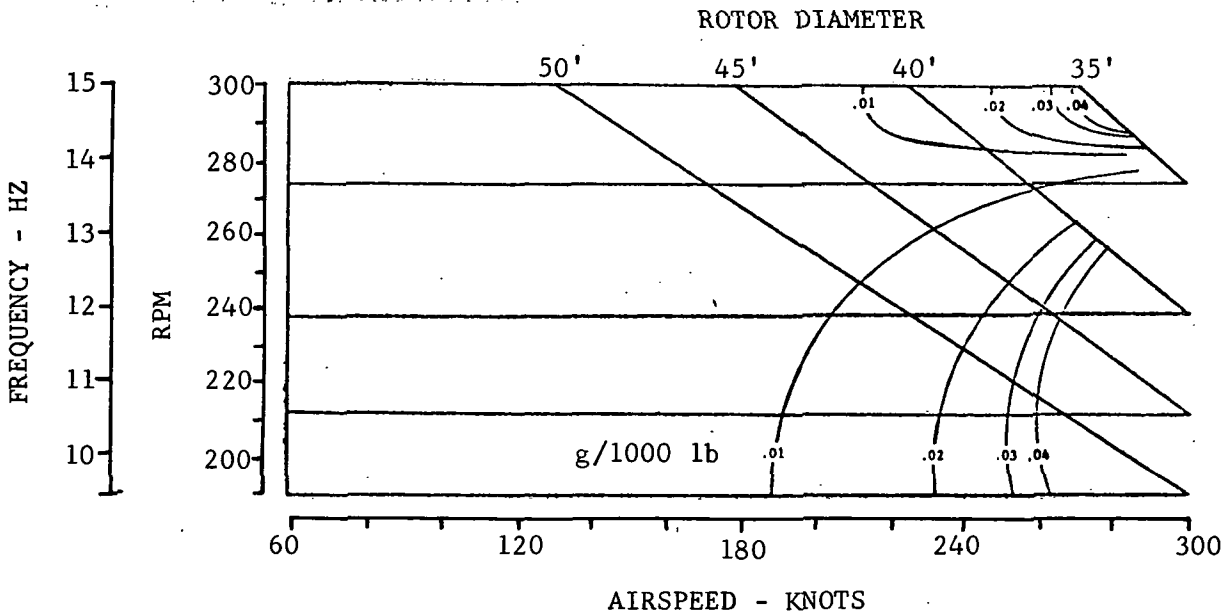


Figure 77(b). Pilot's Station Vertical Response (g/1000-Pound Rotor Lift) to Vertical Excitation for Three-Bladed Rotor.

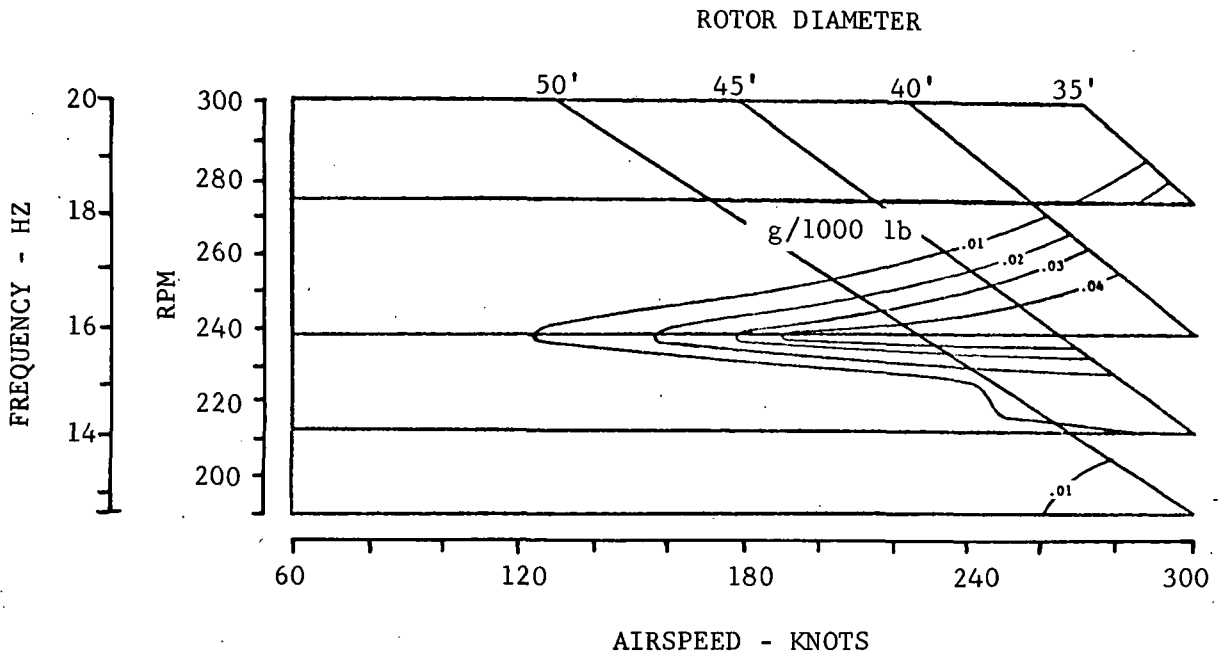


Figure 77(c). Pilot's Station Vertical Response (g/1000-Pound Rotor Lift) to Vertical Excitation for Four-Bladed Rotor.

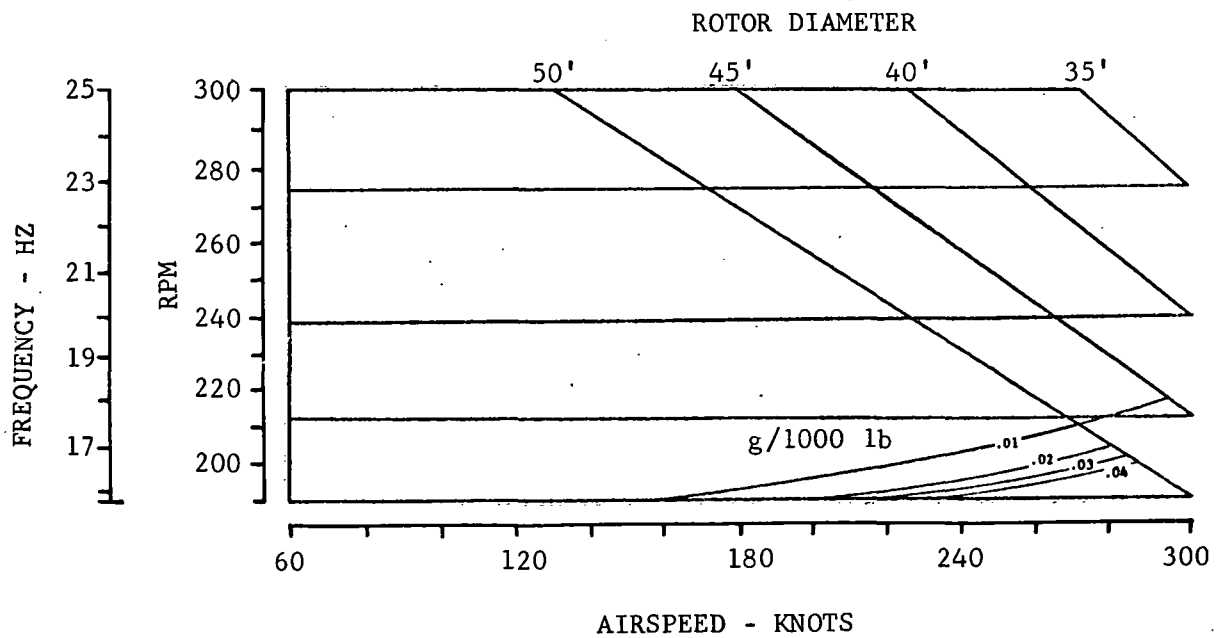


Figure 77(d). Pilot's Station Vertical Response (g/1000-Pound Rotor Lift) to Vertical Excitation for Five-Bladed Rotor.

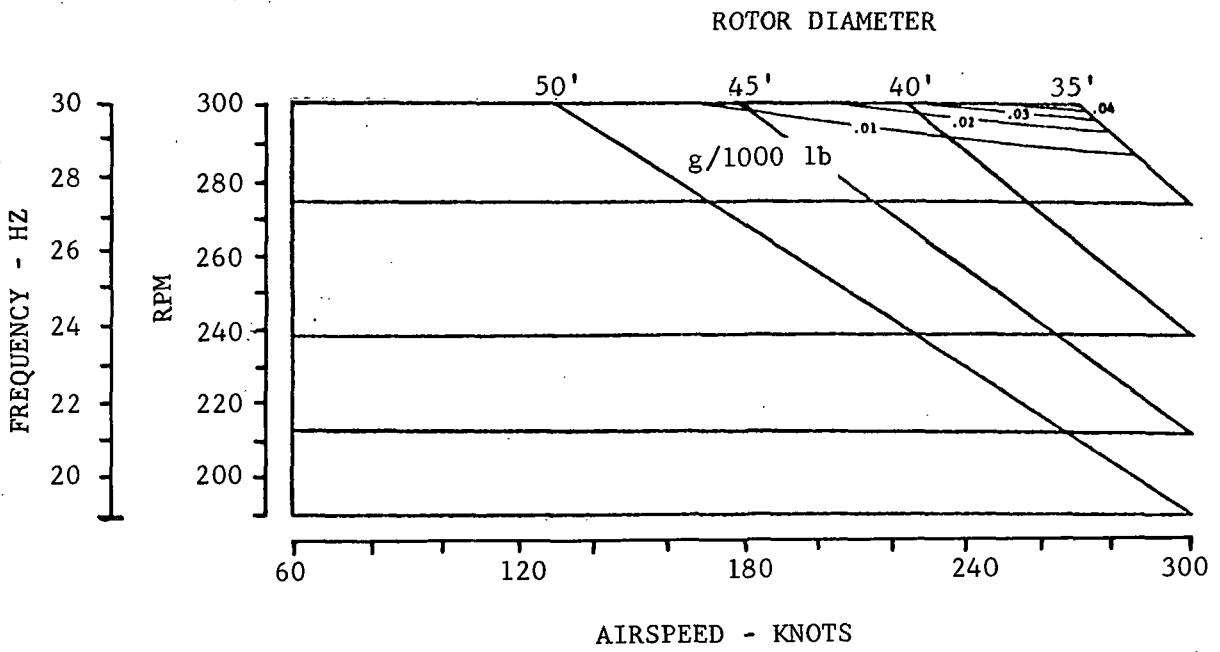


Figure 77(e). Pilot's Station Vertical Response (g/1000-Pound Rotor Lift) to Vertical Excitation for Six-Bladed Rotor.

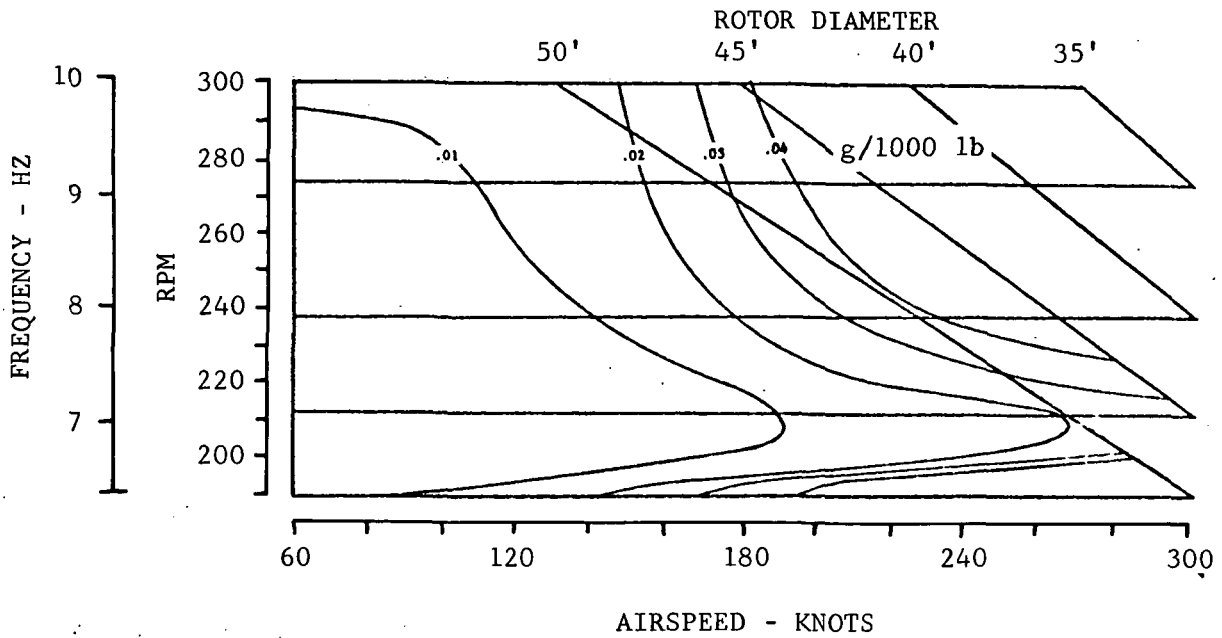


Figure 78(a). Pilot's Station Lateral Response (g/1000-Pound Rotor Lift) to Lateral Excitation for Two-Bladed Rotor.

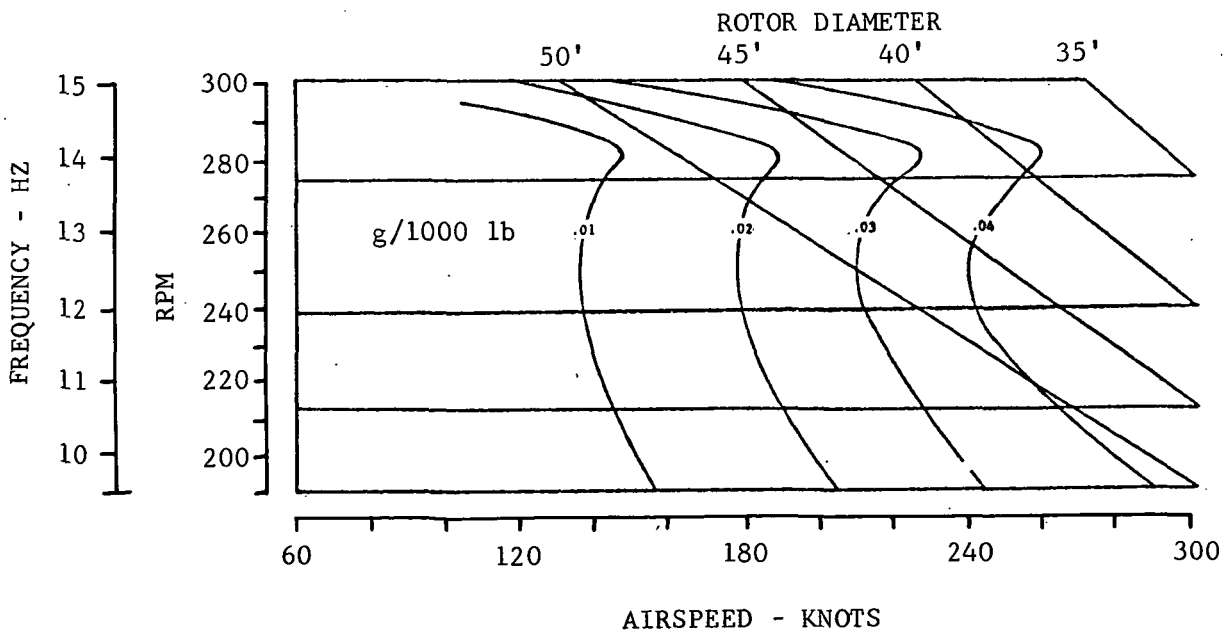


Figure 78(b). Pilot's Station Lateral Response (g/1000-Pound Rotor Lift) to Lateral Excitation for Three-Bladed Rotor.

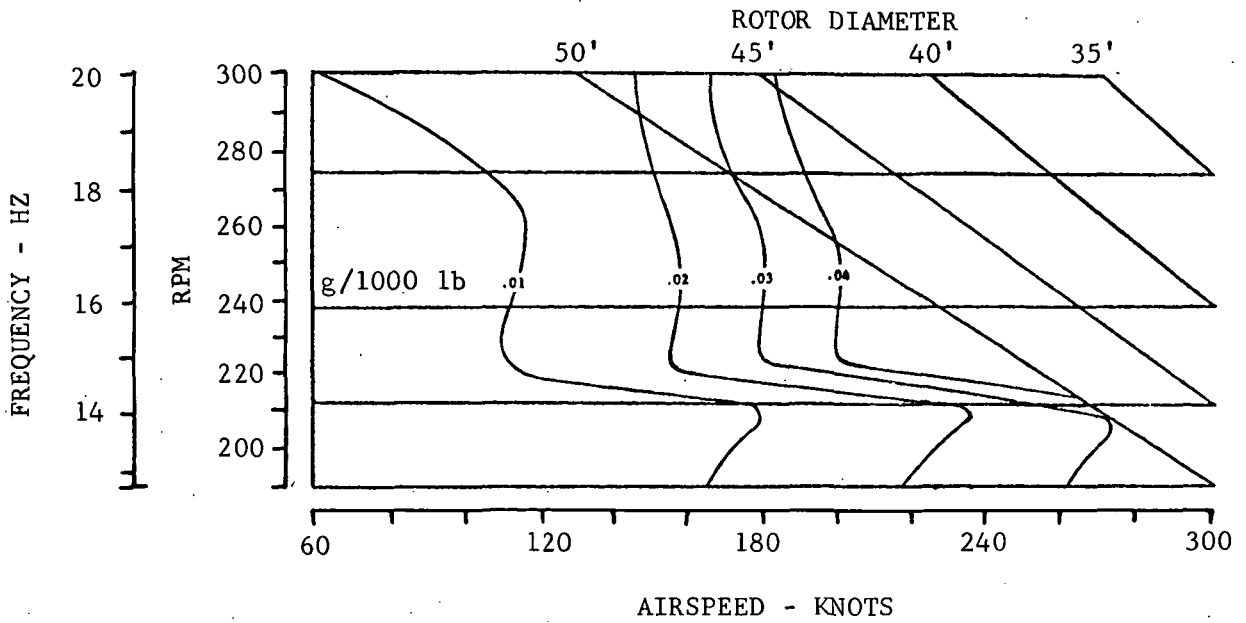


Figure 78(c). Pilot's Station Lateral Response (g/1000-Pound Rotor Lift) to Lateral Excitation for Four-Bladed Rotor.

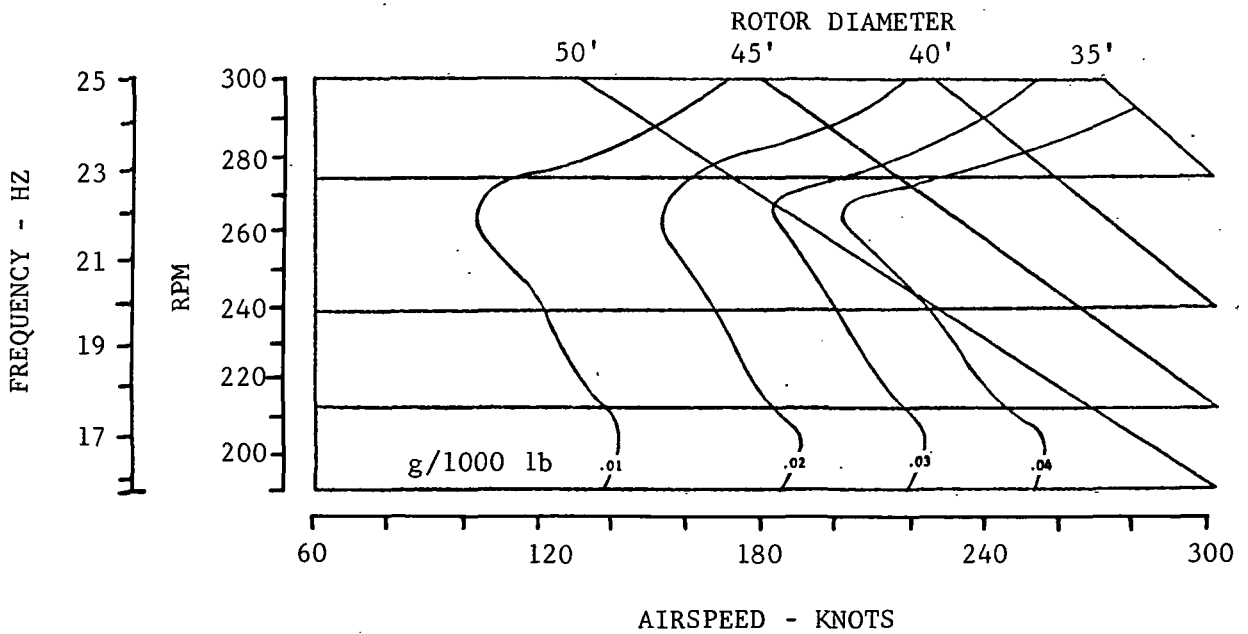


Figure 78(d). Pilot's Station Lateral Response (g/1000-Pound Rotor Lift) to Lateral Excitation for Five-Bladed Rotor.

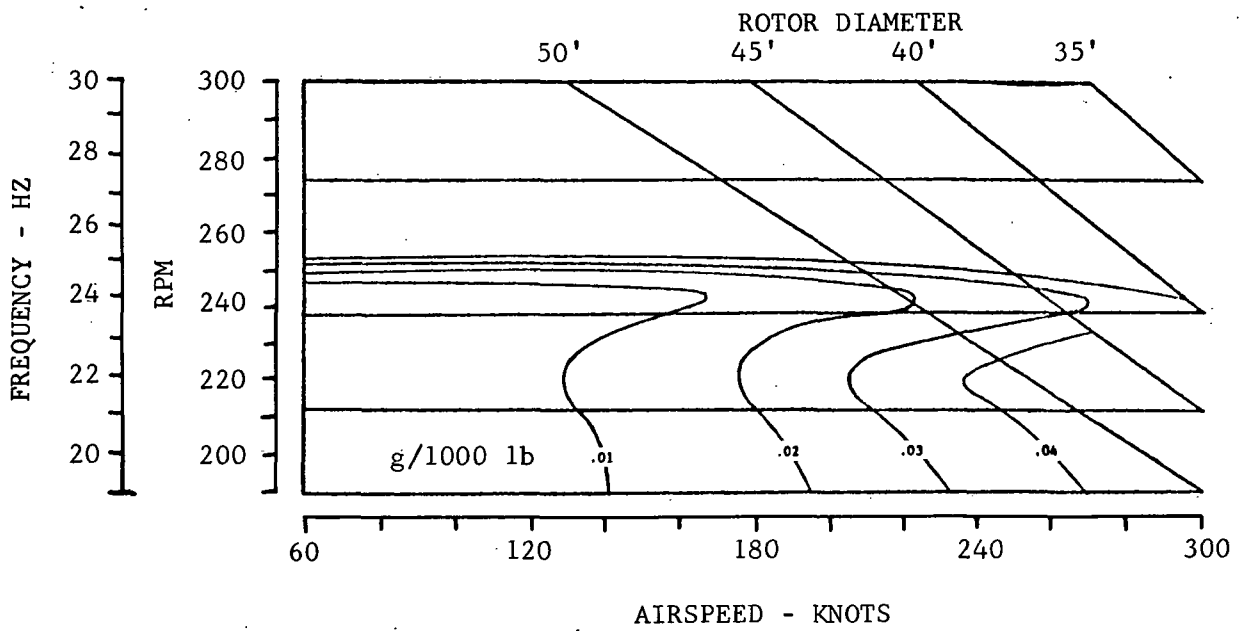


Figure 78(e). Pilot's Station Lateral Response (g/1000-Pound Rotor Lift) to Lateral Excitation for Six-Bladed Rotor.

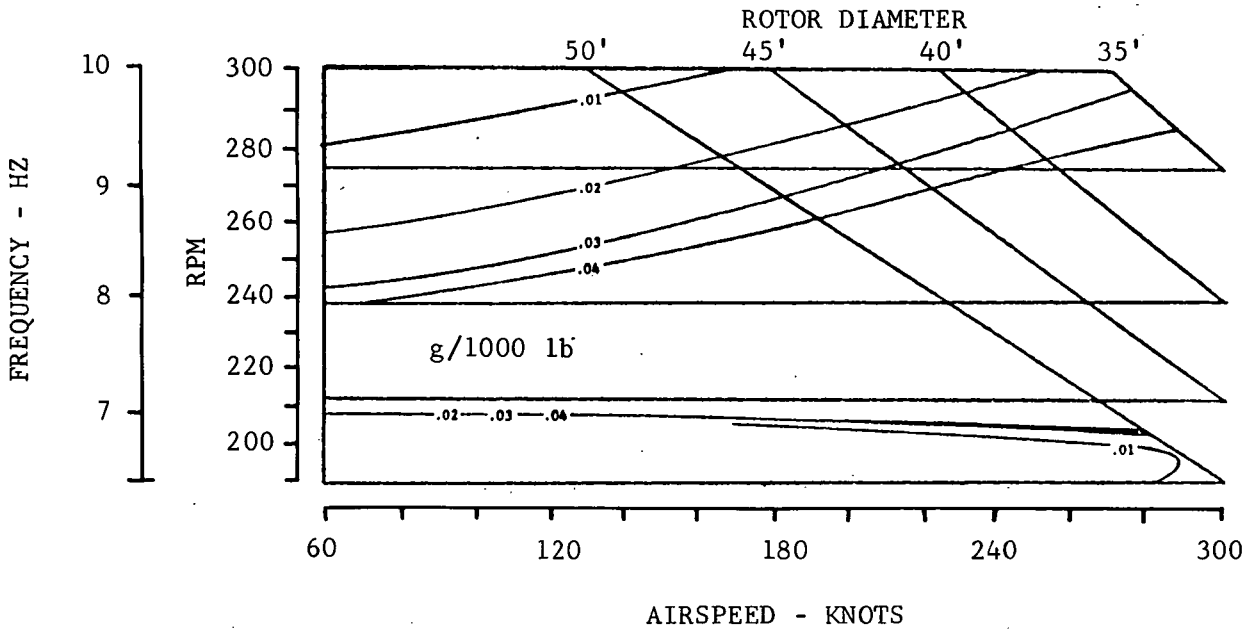


Figure 79(a). Pilot's Station Vertical Response (g/1000-Pound Rotor Lift) to Fore and Aft Excitation for Two-Bladed Rotor.

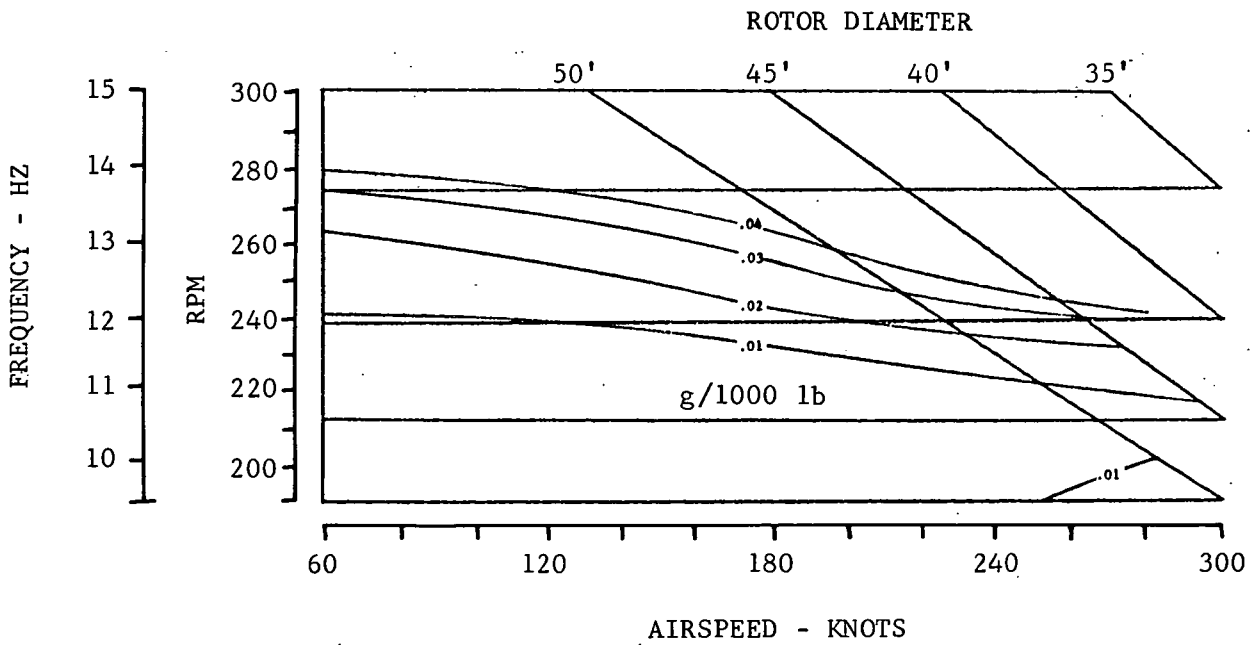


Figure 79(b). Pilot's Station Vertical Response (g/1000-Pound Rotor Lift) to Fore and Aft Excitation for Three-Bladed Rotor.

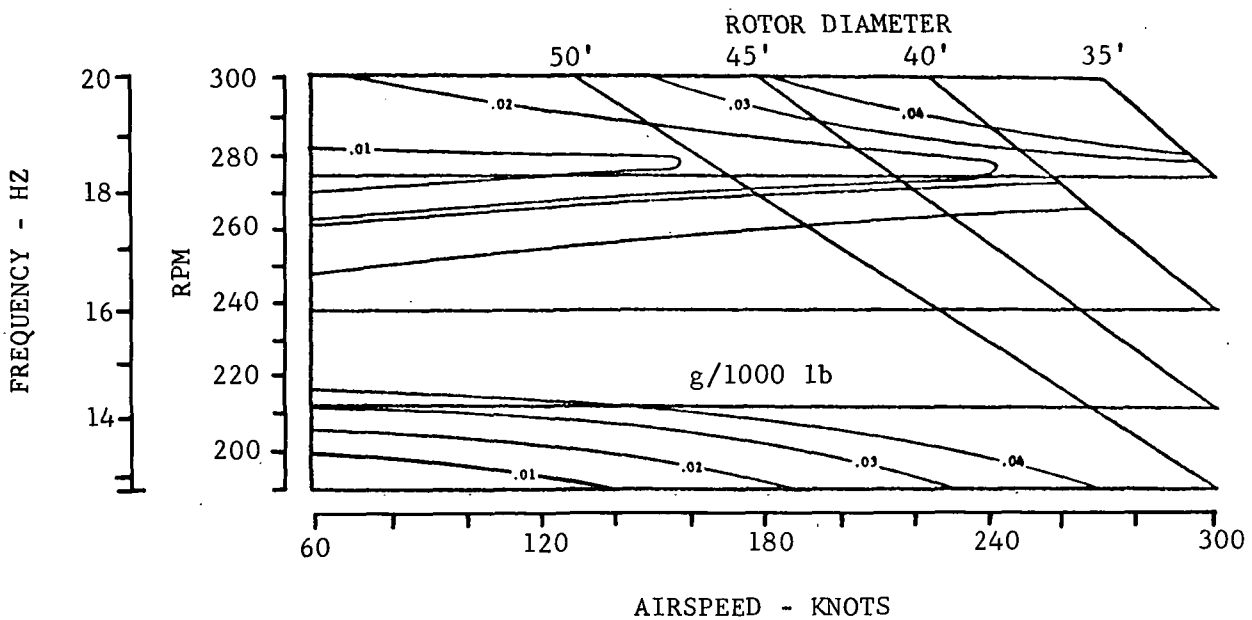


Figure 79(c). Pilot's Station Vertical Response (g/1000-Pound Rotor Lift) to Fore and Aft Excitation for Four-Bladed Rotor.

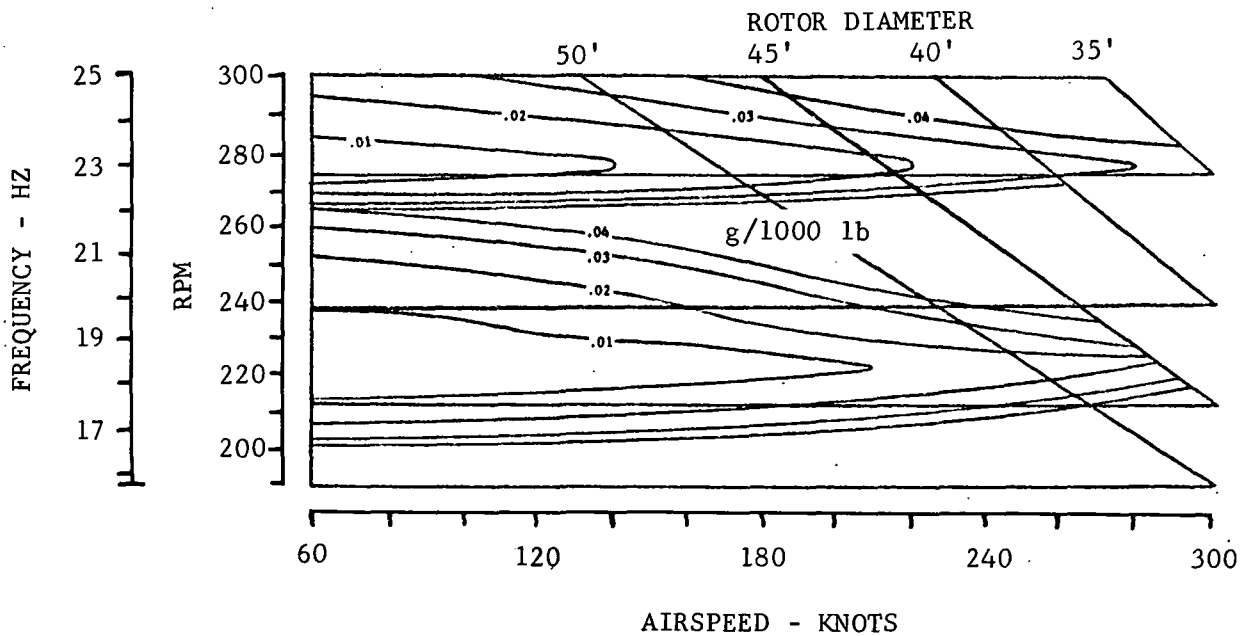


Figure 79(d). Pilot's Station Vertical Response (g/1000-Pound Rotor Lift) to Fore and Aft Excitation for Five-Bladed Rotor.

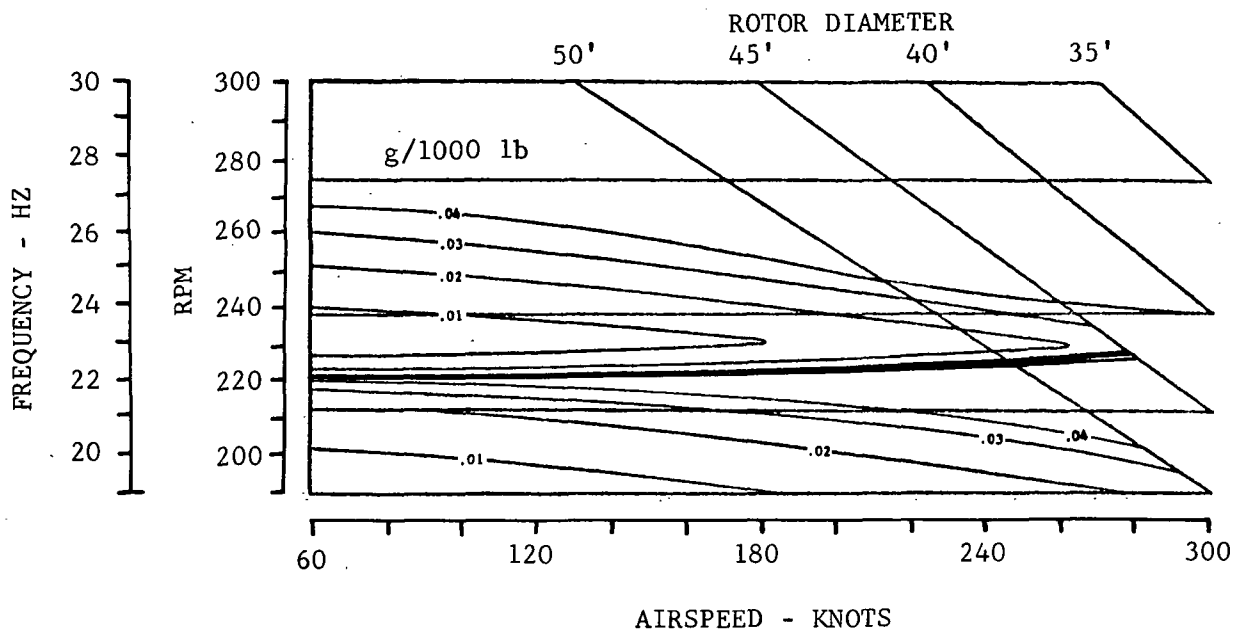
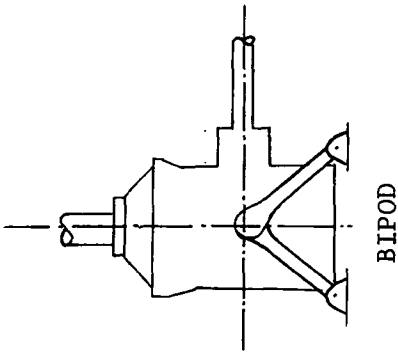


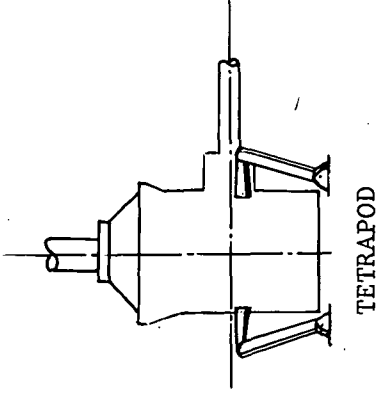
Figure 79(e). Pilot's Station Vertical Response (g/1000-Pound Rotor Lift) to Fore and Aft Excitation for Six-Bladed Rotor.

INPLANE

PASSIVE:



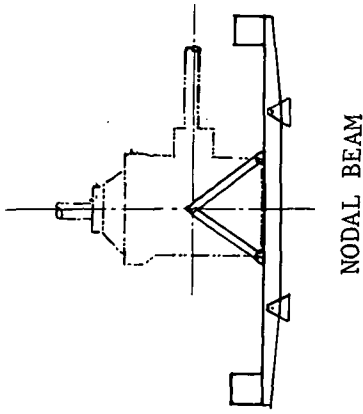
BIPOD



TETRAPOD

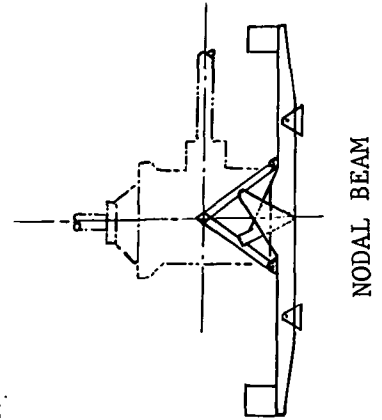
VERTICAL

PASSIVE:

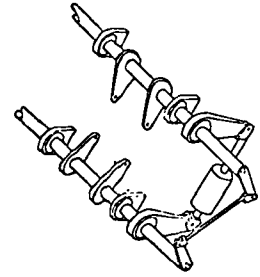


NODAL BEAM

SERVO-CONTROLLED:



NODAL BEAM



SERVO-NULL

Figure 80. Methods of Isolation.

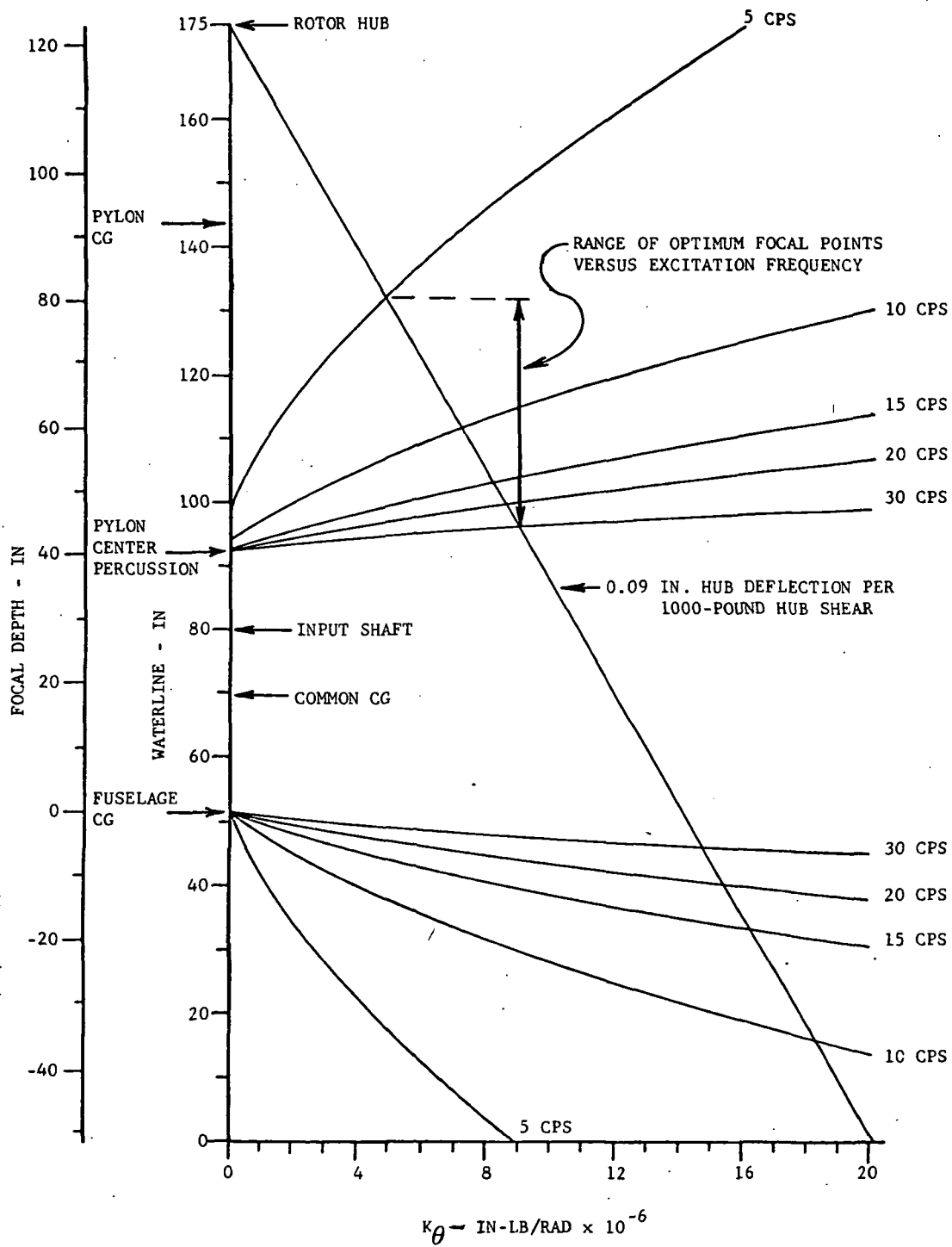


Figure 81. Loci of Minimum Fuselage Response to Hub Force Excitation.

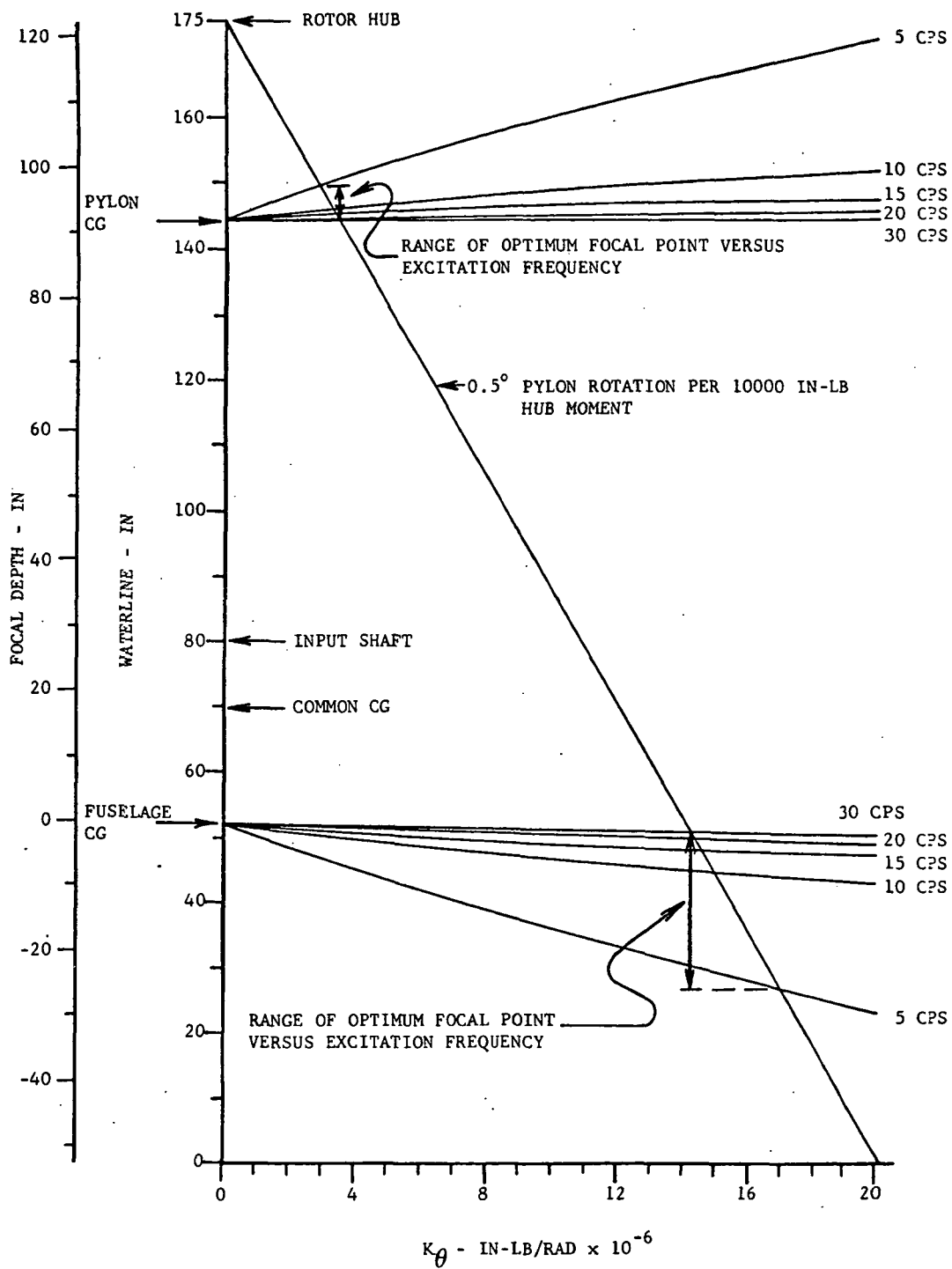


Figure 82. Loci of Minimum Fuselage Response to Hub Moment Excitation.

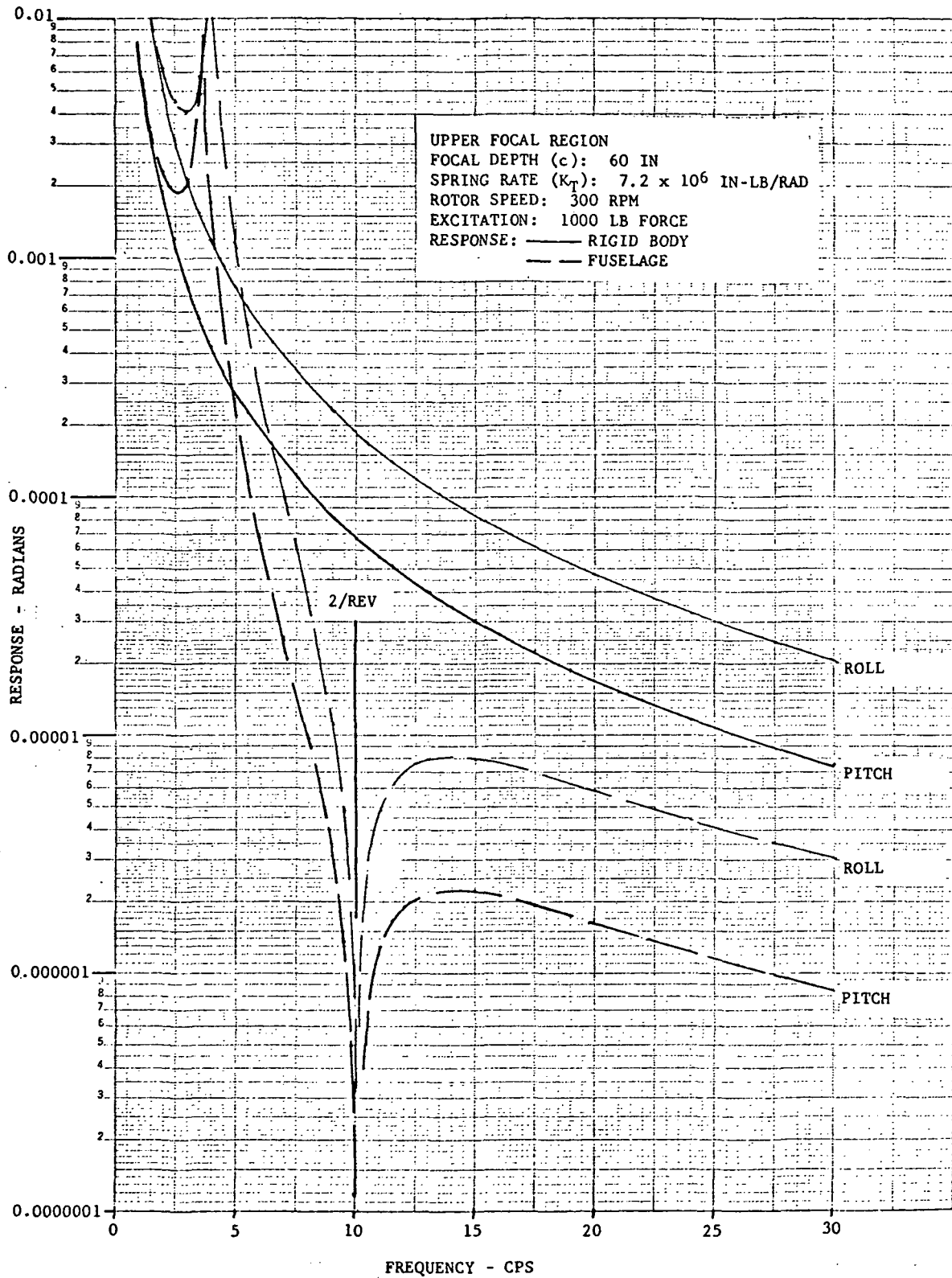


Figure 83. Typical Fuselage Angular Response for Focal Pylon Isolation of Two-Per-Rev, Upper Focal Region, Force Excitation.

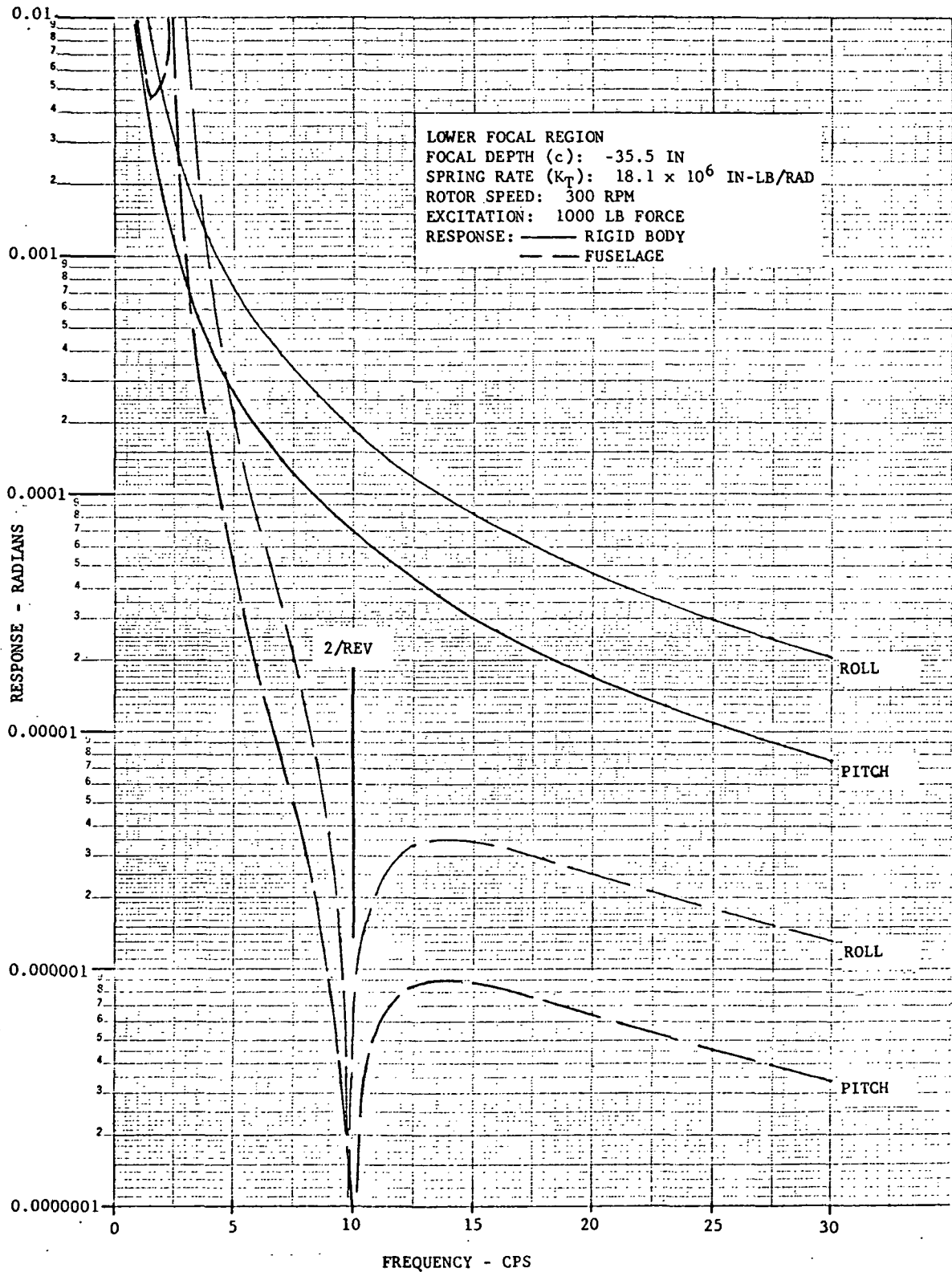


Figure 84. Typical Fuselage Angular Response for Focal Pylon Isolation of Two-Per-Rev, Lower Focal Region, Force Excitation.

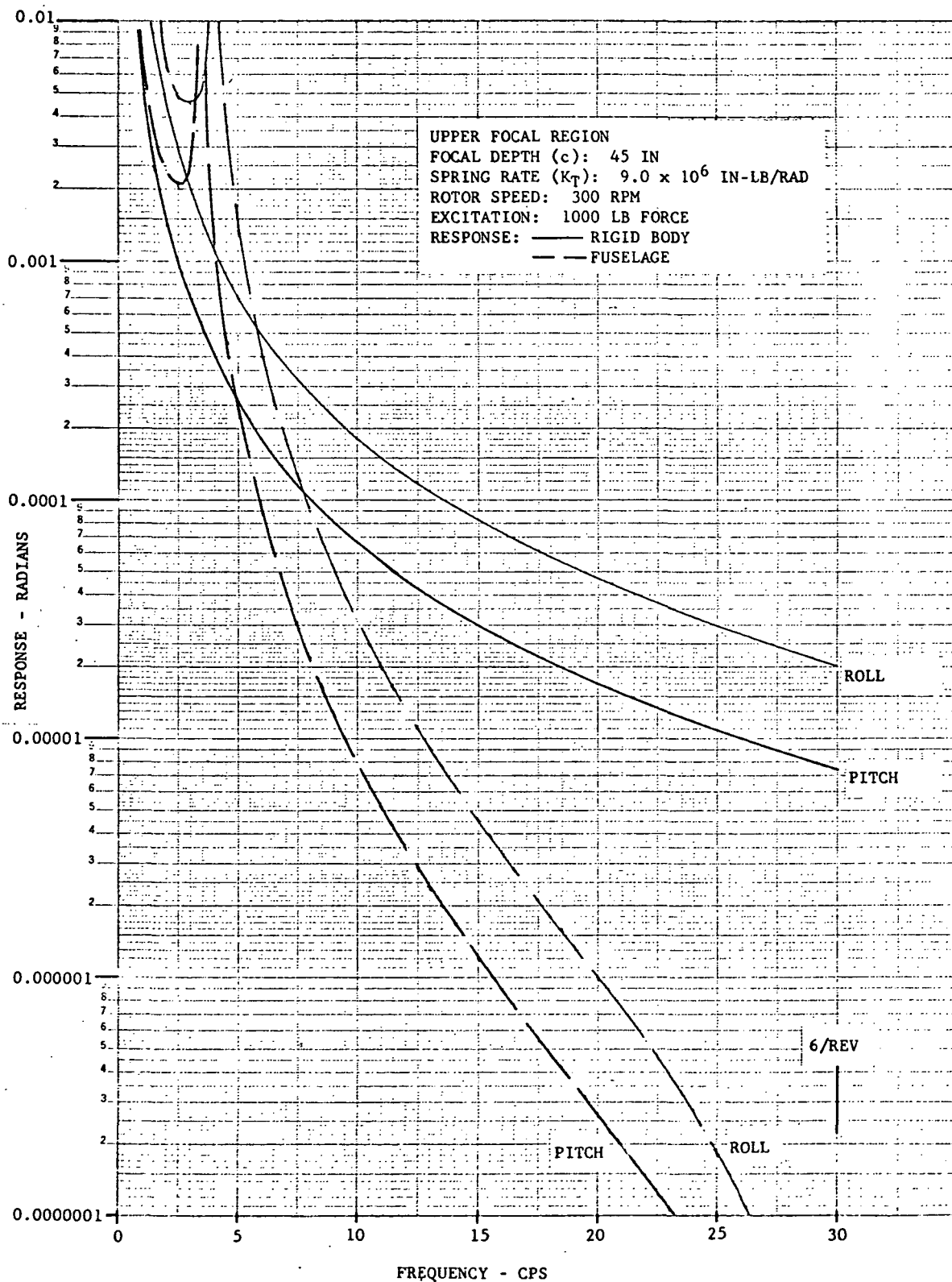


Figure 85. Typical Fuselage Angular Response for Focal Pylon Isolation of Six-Per-Rev, Upper Focal Region, Force Excitation.

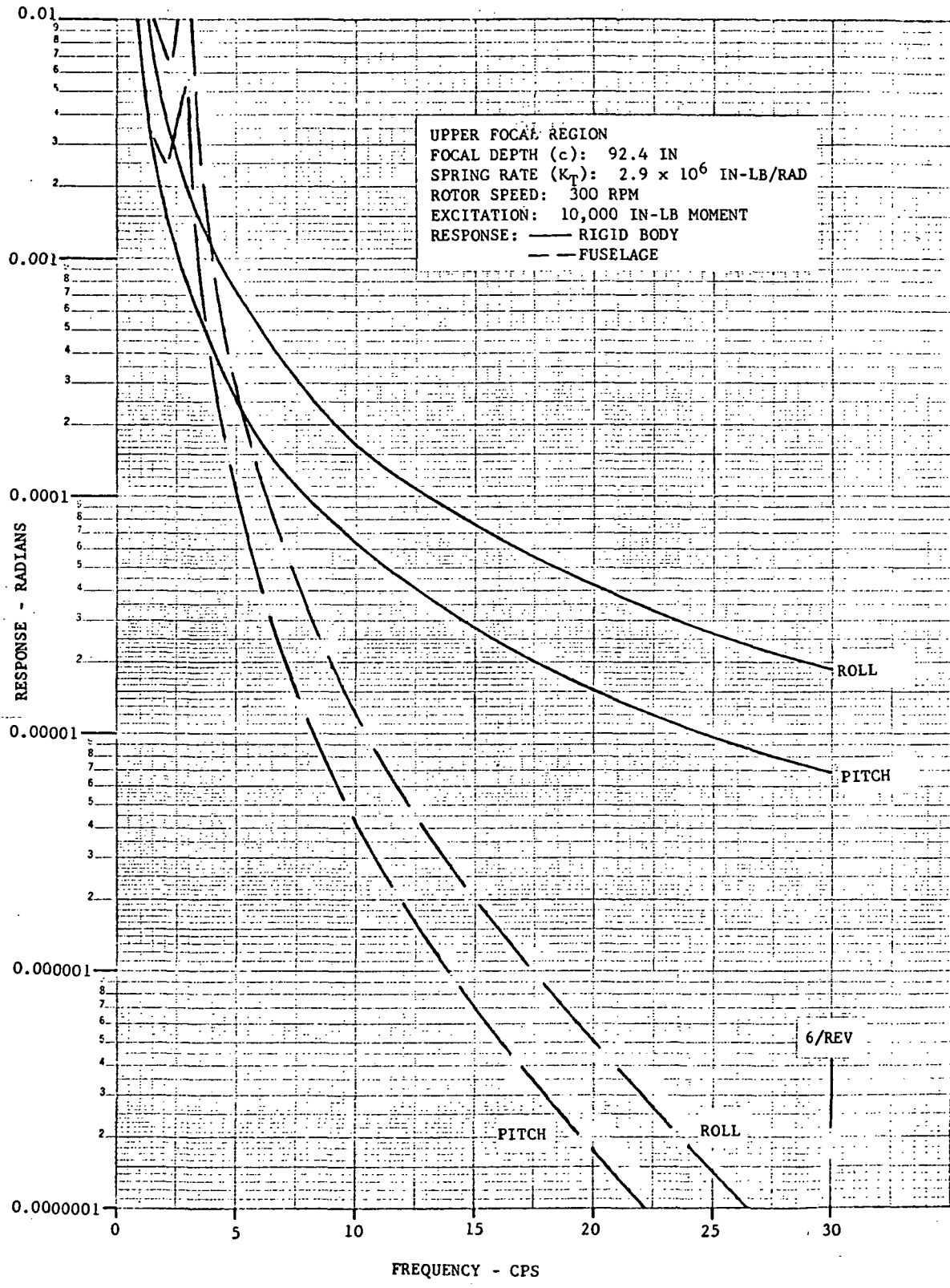


Figure 86. Typical Fuselage Angular Response for Focal Pylon Isolation of Six-Per-Rev, Upper Focal Region, Moment Excitation.

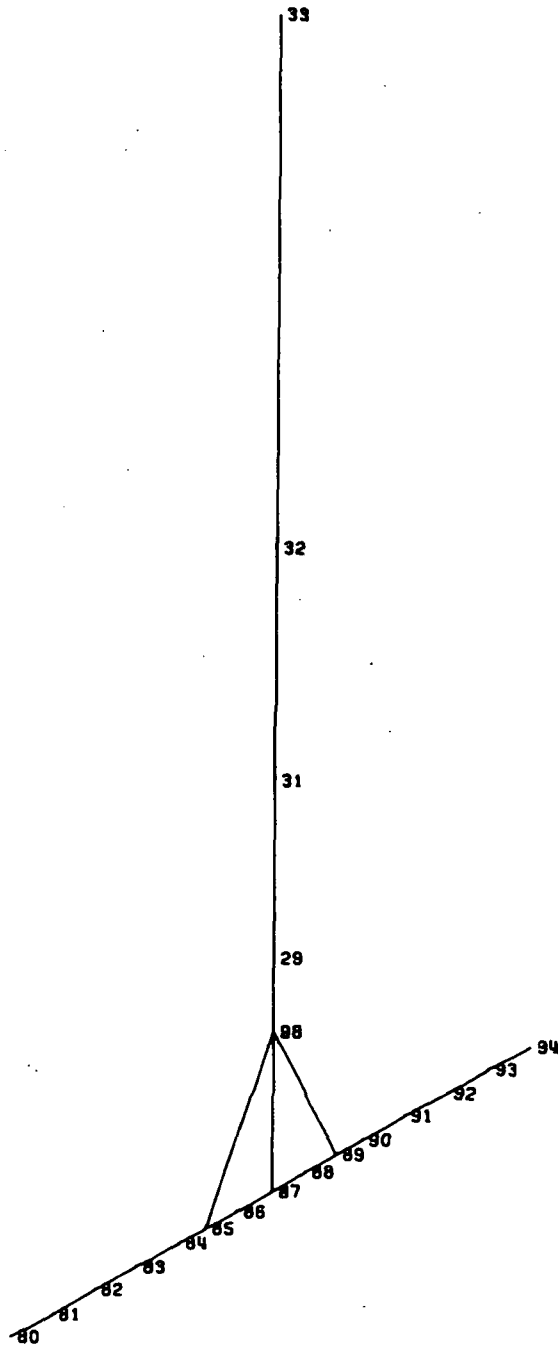


Figure 87. Two-Dimensional Analytical Model of Nodal Beam and Pylon Assembly.

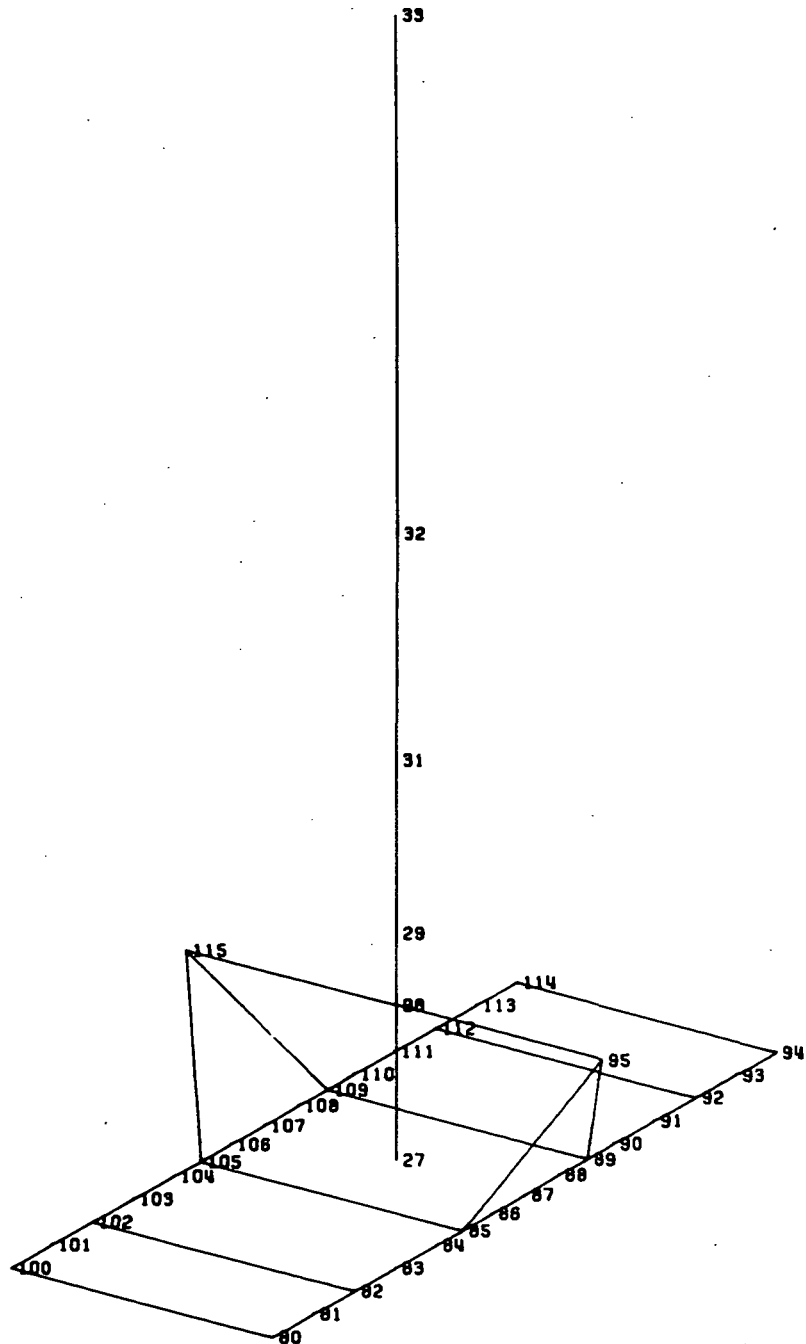
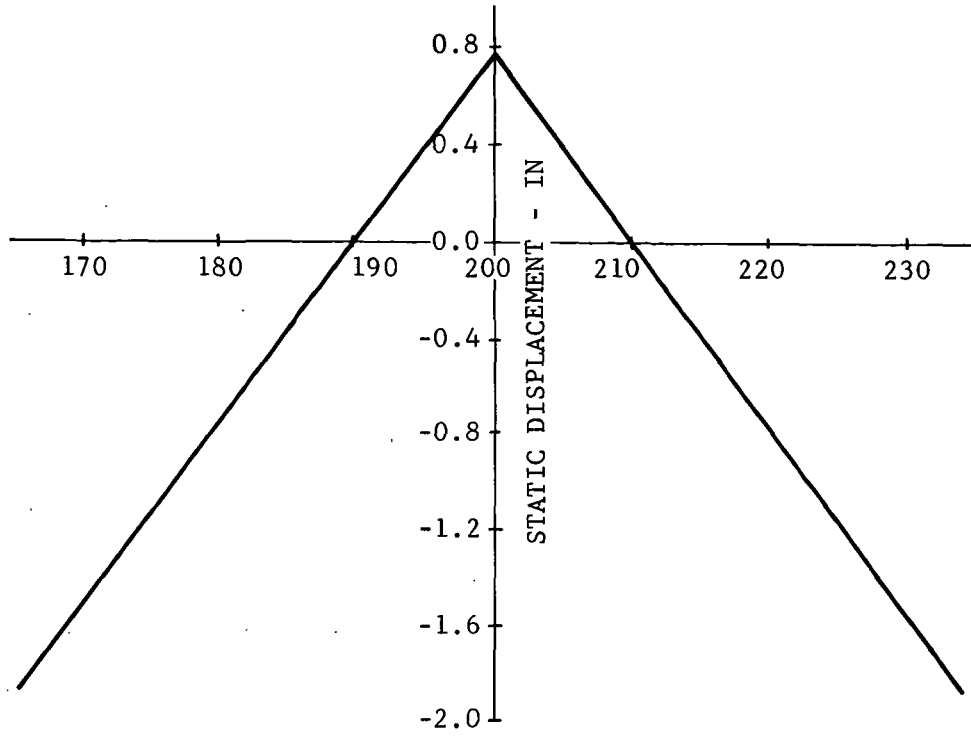
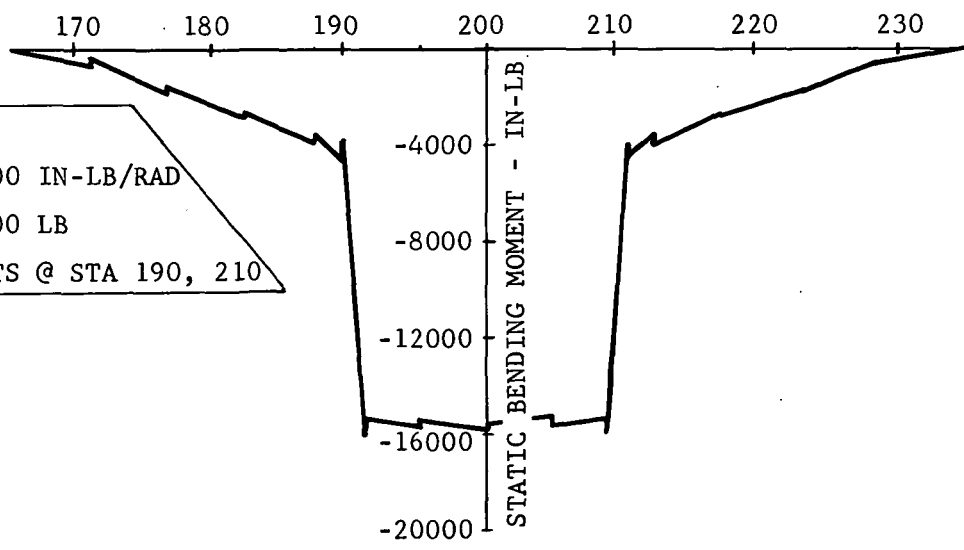


Figure 88. Three-Dimensional Analytical Model of Nodal Beam and Pylon Assembly.



NODAL BEAM STATION - INCHES



NOTE:
 $K_{\theta} = 100,000 \text{ IN-LB/RAD}$
 TIP WT = 200 LB
 NODAL POINTS @ STA 190, 210

Figure 89. Displacement and Bending Moment Distribution for $n_z = 1.0 \text{ g}$ with 15,000 Pounds Lift.

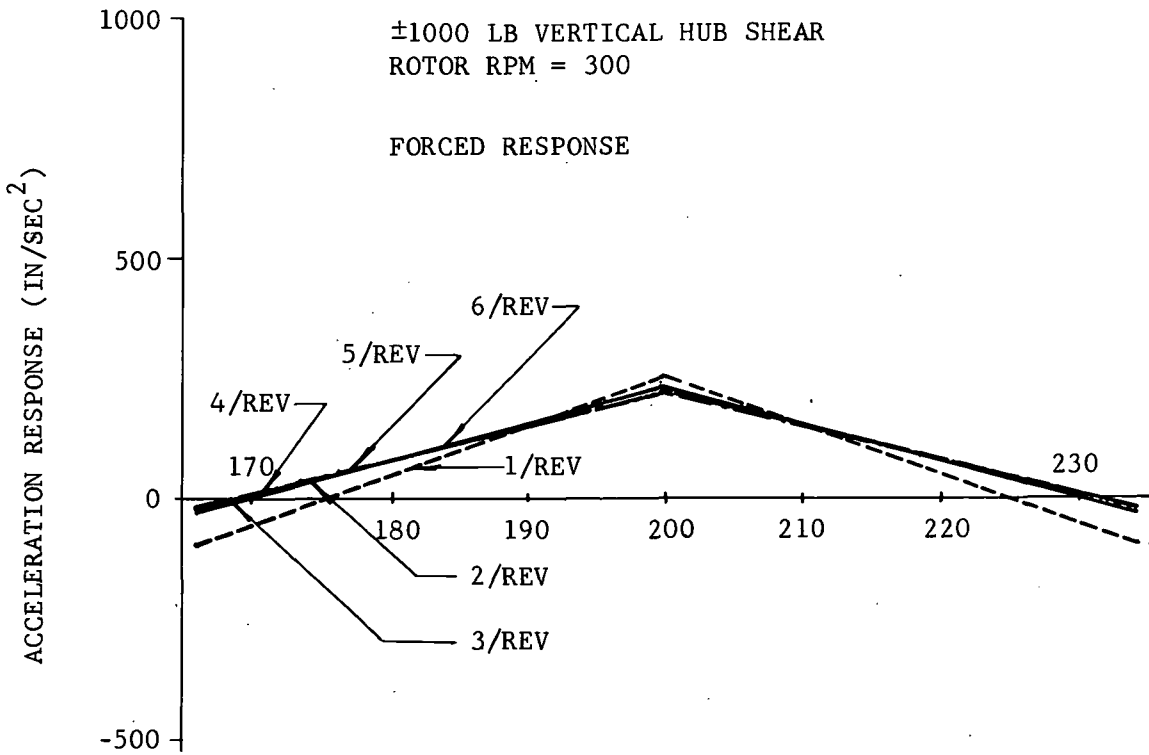
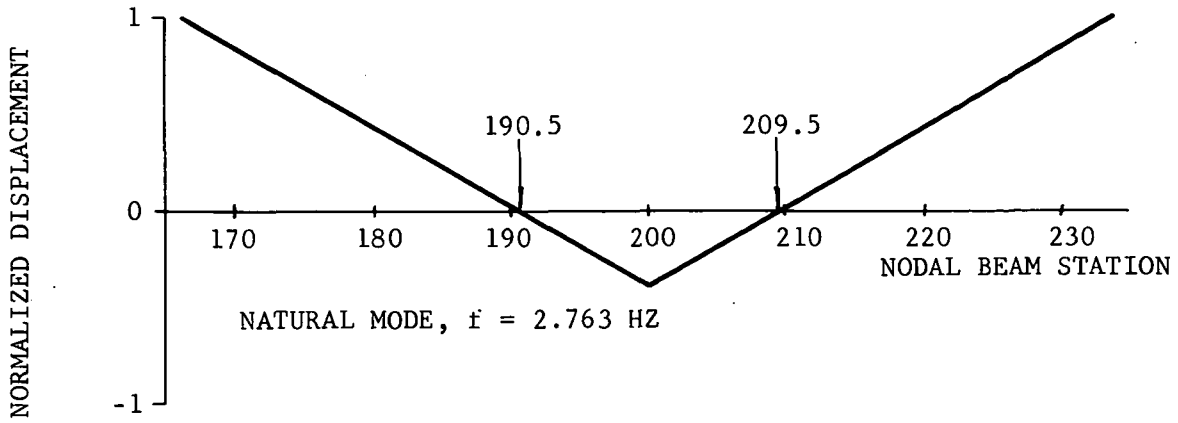


Figure 90. Natural Mode and Forced Response of Pylon and Nodal Beam Assembly with $M_{Tip} = 50$ Pounds, $K_{\theta} = 10,000$ In.-Lb/Rad.

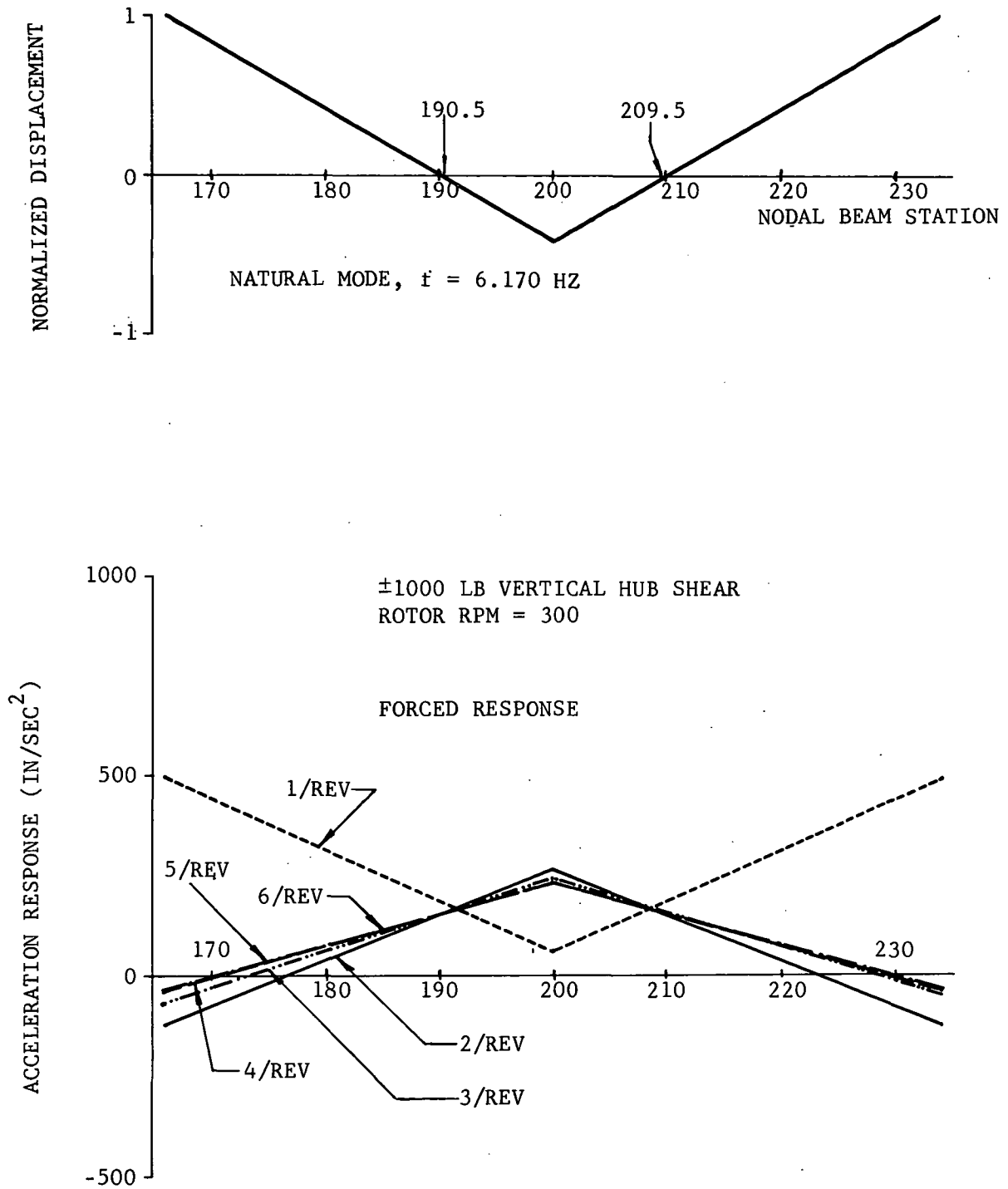


Figure 91. Natural Mode and Forced Response of Pylon and Nodal Beam Assembly with $M_{TIP} = 50$ Pounds, $K_{\theta} = 50,000$ In.-Lb/Rad.

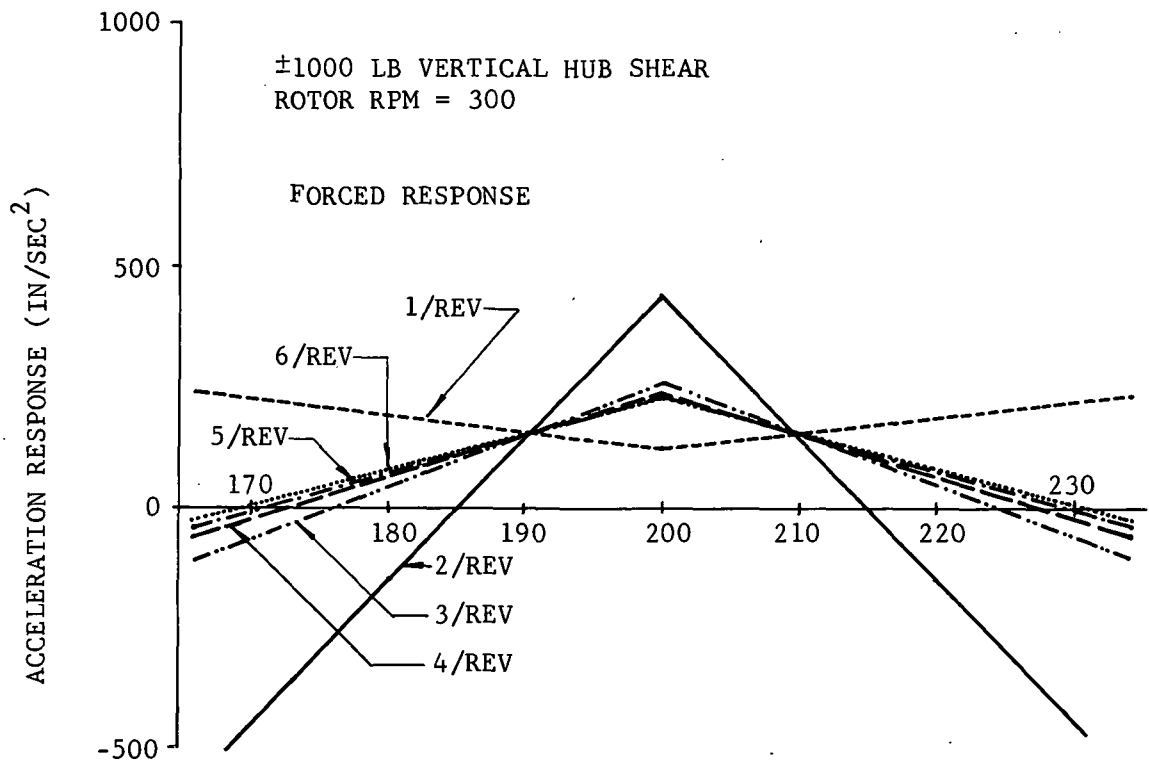
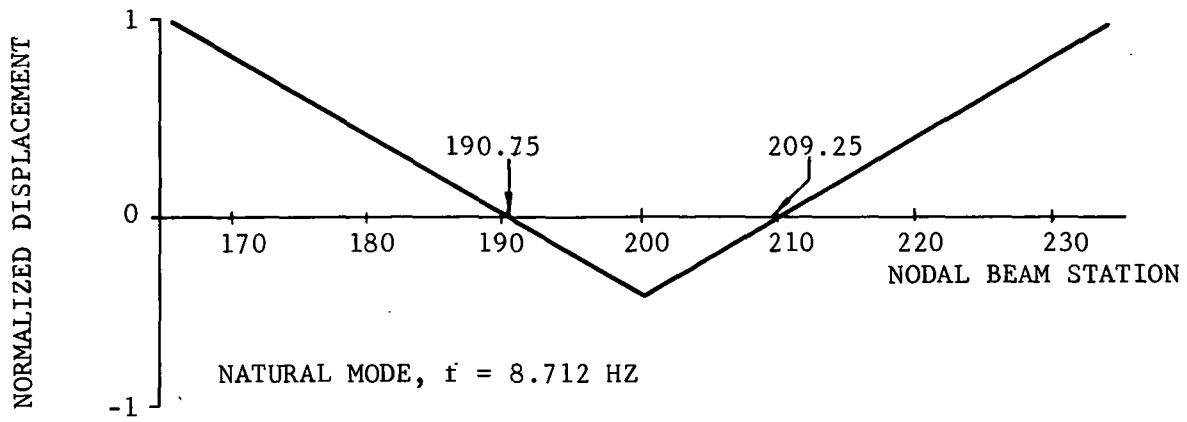


Figure 92. Natural Mode and Forced Response of Pylon and Nodal Beam Assembly with $M_{TIP} = 50$ Pounds, $K_{\theta} = 100,000$ In.-Lb/Rad.

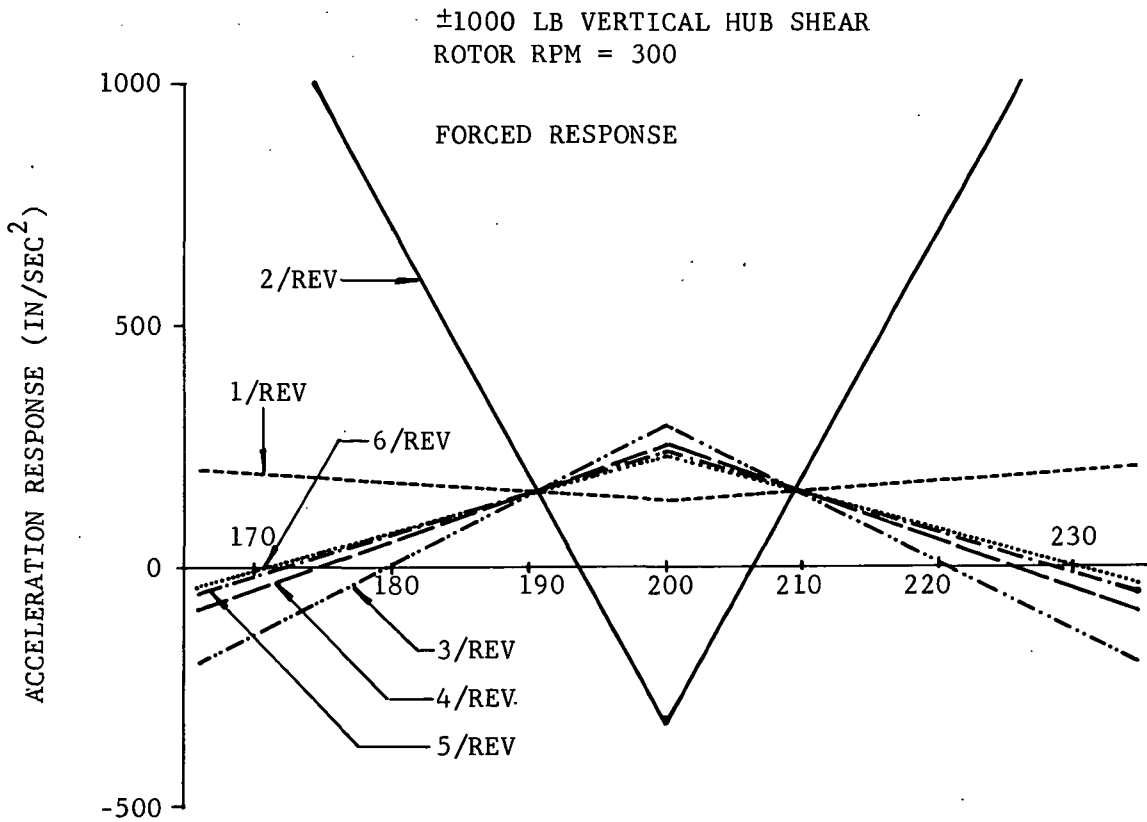
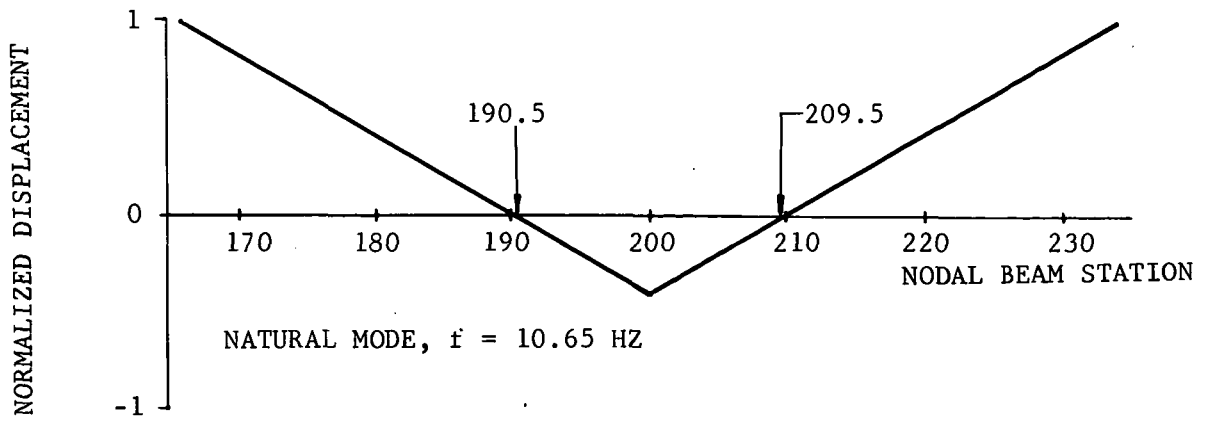


Figure 93. Natural Mode and Forced Response of Pylon and Nodal Beam Assembly with $M_{TIP} = 50$ Pounds, $K_{\theta} = 150,000$ In.-Lb/Rad.

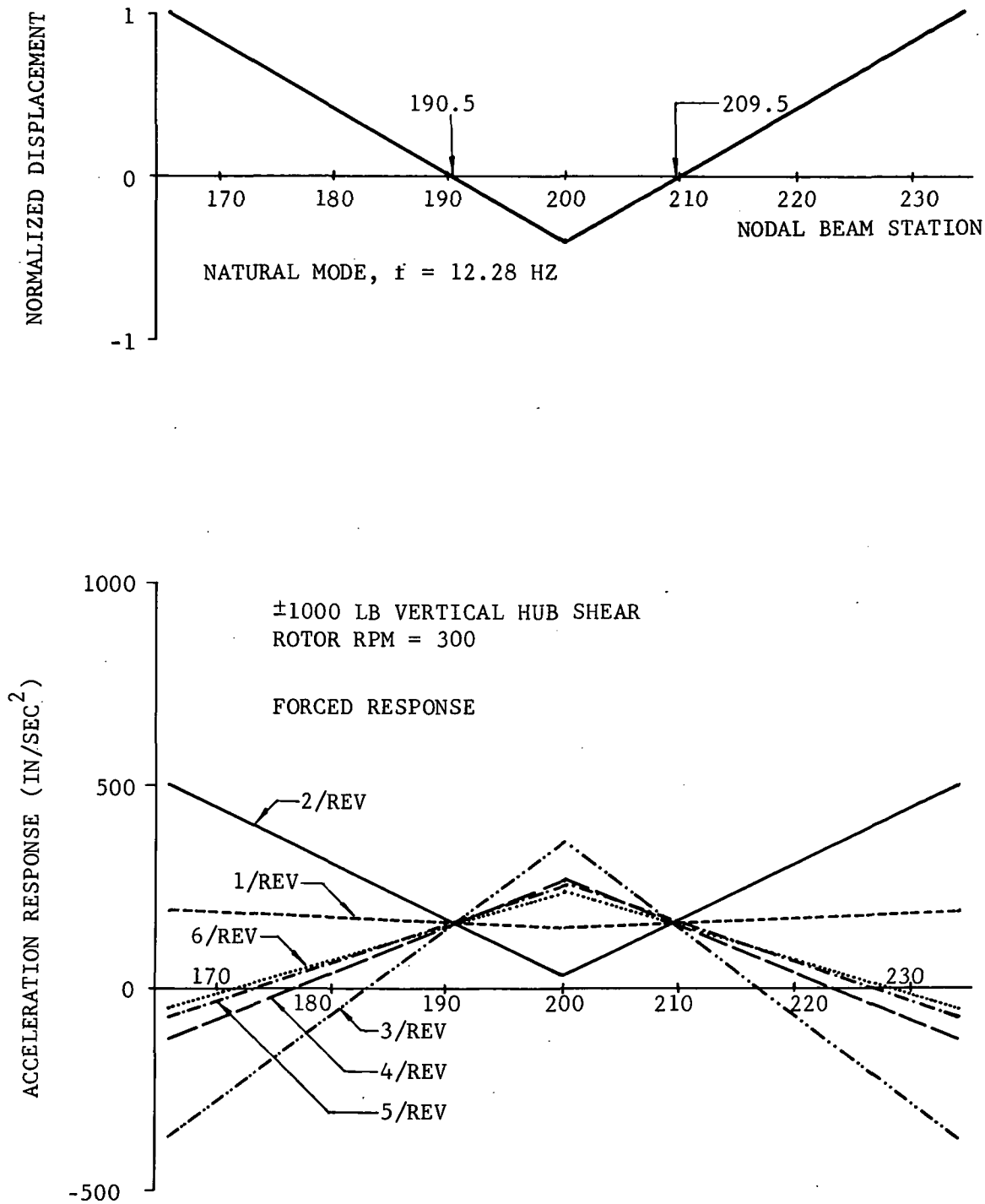


Figure 94. Natural Mode and Forced Response of Pylon and Nodal Beam Assembly with $M_{TIP} = 50$ Pounds, $K_{\theta} = 200,000$ In.-Lb/Rad.

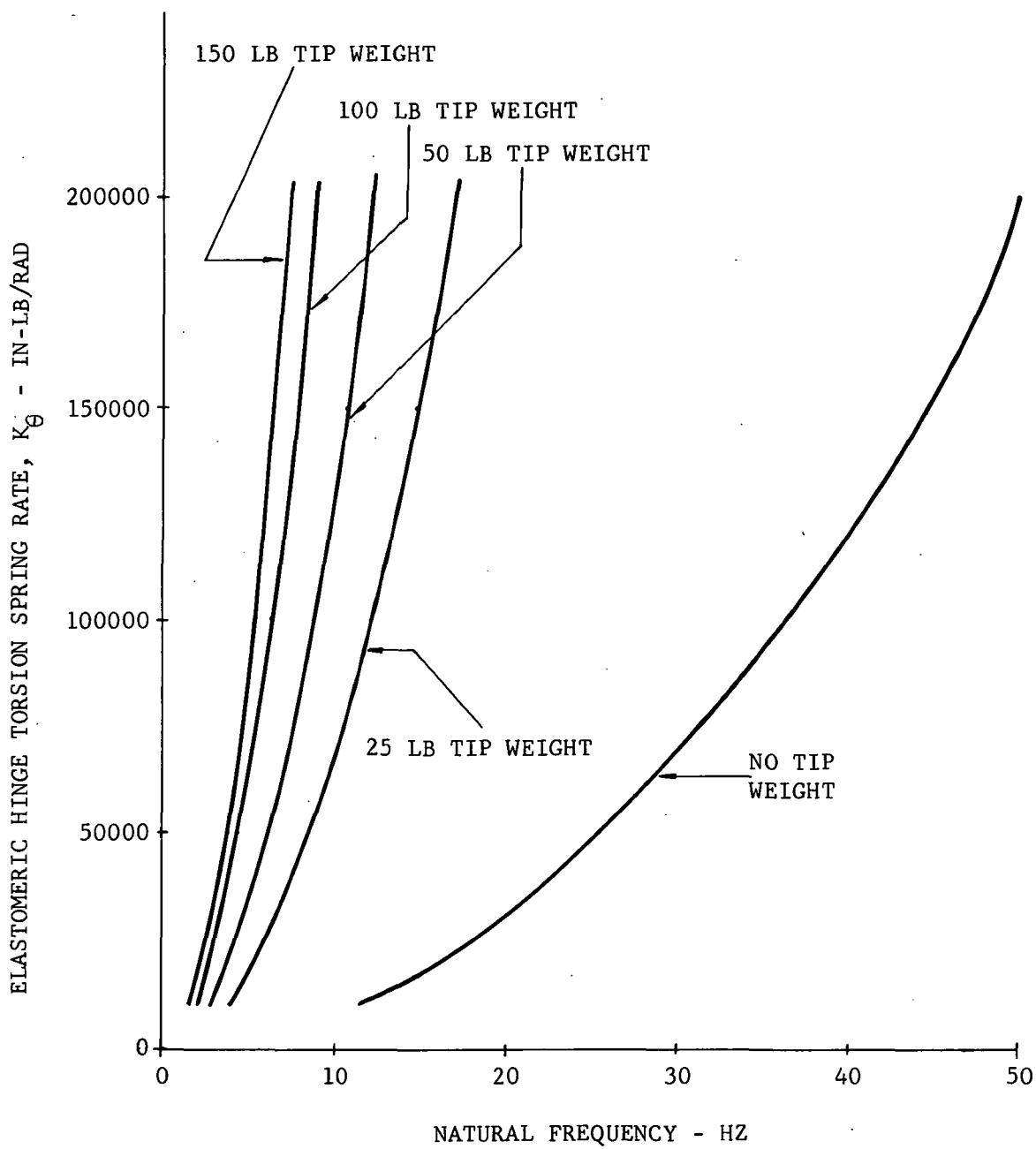


Figure 95. RSRA Nodal Beam Natural Frequency with Variations of M_{TIP} and K_θ .

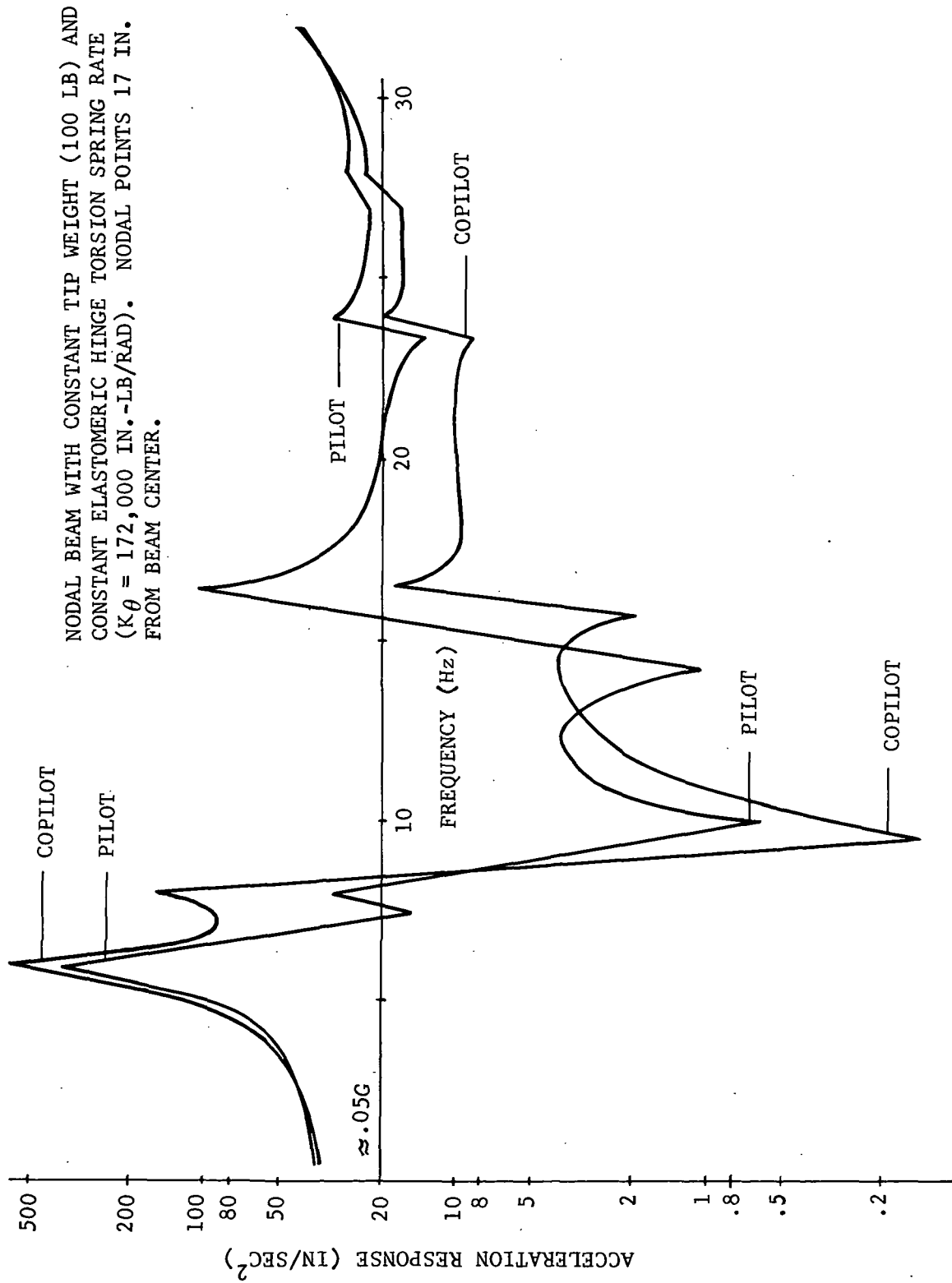


Figure 96. Model 309 Frequency Response to a 1000-Pound Vertical Hub Shear.

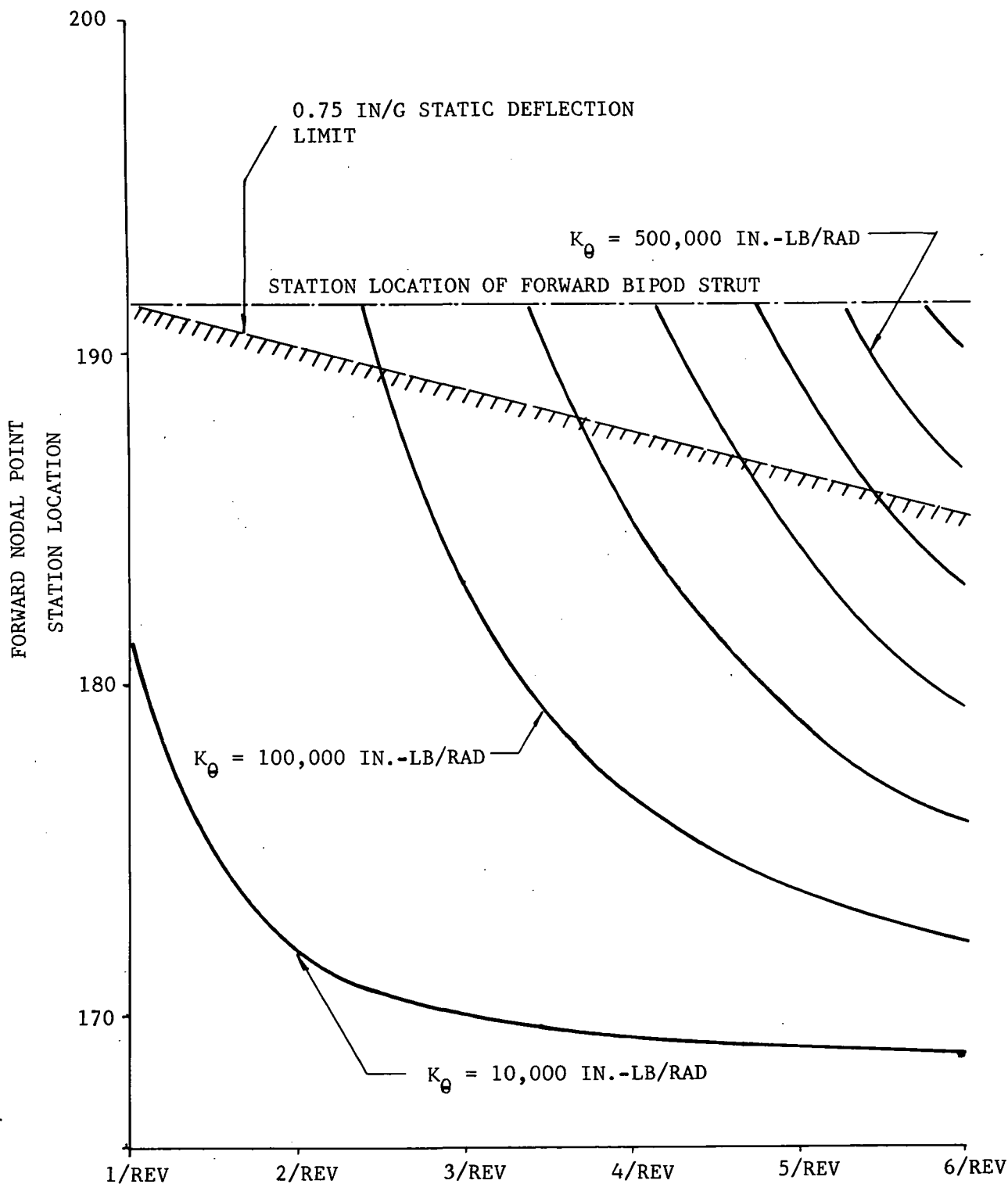


Figure 97. Nodal Point Location as a Function of Frequency and K_θ for RSRA Nodal Beam with $M_{TIP} = 25$ Pounds.

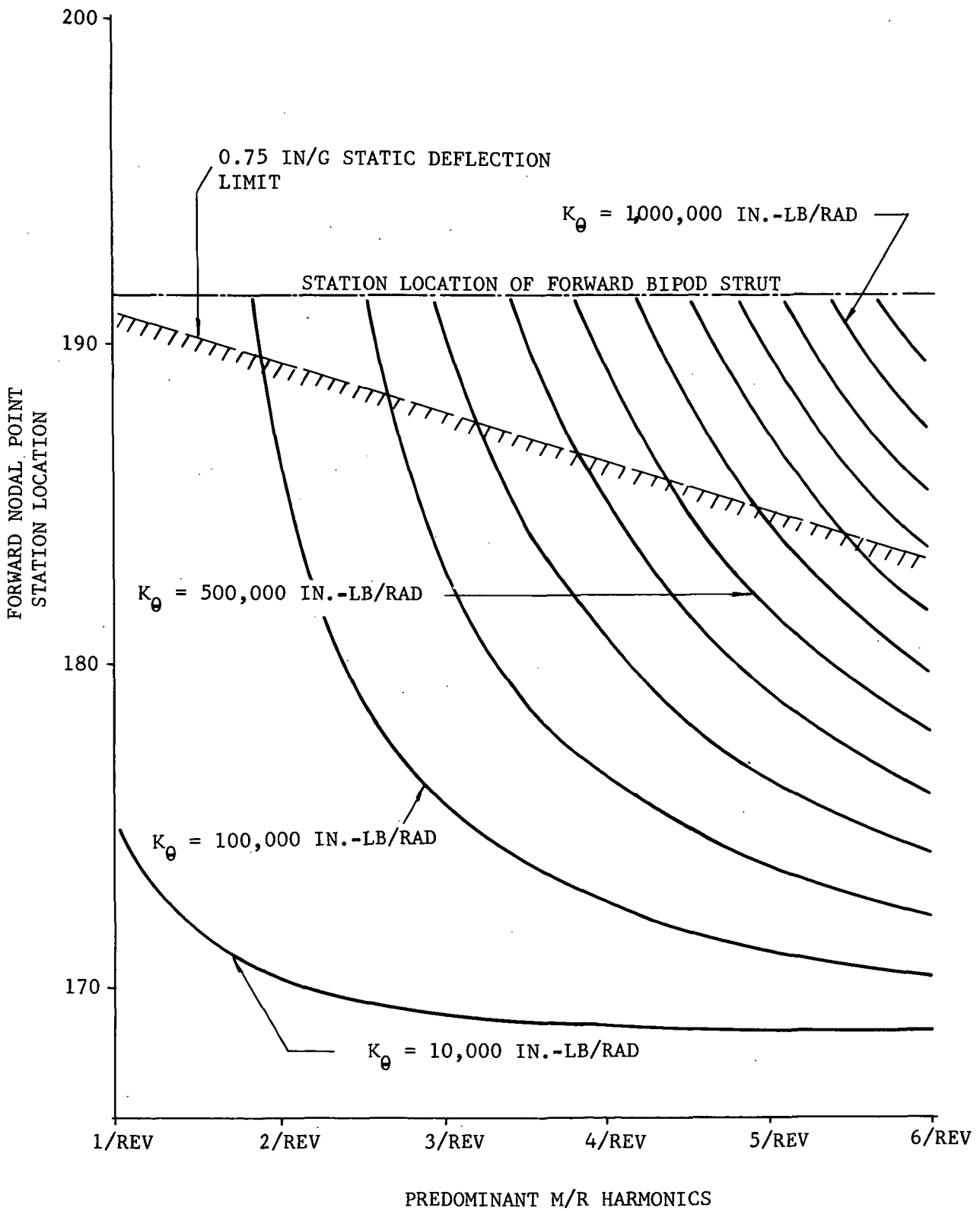


Figure 98. Nodal Point Location as a Function of Frequency and K_{θ} for RSRA Nodal Beam with $M_{TIP} = 50$ Pounds.

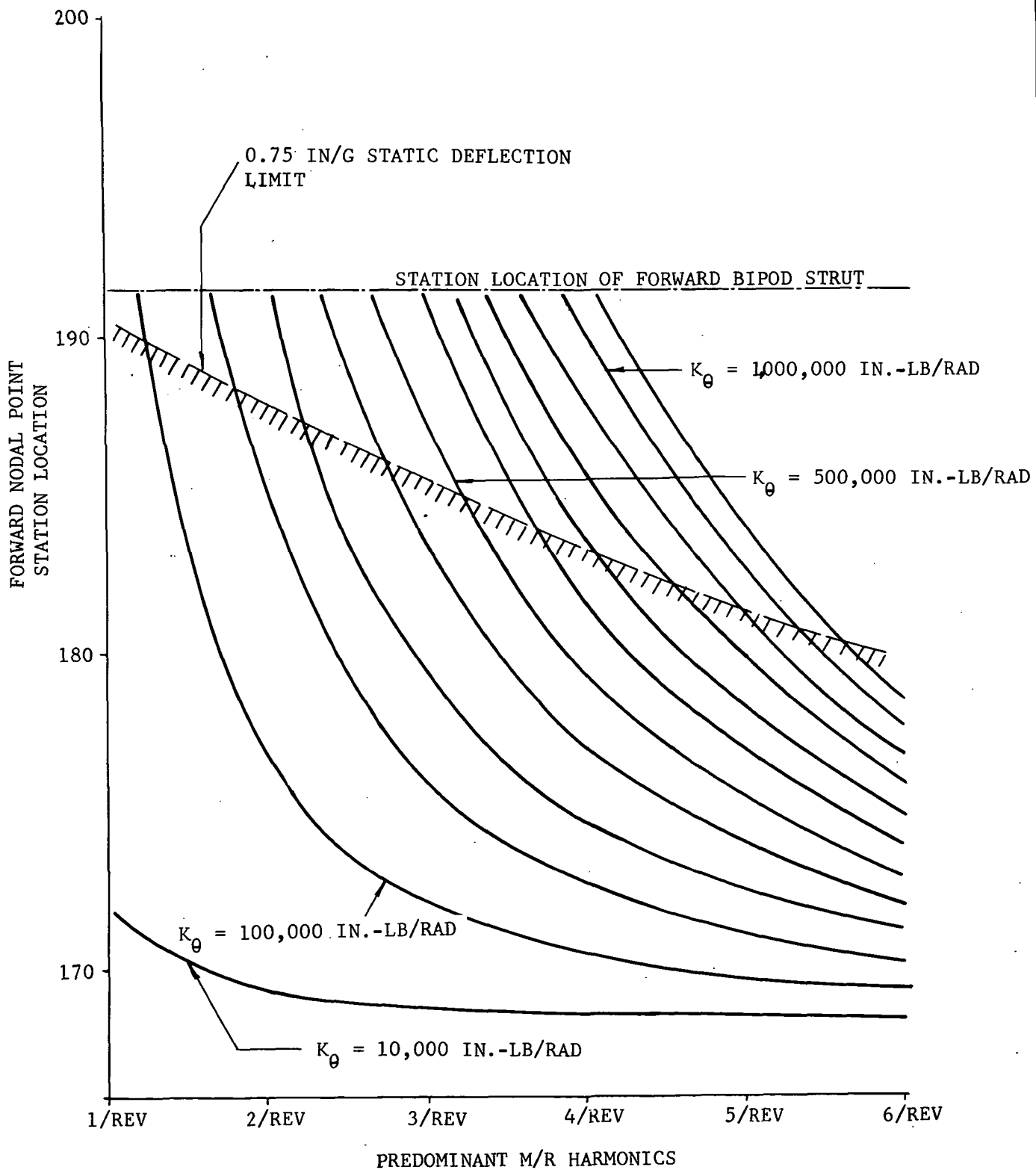


Figure 99. Nodal Point Location as a Function of Frequency and K_θ for RSRA Nodal Beam with $M_{TIP} = 100$ Pounds.

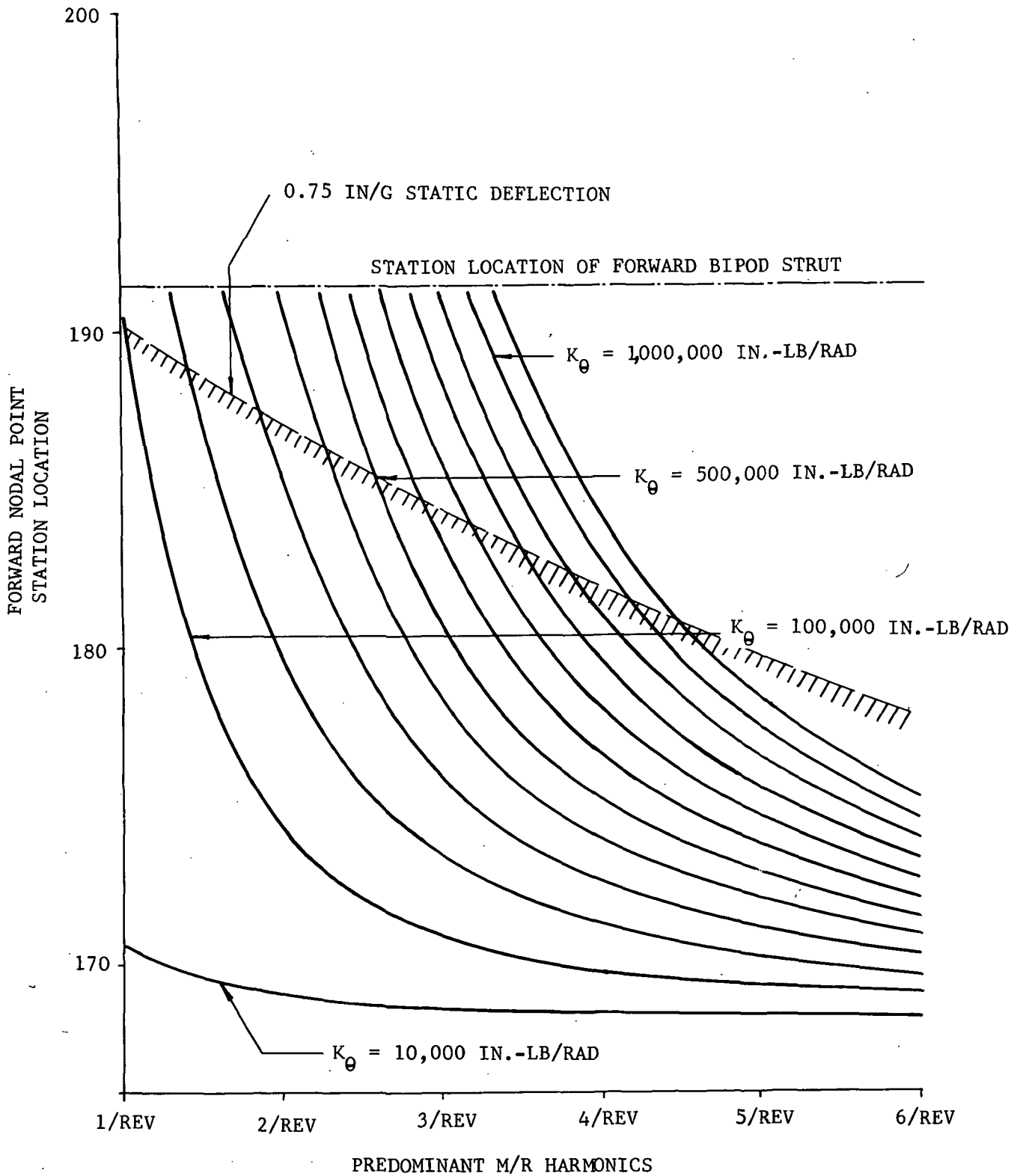


Figure 100. Nodal Point Location as a Function of Frequency and K_{θ} for RSRA Nodal Beam with $M_{TIP} = 150$ Pounds.

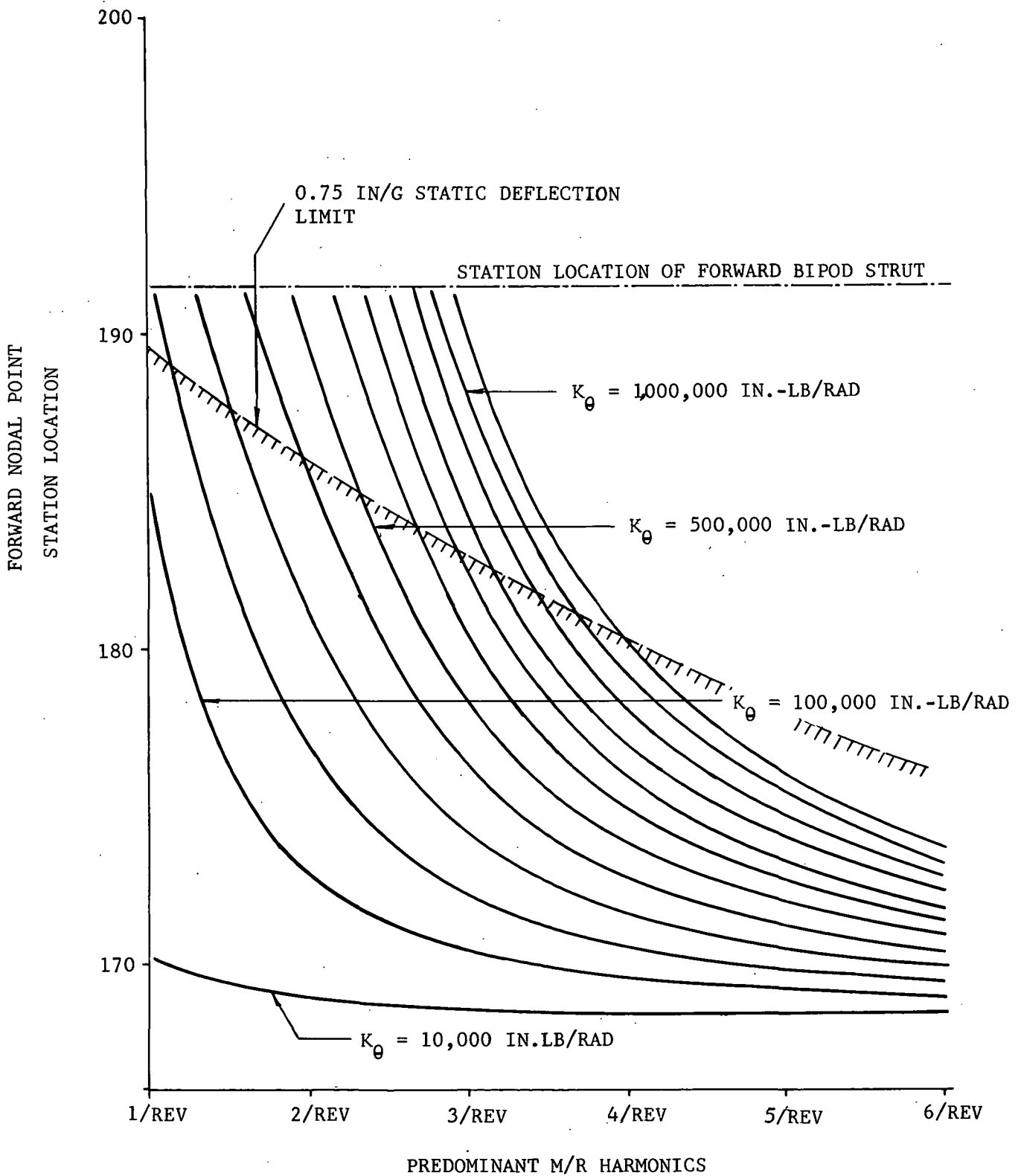


Figure 101. Nodal Point Location as a Function of Frequency and K_{θ} for RSRÁ Nodal Beam with $M_{TIP} = 200$ Pounds.

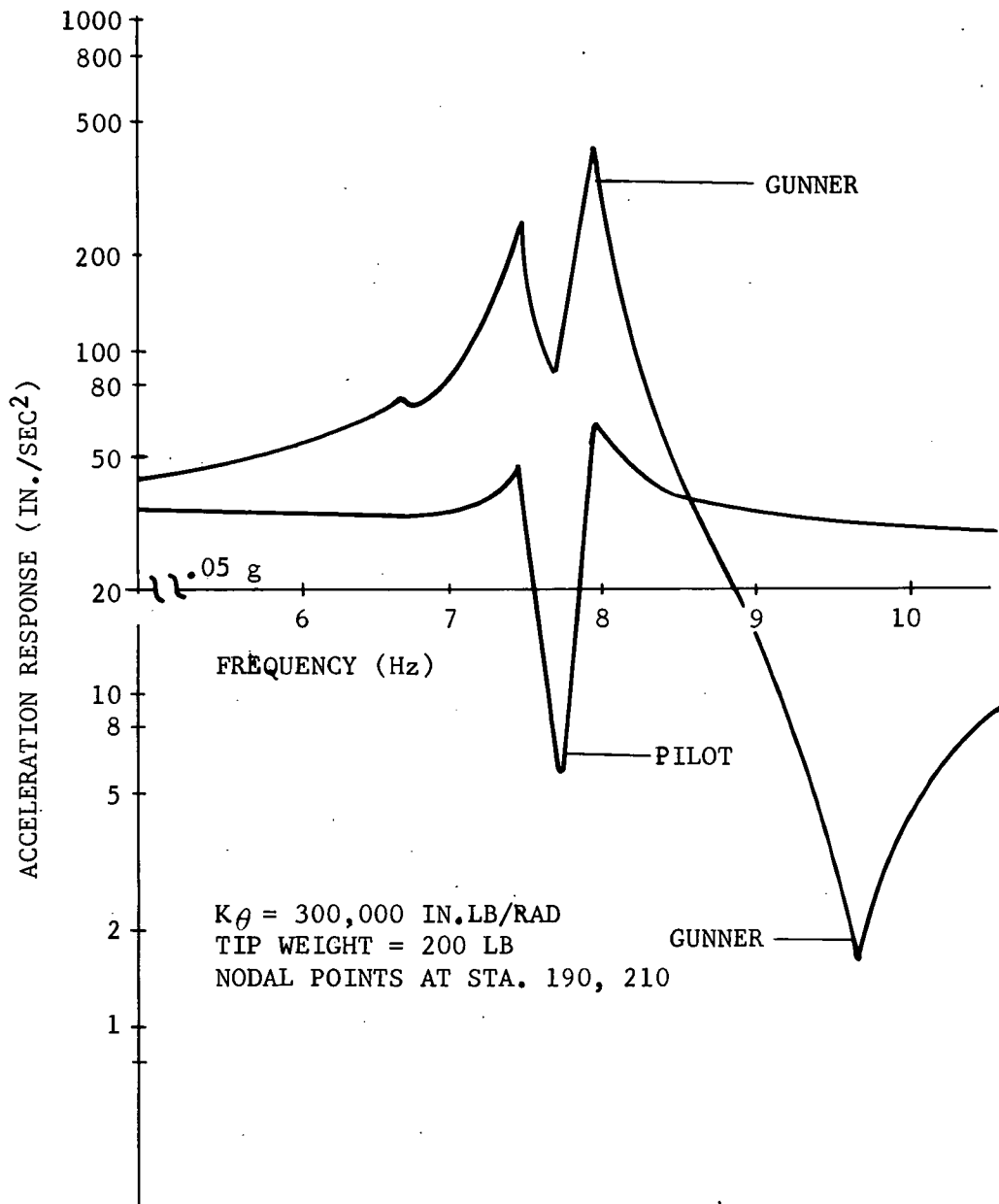


Figure 102. Low RPM Two-Per-Rev Vertical Isolation with Nodal Beam.

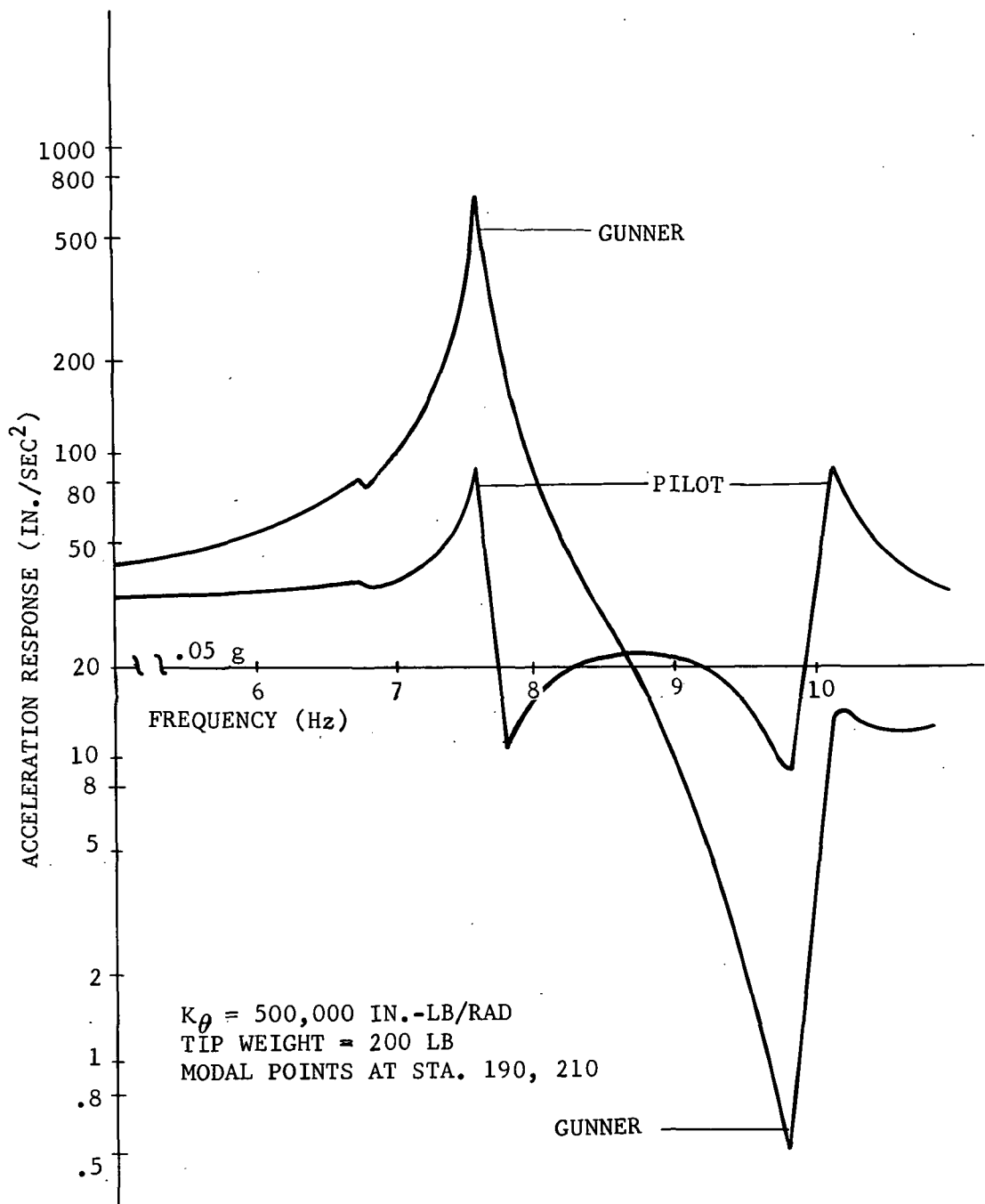


Figure 103. High RPM Two-Per-Rev Vertical Isolation with Nodal Beam.

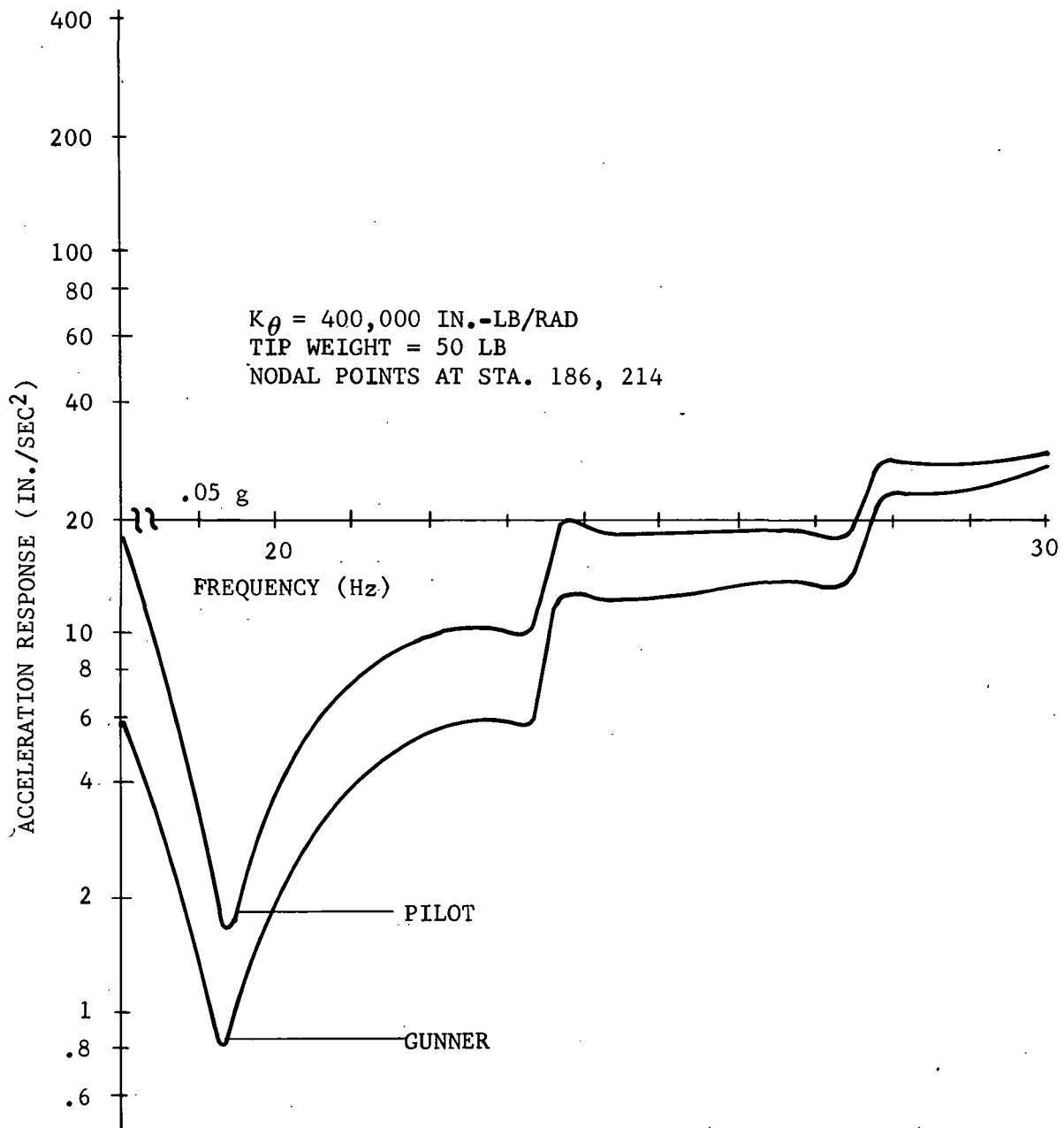


Figure 104. Low RPM Six-Per-Rev Vertical Isolation with Nodal Beam.

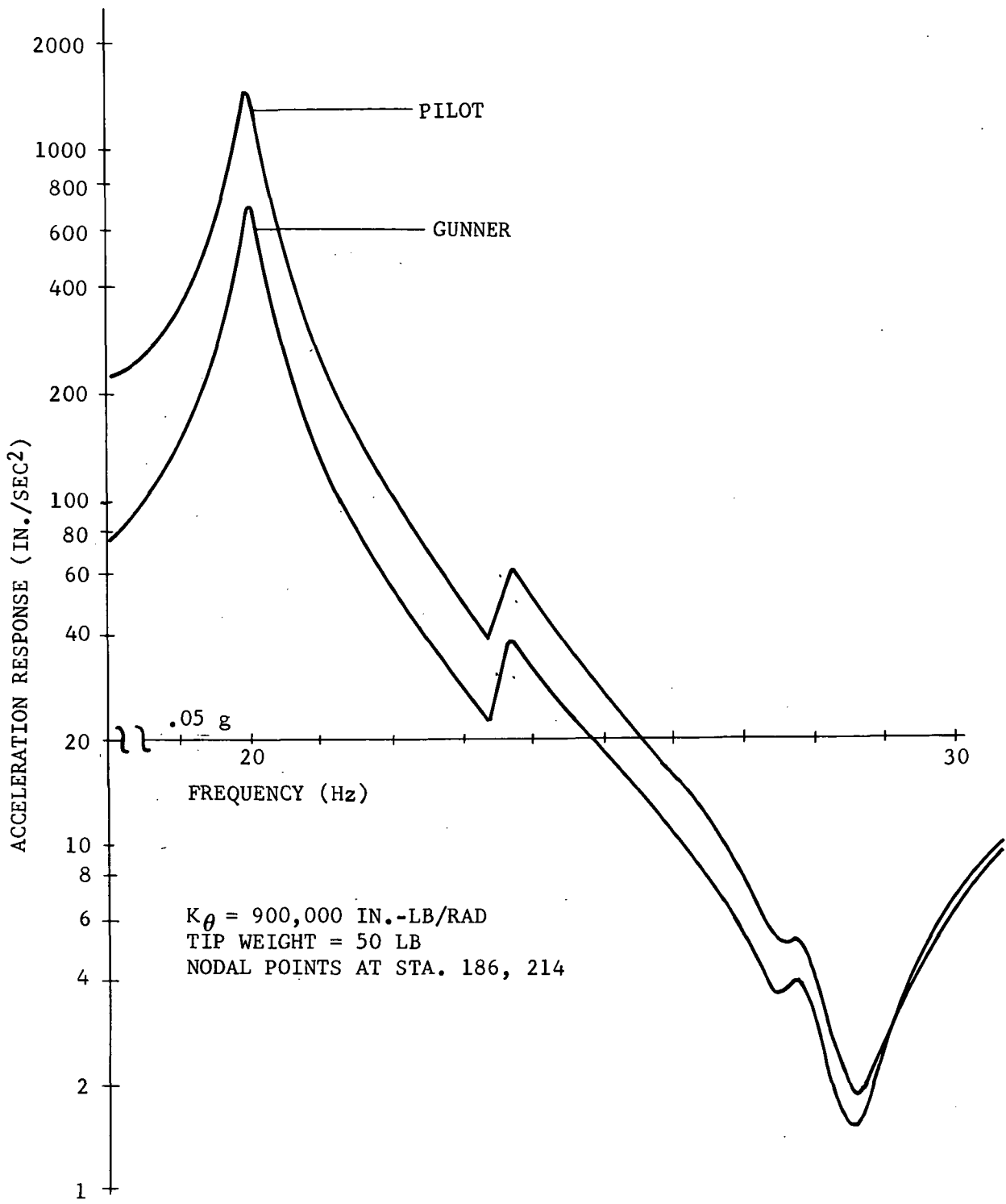


Figure 105. High RPM Six-Per-Rev Vertical Isolation with Nodal Beam.

NODAL BEAM
PYLON ISOLATOR

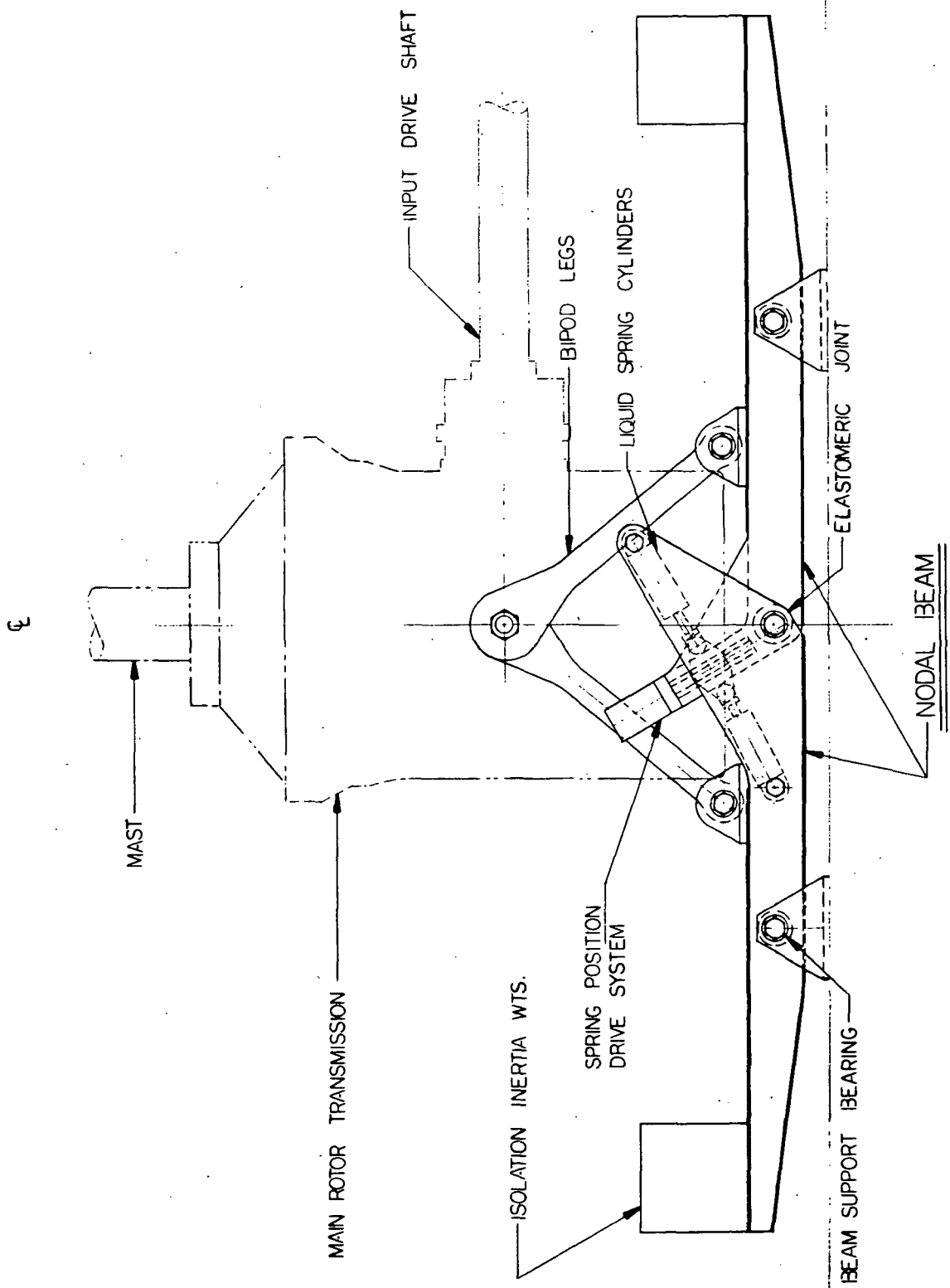


Figure 106. RSRA Nodal Beam Vertical Isolation System.

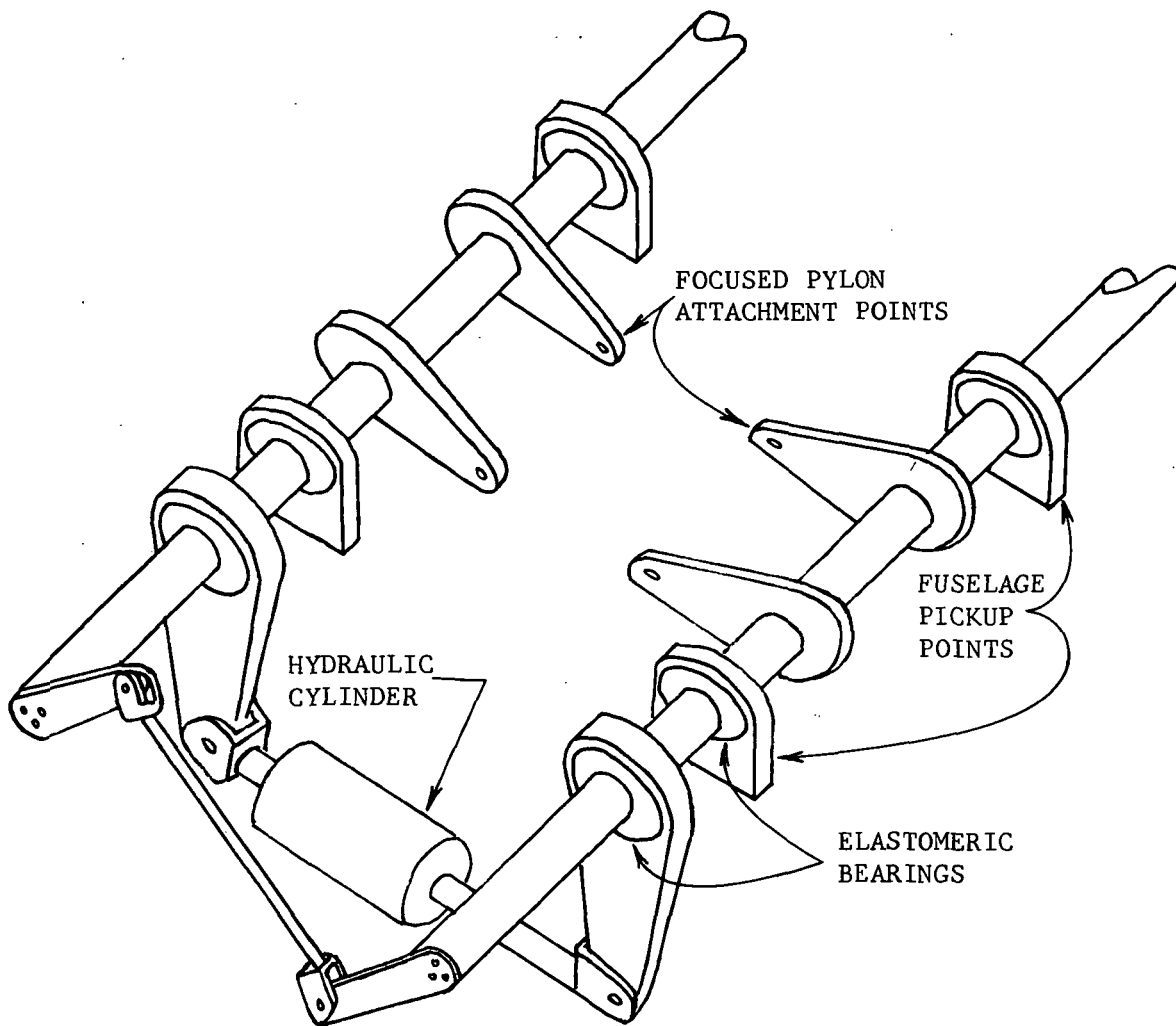


Figure 107. Servo-Null Vertical Isolation System.

646A ROTOR

OPERATIONAL ENVELOPE CONSIDERED AND REGIMES OF BLADE LOAD AMPLIFICATION

4 BLADES
55 FT DIA

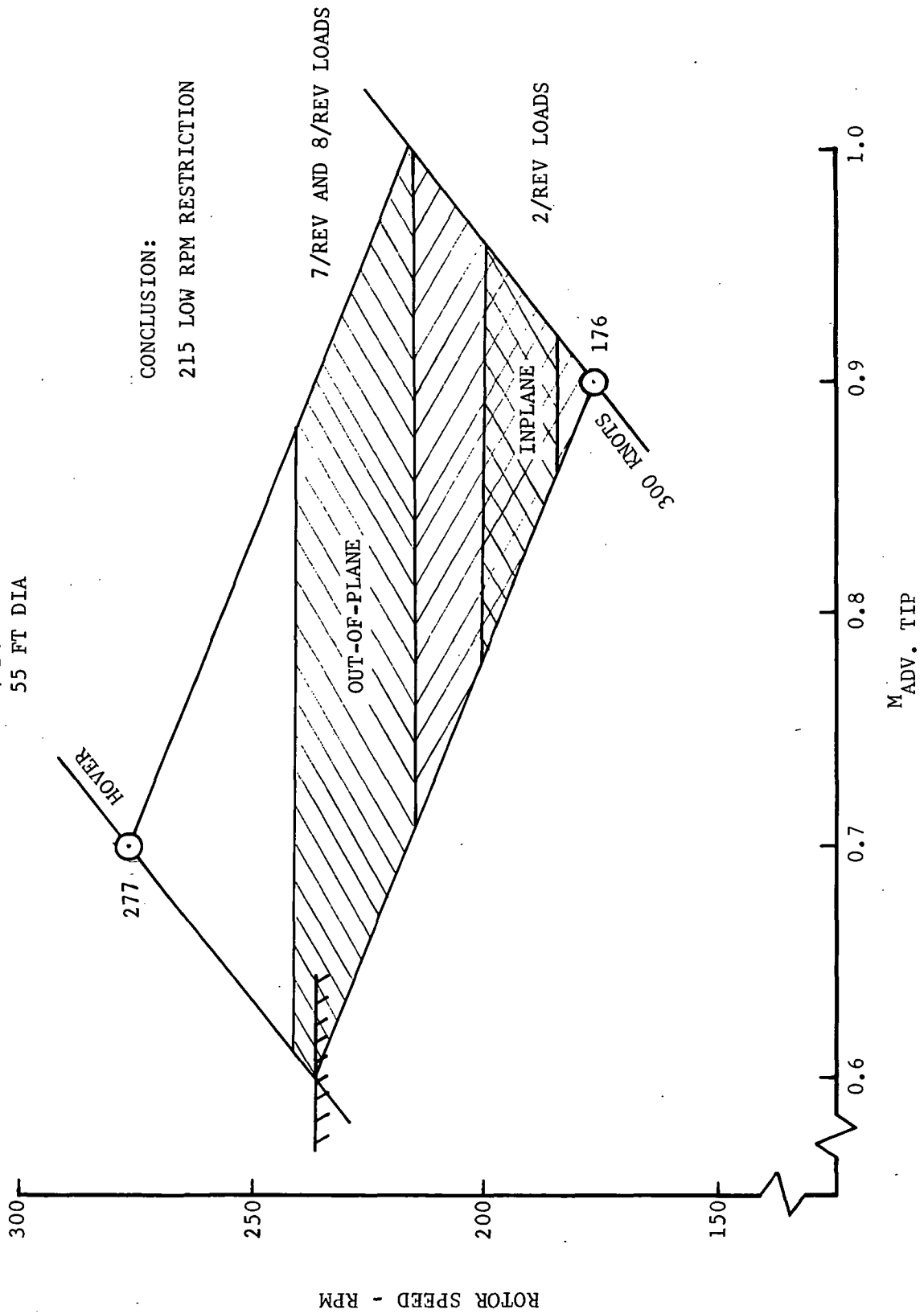
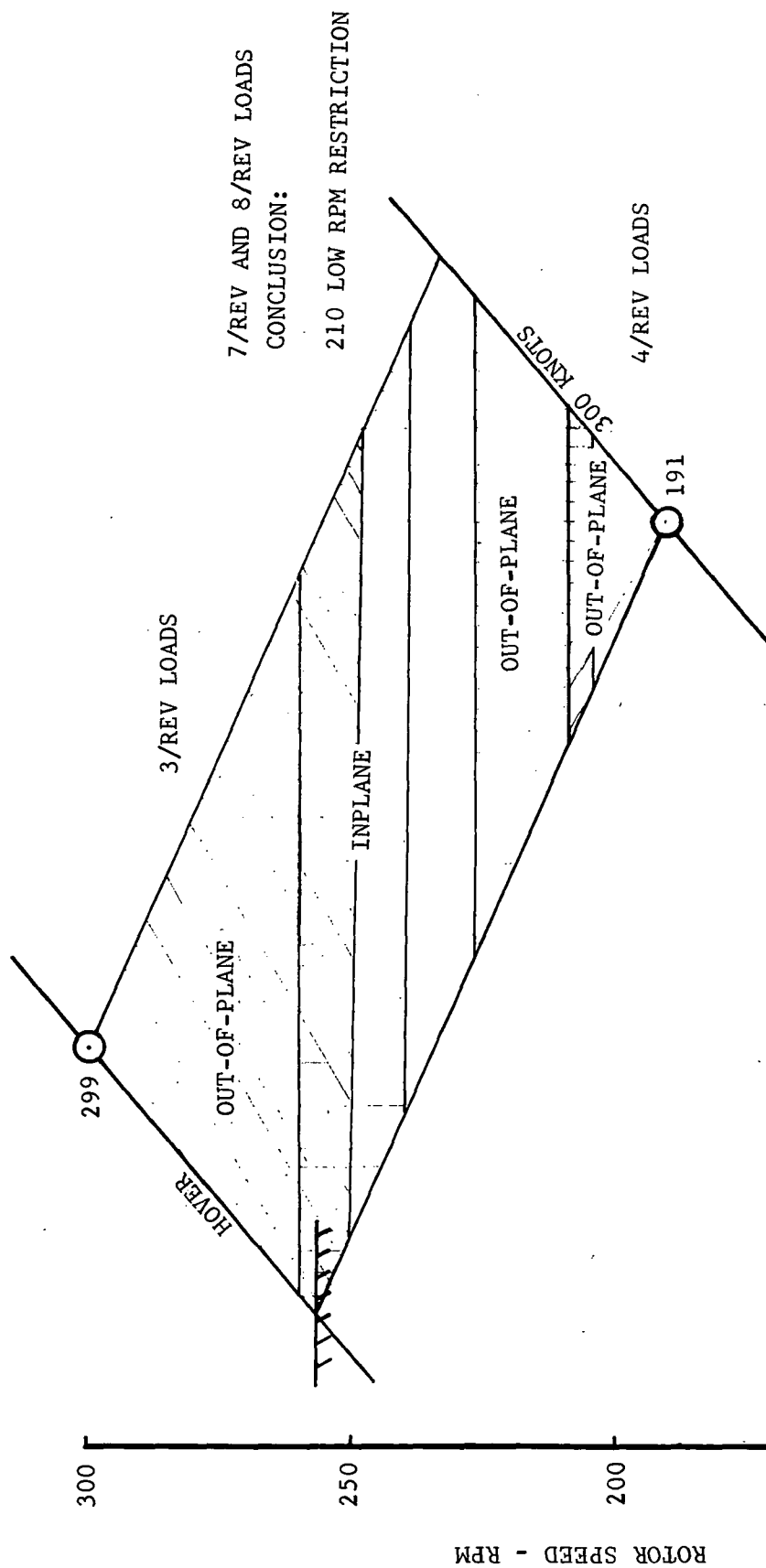


Figure 108. Operational Envelope Considered and Regimes of Blade Load Amplification - 646A.

OPERATIONAL ENVELOPE CONSIDERED AND REGIMES OF BLADE LOAD AMPLIFICATION

2 BLADES
50 FT DIA



CONCLUSION:
210 LOW RPM RESTRICTION

$M_{ADV, TIP}$

Figure 109. Operational Envelope Considered and Regimes of Blade Load Amplification - 646B.

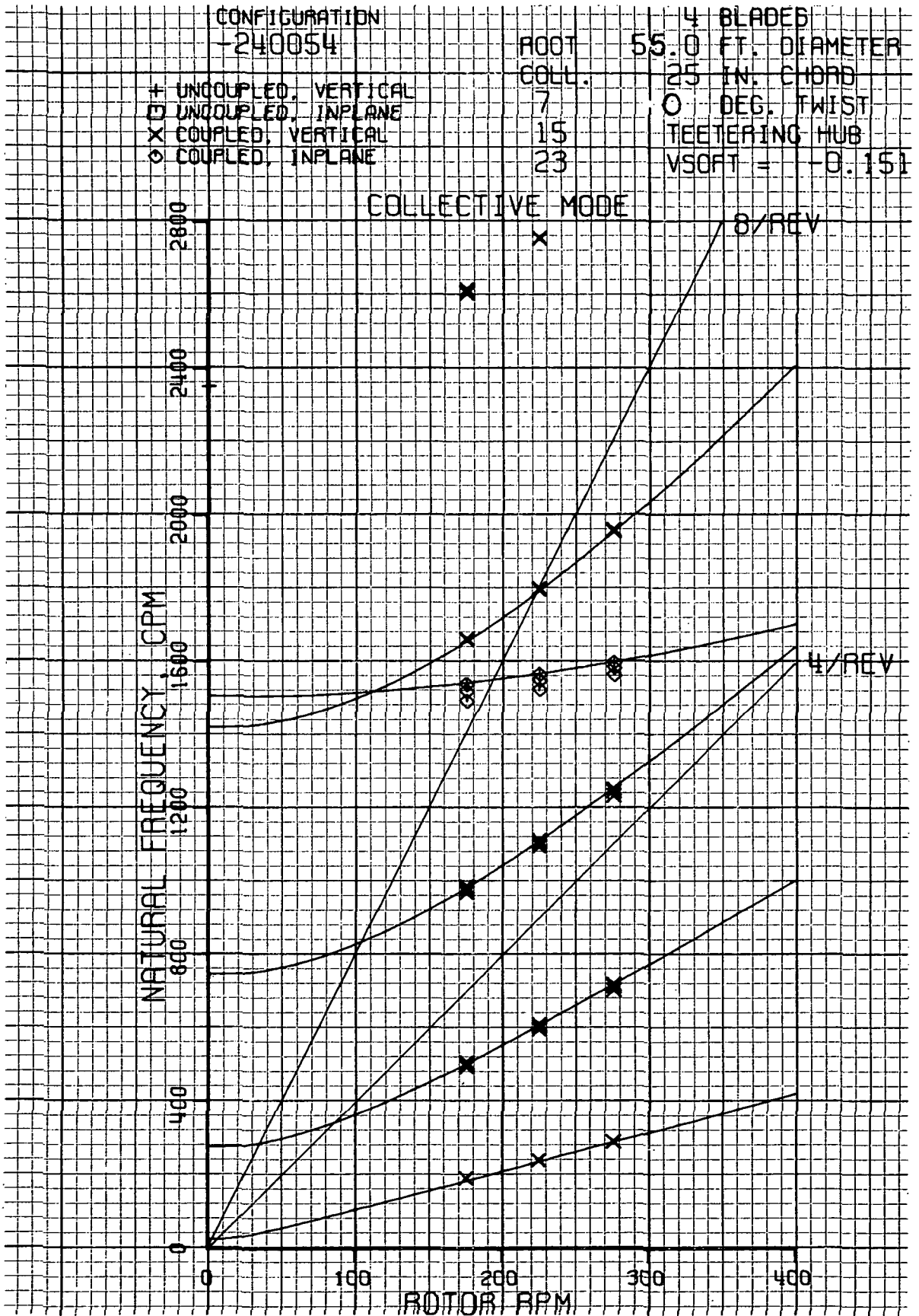


Figure 110. 646A Rotor Coupled Natural Frequencies Collective Mode.

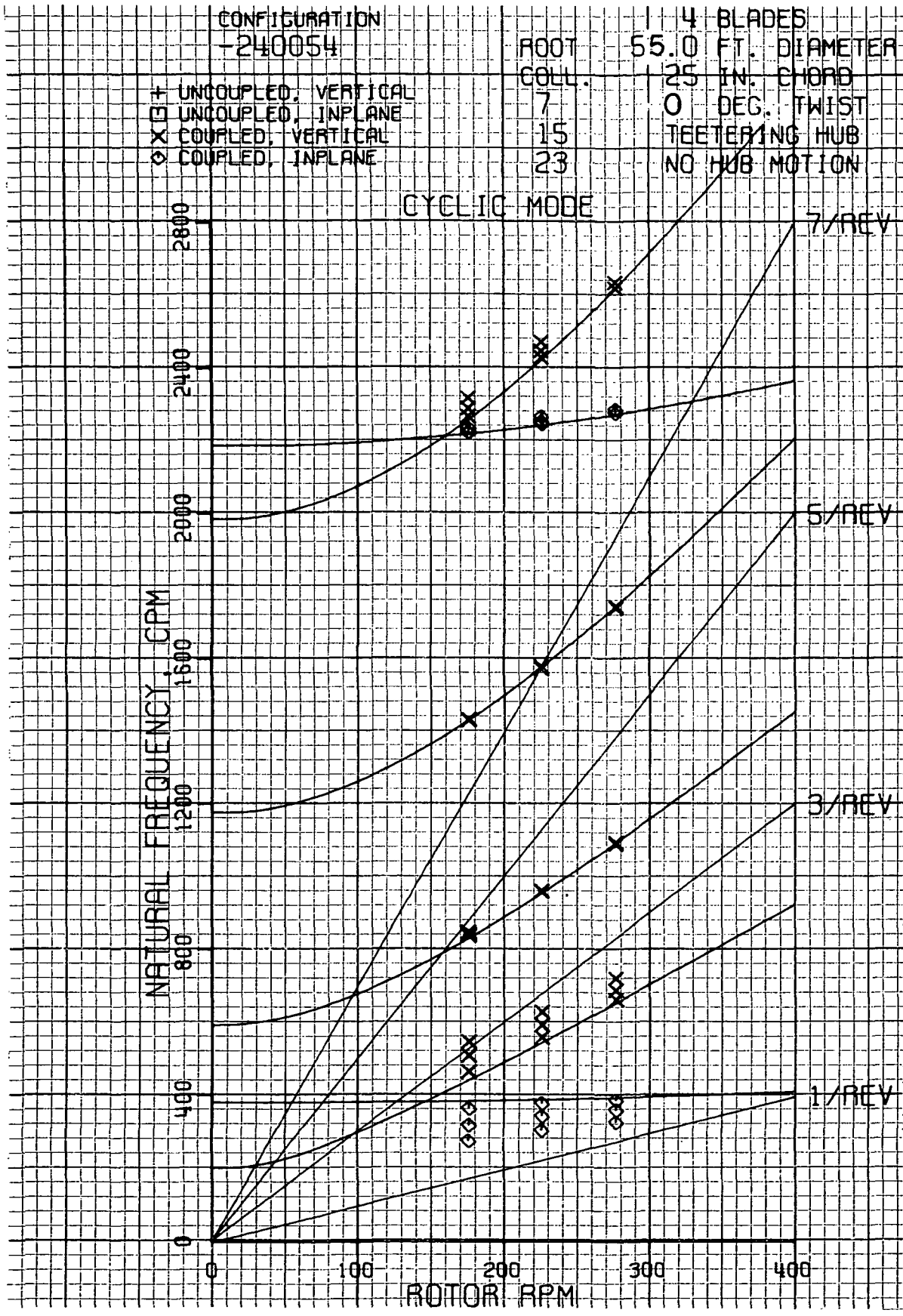


Figure 111. 646A Rotor Coupled Natural Frequencies Cyclic Mode.

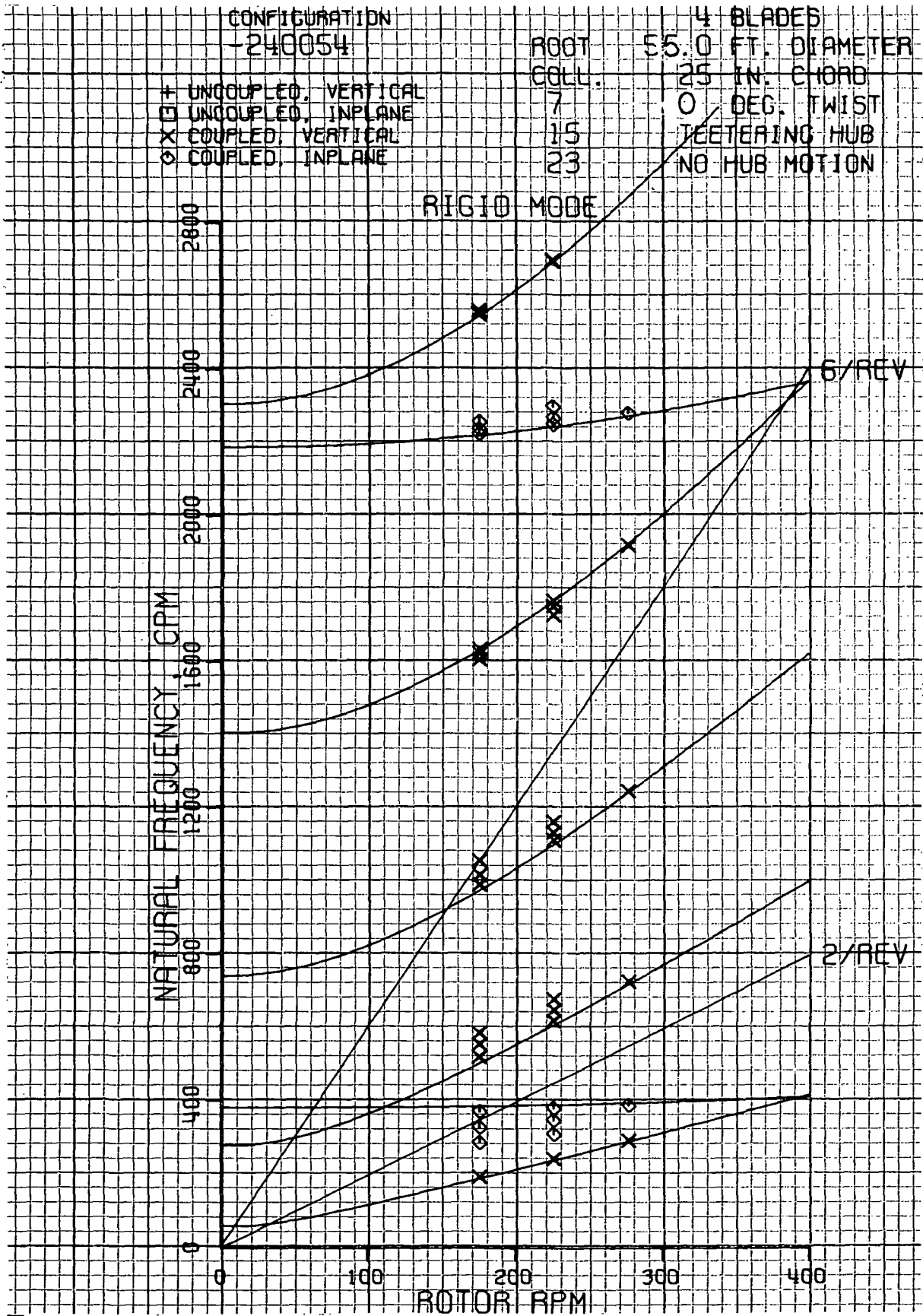


Figure 112. 646A Rotor Coupled Natural Frequencies Rigid Mode.

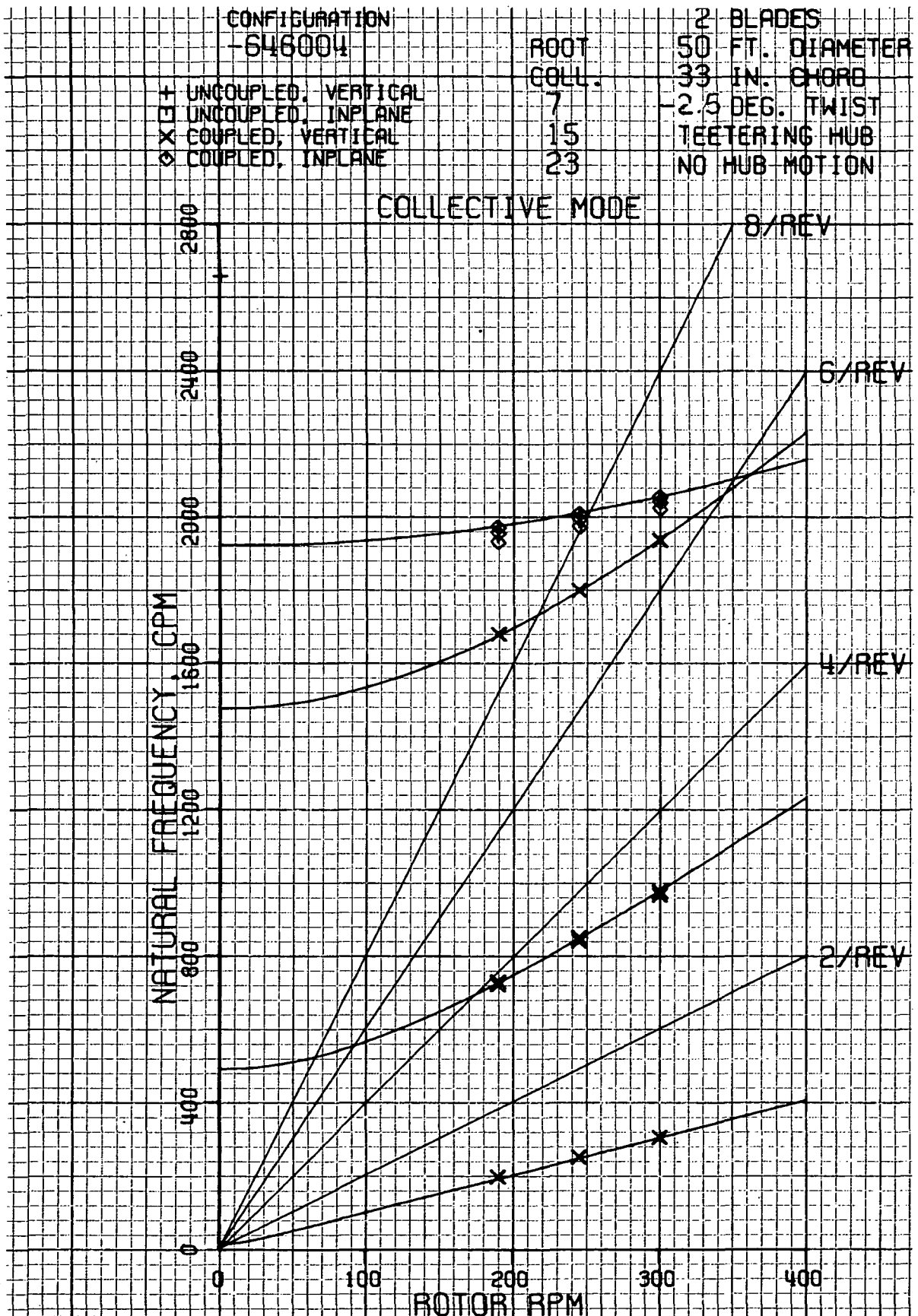


Figure 113. 646B Rotor Coupled Natural Frequencies Collective Mode.

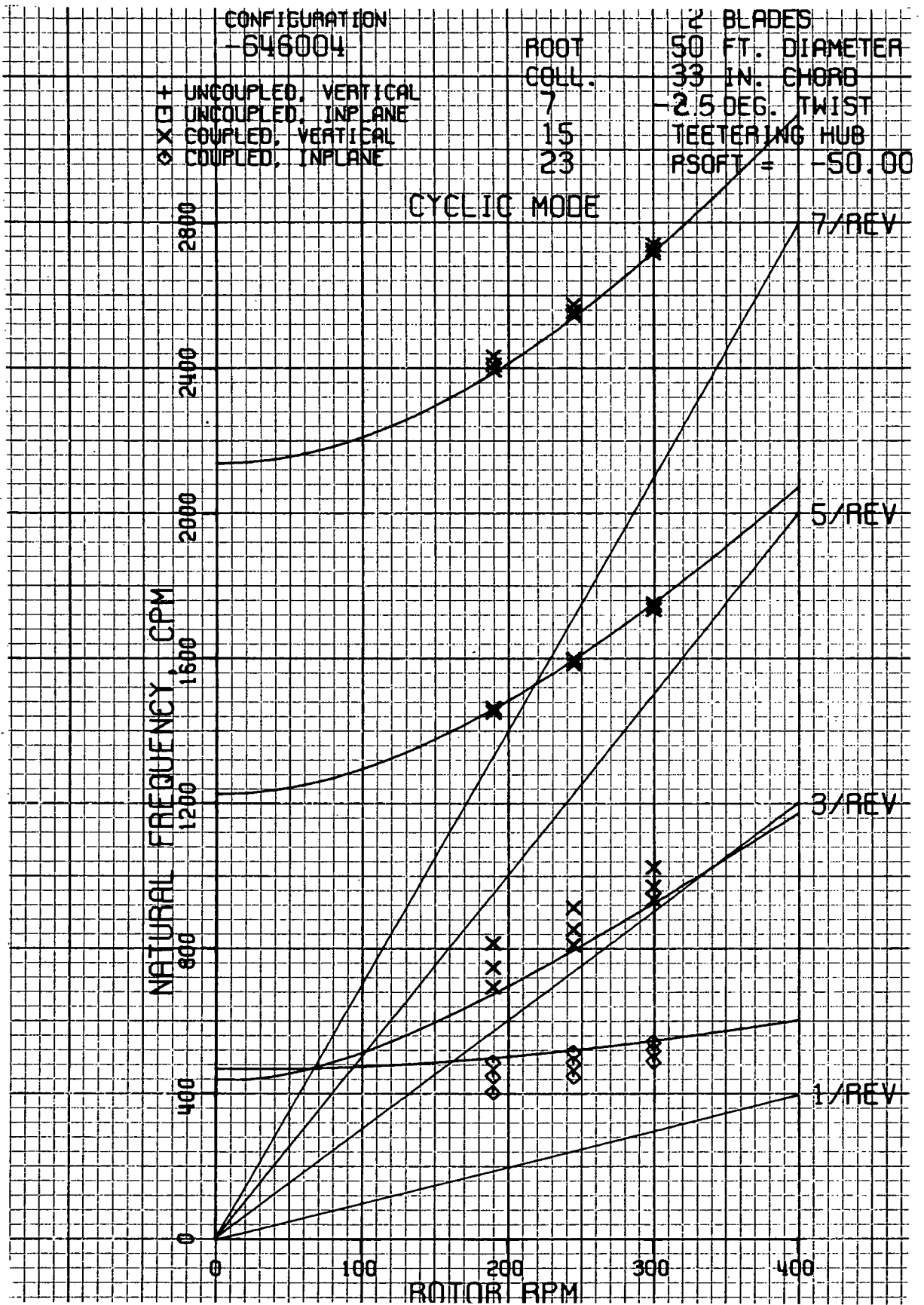


Figure 114. 646B Rotor Coupled Natural Frequencies Cyclic Mode.

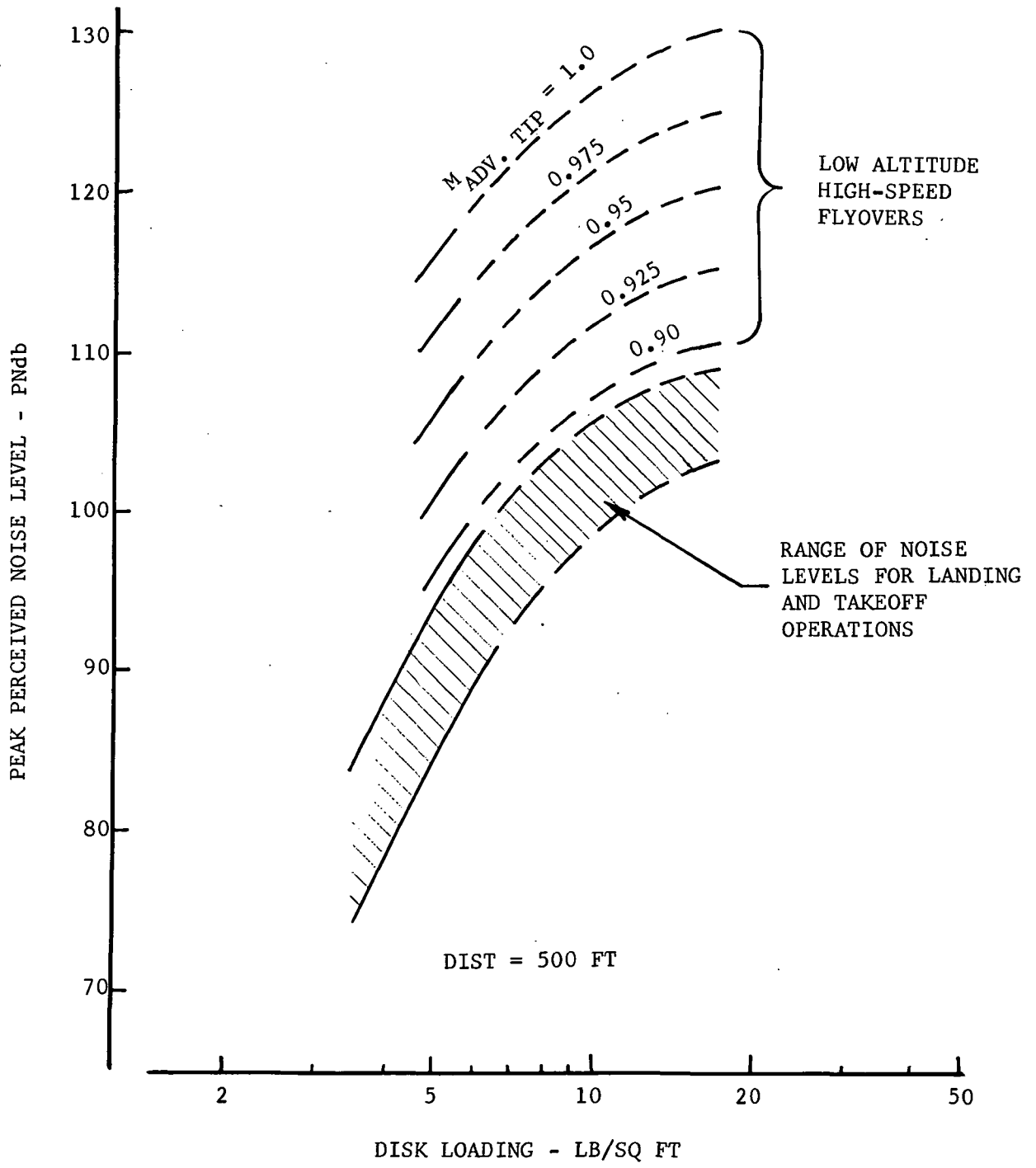
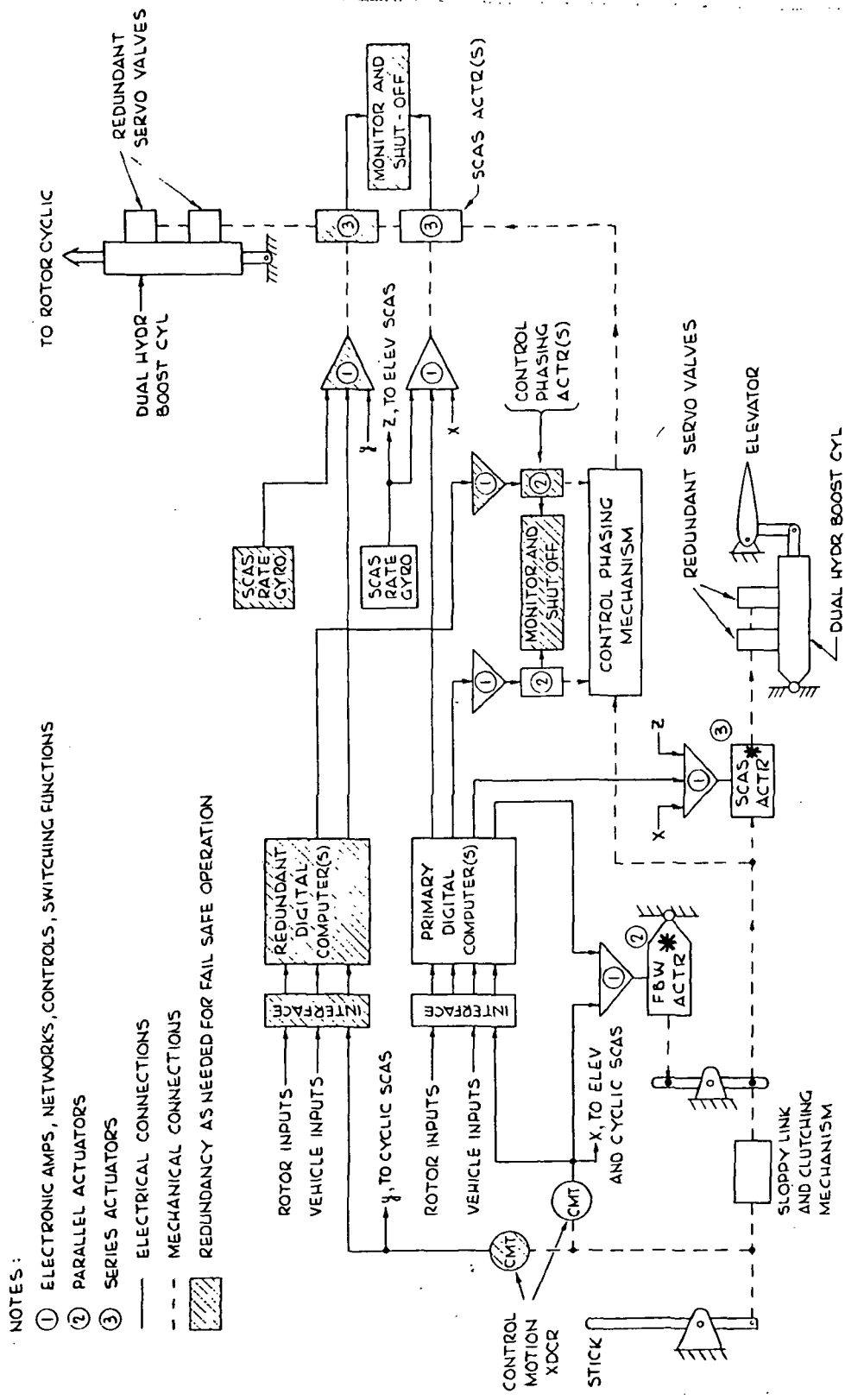


Figure 115. Rotor Noise Generation.



NOTES:

- ① ELECTRONIC AMPS, NETWORKS, CONTROLS, SWITCHING FUNCTIONS
- ② PARALLEL ACTUATORS
- ③ SERIES ACTUATORS
- ELECTRICAL CONNECTIONS
- - - MECHANICAL CONNECTIONS
- ▨ REDUNDANCY AS NEEDED FOR FAIL SAFE OPERATION

* This includes a position transducer.

Figure 116. Control System Concept No. I.

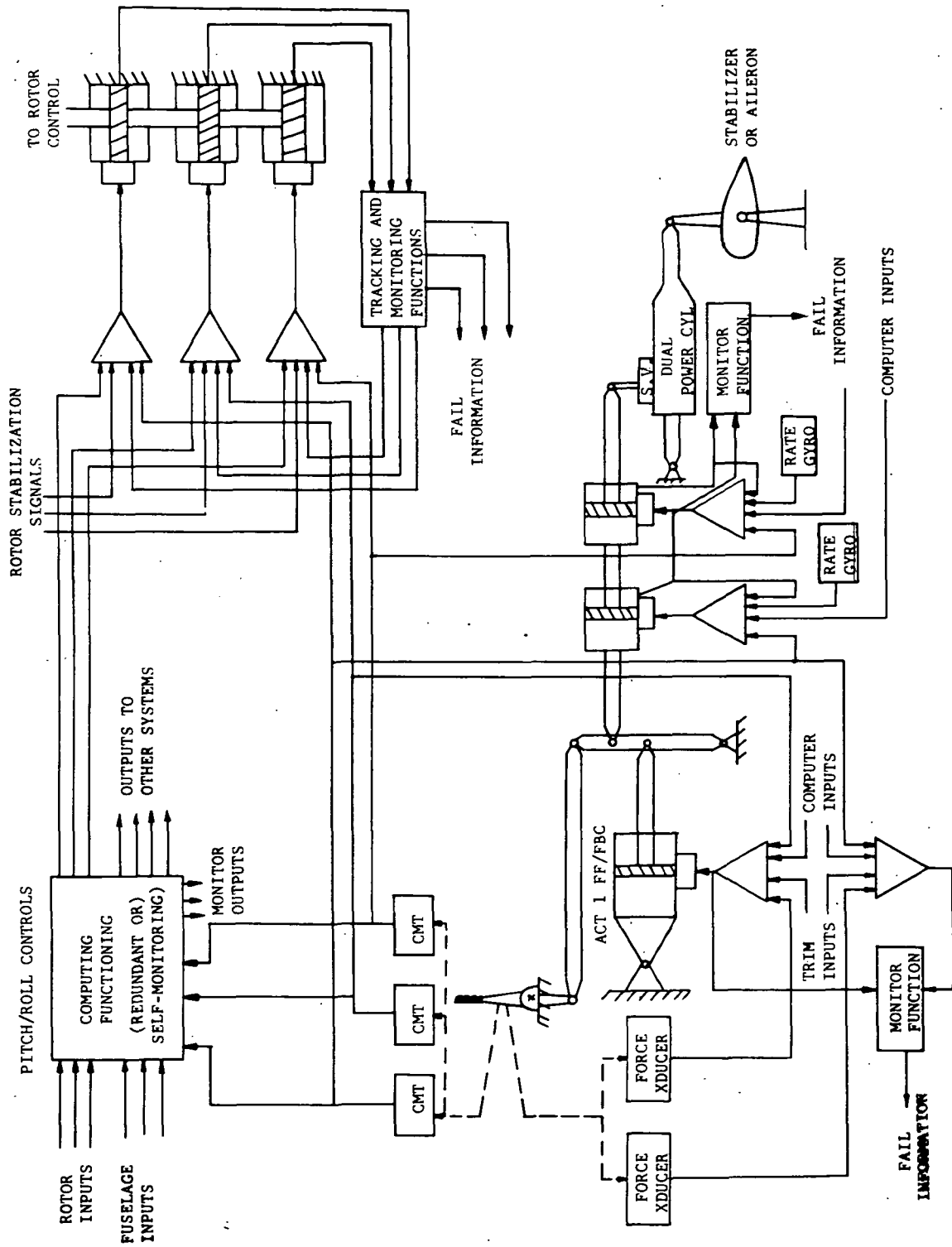
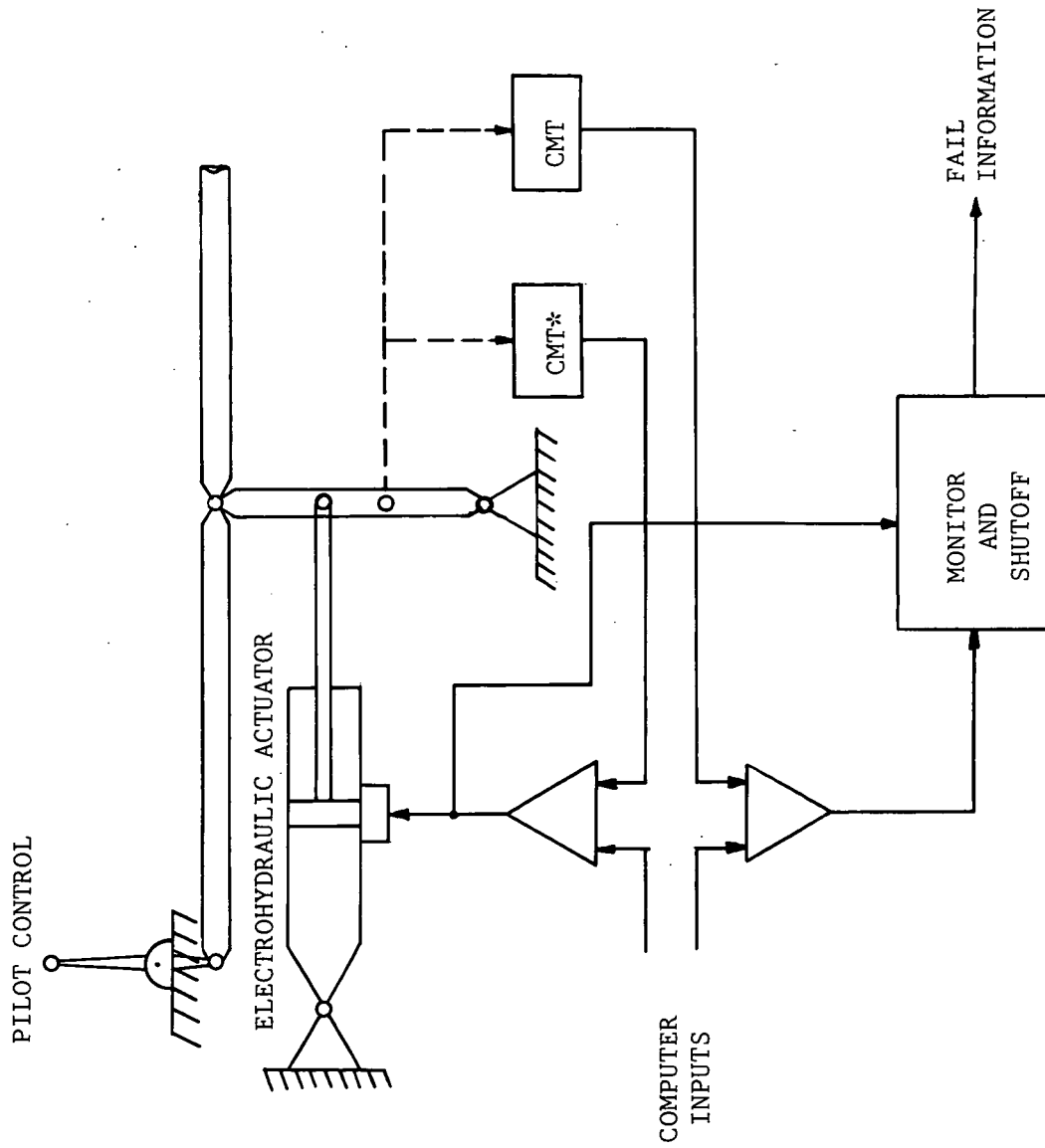


Figure 117. Control System Concept No. II.



*Control Motion Transducer

Figure 119. Throttle Control.

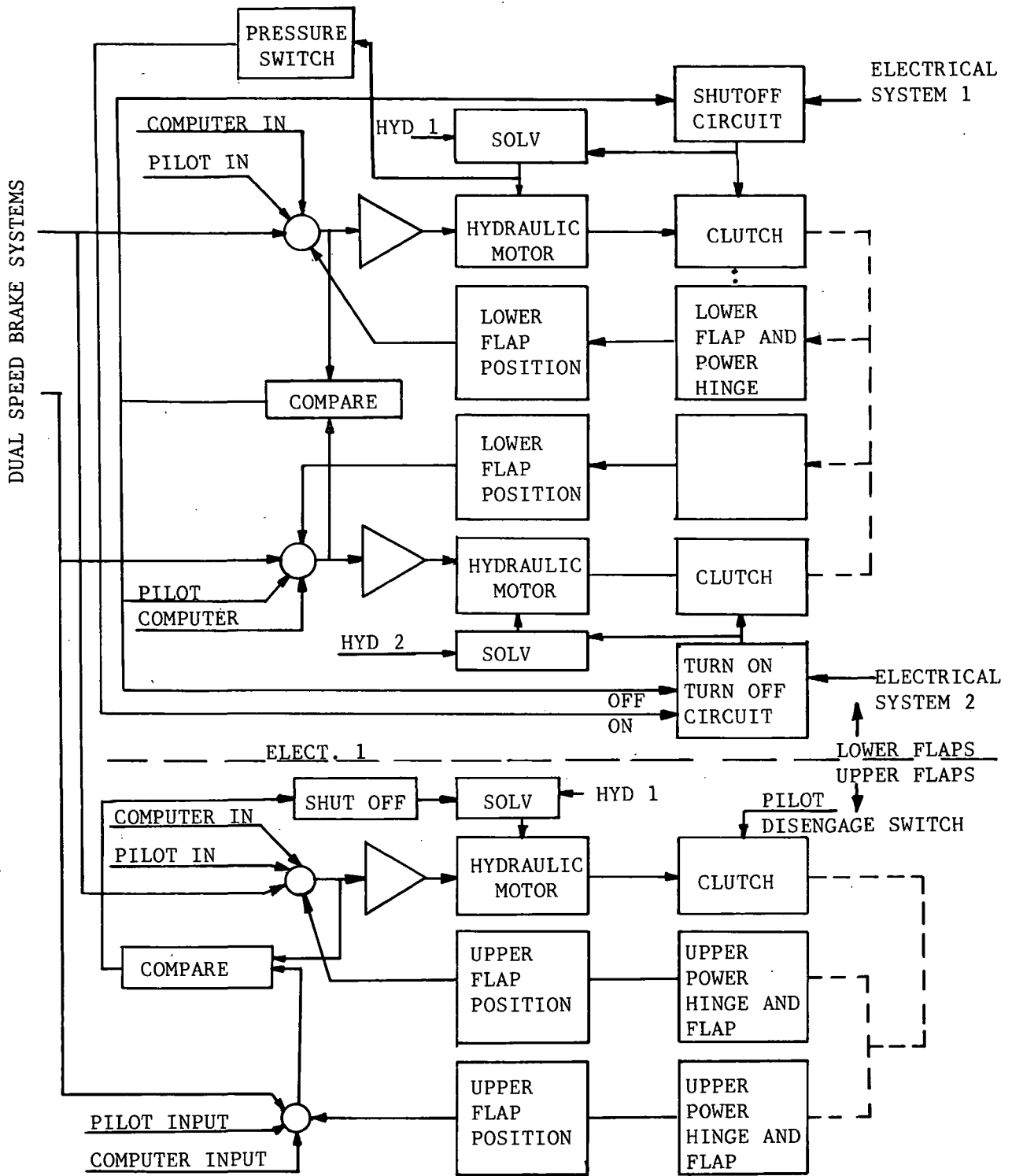


Figure 120.. Flap Controls.

APPENDIX C

TABLES

LIST OF TABLES

<u>Table</u>	<u>Subject</u>	<u>Page</u>
I	Aircraft Description	1
II	Group Weight Statement	4
III	High-Speed Mission Gross Weights	5
IV	Center of Gravity and Inertia Data (Compound Mode)	6
V	Drag Analysis	7
VI	High-Speed Mission Fuel Requirements	8
VII	High-Speed Mission Performance Summary	9
VIII	Hover Test Versatility	10
IX	Summary - Maximum Speed as Pure Helicopters	11
X	Percent Transmissibility of Hub Forces in Pitch	12
XI	Percent Transmissibility of Hub Forces in Roll	12
XII	Percent Transmissibility of Hub Moments in Pitch	13
XIII	Percent Transmissibility of Hub Moments in Roll	13
XIV	Isolation of Bipod Focal Pylon With Fore and Aft Axis at Input Shaft Axis	14
XV	Inplane Isolation System Trade-Offs	15
XVI	Passive Nodal Beam Configurations Required To Cover Entire Frequency Spectrum	16
XVII	Summary of Servo-Null Isolation System Requirements	17
XVIII	Comparison of Control System Concepts	18

TABLE I

AIRCRAFT DESCRIPTION

	<u>Units</u>	<u>Model 646A</u>	<u>Model 646B</u>
<u>DESIGN WEIGHTS</u>			
<u>Compound</u>			
Empty	lb	17,954	13,922
T.O. (Design Mission)	lb	23,738	18,517
Maximum	lb	24,761	19,730
<u>Pure Helicopter</u>			
Empty	lb	13,252	11,742
Maximum	lb	19,210	15,868
<u>Fuel Capacity</u>			
Compound	lb	5,063	5,302
Pure Helicopter	lb	3,358	2,726
<u>Fuselage Dimensions</u>			
Length	ft	51.9	50.4
Width	ft	5.25	3.08
Height	ft	9.60	9.60
<u>Landing Gear</u>			
<u>Main</u>			
Tread	in.	--	94
Tire Size	in.	--	26 x 6.6
Oleo Strut Travel	in.	--	12
Turnover Angle	deg	--	22.5 lat.
<u>Tail Wheel</u>			
Tire Size	in.	--	18 x 5.5
Oleo Strut Travel	in.	--	5
Axle Travel	in.	--	10
<u>Main Rotor</u>			
Type	--	Modified BHC Model 240 Gimbaled	Modified BHC Model 645 Semirigid
Number of Blades	--	4	2
Diameter	ft	55	50
Chord	in.	25	33
Solidity	--	.094	.070
Twist	deg	0	-2.5
Airfoil	--	Mod. Wortmann FX090	Mod. Wortmann FX090
Mast Tilt Range	deg	-4 to -12	0 to -15
Collective Range	deg	18	20
Flapping Range	deg	±10	±12

AIRCRAFT DESCRIPTION (CONTINUED)

	<u>Units</u>	<u>Model 646A</u>	<u>Model 646B</u>
<u>Wing</u>			
Area	sq ft	225	173
Aspect Ratio	--	4	4
Taper Ratio	--	2.0	1.87
Sweep Angle	deg	2.85	2.60
Incidence Range	deg	±20	±20
Section	--	653A618	653A618
<u>INBOARD T.E. CONTROLS</u>			
Type (Upper and Lower)	--	Split Flap	Split Flap
Percent of Chord	--	30	30
Percent of Span	--	100	100
Maximum Deflection	deg	±60	±60
Area	sq ft	118.0	99.2
<u>T.E. CONTROLS</u>			
Percent Chord	--	30	30
Percent Span	--	40	40
Maximum Deflection	deg		
as Flaps (Lower)	deg	30	30
as Ailerons (Upper)	deg	30	30
Area	sq ft	21.7	18.6
<u>Horizontal Stabilizer</u>			
Type	--	Stabilator	Stabilator
Span	ft	14.1	14.1
Area	sq ft	50	50
Aspect Ratio	--	4.0	4.0
Taper Ratio	--	2.0	2.0
Sweep Angle	deg	2.86	2.86
MGC	in.	43.8	43.8
MGC Location	in. B.L.	38.0	38.0
Airfoil	--	12% Sym.	12% Sym.
Maximum Deflection	deg	±15	±15
<u>Vertical Stabilizer</u>			
Area	sq ft	21.2	14.8
Aspect Ratio	--	1.7	1.7
Taper Ratio	--	2.5	2.5
Sweep Angle	deg	47	47
MGC	in.	47	37
MGC Location	in. B.L.	0	0
Airfoil	--	12% Sym.	12% Sym.

AIRCRAFT DESCRIPTION (CONTINUED)

	<u>Units</u>	<u>Model 646A</u>	<u>Model 646B</u>
<u>Rudder</u>			
Area	sq ft	4.3	4.0
Percent Chord	--	30	30
Percent Span	--	50	50
Maximum Deflections	deg	±30	±30
<u>Ventral Fin</u>			
Area	sq ft	17.5	12.3
Aspect Ratio	--	0.75	0.75
<u>Tail Rotor</u>			
Type	--	BHC Model 240	BHC Model 309
Number of Blades	--	4	2
Diameter	ft	10.0	10.2
Solidity	--	0.191	0.146
Twist	deg	0	0
Airfoil	--	FX083	FX083
<u>Main Rotor Engines</u>			
Type	--	T55-L7-C	T53-L-13B
Mil. Power (Uninstalled)	shp	2 x 2650	2 x 1400
Mil. Power (Installed)	shp	2 x 2520	2 x 1325
<u>Auxiliary Engines (Installed)</u>			
	--	F102LD100	JT-12A-8
Mil. S.L. Static Thrust	lb	2 x 7200	2 x 3240
Mil. S.L. Thrust at 300 KTAS	lb	2 x 4100	2 x 2920

TABLE II
GROUP WEIGHT STATEMENT

<u>Group</u>	<u>Model 646A Weight (lb)</u>	<u>Model 646B Weight (lb)</u>
Rotor	1921.0	1600.0
Wing	1209.0	827.0
Tail	236.8	196.0
Body	2700.0	1830.5
Gear	805.0	730.0
Flight Controls	747.0	663.7
Engine Section	1041.8	562.8
Propulsion	5806.7	4400.7
Instruments	119.7	119.7
Hydraulics	165.0	165.0
Electrical	382.0	382.0
Electronics	224.4	224.4
Furnishings and Equipment	159.2	141.0
Air Conditioning	162.0	108.4
Special Provisions		
Pylon Support	280.0	160.0
Crew Escape Systems	324.0	216.0
Wing Tilt and Balance	350.0	325.0
Wing High Lift Systems	150.0	100.0
Instrument Packages	80.0	80.0
Ballast Provision	10.0	10.0
Rotor Tilt Provision	80.0	80.0
Instrumentation	<u>1000.0</u>	<u>1000.0</u>
Weight Empty	17953.6	13922.2

TABLE III

HIGH-SPEED SEA LEVEL MISSION GROSS WEIGHTS

	Model 646A Mission		Model 646B Mission	
	Primary	Alternate	Primary	Alternate
Weight Empty	17953.6 (1b)	17953.6 (1b)	13922.2 (1b)	13922.2 (1b)
Useful Load				
Crew	(3) 600.0	600.0	(2) 400.0	400.0
Fuel	3040.0	5063.0	3062.0	5250.0
Payload (Removable)	2000.0	1000.0	1000.0	-
Engine Oil	53.8	53.8	51.8	51.8
Engine Oil - Trapped	17.2	17.2	17.2	17.2
Oil - Transmission and Gearboxes	54.3	54.3	44.5	44.5
Fuel - Trapped	19.3	19.3	19.3	19.3
Auxiliary Fuel Instl	-	-	-	25.0
Mission Gross Weights	23738.2	24761.2	18517.0	19730.0

TABLE IV

CENTER OF GRAVITY AND INERTIA DATA
(COMPOUND MODE)

	Model 646A			Model 646B		
	<u>Weight Empty</u>	<u>Primary Mission</u>	<u>Alternate Mission</u>	<u>Weight Empty</u>	<u>Primary Mission</u>	<u>Alternate Mission</u>
Weight (lb)	17954	23738	24761	13922	18517	19730
Center of Gravity (in.)						
Longitudinal	FS 229	FS 222	FS 227	FS 208	FS 198	FS 201
Lateral	BL 299	BL 299	BL 299	BL 199	BL 199	BL 199
Vertical	WL 98	WL 92	WL 91	WL 72	WL 64	WL 62
Inertia (slug-ft ²)						
Roll	13719	15066	17226	8508	9924	14364
Pitch	50414	55707	54186	26835	32596	31150
Yaw	51141	55664	55790	24869	29744	31898
I _{XZ}	524	1539	588	944	2005	1549
Principal Axis Inclination	0.8°	2.17°	0.87°	3.30°	5.78°	5.05°

TABLE V. DRAG ANALYSIS

COMPONENT	FLAT PLATE DRAG AREA FT ²					
	AIRPLANE		HELICOPTER		WETTED-AREA	
	TECHNIQUE	646A	646B	TECHNIQUE	646A	646B
Fuselage	1.26	1.17	1.78	1.65	3.09	2.87
Pylon	.16	.11	.25	.18	.31	.22
Shaft Engines	1.16	.30	1.74	.45	.31	.08
Thrust Engines	1.43	.76	2.04	1.08	1.49	.79
Tail Boom	1.01	.58	1.01	.58	1.77	1.02
Wing	1.55	1.27	2.07	1.70	2.55	2.09
Horizontal Tail	.31	.35	.46	.53	.57	.65
Vertical Tail	.22	.23	.34	.35	.42	.43
Tail Rotor Gearbox	<u>.16</u>	<u>.16</u>	<u>.23</u>	<u>.23</u>	<u>.05</u>	<u>.05</u>
	7.26	4.93	9.92	6.75	10.56	8.20
Sub Total	<u>.73</u>	<u>.53</u>	<u>.99</u>	<u>.73</u>	<u>0</u>	<u>0</u>
10% Miscellaneous & Interference	7.99	5.46	10.91	7.48	10.56	8.20
Sub Total	<u>.23</u>	<u>.23</u>	<u>.23</u>	<u>.23</u>	<u>.23</u>	<u>.23</u>
Trim Drag (C _L Tail = 0.1)	8.22	5.69	11.14	7.71	10.79	8.43
Sub Total	<u>0</u>	<u>0</u>	<u>0</u>	<u>0</u>	<u>0</u>	<u>0</u>
Shaft Engine Jet Thrust	8.22	5.69	11.14	7.71	10.79	8.43
Sub Total	<u>.71</u>	<u>.50</u>	<u>.71</u>	<u>.50</u>	<u>2.13</u>	<u>1.51</u>
Tail Rotor Hub	8.23	5.85	8.23	5.85	8.09	5.75
Main Rotor Hub	17.16	12.04	20.08	14.06	21.01	15.69
Sub Total	<u>1.02</u>	<u>.97</u>	<u>1.02</u>	<u>.97</u>	<u>1.02</u>	<u>.97</u>
Induced Drag @ Max Speed*, SLS, 15 Min Mission	18.18	13.01	21.10	15.03	22.03	16.66
Sub Total	<u>5.07</u>	<u>3.00</u>	<u>5.07</u>	<u>3.00</u>	<u>5.07</u>	<u>3.00</u>
Rotor Drag @ 300 Kts	23.25	16.01	26.17	18.03	27.10	19.66
TOTAL						

* Max speed for the alternate configuration is 295 knots, 300 knots for the design configuration.

TABLE VI. HIGH-SPEED MISSION FUEL REQUIREMENTS

ITEM	FUEL WEIGHT-LB.			
	646A		646B	
	SLS	9500'	SLS	9500'
1. Warm-up & Take-Off	314	314	255	255
2. Flight At Minimum Airspeed	129	129	87	87
3. Climb				
(a) 15 Min Mission	0	224	0	187
(b) 30 Min Mission	0	232	0	199
4. Acceleration				
(a) 15 Min Mission	427	208	397	364
(b) 30 Min Mission	442	216	422	386
5. High Tip Speed Cruise				
(a) 15 Min Mission	1756	1363	1933	1532
(b) 30 Min Mission	3514	2719	3888	3067
6. Deceleration	32	22	25	20
7. Descent				
(a) 15 Min Mission	0	119	0	82
(b) 30 Min Mission	0	115	0	78
8. End-Of-Mission Hover	78	78	48	48
9. Reserve				
(a) 15 Min Mission	304	273	305	286
(b) 30 Min Mission	<u>501</u>	<u>425</u>	<u>525</u>	<u>460</u>
TOTAL				
15 Min Mission	3040	2730	3050	2861
30 Min Mission	5010	4250	5250	4600

TABLE VII. HIGH-SPEED MISSION PERFORMANCE SUMMARY

ITEM		646A		646B	
		SLS	9500'	SLS	9500'
1.	Take-Off Gross Weight				
					Lb
	(a) 15 Min Mission	23738	23446	18517	18330
	(b) 30 Min Mission	24761	23996	19730	19070
2.	End-Of-Mission Hover Weight				
					Lb
	(a) 15 Min Mission	21080	21165	15820	15805
	(b) 30 Min Mission	20331	20257	15055	14980
3.	Total Payload				
					Lb
	(a) 15 Min Mission	3000	3000	2000	2000
	(b) 30 Min Mission	2000	2000	1000	1000
4.	Total Fuel Weight				
					Lb
	(a) 15 Min Mission	3040	2730	3050	2860
	(b) 30 Min Mission	5010	4250	5250	4600
5.	Maximum Airspeed				
					Kts
		300	300	295	295

TABLE VIII. HOVER TEST VERSATILITY

CONFIGURATION	646A			646B		
	GROSS WEIGHT (LB)	RADIUS (FT)	SOLIDITY	GROSS WEIGHT (LB)	RADIUS (FT)	SOLIDITY
1. Compound Helicopter						
A. Largest Rotor Heaviest Gross Weight	26,700 28,000	27.5 27.5	0.150 0.096	15,420 15,900	25.0 25.0	0.095 0.068
B. Smallest Rotor	20,500	22.9	0.125	15,420	24.3	0.075
2. Pure Helicopter						
A. Largest Rotor Heaviest Gross Weight	29,300 29,300	27.5 27.5	0.150 0.150	17,950 18,550	25.0 25.0	0.150 0.100
B. Smallest Rotor	15,840	14.4	0.150	13,250	16.3	0.150

TABLE IX

SUMMARY - MAXIMUM SPEED AS PURE HELICOPTERS

VEHICLE	DIAMETER FT	SOLIDITY	GROSS WEIGHT LB	MAXIMUM SPEED KT
646A	55	0.15	29,300	184
	55	0.15	15,840	210
	28.8	0.15	15,840	111
646B	50	0.10	18,550	169
	50	0.15	13,250	167
	32.6	0.15	13,250	164

TABLE X. PERCENT TRANSMISSIBILITY OF HUB FORCES IN PITCH

Focal Point (WL)	$K_{\theta} \times 10^6$ (in-lb/rad)	FREQUENCY - CPS					
		5	10	15	20	25	30
132.5	4.9	0.0	41.6	45.9	47.3	47.8	48.1
112.0	7.2	81.4	0.0	7.3	9.6	10.7	11.2
104.0	8.2	83.7	7.5	0.0	2.4	3.4	4.0
100.0	8.6	81.9	9.7	2.3	0.0	1.0	1.6
96.6	9.0	88.4	11.6	4.0	1.6	0.5	0.0
46.2	14.9	36.7	6.4	2.4	1.0	0.4	0.0
40.2	15.5	31.6	4.9	1.2	0.0	0.6	0.9
33.5	16.3	27.4	3.4	0.0	1.1	1.6	1.9
16.0	18.3	18.5	0.0	2.9	3.8	4.2	4.5

TABLE XI. PERCENT TRANSMISSIBILITY OF HUB FORCES IN ROLL

Focal Point (WL)	$K_{\theta} \times 10^6$ (in-lb/rad)	FREQUENCY - CPS					
		5	10	15	20	25	30
132.5	4.9	0.0	47.8	52.1	53.3	54.1	54.5
112.0	7.2	150.0	0.0	9.6	12.6	13.9	14.6
104.0	8.2	161.7	10.4	0.0	3.3	4.7	5.4
100.0	8.6	159.1	13.7	3.2	0.0	1.4	2.2
96.6	9.0	179.8	16.5	5.5	2.1	0.6	0.0
46.2	14.9	61.9	9.6	3.4	1.5	0.6	0.0
40.2	15.5	51.4	7.2	1.7	0.0	0.8	1.2
33.5	16.3	43.9	4.9	0.0	1.6	2.4	2.7
16.0	18.3	29.3	0.0	4.1	5.5	6.0	6.4

TABLE XII.. PERCENT TRANSMISSIBILITY OF HUB MOMENTS IN PITCH

Focal Point (WL)	$K_{\theta} \times 10^6$ (in-lb/rad)	FREQUENCY - CPS					
		5	10	15	20	25	30
149.5	2.9	0.0	24.6	27.7	28.7	29.1	29.4
145.8	3.3	39.2	0.0	5.4	6.8	7.6	8.0
145.0	3.4	48.0	5.1	0.0	1.6	2.4	2.8
144.5	3.5	39.4	6.3	2.0	0.0	0.2	0.4
144.2	3.5	40.2	6.9	2.6	1.1	0.5	0.0
51.0	14.2	39.3	7.0	2.7	1.2	0.6	0.0
49.8	14.3	36.8	5.7	1.5	0.0	0.5	0.8
48.0	14.5	35.5	4.2	0.0	1.4	2.0	2.3
45.0	14.9	27.4	0.0	3.7	4.9	5.5	5.8
26.8	17.0	0.0	17.3	19.8	20.6	21.0	21.1

TABLE XIII. PERCENT TRANSMISSIBILITY OF HUB MOMENTS IN ROLL

Focal Point (WL)	$K_{\theta} \times 10^6$ (in-lb/rad)	FREQUENCY - CPS					
		5	10	15	20	25	30
149.5	2.9	0.0	25.2	28.3	29.4	29.9	30.1
145.8	3.3	41.6	0.0	5.6	7.2	8.0	8.3
145.0	3.4	51.3	5.4	0.0	1.7	2.5	2.9
144.5	3.5	42.0	6.6	2.2	0.0	0.2	0.4
144.2	3.5	42.8	7.2	2.7	1.2	0.5	0.0
51.0	14.2	67.4	10.3	3.9	1.8	0.9	0.0
49.8	14.3	62.9	8.4	2.2	0.0	0.7	1.2
48.0	14.5	60.8	6.2	0.0	2.0	2.9	3.3
45.0	14.9	46.2	0.0	5.4	7.1	7.9	8.4
26.8	17.0	0.0	25.2	28.5	29.6	30.1	30.3

TABLE XIV. ISOLATION OF BIPOD FOCAL PYLON WITH FORE AND AFT AXIS AT INPUT SHAFT AXIS

$K_{\theta} \times 10^6$ (in-lb/rad)	FREQUENCY - CPS					
	5	10	15	20	25	30
% FORCE TRANSMISSIBILITY IN PITCH						
4.9	25.2	6.9	4.1	3.2	2.7	2.5
6.9	37.0	8.8	4.9	3.6	3.0	2.7
8.9	51.4	10.9	5.7	4.1	3.3	2.9
10.9	69.1	13.0	6.6	4.5	3.6	3.1
12.9	91.5	15.2	7.4	5.0	3.9	3.3
14.9	120.8	17.5	8.3	5.5	4.2	3.5

$K_{\theta} \times 10^6$ (in-lb/rad)	FREQUENCY - CPS					
	5	10	15	20	25	30
% MOMENT TRANSMISSIBILITY IN PITCH						
4.9	66.7	42.5	38.8	37.6	37.0	36.7
6.9	82.6	45.1	39.9	38.2	37.4	36.9
8.9	101.6	47.8	41.0	38.8	37.8	37.2
10.9	125.2	50.7	42.2	39.4	38.1	37.5
12.9	155.1	53.6	43.3	40.0	38.5	37.7
14.9	194.0	56.7	44.4	40.6	38.9	38.0

TABLE XV. INPLANE ISOLATION SYSTEM TRADE OFFS

<u>Consideration</u>	<u>Bipod</u>	<u>Tetrapod</u>
Isolation of Forces		
Pitch	Good	Excellent
Roll	Excellent	Excellent
Isolation of Moments		
Pitch	Moderate	Excellent
Roll	Excellent	Excellent
Torque Restraint	Incorporated	Requires additional components
Provisions for tilting	Easily accommodated by actuator & spring at base of transmission	Requires additional provisions
Weight	Approximately 0.8% of gross weight	Approximately 1.2% gross weight (not including provisions for tilting)
Adaptation to vertical isolation systems (nodal beam & servo-null)	Good	Good

TABLE XVI. PASSIVE NODAL BEAM CONFIGURATION REQUIRED TO COVER ENTIRE FREQUENCY SPECTRUM

CONFIGURATION NO.	FREQ RANGE ISOLATED	CONFIG* TIP MASS	K ϕ	NODAL POINT LOCATION
1	6-9 Hz	100 lb	100,000	Sta 190, 210
2	9-16 Hz	100 lb	200,000	Sta. 190, 210
3	16-23 Hz	50 lb	300,000	Sta. 190, 210
4	23-30 Hz	25 lb	350,000	Sta. 190, 210

$\frac{\text{in-lb}}{\text{rad}}$

$\frac{\text{in-lb}}{\text{rad}}$

$\frac{\text{in-lb}}{\text{rad}}$

$\frac{\text{in-lb}}{\text{rad}}$

* Total Tip Mass - 2 Times Value Shown

TABLE XVII. SUMMARY OF SERVO-NULL ISOLATION
SYSTEM REQUIREMENTS

15,000 POUND FUSELAGE WEIGHT

	RPM	Total Spring Rate About Torque Tube K_{θ}	Mass	in/g*
2/rev	Low	325,000	100	2.25
	High	800,000		0.92
3/rev	Low	375,000	50	1.95
	High	850,000		0.87
4/rev	Low	350,000	27	2.10
	High	800,000		0.92
5/rev	Low	375,000	20	1.95
	High	900,000		0.82
6/rev	Low	400,000	15	1.82
	High	1,000,000		0.74

*Without Servo-Null

TABLE XVIII. COMPARISON OF CONTROL SYSTEM CONCEPTS

	CONCEPT I	CONCEPT II	CONCEPT III
Number of Hydraulic Systems Required	2	3	2
Number of Electrical Systems Required	2	3	2
Mechanical System Ability	Rotor and Fixed-Wing Controls	Fixed-Wing Controls only	Rotor and Fixed-Wing Controls
Computer Output Requirements	Dual Independent Computer Commands	Triple Independent Computer Commands to Rotor (dual to fixed-wing)	Dual Independent Computer Commands
Electronic Complexity	Dual electronics for monitor functions (rotor and fixed-wing controls)	Dual electronics for fixed-wing monitoring. Triple for rotor, with triple force equalization system	Dual electronics for monitor functions (rotor and fixed-wing controls)
Safety Considerations	Dead band exists in sloppy link device with FBW Actuator, until sloppy link centers and locks - other characteristics similar to Concept III	One rotor control system failure is safe. Fixed-wing controls are safe for all electrical system failures.	Rotor and Fixed-Wing Control: Mechanical backup is connected directly. Rotor SCAS failure effect can be limited by rotor gain change. Mechanical system is fail safe. All systems will operate with electrical failures.
Weight Considerations	Sloppy link and clutching is added	Weight saved by using FBW rotor controls is offset by extra hydraulic, electrical and computer requirements.	Some weight savings because of single actuator in gain change mechanism.

TABLE XVIII. (Continued)

	CONCEPT I	CONCEPT II	CONCEPT III
Development Required	Sloppy link and clutching mechanism. Control phasing mechanism.	Triple FBW turn/on turn off and tracking devices. Rotor Stabilization System	Gain change mechanism Rotor Stabilization System
Switchover Complexity	Sloppy link must be closed when going to mechanical backup to eliminate deadband	Mechanical backup is always in fixed wing controls	Mechanical backup is always in all controls
Preflight Check	Test all systems for failure detection system operation and sloppy link and clutch operation	Check that failed rotor command channel disengages automatically	Test all systems for failure detection operation
Operating Options	Mechanical Control. Pilot-controlled FBW. Computer-controlled FBW Computerized rotor control and pilot-controlled fixed-wing control	Mechanical Fixed-Wing Pilot-controlled FBW rotor. Computer-controlled FBW rotor and fixed-wing controls.	Mechanical Control. Computer-controlled FBW. Computerized rotor control and pilot-controlled fixed-wing.
Pilot Confidence	Fair	Bad	Good